University of Glasgow

Neuroinflammatory and protein responses to TBI

Hannah Louise Morgan, BSc (Hons)

A thesis submitted to the University of Glasgow in fulfilment of the requirements for the degree of Doctor of Philosophy.

Graduate School of the College of Medical and veterinary Life Sciences, the University of Glasgow.

Abstract

Background: Traumatic brain injury (TBI) is a leading cause of death and disability world-wide, affecting approximately 69 million individuals each year. It is also recognised as one of the major, modifiable risk factors in the development of neurodegenerative disease in later life, with exposure to moderate to severe single TBI and repetitive, mild TBI both recognised as contributing factors in the development of dementia. However, the neuropathological mechanisms contributing to late neurodegeneration remain uncertain. The complex polypathology emerging from the initial biomechanical injury mirror other neurodegenerative disease and include abnormal aggregation of proteins such as tau and Aß and neuroinflammation, which will be explored in this thesis.

Methodology: Utilising material from the Glasgow TBI archive, in cohorts of patients aged ≤60 exposed to acute and long-term survival following moderate to severe, single TBI and appropriately age-matched controls, the role of the cellular adaptive immune response to injury was assessed through immunocytochemistry for T- and B-lymphocyte populations. These cohorts as well as tissue from patients exposed to repetitive mild TBI (rTBI) and appropriately matched controls were studied to characterise the differential astroglial response to injury across injury subgroups through measurement of GFAP, AQP4 and NQO1 immunoreactivity. A cohort of patients aged ≥60 years who survived acutely following moderate to severe, single TBI compared to age-matched, uninjured controls with no history of neurodegenerative disease, were examined to evaluate the effect of age and TBI using modifications of clinically recognised, standardised, semi-quantitative scoring systems of tau and Aß immunoreactivity. Lastly, a protocol for the assessment of our archival, FFPE tissue was devised to allow comparison of proteomes of cohorts of patients exposed to mild rTBI, AD patients and appropriately matched controls, using liquid-chromatography mass-spectrometry.

Results: There is no histological evidence of a significant cellular response from the adaptive immune system following exposure to moderate to severe, single TBI in patients surviving acutely or long-term after injury, with no increase in T- or B-lymphocytes. There was, unexpectedly, a decrease in T-lymphocytes in long-term survivors of TBI. Contrastingly, there was an increase in reactive astrogliosis

following exposure to TBI; demonstrated by an increase in AQP4-immunoractive astrocytes in acutely surviving patients and increase in GFAP expression in long-term surviving patients and an increase in NQO1 expression in rTBI patients compared to age-matched uninjured controls. There was also an increase in both AQP4 and GFAP expression in elderly uninjured controls compared to younger uninjured controls. Examining the expression of Aß and tau in elderly patients exposed to single, moderate to severe TBI showed an increase in neuritic Aß plaque and in the regional distribution of all plaque compared to uninjured, elderly controls, but no increase in expression or distribution of NFTs. Finally, a protocol for processing archival FFPE resulted in identification of 267 proteins from across rTBI, AD and uninjured, non-NND controls with significantly differential expression in 84 of them.

Conclusions: Together, these findings increase understanding of the neuropathological changes occurring following moderate to severe, single TBI and repetitive TBI. These data demonstrate that there is an astrogliotic but not adaptive cellular response after moderate to severe single TBI whilst also showing that age is correlated with an increase in reactive astrogliosis for several markers. Age was also examined in the examination of proteinopathic changes following acute survival after moderate to severe injury and changes suggest that TBI may occur as a result of increased amyloid pathology as neuritic plaque was observed > 2 weeks after injury. Lastly, that archival FFPE samples were successfully processed to allow identification of proteins from across a range of cohorts, revealing differences in protein expression that underpin the neuropathological changes which contribute to the long-term, post-TBI neurodegenerative process.

Table of Contents

List of Tables

List of Figures

Publications arising from this thesis

Morgan, H.L., Fullerton, J.L., Smith, D.H., Stewart, W. 'PS2.04.199 Traumatic brain injury is not associated with an adaptive immune cell infiltrate in humans'. The 3rd Joint Symposium of the International and National Neurotrauma Societies and AANS/CNS Section on Neurotrauma and Critical Care August 11–16, 2018, Toronto, Canada. *Journal of Neurotrauma*. Aug 2018. A-1-A-285.

Morgan, H.L., Johnson, V., Smith, D.H., Stewart, W. 'DBB-20 Traumatic brain injury leads to widespread acute amyloid-beta deposition in the elderly', Abstracts from The 37th Annual National Neurotrauma Symposium June 29–July 3, 2019, Pittsburgh, Pennsylvania. *Journal of Neurotrauma*. Jul 2019. A-1-A-156.

Morgan, H.L., Johnson, V, Smith, D.H., Stewart, W. 'Traumatic brain injury leads to widespread acute amyloid-beta deposition in the elderly', 2019 Annual Laboratory Poster Day, Queen Elizabeth University Hospital, Glasgow, UK.

List of accompanying material

Acknowledgements

This thesis has been made possible with the help and support of many individuals, whom I would like to take a moment to thank.

Firstly, I owe my primary supervisor Professor William Stewart of the Department of Neuropathology, Queen Elizabeth University Hospital very many thanks for his tireless support in my efforts to complete my PhD and write this thesis. From offering me the initial position, to the final motivation when trying to write up, I am very grateful for all his help over the years. I also owe a great deal of thanks to my second supervisor Dr Josie Fullerton of the School of Cardiovascular and Metabolic Health, who has been brilliant mentor to me throughout this whole process and has never failed to reassure me when I did not believe I could do it. I would not be writing this without her reassurance, guidance and help.

The support team within MVLS have helped me a great deal in getting this thesis completed, including Dr Mick Craig, Ms Audrey Hillis and the members of the Higher Degrees Committee. Several other individuals have helped me over the years with either advice or helping with technical skills, including Dr Kamar Ameen-Ali at Teesside University, and Dr Victoria Johnson and Professor Douglas Smith at the University of Pennsylvania. I would also like to thank, Dr Richard Burchmore, Mrs Suzanne McGill and Dr Stefan Weidt of Glasgow Polyomics as well as Dr John Cole and Dr Sheon Samji who assisted me in carrying out my polyomics work.

I would like to give enormous thanks Dr Jennifer Hay, who has also offered me endless amounts of encouragement and excellent advice, supporting me through every stage of the process and being exceptionally understanding. I'd like to thank Dr Emma Russell who went through this process hand in hand with me - keeping me sane, and all the members staff who have worked with the GBIRG and GTRF over the years offering excellent cake and advice.

All my friends who have always been there for a laugh and a cry these mad last few years, and everyone from GUCC who has given me a regular escape into a whole different world.

Especially I'd like to thank Dr Sophie Boyd and Dr Katy Cooper who have been the most supportive friends and have never ceased to believe in and encourage me.

I need to thank my Mum and Dad and all my siblings – real and muggle, for never needing me to explain why I'm doing a PhD and loving me through everything. I'm looking forward to seeing so much more of you! Xxx

Lastly, thank you Beast/Pudding/Potato/Loaf/Rosie, your indifference keeps me grounded.

Author's Declaration

I declare that, except where explicit reference is made to the contribution of others, that this dissertation is the result of my own work and has not been submitted for any other degree at the University of Glasgow or any other institution.

Printed Name: Hannah Louise Morgan

Signed: _____

Date: 12th February 2023

Abbreviations

µg	Microgram
µl	Microlitre
ACO2	Aconitate hydratase, mitochondrial
ACOT7	Cytosolic acyl coenzyme A thioester hydrolase
AD	Alzheimer's disease
ADD2	Beta-adducin
ADNC	Alzheimer’s disease neuropathologic changes
ADP	Adenosine diphosphate
ALDH9A1	4-trimethylaminobutyraldehyde dehydrogenase
ALS	Amyotrophic lateral sclerosis
ANXA5	Annexin A5
ApoE	Apolipoprotein
APP	Amyloid precursor protein
AQP1	Aquaporin 1
AQP4	Aquaporin 4
ARDS	Acute respiratory distress syndrome
AT	Austria
aTBI	Acute traumatic brain injury
ATP	Adenosine triphosphate
ATP1A2	Sodium/potassium-transporting ATPase subunit alpha-2
ATP2B2	Plasma membrane calcium-transporting ATPase 2
ATP5C1	ATP synthase subunit gamma, mitochondrial
ATP5D	ATP synthase subunit delta, mitochondrial
ATP6V1B2	V-type proton ATPase subunit B, brain isoform
ATP6V1D	V-type proton ATPase subunit D
Aß	Amyloid-beta
BACE1	ß-site APP cleaving enzyme 1
BBB	Blood Brain Barrier
CA	California
CAA	Cerebral amyloid angiopathy
CADM4	Cell adhesion molecule 4
CAMK2G	Calcium/calmodulin-dependent protein kinase type II subunit gamma
CAN	Acetonitrile
CANX	Calnexin

CC	Corpus callosum
CCI	Closed cortical impact
CFL1	Cofilin-1
CFS	Cerebrospinal fluid
CID	Collision-induced dissociation
CKMT1A;CKMT1B	Creatine kinase U-type, mitochondrial
CNP	2,3-cyclic-nucleotide 3-phosphodiesterase
CNS	Central nervous system
CNTN2	Contactin-2
COX-2	Cyclooxygenase-2
COX4I1	Cytochrome c oxidase subunit 4 isoform 1, mitochondrial
CRYAB	Alpha-crystallin B chain
CS	Citrate synthase, mitochondrial
CSP	Cavum septum pellucidum
cTBI	Chronic traumatic brain injury
CTE	Chronic traumatic encephalopathy
CYCS	Cytochrome c
DAB	3,3'-Diaminobenzidine
DAI	Diffuse axonal injury
DBI	Acyl-CoA-binding protein
DE	Germany
dH20	Distilled water
DLB	Dementia with Lewy bodies
MRI	Diffusion MRI
DP	Dementia pugilistica
DTI	Diffusion tensor imageing
DTT	Dithiothreitol
DYNLRB1	Dynein light chain roadblock-type 1
ECH1	Delta(3,5)-Delta(2,4)-dienoyl-CoA isomerase, mitochondrial
EDTA	Ethylenediaminetetraacetic acid
ENPP6	Ectonucleotide pyrophosphatase/phosphodiesterase family member 6
ESI	Electrospray ionisation
FA	Formic acid
FASP	Filter aided sample preparation
FF	Fresh frozen
FFPE	Formalin-fixed, paraffin embedded
FTL	Ferritin light chain

FTLD	Frontotemporal lobular dementia
g	Gravity
GAPDH	Glyceraldehyde-3-phosphate dehydrogenase
GDI1	Rab GDP dissociation inhibitor alpha
GDI2	Rab GDP dissociation inhibitor beta
GFAP	Glial fibrillary acidic protein
GNAI1	Guanine nucleotide-binding protein G(i) subunit alpha-1
GNAO1	Guanine nucleotide-binding protein G(o) subunit alpha
GPX1	Glutathione peroxidase 1
GSTP1	Glutathione S-transferase P
H_20_2	Hydrogen peroxide
HAPLN2	Hyaluronan and proteoglycan link protein 2
HBA1;HBA2	Haemoglobin subunit alpha
HBD	Haemoglobin subunit delta
HDACi	Histone deacetylase inhibitor
HICs	High income countries
HO-1	Heme oxygenase-1
HRP	Horseradish peroxidase
HSPA5	78 kDa glucose-regulated protein
HSPA6	Heat shock 70 kDa protein 6
HSPD1	60 kDa heat shock protein, mitochondrial
htau	Human tau
IAA	Iodoacetamide
IgG	Immunoglobulin G
IGHA1	Ig alpha-1 chain C region
IGHG1	Ig gamma-1 chain C region
IHC	Immunohistochemistry
iNPH	Idiopathic normal pressure hydrocephalus
IR	Infrared
KO	Knock out
LC	Liquid chromatography
LCM	Laser capture microdissection
LCMS	Liquid chromatography mass spectrometry
LDHA	L-lactate dehydrogenase A chain
LFQ	Label free quantification
LGALS3BP	Galectin-3-binding protein
LMICs	Low middle income countries
LOC	Loss of consciousness

LPS	Lipopolysaccharide
Lyc-C	Endoproteinase Lys-C
m/z	mass number / charge number
MAP2	Microtubule-associated protein 2
MAP6	Microtubule-associated protein 6
MBP	Myelin basic protein
MCI	Mild cognitive impairment
MCP1	Monocyte chemoattractant protein 1
MDH1	Malate dehydrogenase, cytoplasmic
mIF	Multiplexed immunofluorescence
miRNA	Micro ribonucleic acid
mM	Millimolar
MMP	matrix-metalloproteinase
MND	Motor neurone disease
mRNA	Messenger ribonucleic acid
MS	Multiple sclerosis
mTBI	Mild traumatic brain injury
MT-CO2	Cytochrome c oxidase subunit 2
NCBI	National Center for Biotechnology Information
NCE	Normalized collision energy
NDD	Neurodegenerative disease
NEFH	Neurofilament heavy polypeptide
NEFM	Neurofilament medium polypeptide
NFT	Neurofibrillary tangles
nLC-ESI-MS/MS	Nanoflow HPLC electrospray tandem mass spectrometry
NO	Nitric oxide
NQO1	NAD(P)H quinone dehydrogenase 1
Nrf2-keap1-ARE	Kelch-like ECH-Associating protein 1
NS	Not significant
OMG	Oligodendrocyte-myelin glycoprotein
OR	Odds ratio
PBS	Phosphate-buffered saline
PCA	Principal component analysis
PCSK1N	ProSAAS
PD	Parkinson's disease
PDD	Parkinson's disease dementia
PEBP1	Phosphatidylethanolamine-binding protein 1
PET	Positron emission tomography

PFN1	Profilin-1
PGK1	Phosphoglycerate kinase 1
PHB2	Prohibitin-2
PKM	Pyruvate kinase PKM
PM	Post-mortem
PRRT2	Proline-rich transmembrane protein 2
PSMB6	Proteasome subunit beta type-6
PSP	Progressive supranuclear palsy
PTA	Post-traumatic amnesia
pTau	hyperphosphorylated tau
PTPRZ1	Receptor-type tyrosine-protein phosphatase zeta
PYGB	Glycogen phosphorylase, brain form
QC	Quality control
RAP1B	Ras-related protein Rap-1b
ROS	Reactive oxygen species
RP	Resolving power
RPS18	40S ribosomal protein S18
rTBI	Repetitive traumatic brain injury
S100B	HSPA6
sAPPα	Soluble amyloid precursor protein α
SDS	Sodium dodecyl-sulphate
SEPTIN7	Septin-7
SEPTIN8	Septin-8
SGL	Superficial glial limitans
SH3GL2	Endophilin-A1
SLC9A3R1	Na(+)/H(+) exchange regulatory cofactor NHE-RF1
SN	Substantia nigra
SNAP25	Synaptosomal-associated protein 25
SNCA	Alpha-synuclein
SNpc	Substantia nigra pars compacta
SOD1	Superoxide dismutase [Cu-Zn]
sTBI	Single moderate or severe traumatic brain injury
SUDEP	Sudden unexplained death in epilepsy
TALDO1	Transaldolase
TBHQ	Tert-Butylhydroquinone
TBI	Traumatic brain injury
TDP-43	Transactive response DNA-binding protein 43
TEM	Transmission electron microscopy

TFA	Trifluoroacetic acid
TKT	Transketolase
TMA	Tandem mass tag
TNF-α	Tumour necrosis factor-α
TPI1	Triosephosphate isomerase
TPPP	Tubulin polymerization-promoting protein
TPPP3	Tubulin polymerization-promoting protein family member 3
Tris	Tris(hydroxymethyl) aminomethane
TSA	Thorn-shaped astrocytes
TUBA1B	Tubulin alpha-1B chain
TUBB3	Tubulin beta-3 chain
UBC	Polyubiquitin-C
uHPLC	Ultra-High-Performance Liquid Chromatography
UQCRC1	Cytochrome b-c1 complex subunit 1, mitochondrial
UQCRFS1	Cytochrome b-c1 complex subunit Rieske, mitochondrial
VDAC1	Voltage-dependent anion-selective channel protein 1
VEGF	Vascular endothelial growth factor
VPA	Valproic acid
WMI	White matter interface
YWHAE	14-3-3 protein epsilon
α-syn	Alpha-synuclein
η^2	Eta-squared

Chapter 1 – General Introduction

Traumatic brain injury (TBI) is a global public health concern and leading cause of death and disability worldwide, with 64-74 million individuals estimated to suffer from TBI each year (Dewan et al., 2019). Age-adjusted incidence of all TBI severities from studies published between 2015 and 2020 varies globally, ranging between 476 per 100,000 individuals in South Korea (H. Kim et al., 2020) to 787 per 100,000 individuals in the US (Maas et al., 2022; Taylor et al., 2017). Moreover, these studies may continue to underestimate the true extent of the issue as incidence continues to rise globally (James et al., 2019), particularly in older populations (Shivaji et al., 2014). Severity of injury can vary, from mild TBI (mTBI; including concussion), through moderate to severe TBI, with severe TBI resulting in a high mortality rate of approximately 30-40% (Rosenfeld et al., 2012).

The main mechanisms of moderate to severe injuries are falls, road traffic incidents and violence, and whilst global trends in mechanism vary due to differences in nation-specific data capture and reporting methodologies. Largely it is suggested that road traffic incidents are the most common cause of injury in low middle income countries (LMICs) (Dewan et al., 2019; James et al., 2019) while individuals from high income countries (HICs) are most likely to be injured due to a fall (Lecky et al., 2021; Maas et al., 2022). Incidence of TBI is higher in LMICs than HICs (Clark et al., 2022; Dewan et al., 2019; James et al., 2019), with a clear connection drawn between mechanism of injury and the UN's Human Development Index (a composite index of life expectancy, education, and per-person income indicators, used to rank countries into tiers of human development: low, medium, high, and very high; **Figure 1-1**, (Maas et al., 2022)).

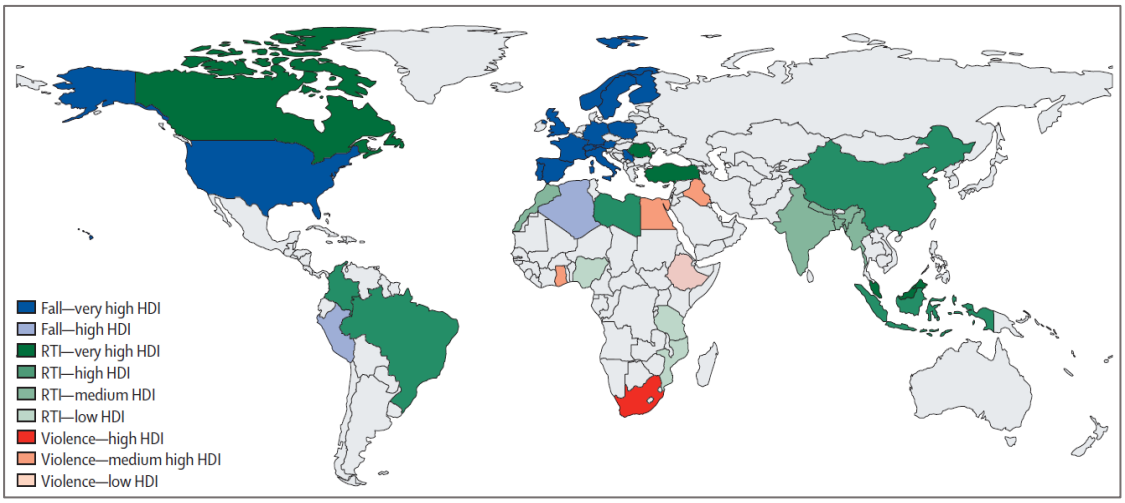

Figure 1-1 Between Country Variations in mechanism of TBI according to UN Human Development Index. RTI = Road Traffic Incident, HDI = Human Development Index (from Maas et al 2022)

Notwithstanding the initial insult, the burden of any TBI may be felt for years after injury where, for example, in the US approximately 4 million individuals are living with a TBI-related chronic condition (Frieden et al., 2015), while in the UK alone, roughly 1.3 million people are living with TBI-related disabilities (Parsonage, 2016). Additionally, TBI may result in substantial socioeconomic consequences lasting many years post-injury (Norup et al., 2020) and an estimated $400 billion is spent for the overall healthcare cost of TBI per year globally (Maas et al., 2017).

1.1 Late neurodegenerative disease and TBI

There is increasing awareness of the connection between TBI and the risk of later development of neurodegenerative disease. The first reporting of the long-term effects of TBI emerged from a series of examinations of professional and amateur boxers exposed to repetitive TBI (rTBI) by Dr Harrison S Martland in 1928, coining the term punch-drunk syndrome (Martland, 1928). Following this, descriptions of isolated cases of brains taken from boxers continued through the latter part of the last century (Brandenburg & Hallervorden, 1954; Critchley, 1957; Mawdsley & Ferguson, 1963; Millspaugh, 1937; Spillane, 1962) where studies described neurodegenerative pathology such as cerebral atrophy and softening, and cavum septum pellucidum, alongside changes in behaviour

including emotional liability, memory impairment and dementia (A. H. Roberts, 1969). Corsellis (1973) examined 15 ex-boxers, providing the first formal description of dementia pugilistica (DP), noting the neuropathological abnormalities of septum pellucidum, degradation of the substantia nigra and occurrence of neurofibrillary tangles, particularly within the medial temporal grey matter, as well as neuropsychiatric symptoms such as speech and motor problems, memory loss and personality changes (Corsellis et al., 1973). Recognition has continued to grow over the subsequent decades, with more recent studies highlighting neuropathological anomalies associated with boxing (Allsop et al., 1990; Castellani & Perry, 2017; Geddes et al., 1997, 1999; G. Roberts et al., 1990; Saing et al., 2012; Schmidt. et al., 2001). However, it is now understood that the pathology is not limited to boxers but extends to the brains of individuals exposed to rTBI in a variety of sports and situations (McKee et al., 2010, 2009; Omalu et al., 2011, 2006, 2005; Omalu et al., 2010; Omalu et al., 2010), veterans exposed to blast injury (Goldstein et al., 2012) and even those who suffer a single, moderate to severe TBI (sTBI) (Dale et al., 1991; Johnson et al., 2013; Johnson et al., 2013, 2012; Roberts et al., 1991; Smith et al., 2013). Chronic traumatic encephalopathy (CTE) is now the diagnostic term used to represent late neurodegenerative disease due to exposure to TBI as opposed to participation in one sport or activity (J. Hay et al., 2016; V. E. Johnson et al., 2017; McKee et al., 2009, 2013; D. H. Smith et al., 2013; Stewart et al., 2016). However, due to the nature of previous studies which have derived data from the review of relatively few cases from singular archives, producing scant data and lack of consensus on the precise neuropathological phenotypes following TBI (E. Lee et al., 2019; Y. Lee et al., 2013; D. Smith et al., 2019; Washington et al., 2016), studies continue with the aim to develop robust, validated neuropathological criteria for a diagnosis of CTE (Bieniek et al., 2021; McKee et al., 2015; D. Smith et al., 2021).

1.2 TBI and Alzheimer's disease

The risk of dementia has historically been linked to a proportion of survivors of single TBI (Fleminger, 2003; Graves et al., 1990; Guo et al., 2000; Molgaard et al., 1990; Mortimer et al., 1991; Plassman et al., 2000) and it is now acknowledged as the strongest environmental risk factor for a range of

neurodegenerative diseases, including Alzheimer's disease (AD) (Collins et al., 2020; Fann et al., 2018; Li et al., 2017; LoBue et al., 2018; Nordström & Nordström, 2018; Schaffert et al., 2018), with estimates suggesting that at least 3% of dementia diagnoses in the general population are attributable to TBI (Livingston et al., 2020; Maas et al., 2022; D. Smith, 2013).

Retrospective examination by Plassman *et al.* (2000) reviewed clinical assessments and interviews of head injured and non-head injured US veterans, 50 years after date of injury. Individuals who sustained a severe TBI (loss of consciousness (LOC) or post-traumatic amnesia (PTA) lasting longer than 24 hours) were 4 times more likely to develop dementia compared to non-head injured soldiers and those who sustained a moderate TBI (LOC or PTA lasting 30 minutes to 24 hours) were 2 times more likely to develop dementia than healthy controls (Plassman et al., 2000). Population-based observational studies of the long-term risks demonstrate that TBI is associated with an increased risk of dementia compared to people without a history of TBI and with people with non-TBI trauma (Fann et al., 2018) with the risk still evident >30 years after injury and the association stronger for individuals who suffer multiple TBIs (Nordström & Nordström, 2018). Studies of 7625 patients with a possible/probable clinical diagnosis of AD (LoBue et al., 2018), and of 2,133 participants with autopsy-confirmed AD (Schaffert et al., 2018) observed that those individuals with a self-reporting history of TBI with LOC had earlier onset of AD-like dementia symptoms, suggesting TBI may be related to an underlying neurodegenerative process related to AD.

1.3 TBI and synucleinopathies

Dementia with Lewy bodies (DLB) is an age-associated dementia characterised by accumulation of aggregated α-synuclein protein in Lewy bodies and neurites, similar to Parkinson's disease (PD) (Baba et al., 1998; C. Simon et al., 2021; Trojanowski & Virginia M-Y.L, 1998) . Relatively little is understood about how history of TBI might contribute as a risk factor for DLB, with data conflicted. By example, a relatively small study of patients diagnosed with DLB (n=147) did not demonstrate TBI as a risk factor for disease progression (Boot

et al., 2013). However, an autopsy study of individuals with history of sTBI where there had been a LOC of ≤1 hour was found to be associated with the presence of Lewy bodies in temporal and frontotemporal areas of the brain, while individuals exposed to LOC for >1 hour did not demonstrate this (Crane et al., 2016). A case study of 2 individuals exposed to moderate to severe TBI in mid-life with early-onset dementia demonstrated the stark variations between the neuropathology an individual exposed to TBI may present (Kenney et al., 2018). Case 1 demonstrated atypical AD with features of CTE but no α-synuclein-positive lesions, while Case 2 had unusually large α-synuclein intraneuronal inclusions, Lewy bodies and Lewy neurites, as well as extracellular α-synuclein, resulting in a diagnosis of DLB. This heterogeneity of pathology can create a barrier to reaching a diagnosis. When examining the effects of rTBI exposure in former contact sport athletes on association with DLB, researchers found and that the number of years played was associated with deposition of neocortical Lewy bodies, with pattern of Lewy body hierarchical clustering similar in CTE and DLB alone, (J. W. Adams et al., 2018) suggesting that participation in contact sport may increase risk of developing neocortical DLB.

PD is a typically slow progressing neurodegenerative disease characterised by the loss of dopaminergic neurons within the substantia nigra (Armstrong & Okun, 2020) and accumulating disability, where the decline can span decades (Bloem et al., 2021). A high degree of heterogeneity is observed within the disease, where even if one of the known, specific genetic causes is identified, the disease can manifest itself in a broad manner of symptoms and progressions (Armstrong & Okun, 2020). The disease manifests as early prodromal symptoms including rapid eye movement, sleep behaviour disorder, loss of smell, and depression (Berg et al., 2015) which will then progress to motor symptoms such as tremors, stiffness, and imbalance once approximately half of cells in the caudal substantia nigra are lost (Fearnley & Lees, 1991). Non-motor symptoms increase with disease burden, frequently leading to cognitive impairment as Parkinson's disease dementia (PDD) for 46% of patients within 10 years (Williams-Gray et al., 2013) and 83% of patients within 20 years (Hely et al., 2008). The hallmark of PD is neuronal aggregates of α-synuclein, forming Lewy bodies and Lewy neurites in a distinctive pattern, predominantly within the

limbic and motor systems (Braak & Braak, 2000). Recently, studies have suggested an association between sTBI and PD (Wilson et al., 2017), with a meta-analysis study demonstrating a pooled odds ratio (OR) of 1.57 for risk of PD following TBI (Jafari et al., 2013) while another study observed a 44% increased risk of developing PD within 5-7 years, for individuals sustaining a TBI over 55 years old (Gardner et al., 2015) and injury severity is correlated with increased risk of PD, even if the injury occurred before the age of 25 (Crane et al., 2016).

Once more, there is a degree of clinical overlap between symptoms associated with CTE and PD, including mood, cognitive, behaviour as well as motor symptoms, but the literature is very limited with regards to the risk of PD following rTBI and the few positive studies are potentially unsatisfactory due to issues such as poor matching of controls (Seidler et al., 1996) or reverse causation (Rugbjerg et al., 2009). The recent, well powered studies from the *Football's InfluencE on Lifelong health and Dementia risk* (FIELD) consortium have demonstrated a 2-fold increase in deaths with PD in former football players compared to matched, general population controls (Mackay et al., 2019; Russell et al., 2019, 2021) but additional studies are required to further examine the true extent of the correlation between PD and rTBI.

1.4 TBI and motor neuron disease

Amyotrophic lateral sclerosis (ALS) is the most common form of motor neuron disease (MND) (C. Lee, 2012), affecting 1-2 per 100,000 individuals each year (Robberecht & Philips, 2013). Upper and lower motor neurons are lost and there is an accumulation of the ubiquitinated protein transactive response DNA-binding protein 43 (TDP-43) in surviving motor neurons (Neumann et al., 2006). Whilst there are some identified hereditary factors in ALS diagnosis, 90-95% of cases, are sporadic (Frakes et al., 2014), and believed to be due to a combination of genetic and environmental factors, including TBI (H. Chen et al., 2007; McKee et al., 2010; Schmidt et al., 2010; Seals et al., 2016; D. Wright et al., 2017).

Limited data indicate that exposure to TBI - including sports-related concussion- may result in an increased risk of ALS/MND (X.-C. Chen et al., 2022; Daneshvar et al., 2021; Lehman, 2013; Pupillo et al., 2020; Seals et al., 2016). While recent studies of association football players by Mackay et al., (2019) and Rugby players by (Russell et al., 2022), demonstrates a high risk of MND when compared to sex, socioeconomic status, and age-matched general population controls. Examination of the effects of sTBI on the susceptibility to ALS is limited. One study noted a nonsignificant trend to higher ALS in those who had experienced a head injury but a significantly increased risk in those who had suffered more than one TBI which required medical attention (OR = 3.1) and a substantial increase in those who suffered more than one injury, more than 10 years previously (OR = 11.3), indicating that head injury may increase the risk of ALS (H. Chen et al., 2007).

1.5 Macroscopic pathology of TBI

The majority of moderate to severe TBIs in the civilian population are caused by falls, road traffic accidents, physical assault, or other exposure to mechanical forces (Frieden et al., 2015; James et al., 2019; Schuchat et al., 2017) and often involve biomechanical rotational acceleration forces being applied to the parenchyma causing shearing forces to the axons within the brain (Meaney et al., 1995; C. Werner & Engelhard, 2007). The variety in cause of injury is reflected in the heterogeneity of primary pathology observed following TBI; contusions, haemorrhage, brain swelling, and ischaemia being commonly observed pathology (Graham & Luntos, 2002; Johnson et al., 2017). TBI pathologies are often divided into “focal” and “diffuse” injury. “Focal” describing localised pathology such as intracerebral and intracranial haemorrhage and cerebral contusions, and “diffuse” used to describe more widespread pathologies including diffuse axonal injury (DAI) brain swelling, ischaemia and vascular injury (Graham and Luntos, 2002). Secondary pathology may follow immediately from injury, with development of physiological and biomolecular alterations, including disturbance in neuroinflammatory homeostasis and the breakdown of the axonal cytoskeleton (Hay et al., 2016). In late stages after TBI, a wide variety of pathological changes have been

observed including cortical atrophy, ventricular enlargement, cavum and fenestrated septum pellucidum, thinning of the corpus callosum, substantia nigra depigmentation, cerebellar scarring and neuronal loss (Bieniek et al., 2021).

1.5.1 Cerebral atrophy

Brain atrophy has frequently been reported from early studies of boxers, (Brandenburg and Hallervorden, 1954; Grahmann and Ule, 1957; Neubuerger et spillaal., 1959; Spillane, 1962), within frontal (Mawdsley & Ferguson, 1963; Neubuerger et al., 1959) and temporal (Areza-Fegyveres et al., 2007; Drachman, 1999) lobes, and the cerebellum (Grahmann & Ule, 1957; D. Williams & Tannenberg, 1996). Examination of non-boxer athletes demonstrates a mild degree of global atrophy, thinning of the corpus callosum and overall reduction in brain weight (McKee et al., 2013, 2009; Omalu et al., 2011, 2006; Bennet I Omalu et al., 2010; Bennet I. Omaluet al., 2010) and widespread brain atrophy is observed across survival periods following moderate or severe sTBI in both imaging and autopsy studies (Ariza et al., 2006; Cole et al., 2018; Farbota et al., 2012; Ng et al., 2008; Ross, 2011; Ross et al., 2012; Tate & Bigler, 2000; Tomaiuolo et al., 2004; Warner et al., 2010) (**Figure 1-2**). MRI demonstrates increased hippocampal atrophy following moderate to severe sTBI, correlated to both injury severity and cognitive deficits such as verbal and general memory (Ariza et al., 2006; Tate & Bigler, 2000). Furthermore, thinning of the corpus callosum has been shown *in vivo* in MRI studies (Henry-Feugeas et al., 2000; Levin et al., 1990), and is also demonstrated to persist chronically in examination of autopsy tissue taken from sTBI patients with over 1-year survival after injury (Johnson et al., 2013; D. Smith et al., 2013a).

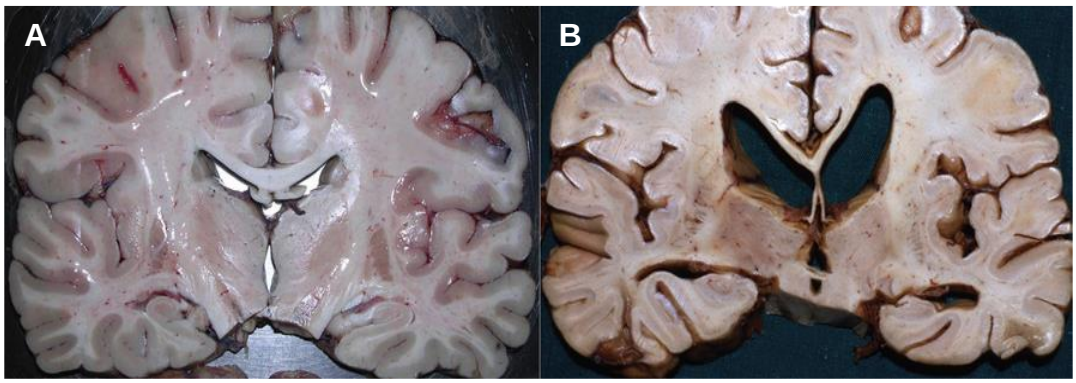

Figure 1-2 Representative images of macroscopic pathology after survival from a single, moderate to severe TBI. (A) brain of 24-year-old who died within hours of an assault. (B) Brain of a 40-year-old patient who survived 4 years following an injury showing notable gyral atrophy, ventricular enlargement, and a thinned corpus callosum. (Smith, et al.,2013).

1.5.2 Cavum septum and ventricular enlargement

In most descriptions of CTE in boxers (Corsellis et al., 1973; Mawdsley & Ferguson, 1963; Nowak et al., 2009; Payne, 1968; Saing et al., 2012; D. Smith, 2013) and other non-boxer athletes (McKee et al., 2009; D. Smith et al., 2019; Stanwell et al., 2022; Stewart et al., 2016), abnormalities of the septum pellucidum are commonly described, one review noting its presence in 65% of cases examined (D. Smith et al., 2013a). Cavum septum pellucidum (CSP), when an opening forms within the leaflet separating two ventricles of the brain, may be accompanied by septal fenestration with detachment from the fornix or corpus callosum potentially due to mechanical strain during trauma (J. H. Adams et al., 1982, 1989; Geddes et al., 1997; Johnson, Stewart, Begbie, et al., 2013) or changes in intracranial pressure (Mawdsley & Ferguson, 1963). CSP is observed in autopsy studies of those exposed to rTBI (Gardner et al., 2014; Grahmann & Ule, 1957; Mawdsley & Ferguson, 1963; McKee et al., 2009; Neubuerger et al., 1959; Nowak et al., 2009; Omalu et al., 2006, 2011; Omalu, Fitzsimmons, et al., 2010; Omalu, Hamilton, et al., 2010; A. H. Roberts, 1969; G. Roberts et al., 1990; Saing et al., 2012; Spillane, 1962; D. Williams & Tannenberg, 1996). *In* vivo radiological studies of boxers with neuropsychiatric symptoms have also demonstrated CSP (Casson et al., 1984; Jordan et al., 1992; Mawdsley & Ferguson, 1963; D. Smith et al., 2019). Interestingly, CSP is absent as a feature of survival following sTBI (D. Smith, 2013) and its diagnostic

value remains uncertain as it is noted in up to a third of the healthy population (Corsellis et al., 1973).

1.5.3 Microscopic pathology of late TBI

The pathology of survival from TBI is often described as a polypathology due to the fact that there is such a wide range of associated pathologies including multiple proteinopathies, neuroinflammation, white matter degeneration neuronal loss and blood-brain barrier (BBB) disruption. Among the most widely observed pathologies are proteinopathies such tau and amyloid-beta (Aß) abnormalities, both of which are hallmark histological markers for a wide array of other neurodegenerative diseases.

1.5.4 Tau

The mechanical forces exerted in TBI result in the breakdown of axonal microtubules leading to disruption of axonal transport and DAI, with liberation of the microtubule-associated protein tau, its subsequent phosphorylation and formulation of neuropil threads and neurofibrillary tangles (NFTs – **Figure 1-3**). Accumulation of hyperphosphorylated NFTs is another observed change in ageing (Braskie et al., 2010; Pontecorvo et al., 2019; Schöll et al., 2016) and a diagnostic hallmark of AD (Braak H; Braak E, 2000), where it follows a characteristic pattern of staging throughout anatomical regions within the brain.

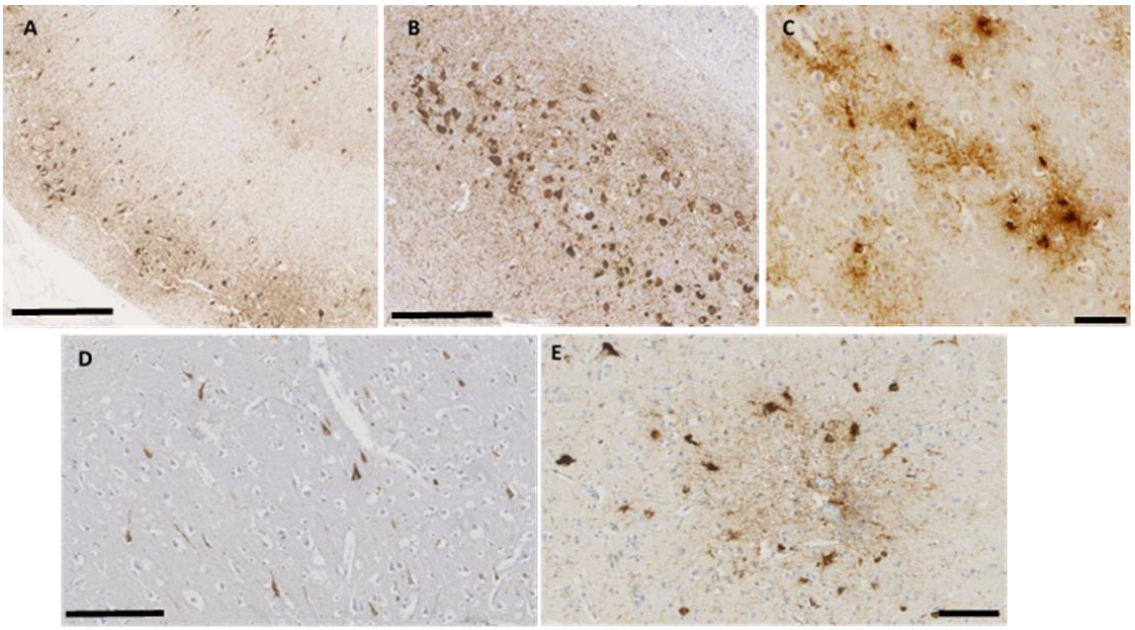

Figure 1-34 Representative images of immunohistological staining of tau pathology.
(A) Bands of NFT and fibrillar tau pathology in the entorhinal cortex of an 87-year-old woman with no history of TBI or neurodegenerative disease (Scale bar 500 µm). (**B**) Pick's bodies in the CA1 region of the hippocampal formation in a 76-year-old woman with no history of TBI or neurodegenerative disease (Scale bar 250µm). (**C**) NFTs and TSA concentrated at the depths of cortical sulcus in tissue from a former American football player (Scale bar 100 µm). (**D**) NFTs in the fusiform gyrus of a 48-year-old man who dies 3 years following a fall (Scale bar 250 µm). (**E**) NFTs and TSA concentrated at the depths of cortical sulcus in tissue from a patient who survived many years following a severe sTBI (Scale bar 100 µm). (Images C and E, Arena et al 2020).

Interestingly, examination of post-mortem tissue taken from patients who survived up to 4 weeks after injury demonstrated no increase in the levels of hyperphosphorylated tau (p-tau) NFTs in the acute period (C. Smith, 2013). However, NFTs and neuropil threads have been observed in 30% patients aged under 60 years of age, who survive 1 year or longer following single, moderate or severe TBI (D. Smith et al., 2013a) and in CTE. Indeed, CTE is commonly descried as a tauopathy (Höglinger et al., 2018; Kovacs, 2018; A. McKee et al., 2009; Orr et al., 2017). For CTE, the pathognomic lesion is defined as neuronal tau deposition, with or without accompanying p-tau immunoreactive astrocytes – thorn-shaped astrocytes (TSA), at the depths of cortical sulci, in a characteristic patchy involvement (Bieniek et al., 2021). There may also be typical involvement of superficial neocortical layers and sector CA2 of the hippocampal formation (Arena et al., 2020; Goldfinger et al., 2018)

1.5.5 Amyloid-beta

Accumulation of amyloid-ß (Aß) is a hallmark AD pathology, where progressive deposition of Aß is considered contributory to the disease (Ittner & Götz, 2011; Selkoe & Hardy, 2016; Sisodia & Price, 1995). Early disease is characterised by diffuse plaques of Aß peptides (Behrouz et al., 1991; Dickson & Vickers, 2001; Malek-Ahmadi et al., 2016; Morris, Storandt, McKeel, et al., 1996) before progressing to neuritic plaques once the clinical stage of AD has been reached (Mirra et al., 1991) (**Figure 1-4**). Normal ageing also demonstrates the accumulation of Aß peptides, where diffuse plaques are observed in non-cognitively impaired individuals (Malek-Ahmadi et al., 2016; Morris, Storandt, McKeel, et al., 1996; Teissier et al., 2020a). Accumulation of ß-amyloid precursor protein (APP) within axonal swellings is observable within hours of injury (Gentleman et al., 1993; Graham et al., 1995; V. Johnson et al., 2012; Sherriff et al., 1994). Further, accumulation of Aß in swollen axons shortly after TBI has been observed in post-mortem tissue (Smith et al., 2003) as well as intra-axonal accumulation of Aß (X. H. Chen et al., 2004) in long-term survivors of moderate or severe TBI. Enzymes such as presenilin-1 (PS-1) and ß-site APP cleaving enzyme-1 (BACE1) required for Aß cleavage are known to accumulate at the site of axonal injury following TBI (X. H. Chen et al., 2009; Uryu et al., 2007) and it is hypothesized that this cleavage of APP and break down of damaged axons may result in aggregation of Aß-peptides which go on to form Aß plaques (X. H. Chen et al., 2004; D. Smith, 1999), with one study demonstrating rapid formation of Aß-oligomer and protofibrils in patients surviving acutely following severe TBI (Abu Hamdeh, Waara, et al., 2018). The accumulation of elevated levels of APP within damaged axons and neurons after TBI may or may not play a contributing role in furthering TBI pathology, with some animal model studies suggesting a neuroprotective role for APP following TBI, where APP metabolite soluble peptide APPß (sAPPα) provides several neuroprotective functions (Corrigan et al., 2012; Hefter & Draguhn, 2017; Plummer et al., 2016; Thornton et al., 2006).

Aß plaques have been shown to occur in up to 30% of patients dying in the acute period following moderate to severe injury (Graham et al., 1995; Hong et al., 2014; Roberts et al., 1994, 1991, 1990; Smith et al., 2003) and in excised

contusional tissue from TBI patients (DeKosky et al., 2007; Ikonomovic et al., 2004). Aß plaques found in these early periods following injury have a diffuse appearance, similar to those observed in normal ageing and in the early stages of AD. In contrast, plaques seen in patients who survive many years after moderate to severe TBI resemble those observed in the clinical stages of AD, with a more neuritic appearance (Johnson et al., 2010, 2012). The development of these plaques may not solely be due to accumulation of APP but also due to failures in the clearance processes which would typically remove Aß. One such degrading enzyme is neprilysin, which degrades both monomeric and oligomeric forms of Aß (Kanemitsu et al., 2003) and is implicated in post-TBI Aß metabolism as it has been shown to accumulate in macrophages and microglia in the acute survivors of TBI specifically in cases with lower levels of Aß plaque formation (X. H. Chen et al., 2009).

Early on, Aß emerged as an important finding in individuals exposed to rTBI (G. Roberts et al., 1990) where in examination of tissue from patients who had experienced multiple rTBI, 95% of cases demonstrated diffuse Aß plaque, and accelerated deposition is also observed in animal models of rTBI (Conte et al., 2004; Uryu et al., 2007). However, conflicting reports question the universal nature of Aß deposition with some studies identifying it in only 44% of cases (A. McKee et al., 2013) while others identify accelerated Aß deposition in CTE patients independent of normal ageing (Stein et al., 2015) suggesting further work is required to breakdown the relationship between Aß plaque formation following TBI.

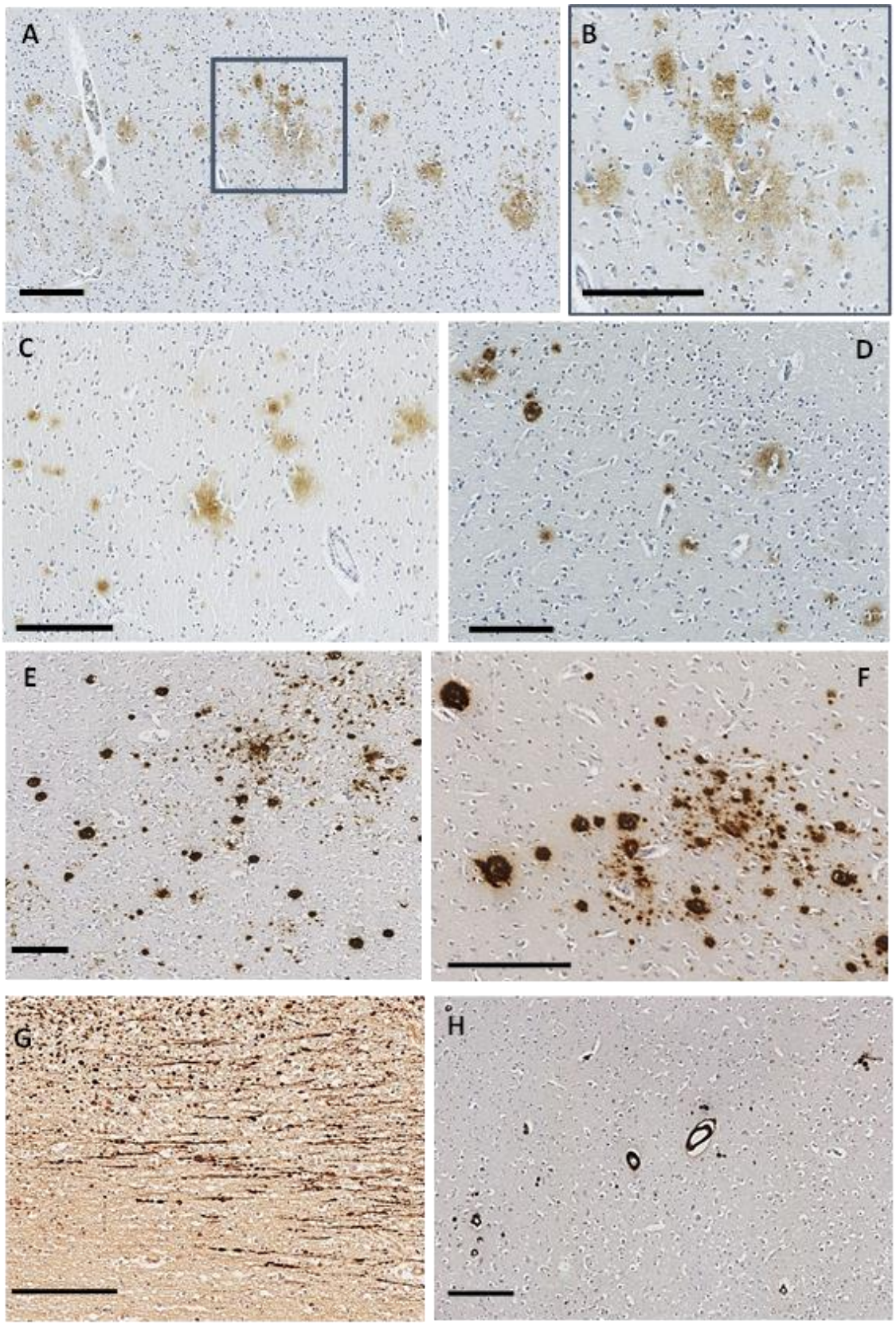

Figure 1-4 Representative images of Amyloid-ß (Aß) pathology: (A & B) Diffuse Aß plaque in the cingulate gyrus of a 76-year-old male with no history of TBI or NDD. (C) Diffuse Aß plaque in the cingulate gyrus of a 50-year-old male who dies 11 days following a fall. (D) Neuritic and diffuse Aß plaque in the insula cortex of a 47-year-old female who died 11 years after a fall. (E) Neuritic Aß plaque in the cingulate gyrus of a 79-year-old male, former rugby player. (F) Neuritic Aß plaque in the hippocampal entorhinal cortex of a 74-year-old male, with a diagnosis of AD. (G) APP-immunoreactive varicosities and axonal bulb formation in the corpus callosum of an 18-year-old male who survived 11 hours following a fall. (H) Cerebral amyloid angiopathy in a 49-year-old male who survived 12 months following an assault. Scale bars 250µm.

1.5.6 Diffuse axonal injury and white matter degeneration

Diffuse axonal injury (DAI) is one of the most common consequences of TBI across all severities (J. H. Adams et al., 1982, 1989; Graham et al., 1988; Johnson, Stewart, & Smith, 2013; Povlishock, 1992; Povlishock & Katz, 2005; D. Smith, 2016; D. Smith & Meaney, 2000). Mechanical loading through rapid head acceleration initiates a cascade of damage to axons, disruption of axonal transport, swelling of axons and generation of axonal bulbs with secondary axotomy through Wallerian degeneration (Maxwell et al., 2015; D. Smith & Meaney, 2000). Axonal pathology may also persist many years following injury, instigating a long-term neurodegenerative process of Aß protein Alzheimer's-like pathologies in both the acute and long-term phases after injury (Chen et al., 2009, 2004; Johnson et al., 2010; Smith et al., 2003; Smith, 1999). Diffusion MRI (dMRI) studies demonstrate that DAI is a strong predictor of post-traumatic neurodegeneration, improving prognostic accuracy and in identifying those at greatest neurodegenerative risk (Graham et al., 2020).

Ongoing axonal pathology has been shown to persist for years after injury in both animal models (X. H. Chen et al., 2004; Pierce et al., 1996) and in human studies (X. H. Chen et al., 2009) of TBI. This persistent axonal pathology is demonstrated through marked thinning of the corpus callosum, with a 25% reduction in corpus callosum thickness in individuals surviving more than 1 year after moderate-severe sTBI (Johnson, et al., 2013). Limited research has been carried out to investigate the prevalence of white matter degeneration following repeated mTBI, but the current literature of largely retrospective cohort studies indicates that white mater degeneration is a common comorbidity in CTE (Corsellis et al., 1973; A. McKee et al., 2013), where career length is associated with more severe white matter rarefication in a study of former NFL players (Alosco et al., 2019). Animal models of rTBI suggest that long-term white matter disruption may be observed through diffusion tensor imaging (DTI) and transmission electron microscopy (TEM) up to 60 days after controlled cortical impact (CCI) (Donovan et al., 2014) and human tau (hTau) mice exposed to a CCI model of mild rTBI develop chronic axonal injury and corpus callosum thinning paired with impaired visuospatial memory (Mouzon et al., 2019), however no increase in tau pathology. These studies suggest that

axonal damage may play a significant role in the neuropathological events developing after both sTBI and rTBI.

1.5.7 TDP-43

Another proteinopathy associated with TBI and various neurodegenerative diseases involves 43kDa TAR-DNA binding protein (TDP-43), which is usually located within the nucleus of cells throughout the body, but in a diseased state can translocate to the cytoplasm and form polyubiquinated and hyperphosphorylated inclusions (Geser et al., 2009; Hay et al., 2016). Highly associated with neurodegenerative conditions such as ALS and frontotemporal lobular dementia (FTLD) (Chen-Plotkin et al., 2010; Geser et al., 2009; Neumann et al., 2006, 2007) but changes are also observed following TBI. In both acute and long-term survivors of sTBI, an increase in levels of cytoplasmic phosphorylation-independent TDP-43 has been observed compared to uninjured control cases. However, no increase in pathological, phosphorylated TDP-43 was observed (Johnson et al., 2011). This contrasts with observations made of cases of rTBI, where an increase in the presence of abnormal cytoplasmic TDP-43 is observed in a similar distribution to that of FTLD throughout the hippocampus, temporal neocortex and amygdala and extending to the spinal cord (King et al., 2010; A. McKee et al., 2010, 2013).

1.5.8 α-synuclein

The neuronal protein α-synuclein is involved in the regulation of synaptic vesicle trafficking and subsequent neurotransmitter release but aggregates to form insoluble fibrils within neurons, or Lewy bodies in neurodegenerative diseases (NDD) such as PD, DLB and multiple system atrophy (Braak H; Braak E, 2000; Lücking & Brice, 2000; Mezey et al., 1998; Spillantini et al., 1997; Stefanis, 2012), characteristically within the substantia nigra (SN) of the brainstem (Ulusoy & Di Monte, 2013). A single study has demonstrated α-synuclein deposited in axonal swellings in 2 cases of acute survival from TBI (Newell et al., 1999). A CCI model of long-term survival of TBI suggests α-synuclein as a link between the chronic effects of TBI and PD symptoms such

as extrapyramidal motor features, where there is overexpression of α-synuclein within the SN of rats exposed to TBI (Acosta et al., 2015). Elsewhere, examination of cerebrospinal fluid (CSF) of patients admitted for severe TBI showed substantial increase in levels of CSF α-synuclein in patients who died compared to those who survived at 6 months post-injury, indicating the possibility of α-synuclein as a prognostic marker for TBI (Mondello et al., 2013).

1.5.9 Neuronal loss and substanita nigra pathology

In autopsy studies, material from patients exposed to rTBI, neuronal loss is described in most cases of CTE, including both boxer and non-boxer individuals (Corsellis et al., 1973; Grahmann & Ule, 1957; Hof et al., 1992; Neubuerger et al., 1959; Nowak et al., 2009; Omalu et al., 2005, 2006, 2011; Omalu, Fitzsimmons, et al., 2010; Omalu, Hamilton, et al., 2010; Schmidt. et al., 2001), with neuronal dropout across the cerebral cortex and sometimes localised in areas of the neocortex, the SN, locus coeruleus and cerebellum. The degree of loss has been described as “patchy” to widespread and diffuse (D. Smith, 2013). Within the SN, there may be reduction in pigmentation, tau NFTs and neuronal dropout microscopically. Interestingly, although Parkinsonian symptoms are commonly observed in individuals with CTE (Royal College of Physicians of London. Committee on Boxing, 1969; D. Smith, 2013), the characteristic synuclein-associated Lewy Bodies of Parkinson’s are less frequently reported in CTE (Brandenburg & Hallervorden, 1954; Corsellis et al., 1973; Drachman, 1999; Neubuerger et al., 1959; Omalu et al., 2005, 2006).

With regards to sTBI, both acute and chronic loss of neurons has been examined, with a marked generalised loss observed in the acute phase found, perhaps unsurprisingly, in association with other pathologies including traumatic axonal injury, inflammation, and ischaemic injury (Maxwell et al., 2003; Shaw et al., 2001). This loss of neurons is believed to continue beyond the immediate acute phase in patients who suffer moderate-severe injury, with active degeneration observed in hippocampal and thalamic regions in patients surviving more than 1 year after injury (Maxwell et al., 2003, 2006; S. Williams et al., 2001).

1.5.10 Blood-brain barrier pathology

Blood-brain barrier (BBB) disruption occurs as an early event in neurodegenerative diseases such as multiple sclerosis (Kirk 2003) and AD, as well as ageing, where it is believed to contribute to disease progression through impaired Aß clearance (Bell & Zlokovic, 2009; Grammas et al., 2011; Montagne et al., 2015; Zlokovic, 2008; Zlokovic et al., 2010). Animal models of TBI demonstrate that BBB disruption occurs in the minutes and hours following injury (Baldwin et al., 1996; Baskaya et al., 1997). In humans, acute permeability of the BBB is demonstrated through increased levels of markers such as S100ß and serum albumin in the CSF following severe sTBI (Blyth et al., 2009; Saw et al., 2014; Stahel et al., 2000), with an association between injury severity and outcome (Ho et al., 2014) and imaging studies also provide evidence of BBB disruption following both mild to severe sTBI (Tomkins et al., 2011) and rTBI patients (Leaston et al., 2021; Weissberg et al., 2014). Post-mortem evidence of widespread BBB disruption has been observed after single moderate to severe TBI in the initial acute phase but also persisting in a high proportion of later survivors (J. Hay et al., 2015).

1.5.11 Neuroinflammation

Neuroinflammation is increasingly viewed as a central aspect in the neuropathological response to both neurodegenerative disease, such as AD (Kwon 2020), and TBI. Chronic traumatic neuroinflammation may be the most important cause of post-traumatic neurodegeneration in terms of prevalence (Faden & Loane, 2015a) and may present a key target for anti-inflammatory treatment options following TBI. With both an internal, innate, and external, adaptive immune system to protect against threats, the brain is well equipped to deal with the wide range of pathologies which may develop following injury, however it is also believed to contribute to the development of persistent pathology (Burda et al., 2017; Faden & Loane, 2015b; Morganti-Kossmann et al., 2019; D. W. Simon et al., 2017).

1.5.11.1 Adaptive immune response

The cellular adaptive immune system engages in the development and progression of several neurodegenerative diseases such as AD (Bryson & Lynch, 2016; McManus et al., 2015; Mittal et al., 2019), ALS (Graves et al., 2004; Kawamata et al., 1992; Troost et al., 1989) and multiple sclerosis (MS) (Dendrou et al., 2015; Fletcher et al., 2010; Hemmer et al., 2015; Nylander & Hafler, 2012). However, relatively little is understood about the involvement of the adaptive cellular response to brain injury.

In the healthy central nervous system (CNS), circulating peripheral immune cells pass through the BBB- to surveil the brain and spinal cord, with low levels of T- and B-lymphocytes found within the brain (Loeffler et al., 2011). Studies show BBB disruption occurs acutely following injury and may remain so for months and years following injury (J. Hay et al., 2015; Tomkins et al., 2011) and it is thought that a simultaneous inflow of peripheral adaptive immune cells follows. Infiltration of circulating immune cells is observed within hours of injury in studies using rat models of TBI where BBB disruption contributed to entry of cells into the brain parenchyma (Holmin et al., 1995; Holmin & Mathiesen, 1999; Soares et al., 1995; Stahel et al., 2000). Examination of biopsies taken from surgically removed contusional TBI tissue has shown CD4- and CD8-positive T-cells within the parenchyma (Holmin et al., 1998), in conjunction with infiltration of leucocytes and reactive microglia, however more research is required to understand what the cellular adaptive immune response is diffusely across the brain and not just in excised contusional tissue.

1.5.11.2 Microglia

The innate immune system of the CNS plays a heterogeneous role, with both neuroprotective and damaging to external stimuli (Hickman et al., 2018; Laird et al., 2008; Myer et al., 2006; Perry et al., 2010; Song & Colonna, 2018) with activation of resident microglia (Johnson, Stewart, Begbie, et al., 2013; Loane & Byrnes, 2010; Ziebell & Morganti-Kossmann, 2010) resulting in morphological changes to these microglia, which express a range of inflammatory mediators

that contribute to neuroinflammatory pathways (Gentleman et al., 2004; Loane and Byrnes, 2010; Morganti-Kossmann et al., 2002, 1999; Rodney et al., 2018; Thelin et al., 2017; Ziebell and Morganti-Kossmann, 2010). Microglia may enter an altered state, from the "resting", dendritic, ramified cells which are their quiescent, surveillance state, to an activated, ameboid state (Hay, 2018; Walker et al., 2014), where cells are more densely packed and demonstrate shortened, cellular processes, and more closely resemble their blood-borne counterparts (Johnson et al., 2013).

These morphological changes occur within minutes of TBI with microglia proliferating rapidly and releasing inflammatory mediators such as nitric oxide (NO), cytokines, and reactive oxidative substances (ROS) (Ii et al., 1996; Johnson et al., 2013; Qin et al., 2002). Once activated, microglia enter a pro-inflammatory state where they may initiate neuronal damage either through recognition of pro-inflammatory stimuli such as lipopolysaccharide (LPS) and monocyte chemoattractant protein 1 (MCP1), or through exposure to neuronal damage (Block & Hong, 2005; Conductier et al., 2010; Liddelow et al., 2017). However, microglia may also play a beneficial role, demonstrated where trials of immunosuppressive treatments following TBI, such as corticosteroids, results in less favourable recovery and even increased mortality at 6 months following injury (Bergold, 2016; Edwards, et al., 2005; Russo & McGavern, 2016).

Microglial activation can also persist for many years following single, moderate, or severe TBI correlating with damage to white matter tracts, with ongoing axonal degeneration and tissue atrophy (Johnson, Stewart, Begbie, et al., 2013). However, whilst neuroinflammation has been implicated in the pathogenesis of CTE (Cherry et al., 2016, 2020; Collins-Praino & Corrigan, 2017), understanding of the role played by microglia in the development of neurodegenerative change following rTBI is still lacking.

1.5.11.3 Astrocytes

Astrocytes are specialised glial cells which make up a substantial proportion of the cells within the parenchyma of the brain (Laird et al., 2008). They exert

multiple complex supportive roles within the CNS, maintaining cellular homeostasis of ion, water and blood flow via their contribution to tight junctions within the BBB (Abbott, 2005; Abbott et al., 1992; Cabezas et al., 2014; Hayashi et al., 1997), whilst also acting as key regulators of provision of metabolic substrates and regulation of oxidative balance within the brain (Bouzier-Sore et al., 2002; Pellerin et al., 2007; Vasile et al., 2017). Additionally, astrocytes have a central role in the innate immune system. Reactive astrogliosis is recognised as a potential driver of neurodegenerative disease such as AD (Beach et al., 1989; Beach & Mcgeer, 1988; Blasko & Grubeck-Loebenstein, 2003; Itagaki et al., 1989; Oberstein et al., 2015; Perez-Nievas & Serrano-Pozo, 2018), where disease progression is influenced by a cytokine cascade (Griffin et al., 1998), Braak staging (Simpson et al., 2010). Cognitive performance (Kashon et al., 2004) is also coupled with increased expression of glial fibrillary acidic protein (GFAP) – the prototypic protein expressed in reactive astrocytes. Astrocytes are also believed to be a key responder to TBI, initiating and mediating the neuroinflammatory response to injury (Burda et al., 2016; Karve et al., 2016; Laird et al., 2008).

During reactive astrogliosis, astrocytes rapidly proliferate and undergo morphological transformation, changing from individually zoned cells with fine processes, to overlapping, hypertrophied cells with intertwined processes (Sofroniew, 2009, 2015; Zhou et al., 2019). As with microglia, astroglia are heterogeneous in nature, providing both neuroprotective and detrimental effects in health and disease (Bardehle et al., 2013; Laird et al., 2008; Myer et al., 2006; Pekny et al., 2014; Sirko et al., 2015). Therefore, astrogliosis is an essential response to injury, creating a protective barrier around inflamed tissue as it recovers, preventing propagation of the neuroinflammatory processes (Sofroniew, 2009; H. Wang et al., 2018) and providing a homeostatic buffer within the brain. However, a chronic astrocytic response may contribute to late neurodegenerative disease (D'Ambrosi & Apolloni, 2020; Vasile et al., 2017) through production of immunomodulatory modulators such as matrix-metallopeptidase 9 (MMP-9), tumour necrosis factor-α (TNF-α) and cyclooxygenase-2 (COX-2) (Akiyama et al., 2000; Burda & Sofroniew, 2017; Chung, 1990; Habbas et al., 2015; Hsieh et al., 2012; Kamat et al., 2014; Sofroniew, 2013, 2015; Sofroniew & Vinters, 2010; Teismann et al., 2003) which

interact with surrounding glia, neurons and astrocytes, so expanding the neuroinflammatory response .

An integral component of the BBB, astrocytic end foot processes, participate in ionic, amino acid and water homeostasis within the brain (Abbott et al., 2006). Aquaporin 4 (AQP4) is the major, bidirectional water channel in the brain (Nielsen et al., 1996; Rash et al., 1998; Venero et al., 2001) and has a polarized location within the astrocytic foot processes, highlighting the role of AQP4 and astrocytes in water transport between the parenchyma of the brain and the blood (Aoki-Yoshino et al., 2005; Papadopoulos et al., 2004; Papadopoulos & Verkman, 2007). Examination of a small cohort of AD cases demonstrating colocalization of cerebral amyloid angiopathy (CAA) and AQP4 (Hoshi et al., 2012) suggests a link between a breakdown in amyloid clearance and activated astrocytes/BBB disruption (Fukuda & Badaut, 2012). Interestingly, AQP4-knockout mice developed increased deposition of Aß fibrillar plaques, intraneuronal Aß and a decrease in GFAP expression in astrocytes closest to Aß plaques (A. Smith et al., 2019), suggesting an additional protective role for astrocytes arounds plaques in AD. Disruption to the BBB in TBI may occur through both mechanical forces and through vasogenic oedema, where the basal lamina of the BBB is degraded by pro-inflammatory cytokines such as matrix metalloproteinases (MMPs) (Candelario-Jalil et al., 2009). The effects on AQP4 expression and distribution in animal models of TBI are conflicting. CCI models demonstrate both an increase (Sun et al., 2003) and a decrease in AQP4 expression in the acute period following injury (Blixt et al., 2015). In contrast, in a closed skull, ‘hit and run’ model of injury loss of characteristic AQP4 localization was reported within the astrocytic end-feet for both mild and moderate TBI, which increased up to 7 days post-injury, continuing into the weeks after (Ren et al., 2013). This was despite a short term rise in intracranial pressure (ICP) and oedema, suggesting AQP4 reorganisation as a general feature within reactive astrocytes, which may not be driving oedema, but acting to return levels to normal.

In humans, examination of contusional tissue taken from 6 patients within 72 hours of injury with cerebral oedema, demonstrated co-expression of aquaporin 1 (AQP1), AQP4 and vascular endothelial growth factor (VEGF) in proximity to cerebral blood vessels (Suzuki et al., 2006). Also, a study of

patients who survived up to 30 days following severe TBI, demonstrated upregulation in AQP4 expression in those who survived 7-30 days post-injury compared to those surviving only hours and uninjured controls, paired with a higher expression of GFAP and a trend to increased oedema in those surviving more than 14 days after injury (Neri et al., 2018), suggesting a link between activation of astrocytic aquaporin channels and reduction in oedema following injury.

The interactions between the roles played by astrocytes in the response to inflammation and injury may well contribute further to the progression of neurodegeneration, where for example, oxidative stress has been found to contribute to water permeability of the BBB through AQP4 upregulation (Chongshan et al., 2017). Oxidative stress can be instigated through a simple imbalance of reactive oxygen species (ROS) and antioxidants (Halliwell, 2012, 1992; Ray et al., 2012), resulting in dysregulation of the inflammatory response (Rivas-Arancibia et al., 2009; Solleiro-Villavicencio & Rivas-Arancibia, 2018). It is a key factor in progression of neurodegenerative disease such as AD (X. Chen et al., 2012; G. H. Kim et al., 2015; Zhao & Zhao, 2013; Zhu et al., 2005) , where it has been found to alter cell signalling, inducing Aß and tau toxicity in APP/PS1 transgenic mice (Giraldo et al., 2014) and also contributing to production of Aß through upregulation of BACE1 expression (L. Chen et al., 2008). ROS have also been long associated with neurodegeneration in ageing (Beal, 1995; Mecocci et al., 2018; Urano et al., 1998; Williams, 1995), where accumulation of ROS has been observed in the ageing brain (Grimm & Eckert, 2017; López-Otín et al., 2013; Mecocci et al., 1993). As the main supportive cell of the CNS, astrocytes are deeply involved in the regulation of oxidative stress; a potential source of excessive ROS through mitochondrial impairment (Grimm & Eckert, 2017; Jackson & Robinson, 2018), which may then promote astrogliosis and glial scar formation (Sofroniew, 2009).

Astrocytes also protect the brain through endogenous antioxidant systems such as the Nrf2-keap1-ARE antioxidative pathway (Chen et al., 2020; Zgorzynska et al., 2021). Nrf2 is a transcription factor which is activated in response to oxidative stress, producing antioxidant enzymes such as Heme oxygenase-1 (HO-1) and NAD(P)H quinone dehydrogenase 1 (NQO1). NQO1 is upregulated in

neurodegenerative disease (Liddell, 2017; Raina et al., 2013; Vargas & Johnson, 2017; Y. Wang et al., 2000) where it is expressed in astroglial and endothelial cells in the substantia nigra pars compacta of PD patients (Van Muiswinkel et al., 2004) and colocalises closely in astrocytes and neurites surrounding senile plaques in AD (SantaCruz et al., 2004). Nrf2-ARE pathways were upregulated in the brain of rats following CCI (Y. Hong et al., 2010), with an increase in NQO1 and HO-1 mRNA levels (Yan et al., 2008), while astrocyte activation was suppressed by activation of this pathway through administration of the antioxidant compound tert-butylhydroquinone (TBHQ) (Z. W. Zhang et al., 2020), highlighting the neuroprotective role upregulation of this enzyme plays in relation to TBI. Proteomic analysis of fresh frozen tissue from individuals diagnosed with CTE revealed increased enrichment of NQO1, in correlation with CTE pathology staging, with NQO1 immunoreactive cells also positive for GFAP and colocalized with hyperphosphorylated tau (Cherry et al., 2018) suggesting a further role for astrocytes in the neuroinflammatory response to TBI.

Acute elevation in levels of GFAP in the CSF of both amateur and professional boxers who have experienced rTBI have been reported, with evidence this might persist in the recovery period (Hansson et al., 2006; Metting et al., 2012; Neselius et al., 2012; Zetterberg et al., 2013), highlighting the potential of GFAP as a biomarker for tracking astrogliosis following rTBI. A study, examining GFAP-immunoreactive astrocytes in post-mortem tissue from a small cohort of blast-related injuries showed reactive astrocytes and astroglial scarring at the grey-white matter interface, at the subpial glial plate and in the perivascular parenchyma, which was not observed in cases with no history of impact TBI or substance abuse (Shively et al., 2016). Interestingly, Shively et al (2016) did not observe a similar pattern of pathology in individuals exposed to sTBI; however, this study was limited by small cohort size.

1.6 Hypotheses and aims

Whilst it is understood that TBI represents a major environmental risk factor for later development of neurodegenerative disease, current understanding highlights the diversity in pathophysiological mechanisms and pathologies emerging following TBI. In particular, the neuroinflammatory response to injury presents a potential late driver of progressive neurodegeneration which remains poorly understood in human TBI.

Table 1-1 Hypotheses and aims

Hypothesis	Background Summary	Aims
sTBI results in acute and long-lasting influx of adaptive immune cells	The innate neuroinflammatory response is recognised in both the acute and chronic phase after TBI and the adaptive cellular response is known to contribute to recovery and neurodegeneration in conditions such as MS. But little is understood of the adaptive cellular response to TBI	To characterise the pattern and timeframe of the adaptive immune cell response across a variety of survival time points after TBI
sTBI and rTBI result in an increase in reactive astrogliosis associated with increase in expression of the relevant markers GFAO, APQ4 and NQO1	Astrocytes perform a number of supportive roles within the parenchyma that are then disrupted following TBI. Reactive astrogliosis can be both a major driver of neurodegeneration but also work to protect the brain.	To characterise astroglial response to injury in cohorts of both sTBI and rTBI, across survival timeframes and the association with GFAP, AQP4 and NQO1 expression
In aged individuals, sTBI results in an acute Aß plaque deposition but no increase in hyperphosphorylated tau	Neurodegeneration is known to occur with age, but TBI is particularly problematic in older adults, with increased severity of injury and worse outcomes. Further research is needed to better understand the connection between age and neuropathological change from TBI	To characterise Aß and tau pathology in an aged population of individuals
Identification of peptides is possible from across TBI and NND cohorts from FFPE archival tissue	FF tissue has been successfully used to identify unique markers of disease from TBI and NND studies, but FFPE tissue is largely left unused due to issues with protein extraction and peptide identification. A successful protocol will allow us to utilise enormous archives of human tissue.	To generate a protocol for the successful identification of a proteome from archival tissue

Chapter 2 - General materials and methods

2.1 Ethical approval for use and source of human tissue

Human brain tissue used in the following studies was selected from the Glasgow Traumatic Brain Injury Archive located in the department of Neuropathology at the Queen Elizabeth University Hospital, Glasgow, UK. The Glasgow TBI archive consists of over 2000 cases of moderate to severe TBI, as well as uninjured control cases, material from former contact sports participants exposed to repetitive mild TBI and tissue from individuals diagnosed with Alzheimer's Disease. All cases held in the archive have accompanying post-mortem reports available, supplemented by corresponding forensic and clinical records. The Archive dataset, therefore, contains information on patient demographics, clinical data, and neuropathological findings from the original post-mortem. All procedures were undertaken in accordance with approval granted by the South Glasgow and Clyde Research Ethics Committee (Project ID 225271) and the Greater Glasgow and Clyde Bio-repository Governance Committee (Application number 340) (**Appendix 1**).

2.2 Studies using post-mortem tissue

Tissue was available for use as formalin-fixed, paraffin embedded blocks which were obtained at routine diagnostic post-mortem autopsy. Whole brains were immersed in a 10% formalin saline solution for a minimum of 2 weeks. Dissection was then undertaken using a standardised block selection protocol, with blocks processed to paraffin using standardised techniques. Upon addition to the Glasgow TBI Archive, each case was anonymised with no patient-identifying information available to the researcher.

Cases used in studies of single TBI (sTBI) had a confirmed diagnosis of moderate to severe TBI based on the neuropathological and clinical diagnosis stated in the post-mortem report. For the purpose of this thesis, acute survival was defined as survival less than 2 weeks after injury, and long-term survival as

those patients surviving a year or more from injury. Cases used in studies of sports participants were exposed to repetitive mild TBI (rTBI) through involvement in rugby, football, or boxing based on patient history acquired from family members.

The age range of all TBI cases selected for inclusion in studies ranged 9 to 89 years old. Where studies focused on TBI in an elderly cohort, elderly was defined as cases aged 60 or over. Age-matched, uninjured controls were identified as individuals with no known history of TBI or neurological disease. Demographic data including post-mortem (PM) delay, sex, cause of injury and cause of death for cases in each study are provided in **Appendix 2**.

2.3 Tissues preparation and immunohistochemistry

From each tissue block, 8µm-thick sections were cut using a rotary microtome (Thermo Scientific, Loughborough, UK) and mounted onto charged microscope slides. These sections were then placed into an oven set to 37°C for a minimum of 3 days to maximise adherence of tissue, prior to placing in an oven at 60°C for 1 hour to remove excess paraffin. Sections were then deparaffinised through multiple washes in xylene solution (3 x 2 minutes) and rehydrated through sequential washes in 100% methanol (3 x 2 minutes) and 95% methanol (2 x 2 minutes) before finally being placed in running tap water for 5 minutes. Sections were next immersed in 3% hydrogen peroxide (H_2O_2) whilst on a Belly Dancer Agitator (Stovall, Life Science Inc, Greensboro, USA) for 15 minutes to quench endogenous peroxidase activity followed by immersion in dH_2O for 5 minutes.

Antigen retrieval was then performed, which was specific to the optimisation of each antibody. Information regarding antigen retrieval and dilutions for each antibody are provided in **Appendix 3**. Where the formic acid protocol for antigen retrieval was required, sections were placed into 98% formic acid (VWR Chemicals, Fontenay-sous-Bois, FR) for 5 minutes and then into running water for a further 5 minutes. Utilising the heat/pressure method, slides were immersed in preheated Tris EDTA buffer or sodium citrate buffer in a

microwave pressure cooker and heated for 8 minutes on high power. Tris EDTA buffer was prepared using 3.7g of laboratory grade ethylenediaminetetraacetic acid (EDTA) and 5.5g of Tris base (Sigma-Aldrich, Gillingham, UK) in 10 litres of dH_2O to pH 8.0. Sodium citrate buffer was prepared using 29.4g of tri-sodium citrate dihydrate in 10 litres of dH_2O to pH 6.0.

To ensure even distribution of heat, the same number of slides were placed in the pressure cooker on each run of antigen retrieval and the seal pin on the pressure cooker was observed to pop at 3 minutes into each run, to guarantee that the sections were immersed in boiling buffer solution for exactly 5 minutes. The lid of the pressure cooker was then carefully removed, and the sections left to cool in buffer for 10 minutes, followed by a staged introduction to cold water to slowly decrease slide temperature back to ambient. Once cooled, sections were placed into 10x phosphate buffered saline/Tween 20 buffer for 5 minutes and then blocked for 30 minutes using 50µl horse serum blocking agent (Vector Labs, Burlingame, CA, UK) per 5ml Optimax buffer (Biogenex, San Ramon, CA, USA). Phosphate buffered saline (PBS)/Tween 20 (0.1M PBS, 0.5%Tween 20) was made up using 54.5g of sodium phosphate dibasic, 16g of sodium phosphate monobasic, 450g of sodium chloride added to 5L of dH_2O to pH7.4, with 25ml of Tween 20.

Each primary antibody was diluted in Optimax buffer (BioGenex, San Ramon, CA. See specific antibody dilutions in **Appendix 3**) and applied to the sections for 20 hours at 4°C. After incubation with the primary antibody, sections went through 3 washes in PBS/Tween solution for 10 minutes under agitation on a Belly Dancer. Biotinylated secondary antibody (100µl horse serum and 100µl secondary antibody per 5ml Optimax buffer - Universal Elite Kit, Vector Labs, Burlingame, CA, USA) was then applied to the sections for 30 minutes at room temperature, after which sections underwent 3 x 10 minutes washes under agitation in PBS/Tween. An avidin/biotin horseradish peroxidase (HRP) complex (100µl Avidin DH solution and 100µl biotinylated enzyme per 5ml Optimax buffer - Universal Elite Kit, Vector Labs, Burlingame, CA, USA) was subsequently applied to the sections for 30 minutes at room temperature, followed by another set of 3x 10-minute washes under agitation with PBS/Tween.

For visualisation, 3,3'-diaminobenzidine (DAB) HRP substrate kit (Vector Labs, Burlingame, CA, USA) was used (84µl buffer stock, 100µl DAB stock and 80µl H_2O_2 per 5ml dH_2O, as per manufacturers instruction). The sections were then rinsed in dH_2O for 5 minutes before being counterstained by immersion in Mayer's haematoxylin for approximately 1 minute, rinsed in dH_2O again before being 'blued' in Scott's Tap Water Substitute for approximately 30 seconds. Slides were then dehydrated in sequential washes of 95% methanol (2 x 2 minutes) and 100% methanol (3 x 2 minutes) before being immersed in multiple washes of xylene (3 x 2 minutes) to clear the sections and then coverslipped using Pertex mounting medium (Histolab, Göteborg, SE). True negative controls were used for each immunostaining run to establish the absence of non-specific binding, with the primary antibody not applied to these sections and only Optimax buffer. Positive controls were also included in each immunostaining run to establish the presence of each specific antibody correctly located in each batch of staining.

All sections were directly viewed using a Leica DMRB light microscope (Leica Microsystems, Wetzlar, DE) and scanned using a 20x objective on a Hamamatsu Nanozoomer 2.0-HT slide scanner (Hamamatsu, Shizuoka, JPN) which has a 0.75NA and scans images at a digital resolution of 0.46µm per pixel. Digitized slide scans were viewed using the SlidePath Digital Image Hub application (Leica Microsystems, UK), NDP.view2 viewing software (Hamamatsu, Shizuoka, JPN) and analysis was undertaken using Fiji ImageJ software (ImageJ, U. S. National Institutes of Health, Bethesda, Maryland, USA) and NDP.view2 with observations blind to all demographic and clinical data for each case.

2.4 Laser capture microdissection

Tissue sections were prepared for laser capture microdissection (LCM)using the same method as stated in section **2.3**, with the use of both formic acid and citrate buffer (pH8.0) antigen retrieval, and the primary antibody selected to reveal amyloid-ß (clone 6F3D; 1:75; Dako, Santa Clara, CA). The exception being that sections were not coverslipped but left to air dry.

Microdissection of Aß plaques was undertaken using the Arcturus® XT system and CapSure® Macro LCM caps (Applied Biosciences, Foster City, California, USA). A stained slide and fresh CapSure® cap cartridge were placed on the device stage, the section scanned, and an overview of the section loaded onto the software. The cap was placed onto the section and the appropriate power, duration, and diameter for the infra-red (IR) laser spot to collect Aß plaques, by testing the spot size, location, and polymer wetting, were correct.

The magnification was set to 10x on the Arcturus® XT system and Aß plaques selected on the designated area of the cap, filling the surface of the cap as much as possible. The IR laser was fired using "IR capture only" mode and targets collected onto the thermo-polymer coating of the CapSure® cap, which was subsequently moved to the QC station to estimate the efficiency of microdissection of desired Aß plaques. The cap was then repositioned onto the section to allow further collection of Aß plaques from a different location on the section, with a minimum of 300 plaques collected per cap. Once the polymer surface of the cap was as covered with as much plaque as possible (approximately 300 plaques), it was moved to the quality control (QC) station again and another cap placed onto the section from the cartridge. Once all 4 slots on the QC station were full the caps were placed into sterile microcentrifuge tubes. The caps were then stored at -80°C until Aß plaque collection was complete.

2.5 Proteomics

2.5.1 Whole tissue section curl collection

From each tissue block, 20µm-thick sections were cut and placed into a sterile 15ml centrifuge tube using sterile disposable forceps until each sample of formalin-fixed, paraffin embedded (FFPE) tissue weighed 0.9g. To ensure a sterile working environment for each case and reduce cross-contamination, fresh gloves, forceps, and microtome blades were used for each case and the workspace thoroughly cleaned using 99% ethanol. Samples were then stored at room temperature.

2.5.2 Dewaxing and deparaffinisation

To each sample, 2ml of xylene was added and incubated with gentle agitation for 5 minutes. The samples were then centrifuged at 5,000 x *g* (Eppendorf 5415D; Hamburg, Germany) for 5 minutes and the excess xylene removed before repeating the process. To each sample, 2ml of absolute ethanol was then added, samples centrifuged at 5000 x *g* for 5 minutes and waste ethanol removed before repeating this process. Each sample was then divided between two sterile 1.5ml microcentrifuge tubes before being placed in a centrifugal vacuum (Thermo Scientific Savant SPD1010 SpeedVac Concentrator; Massachusetts, US) for 30 minutes to dry the tissue. Each tube was then weighed to enable accurate calculation of trypsin dilution required in later steps.

2.5.3 Cell lysis and protease inhibition

The universal protein extraction buffer (UPX - FFPE FASP Kit, Expedeon, San Diego, CA, USA) was then made up with protease inhibitor (Expedeon, San Diego, CA, USA) to obtain a 1x concentration (5mM). Each sample was homogenised with UPX buffer/protease inhibitor solution using a dounce homogenizer and each sample tube covered with Parafilm (M Laboratory, Bemis, Wisconsin, US) whilst incubated at 150°C for 30 minutes with agitation on a (Cole-Palmer, Stuart miniorbital shaker SSM1, Cole-Palmer UK, Cambridgeshire, UK). The samples were then cooled to room temperature and centrifuged at 14,000 x *g* for 15 minutes to separate into lysate and tissue pellet. The lysate for each sample was then collated from the two microcentrifuge tubes, using a pipette to reduce any cellular debris or lipids, and placed in a freezer at -80°C overnight.

2.5.4 Trypsin digestion and filter aided sample preparation (FASP) using FFPE-FASP kit

Once defrosted, samples were spun at 14,000 x *g* for 10 minutes to separate any cellular debris or lipids and 50µl of each sample was aliquoted into a spin filter unit and the remainder of the sample placed into a -80°C freezer. To each sample, 200µl of urea solution (1ml of Tris hydrochloride per tube of urea – FFPE FASP kit, Expedeon, San Diego, CA, USA) was added and the sample spun at 14,000 x *g* for 30 minutes. This was then repeated, and the sample spun for 20 minutes. The flow through from the collection tube was discarded and 90µl of urea solution and 10µl of 10x iodoacetamide (IAA) solution (100µl of urea per black tube of IAA - FFPE FASP kit, Expedeon, San Diego, CA, USA) added to each spin filter which was then incubated in the dark for 20 minutes without agitation. Each spin filter was then spun at 14,000 x *g* for 10 minutes. To each spin filter, 100µl of urea solution was added and all samples were spun at 14,000 x *g* for 15 minutes, this was repeated twice. Subsequently, 100µl of 50mM ammonium bicarbonate (FFPE FASP kit, Expedeon, San Diego, CA, USA) was added to each spin filter which was spun at 14,000 x *g* for 10 minutes, and this process repeated twice. The flow through from each collection tube was then discarded. Trypsin solution was then added to each spin filter (75µl made up to a 1µg trypsin: 100µg protein dilution in 50mM ammonium bicarbonate – Sequencing grade Trypsin, Promega, Madison, WI, US), vortexed for 1 minute and incubated at 37°C for 18 hours with the spin filter wrapped in Parafilm to minimise the effects of evaporation of the digest.

Any sample which had condensed onto the lid of the spin filter was then pipetted back into the spin filter which was then placed into a new collection tube and spun at 14,000 x *g* for 10 minutes. To each spin filter, 50µl of 50mM ammonium bicarbonate was added and the samples spun at 14,000 x *g* for 10 minutes before 50µl of acetyl nitrile was added and the sample spun again at 14,000 x *g* for 10 minutes. Lastly, 1µl of trifluoroacetic acid (TFA – Sigma Aldrich, St Louis, MI, US) was added to the collection tube and vortexed to produce the final protein digest.

To prepare the sample for liquid chromatography-mass spectrometry (LCMS), 100µl of the sample was then placed into a multiwell liquid chromatography-mass spectrometry tray and transferred to the centrifugal vacuum dryer to dry before repeating this process to utilise all the protein digest sample.

2.5.5 Nanoflow HPLC electrospray tandem mass spectrometry (nLC-ESI-MS/MS)

Dry peptides residues were solubilized in 20µl 5% acetonitrile with 0.5% formic acid using the auto-sampler of a nanoflow uHPLC (Ultra-High-Performance Liquid Chromatography) system (Thermo Scientific RSLCnano). Online detection of peptide ions was by electrospray ionisation (ESI) mass spectrometry MS/MS with an Orbitrap Elite MS (Thermo Scientific, Massachusetts, US). Ionisation of LC eluent was performed by interfacing the stainless steel nanobore needle with an electrospray voltage of 2.0kV. An injection volume of 5µl of the reconstituted protein digest were desalted and concentrated for 12 min on trap column (0.3 × 5 mm) using a flow rate of 25µl/min with 1% acetonitrile with 0.1% formic acid.

Peptide separation was performed on a Pepmap C18 reversed phase column (75cm × 75µm, particle size 2µm, pore size 100Å, Thermo Scientific) using a solvent gradient at a fixed solvent flow rate of 0.3µl/min for the analytical column inside a thermostat column oven held at a constant 60°C. The solvent composition was: - (a) 0.1% formic acid in water and (b) 0.08% formic acid in 80% acetonitrile 20% water. The solvent gradient was 4% for 12 min, 4 to 60% for 102 min, 60 to 99% for 14 min, held at 99% for 5 min. A further 9 minutes at initial conditions for column re-equilibration was used before the next injection.

2.5.6 Protein identification

The Orbitrap Elite acquired full-scan MS in the range 300 to 2000m/z for a high-resolution precursor scan at 60,000RP (at 400m/z), while simultaneously acquiring up to the top 20 precursors were isolated at 0.7m/z width and subjected to CID fragmentation (35% NCE) in the linear ion trap using rapid scan mode. Singly charged ions are excluded from selection, while selected precursors are added to a dynamic exclusion list for 30s. Protein identifications were assigned using the MaxQuant search engine (v1.6.5.0, Max Plank Institute, DE) to interrogate protein sequences in the UniProt database using human taxonomy (uniprot-proteome_UP000005640_human_22042020). Perseus software (v1.6.1.5, Max Plank Institute, DE) was subsequently used to process results to filter by: site, reverse, contaminants, identification by > 1 peptide, before being grouped into cohorts and filtered so as to only include proteins identified in ≥70% of cases within a cohort.

2.6 Statistical analysis

Statistical analyses were performed using IBM SPSS statistics software (version 27; SPSS Inc., Chicago, Illinois, USA) and R Project (R Foundation for Statistical Computing, AT). The exact details of each test are given in each chapter. Quantitative data of density of immunoreactive B- and T-Lymphocytes (**Chapter 3**) were analysed using Fisher's exact test, two way mixed-model ANOVA, Mann-Whitney U, and Wilcoxon signed-rank tests were used to assess differences between non-parametric data. The Mann-Whitney U Test, Student's t-test were used to assess the differences in GFAP-, AQP4- and NQO-1-immunoreactivity data between and within cohorts where applicable. Pearson's correlation coefficient was used to measure the linear correlation between 2 sets of data (**Chapter 4**). Semi-quantitative data of the presence, severity and distribution of Aß plaques and NFTs were analysed using Pearson's chi-squared test, Mann-Whitney U test and Fisher's exact test, as appropriate, with Cramer's V and partial Eta squared (η_p^2) used to determine effect size (**Chapter 5**). One-way ANOVA tests with Tukey post hoc test, were used to assess the differences in data between and within cohorts where applicable

using IBM SPSS statistics software, while Searchlight in R Project (Cole et al., 2021), generated principal component analyses and Student's t-test to compare protein expression between cohorts. (**Chapter 6**). Effect size was measured using η_p^2; where 0.01 represents small effect size, 0.06 medium effect size, and > 0.14 large effect size. Alternatively, Cohen's d was calculated to determine the effect size and to indicate the standardized difference between two means, where Cohen's d value of 0.2 suggested a small effect, a value of 0.5 suggested a medium effect and a value of 0.8 suggested a large effect. All tests were used to assess differences in scoring and to establish correlations between and within cohorts, and all effects were considered statistically significant when $p < 0.05$.

.

Chapter 3 - Traumatic brain injury is not associated with an adaptive immune cell infiltrate in humans

3.1 Introduction

Traumatic brain injury (TBI) is recognised as a major, potentially modifiable risk factor for neurodegenerative disease, such as Alzheimer's disease (AD) (Collins et al., 2020; Fann et al., 2018; Li et al., 2017; Livingston et al., 2020; LoBue et al., 2018; Nordström & Nordström, 2018; Tolppanen et al., 2017; Washington et al., 2016) and chronic traumatic encephalopathy (CTE), (Edwards et al., 2017; E. Lee et al., 2019; McKee et al., 2009, 2013, 2015; Omalu et al., 2011; D. Smith et al., 2013a, 2019; Zanier et al., 2018), with an estimated 3 to 10% of dementia in the community attributable to TBI (Livingston et al., 2020). However, the biological processes driving an acute, biomechanical injury to a late and progressive neurodegenerative process remain poorly understood. Among the complex of pathologies emerging after TBI, a prominent neuroinflammatory response is recognised which remains detectable to late survival timepoints (Clark. et al., 2019; Loane & Kumar, 2016; Ramlackhansingh et al., 2011; Scott et al., 2015; C. Smith, 2013; Zanier et al., 2015). Although, studies have focused on characterising the innate immune cell response following TBI, there is growing awareness of a potential role for the cellular adaptive immune response in the development and progression of a range of neurodegenerative diseases (NDDs), including AD (Bryson & Lynch, 2016; McManus et al., 2015; Mittal et al., 2019), amyotrophic lateral sclerosis (ALS) (Graves et al., 2004; Kawamata et al., 1992; Troost et al., 1989) and multiple sclerosis (MS) (Dendrou et al., 2015; Fletcher et al., 2010; Hemmer et al., 2015; Nylander & Hafler, 2012). To date, however, the infiltrative peripheral cellular adaptive response to TBI in humans remains largely unknown.

Retrospective cohort studies demonstrate the association between TBI and increased risk of dementia (Graves et al., 1990; Nordström & Nordström, 2018;

O'Meara et al., 1997; Raj et al., 2022; Schofield et al., 1997; Sivanandam & Thakur, 2012; van den Heuvel et al., 2007; H. K. Wang et al., 2012). TBI resulting in loss of consciousness (LOC) is estimated to increase risk of dementia by approximately 50% (Fleminger, 2003), while studies place the relative risk of dementia in individuals who have suffered a moderate-severe TBI (Plassman et al., 2000) or requiring hospitalisation (Guo et al., 2000) as between 2- and 4-fold. However, the impact of TBI-induced pathology is most likely underrepresented, with definitive diagnosis of TBI-induced neuropathological disease, such as CTE, only possible at post-mortem, resulting in the incidence of TBI-related dementia likely to be at greater levels than previously thought (Lye & Shores, 2000).

Evidence from both pre-clinical models and clinical research demonstrates that TBI induces a rapid, complex neuroinflammatory response. By example, animal models of TBI report infiltration of blood-borne, inflammatory cells within hours of injury (Holmin et al., 1995; Soares et al., 1995). In humans, limited evidence shows activation of the innate immune cell response following TBI, with recruitment of resident microglia (Engel et al., 2000; Ramlackhansingh et al., 2011; C. Smith, 2013) and astrocytes (Y. Chen & Swanson, 2003; X. Cheng et al., 2019; Laird et al., 2008) and elevation of serum and cerebrospinal fluid (CSF) proinflammatory cytokines, in turn, associated with patient outcomes (Hayakata et al., 2004; Shiozaki et al., 2005; Singh et al., 2019). While in a majority of instances, this acute phase neuroinflammatory response resolves as the natural evolution of healing and repair, in a proportion of individuals exposed to single moderate or severe TBI, microglial activation persists to late stages, as demonstrated through imaging evidence of continued neuroinflammation (Farbota et al., 2012; Narayana, 2017) and histological evidence of ongoing white matter degradation (Victoria E Johnson et al., 2013; Victoria E. Johnson et al., 2013).

In contrast to the growing understanding of the innate cellular response, little is known about the time course and distribution of the adaptive immune cell response to TBI. Cells of the adaptive immune system are known to periodically surveil the healthy CNS (Becher et al., 2000; Hickey, 1999, 2001), with both CD3+ T-lymphocytes and CD20+ B-lymphocytes found to varying degrees

throughout the healthy brain (Loeffler et al., 2011). Following human spinal cord injury (SCI), blood-borne CD4 and CD8 immunoreactive T-cells cross the blood-brain barrier (BBB) (Dardiotis et al., 2012; J. Hay et al., 2015; Shlosberg et al., 2010; Tomkins et al., 2011) and infiltrate the spinal cord in the days and months after injury, in conjunction with microglial activation (Fleming et al., 2006). Biopsies of human peri-contusional brain tissue taken acutely following severe TBI reveal infiltration of T-cells into brain parenchyma (Holmin et al., 1998), with alteration of peripheral cellular and cytochemical homeostasis in proximity to contusions (Hausmann et al., 1999; Kossmann et al., 1995). However, whilst TBI is thought to stimulate an influx of adaptive immune cells through a damaged BBB, the scale and duration of cellular adaptive immune infiltration following diffuse TBI remains poorly understood. Therefore, here we examine the extent, distribution, and time course of the lymphocytic cellular response to TBI in comparison with age-matched uninjured controls, with the hypothesis that single moderate or severe TBI results in an immediate and long-lasting, diffuse, mixed T- and B-lymphocytic inflammatory response.

Aim: To characterise the pattern and timeframe of the adaptive immune cell response across a variety of survival time points after moderate to severe sTBI.

3.2 Specific methods

3.2.1 Case selection

All material was obtained from the Glasgow TBI Archive of the Department of Neuropathology, Queen Elizabeth University Hospital, Glasgow, UK. Tissue samples were acquired at routine diagnostic autopsy, with approval for their use in research obtained from the Greater Glasgow and Clyde Bio-repository Governance Committee.

From the Glasgow TBI Archive, material from patients aged 60 years or younger at death and exposed to a single, moderate, or severe TBI was selected as acute (survival <2 weeks from injury; mean 79 hours [range 6 hours-10 days]; n=26) or long-term (≥1 year; mean 8.9 years [range 1-47 years]; n=27) TBI survival. Age-matched controls aged 60 years or younger at time of death and with no known history of TBI or neurological disease were selected from the same archive (n=23). Comprehensive diagnostic neuropathological and forensic reports were available for all cases, with all TBI cases fulfilling standard definitions of moderate or severe TBI by Glasgow coma scale. Full clinical and demographic information, including causes of death are listed in **Table 3-1**.

3.2.2 Brain tissue preparation

At autopsy, whole brains were immersion fixed in 10% formal saline for a minimum of 3 weeks and subsequently dissected, sampled following standardised block selection, and processed to paraffin using standard techniques. For this study, paraffin tissue blocks were selected from a coronal slice of the cerebral hemispheres at the level of the lateral geniculate nucleus to include the thalamus and the corpus callosum, with adjacent cingulate gyrus.

Table 3-1 Demographic and clinical information of chapter 3 cohorts

	TBI: Acute Survival (n=26)	TBI: Long-Term Survival (n=27)	Controls (n=23)
Mean age (range), years	42.7 (9-60)	46.5 (19-60)	38.5 (14-60)
Males, n (%)	17 (65)	26 (96)	11 (58)
Mean post-mortem delay (range), hours	55.7 (3-239)	61.9 (3-185)	71 (12-168)
Mean survival interval (range)	79.3 hours (6-240 hours)	8.9 years (1-47 years)	n/a
Cause of TBI, n (%)			
Fall	15 (57.7)	13 (48)	-
RTA	7 (27)	5 (18.5)	-
Assault	3 (11.5)	6 (22)	-
Unknown	1 (3.8)	3 (11)	-
Cause of death, n (%)			
Head injury	24 (92.3)	-	-
Bronchopneumonia	2 (7.7)	3 (11)	-
ARDS	-	1 (3.7)	-
Pulmonary Thromboembolism	-	-	1 (4.3)
Heart disease	-	8 (29.6)	5 (21.7)
Alcohol related	-	2 (7.4)	-
Pyelonephritis	-	1 (3.7)	-
Renal Failure	-	1 (3.7)	-
GI haemorrhage	-	1 (3.7)	-
Polytrauma	-	1 (3.7)	-
Drug overdose	-	-	4 (17.4)
SUDEP	-	7 (26)	7 (30.4)
Pulmonary oedema	-	-	-
Septicaemia	-	-	3 (13)
Inhalation of gastric contents	-	-	2 (8.6)
Acute purulent meningitis	-	1 (3.7)	-
Hepatic encephalopathy	-	1 (3.7)	-
Hypothermia	-	-	1 (4.3)
Unknown	-	-	-
TBI pathologies, n (%)			
Skull fracture	19 (73)	14 (52)	n/a
DAI	9 (34.6)	4 (15)	n/a
Brain swelling	12 (46)	-	n/a
SDH	20 (77)	13 (48)	n/a
EDH	1 (3.8)	1 (3.7)	n/a
SAH	14 (53.8)	1 (3.7)	n/a

ARDS, Acute respiratory stress disorder; DAI, diffuse axonal injury; EDH, extra dural haematoma; GI, gasterointestinal; RTA, road traffic accident; SAH, subarachnoid haematoma; SDH, subdural haematoma; SUDEP, sudden unexplained death in epilepsy

3.2.3 Immunohistochemistry

From each tissue block, 8μm-thick sections were prepared, deparaffinised in xylene, rehydrated to water through decreasing concentrations of demethylated spirit, and then immersed in aqueous solution of 3% hydrogen peroxide (H_2O_2) for 15 minutes to quench endogenous peroxidases. Antigen retrieval via microwave pressure cooker was performed for 8 minutes in preheated 0.1 mol/L citrate buffer with ensuing blocking achieved by applying 50mL of normal horse serum (Vector Laboratories, Peterborough, UK) per 5mL of Optimax buffer (BioGenex, San Ramon, CA) for 30 minutes. Once blocked, overnight incubation with primary antibodies to either CD3 (pan T-lymphocyte marker, monoclonal mouse anti-CD3, clone SP7, 1:100, ThermoFisher Scientific, San Diego, CA) or CD20 (pan B-lymphocyte marker, monoclonal mouse anti-CD20, clone L26, 1:200, Leica Biosystems, Newcastle-upon-Tyne, UK) was performed at 4°C for 20 hours. Following overnight incubation, biotinylated secondary antibody was then applied for 30 minutes (IgG, 1:200), followed by avidin-biotin complex as per the manufacturer's instructions (1:50; Vectastain Universal Elite kit, Vector Laboratories). Lastly, visualisation was achieved using 3,3'-diaminobenzidine (DAB) peroxidase substrate kit (Vector Laboratories) and sections were counterstained with haematoxylin. As controls for antibody specificity, sections from a case with MS and sections with primary antibody omitted were stained in parallel with test sections.

All sections were viewed using a Leica DMRB light microscope (Leica Microsystems, UK) and digitized by scanning at 20x using a Hamamatsu Nanozoomer 2.0-HT slide scanner, with the resultant images viewed via the SlidePath Digital Image Hub application (Leica Microsystems, UK).

3.2.4 Analysis of immunohistochemistry

All observations were performed blind to demographic and clinical information by two independent observers (HM and J Fullerton [postdoctoral research assistant]). Inter-rater reliability for scoring was strong (Cohen's Kappa 0.83). Cases where there was a discrepancy were reviewed by both observers and a

final, consensus score attained. Quantitative assessment of the density of immunoreactive cells was performed using the manual cell count application within the SlidePath Digital Image Hub, with cells defined as immunoreactive profiles with identifiable nuclei. Anatomical regions of interest (ROI) for assessment were selected as: neocortical grey of the cingulate gyrus; corpus callosum from midline to lateral extent; thalamic nuclei; and internal capsule (**Figure 3-1**). Density of immunoreactive profiles within each ROI was expressed as cells per unit area (cells/mm^2). When an ROI had floated in the staining process that section's ROI was excluded for analysis.

3.2.5 Statistical analysis

Data were analysed using IBM SPSS Statistics Software (version 27; SPSS Inc., Chicago, Illinois, USA). Fisher's exact test was used to assess non-random associations between categorical data. Two way mixed-model ANOVA, Mann-Whitney U, and Wilcoxon signed-rank tests were used to assess differences between non-parametric data. Effects were considered significant when $p<0.05$. Cohen's d was calculated to determine the effect size and to indicate the standardized difference between two means. A Cohen's d value of 0.2 suggested a small effect, a value of 0.5 suggested medium effect and a value of 0.8 suggested a large effect. Outliers were identified using SPSS and removed from the dataset where the value was greater than the third quartile added to 1.5 times the interquartile range for data sets in a cohort.

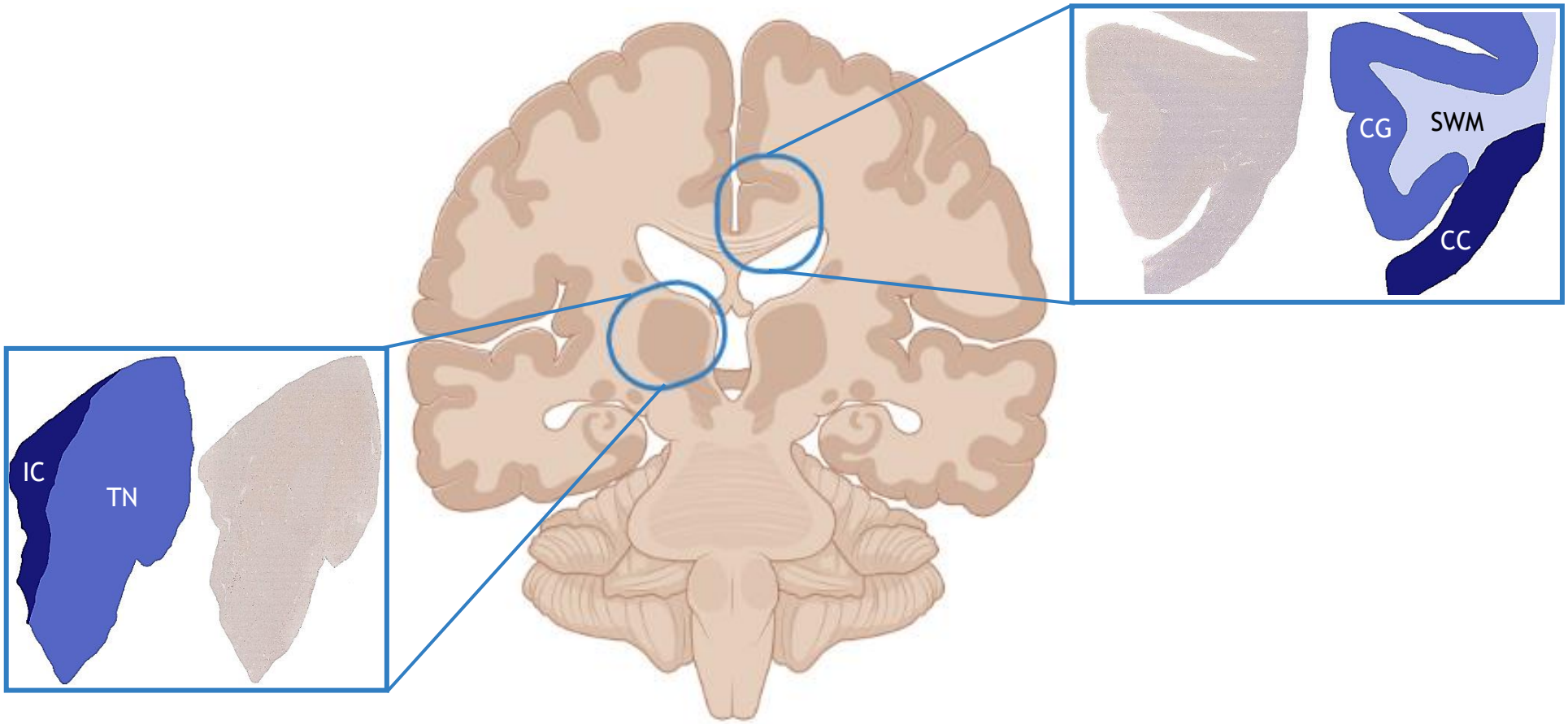

Figure 3-1 Representative images of the regions of interest examined in this study. Cingulate regions consist of the corpus callosum (CC), cingulate gyrus (CG) and superficial white matter (SWM). Thalamic regions were made up of the internal capsule (IC) and thalamic nucleus (TN). Created with BioRender.com.

3.3 Results

3.3.1 No evidence of a CD3-immunoreactive cellular response after TBI

In all 22 uninjured controls, CD3-immunoreactive profiles were present in low numbers in all cingulate and thalamic grey and white matter ROI, located sporadically within the perivascular space and adjacent neuropil (**Figure 3-2**). Similarly, in acute and late survivors of TBI, CD3-immunoreactive profiles were observed in low numbers within both grey and white matter in all ROI; again, localised to the perivascular space and neighbouring neuropil (**Figure 3-2**). Across all groups, CD3-immunoreactive profiles were observed at higher density in white matter than in grey matter ($Z=-1.863$, $p=<0.0001$, Wilcoxon signed-rank test, **Table 3-2A**).

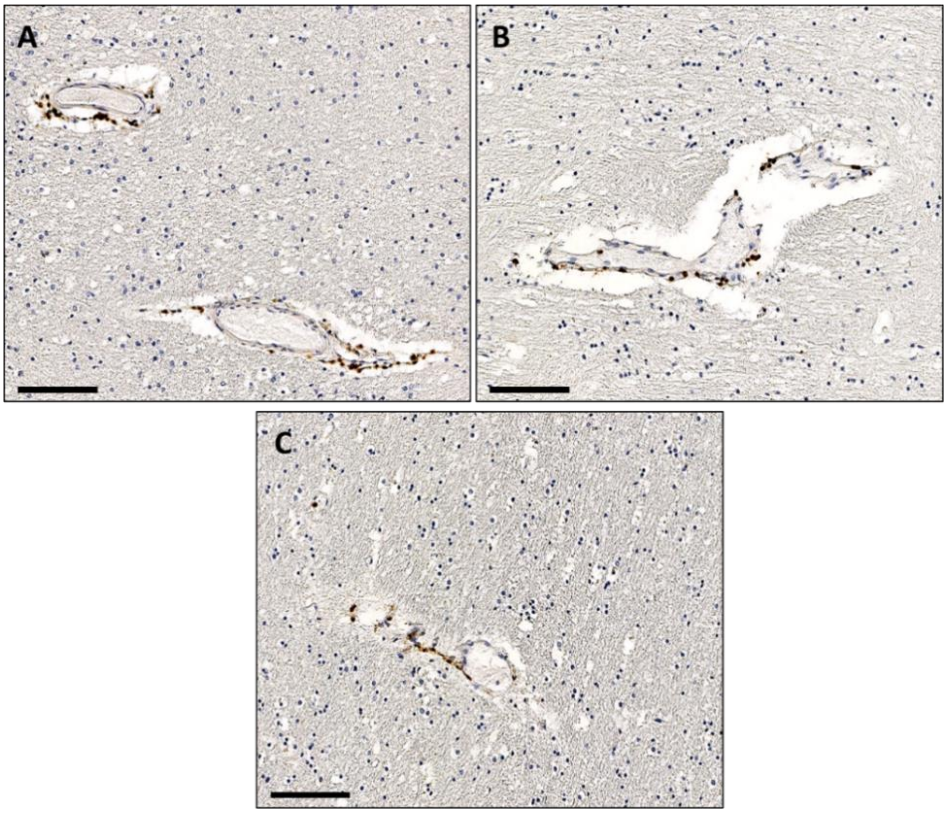

Figure 3-26 Representative images of CD3 immunoreactivity in the subcortical white matter (SWM) after traumatic brain injury and in uninjured controls. Similar CD3-immunoreactive profile density within the SWM of (**A**) an uninjured 46-year-old male, (**B**) a 16-year-old male surviving 7 days after a road traffic accident (RTA), and (**C**) a 52-year-old male who survived 4 years following an assault. In both acute and long-term survivors of a single moderate or severe TBI, CD3-immunoreactive profiles were typically present in a pattern, distribution and density corresponding to that seen in uninjured, controls. Specifically, sparse, perivascular, and occasionally neuropil-located CD3-immunoreactive profiles were present at all time points. Scale bar = 100μm.

Table 3-2 Regional expression of CD3 and CD20 immunoreactive profiles

(A)

CD3 immunoreactive cells/mm²					
	Corpus callosum	**Superficial white matter**	**Internal capsule**	**Cingulate gyrus**	**Thalamic nucleus**
Mean	0.981	1.170	0.880	0.275	0.362
Median	0.816	1.144	0.789	0.185	0.348
SD	0.780	0.800	0.699	0.281	0.268

	White matter	**Grey matter**
Mean	0.985	0.321
Median	0.895	0.308
SD	0.613	0.235
Wilcoxon	p<0.0001	
Cohen's *d*	1.431	

(B)

CD20 immunoreactive cells/mm²					
	Corpus callosum	**Superficial white matter**	**Internal capsule**	**Cingulate gyrus**	**Thalamic nucleus**
Mean	0.014	0.021	0.029	0.011	0.024
Median	0.000	0.013	0.017	0.000	0.014
SD	0.031	0.026	0.040	0.023	0.028

	White matter	**Grey matter**
Mean	0.018	0.022
Median	0.013	0.017
SD	0.021	0.023
Wilcoxon	p<0.0001	
Cohen's *d*	0.182	

There was no increase in prevalence of cases with infiltrating CD3-immunoreactive profiles among acute TBI cases versus age-matched controls (p=1.00, Fisher's test). Specifically, low numbers of CD3-positive profiles were identified across the cingulate ROIs of 22 of 23 assessable acute cases (p=0.510) (**Figure 3-2**) and the thalamic ROIs in all available cases (p=0.520). Similarly, there was no difference in prevalence of late TBI cases with CD3-immunoreactive profiles compared to controls in all ROI examined (p=1.0).

While there was no demonstrable difference in CD3-immunoreactive cell density comparing acute TBI to age-matched controls, CD3-immunoreactive cell density was lower in the cingulate gyrus, internal capsule, and thalamic nuclei among late survivors of TBI when compared to uninjured, age-matched controls (p=0.008 (Cohen's d=0.828), p=0.014 (Cohen's d=0.637) and p=0.02 (Cohen's d=0.464) respectively; Mann-Whitney U test, **Figure 3-3**, **Table 3-3** [supplementary]).

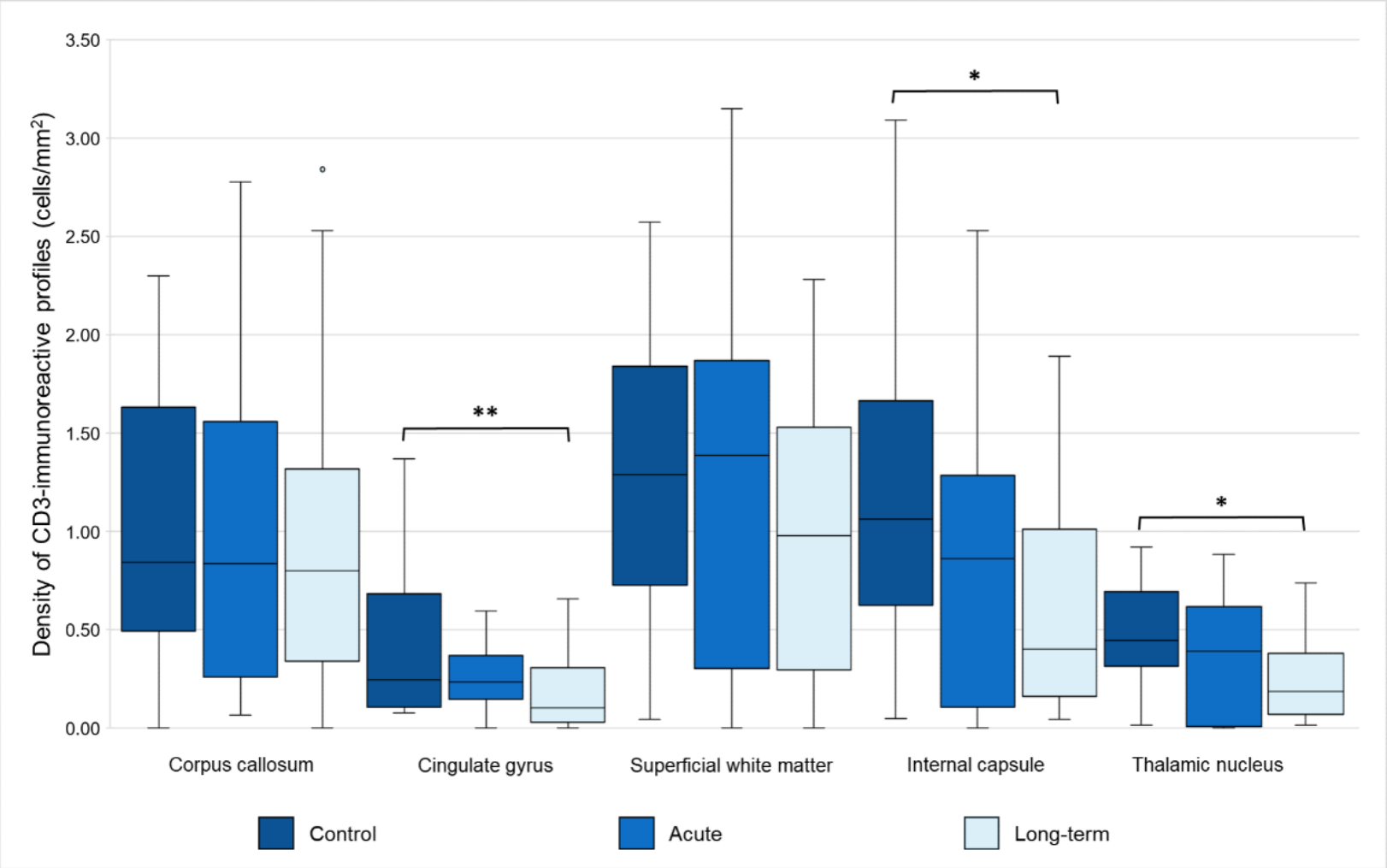

Figure 3-3 Density of CD3-immunoreactive profiles within ROI in acute and late TBI survival compared to uninjured controls. No increase in CD3-immunoreactive T-lymphocytes in any regions across all cohorts examined. A significant decrease in CD3-immunoreactive T-lymphocytes within the cingulate gyrus, internal capsule and thalamic nucleus in long-term survivors compared to uninjured, age-matched controls (* $p < 0.05$, ** $p < 0.01$; Mann-Whitney U test).

3.3.2 No evidence of a CD20-immunoreactive cellular response after TBI

In uninjured controls, CD20-immunoreactive profiles were present within the perivascular space and, sporadically, in the bordering neuropil of the cingulate and thalamic regions in 18 of 22 controls examined. Likewise, CD20-immunoreactive profiles were present in similar prevalence and distribution among cases of acute and late survival following TBI (**Figure 3-4**), with CD20-immunoreactive profiles present in the cingulate ROIs of 21 of 24 acute cases examined (NS, Fisher's exact test) and the thalamic ROIs of 19 of 26 cases assessed (NS). Similarly, long-term survivors of TBI demonstrated sparse CD20-immunoreactive profiles within the perivascular space and adjoining neuropil of in cingulate ROIs of 21 of 26 cases examined (NS; **Figure 3-4**) and thalamic ROIs in 19 of 27 cases analysed (NS).

Overall, CD20 immunoreactive profiles were observed at lower density in white matter ROI than in grey matter ROI ($Z=-1.928$, $p=<0.0001$, Wilcoxon signed-rank test, **Table 3-2B**). There was no measurable difference in density of CD20-immunoreactive profiles therefore between cohorts examined (**Figure 3-5, Table 3-3** [supplementary]).

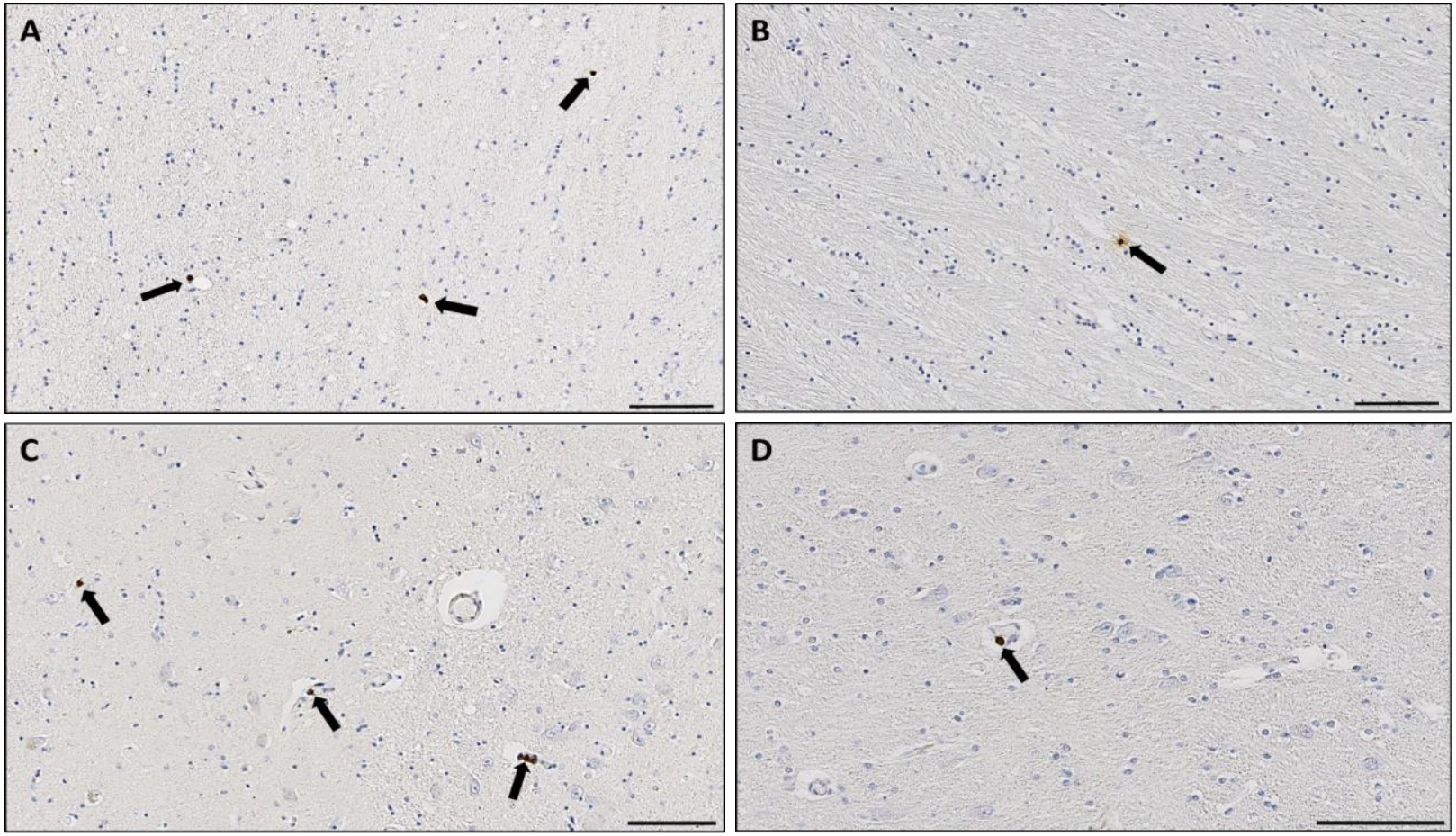

Figure 3-477 Representative images of CD20-immunoreactivity in the internal capsule and thalamic nuclei after TBI and in controls. (**A**) Multiple neuropil CD20-immunoreactive profiles located in the internal capsule of a 60-year-old male with no history of head injury compared to (**B**) a single CD20-immunoreactive profile within the internal capsule of a 19-year-old male who died 5 years following an assault. (**C**) Numerous CD20-immunoreactive profiles in the perivascular space within the thalamic nuclei of a 25-year-old male uninjured control case, in contrast to (**D**) a single perivascular CD20-immunoreactive profile within the thalamic nuclei of a 20-year-old male who died 24 after an assault. In both acute and long-term survivors of moderate to severe TBI, scant CD20-immunoreactive profiles were typically present in a perivascular and periodically neuropil distribution. Scale bars = 100μm.

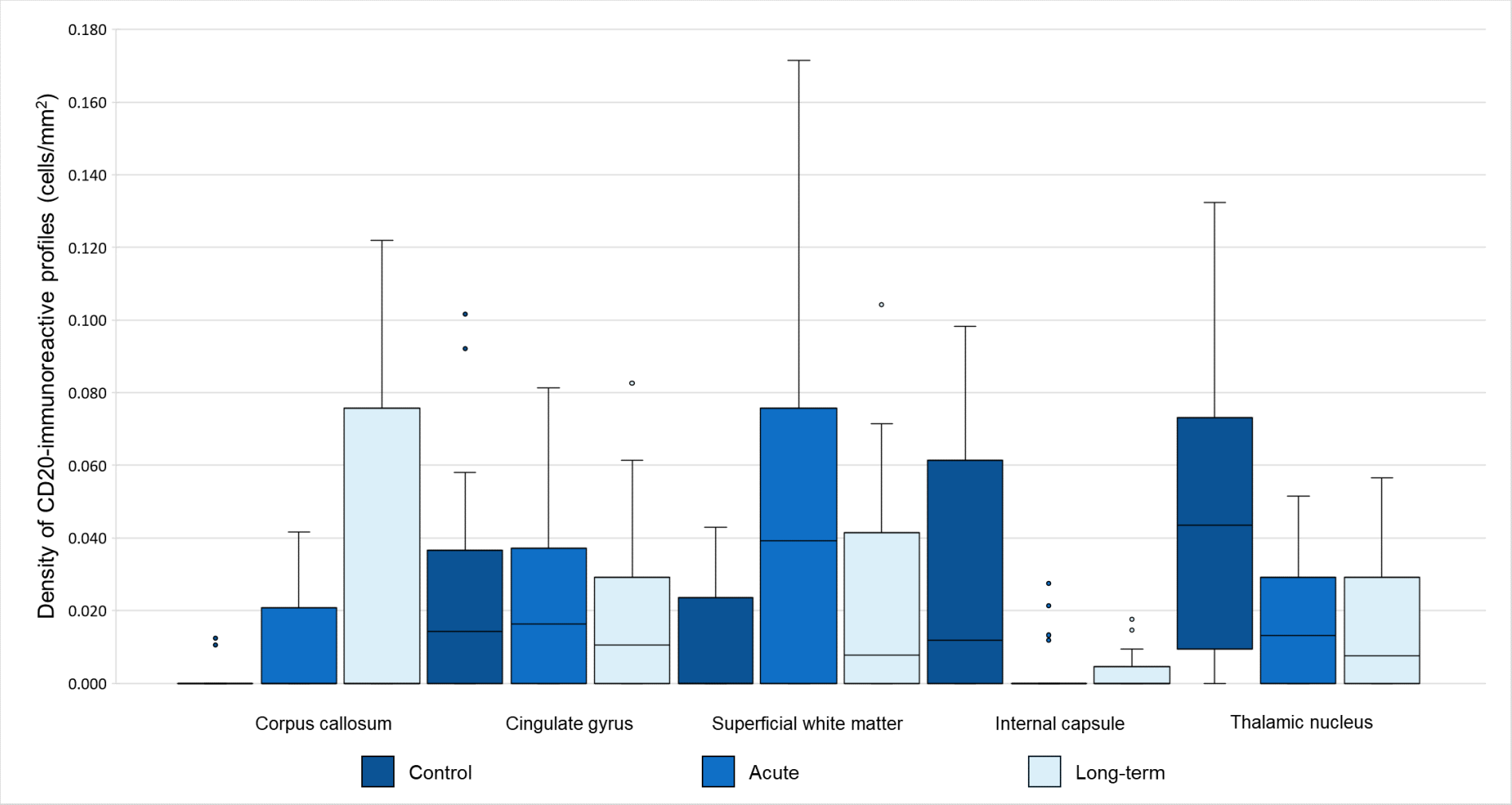

Figure 3-5 Density of CD20-immunoreactive profiles within ROI in acute and late TBI survival compared to uninjured controls. No significant increase in CD20-immunoreactive B-lymphocytes in any regions across all cohorts examined (NS, Mann-Whitney test).

3.4 Discussion

These data demonstrate that, when compared to non-injured, age matched controls there is no histological evidence of a significant cellular response from the adaptive immune system in the brains of patients following a single moderate or severe TBI, with survivals spanning the acute phase to the late timepoints some years after TBI. Specifically, we found no evidence of increased CD3- or CD20-immunoreactive profiles across TBI survival cohorts in any of multiple grey and white matter regions examined. Indeed, paradoxically, we observed decreased CD3-immunoreactive cell density in long-term TBI survivors compared to controls in the cingulate gyrus, thalamic nucleus, and internal capsule.

The central nervous system (CNS) is described as an immunologically privileged environment, uniquely shielded by the BBB, preventing diffusion of inflammatory molecular and cellular components into the neuropil and the spread of infectious agents (Hickey, 2001; Ousman & Kubes, 2012). Constant immune surveillance is carried out by resident microglia, but a healthy BBB is also responsible for the surveillance of the CNS in health, through the passage of low numbers of migrating macrophages, lymphocytes, and monocytes (Hickey, 1999, 2001; Ousman & Kubes, 2012) into the parenchyma, which is heightened when there is a strong immunological stimulus out with the CNS (Hickey & Kimura, 1987). However, the CNS still demonstrates far lower levels of peripheral cell immunological surveillance compared to other organs (Flügel et al., 1999; Yeager et al., 2000) and levels of migration also differ the within the CNS, with the cerebrum demonstrating lower levels of infiltration than the spinal cord (Phillips & Lampson, 1999; Yeager et al., 2000), and CD3 and/or CD20 immunoreactive cells not commonly found in the brains of healthy patients (Bogerts et al., 2017). This is supported by this study, where both CD3- and CD20-immunoreactive profiles were identified in low numbers across cohorts.

However, evidence supports BBB disruption both acutely and in late survival following TBI (J. Hay et al., 2015; Sulhan et al., 2020; Takata et al., 2021; Tomkins et al., 2011). Further, BBB disruption occurs in a variety of neurological conditions such as AD (Bell & Zlokovic, 2009; Zlokovic, 2008, 2011), and MS (Kirk et al., 2003; Leech et al., 2007; Minagar & Alexander, 2003; Ortiz et al., 2014), and is suggested

might contribute to the inflammatory progression of these disease processes. In contrast, the findings in this study, however, do not support the hypothesis that an influx of either CD3- or CD-20- immunoreactive cellular components occurs through a disrupted BBB, either acutely or in the chronic, late-phase after injury. Indeed, paradoxically grey matter regions previously identified as vulnerable to BBB damage (J. Hay et al., 2015) and examined in this study, show a reduction in CD3-immunoreactive profiles in individuals surviving a year or more from single moderate or severe TBI.

In pre-clinical studies, a transient increase in T-cell infiltration is observed after controlled cortical impact (CCI) in rats (Jin et al., 2012), although only a small proportion of infiltrating T-cells cells were directly involved in the inflammatory response within the brain. Further, depletion of mature T- and B-lymphocytes in a murine model of TBI resulted in no reduction in astrogliosis or neuronal death or changes to levels of pro- and anti-inflammatory mediators or cytokines (Weckbach et al., 2012). This indicates that a lack of the adaptive cellular response did not noticeably affect the neuroinflammatory reaction in these animals and aligns with our studying suggesting a limited role for adaptive cells within the brain after injury.

Notably, data from studies of human tissue which do observe an increase in T-cell infiltration utilise surgically resected contusion tissue (Holmin et al., 1998) and cortical contusions (Hausmann et al., 1999); examples of focal, haemorrhagic TBI pathology. In contrast, this study scrutinises a more diffuse tissue response to TBI. Cases within the cohorts examined were known to have suffered from contusional injuries - 81% of acute cases and 96% of long-term cases. However, none of the regions examined contained any contusional damage, as this study aimed to examine the adaptive cellular response remote to focal pathology and in regions of known vulnerability to pathological changes following TBI. Additional studies looking at the cellular response in proximity to constitutional injury may be of merit.

The reduction in CD3-immunoreactive profiles observed across regions examined in this study is not discussed widely in the literature, with spinal cord injury (SCI) studies finding an influx of both T- and B-lymphocytes (Ankeny et al., 2006;

Ankeny & Popovich, 2009), and the increased synthesis of autoantibodies like those seen in MS (Ankeny et al., 2009). Although, a reduced inflammatory response after SCI, possibly induced by the depletion of CD20-immunoreactive B-cells (Casili et al., 2016), highlights the potential immunomodulating importance of the adaptive cell response in CNS injury and the possibility that a lack of lymphocytes within the brain after injury may proffer some form of neuroprotection.

Generation of autoantibodies by the systemic immune system in TBI is recognised to occur within days of injury, manifest as antibodies against glial fibrillary acidic protein (GFAP) and myelin basic protein (MBP) fragments within the serum and cerebral spinal fluid (CSF) samples of patients (Cox et al., 2006; Susie Zoltewicz et al., 2012; K. Wang et al., 2016; Z. Zhang et al., 2014). The possible exposure of peripheral 'memory' immune cells to self-antigens has significance for cases of secondary insult or infection, where repeated disruption to the BBB results in the appearance of post-traumatic syndromes (Nizamutdinov & Shapiro, 2017). Demonstration of MBP auto-reactive T-cells in the periphery after TBI (Cox et al., 2006) may impact understanding of white matter loss and axonal degradation occurring concurrently with chronic inflammation following TBI (Johnson, Stewart, Begbie, et al., 2013). A marked absence of an adaptive cell response, even in regions such as the corpus callosum which are anatomically vulnerable to white matter loss and concurrent chronic innate inflammatory response in late survivors of injury (Victoria E. Johnson et al., 2013; C. Smith, 2013; Tomaiuolo et al., 2004), suggests white matter loss in MS and TBI may follow different pathways.

Data from this study suggest that a cellular lymphocytic response may not play a large role within the brain in the evolution of late TBI neuropathology, unlike that seen in other neurodegenerative diseases such as AD (Bryson & Lynch, 2016; McManus et al., 2015; Mittal et al., 2019), MS (Dendrou et al., 2015; Hafler, 2009) and ALS (Beers et al., 2017; Kawamata et al., 1992; Sheean et al., 2018), and contusional TBI (Hausmann et al., 1999; Holmin et al., 1998). However further studies could go on to examine how the adaptive cellular response may act to alter the homeostatic balance within the CNS after TBI. Modulation of the innate inflammatory cell response to injury may be triggered by changes in circulating pro- and anti-inflammatory cytokines, which are observed widely in both the acute and chronic stages following injury and contributes broadly to secondary damage

(Ferreira et al., 2014; Kumar et al., 2015; Morganti-kossmann et al., 2002; Ziebell & Morganti-Kossmann, 2010). Further peripheral adaptive immune responses, such as antigen processing and presentation by circulating lymphocytes affecting neurodegeneration (Tobin et al., 2014), as well as TBI-induced systemic immunosuppression (Das et al., 2012; Ritzel et al., 2018) poses questions of how TBI may shape and exacerbate these downstream neuroinflammatory responses.

In conclusion, we present data indicating that, following single, moderate to severe TBI, there is no histological evidence of a cellular T- or B-lymphocyte infiltrative response within the brain parenchyma across acute to late survival time points. This demonstrates that the cellular component of the adaptive immune system may not influence the progression of TBI pathology locally, as previously speculated.

Chapter 4 – The astrocytic response to TBI

4.1 Introduction

TBI is a global health concern, associated with high rates of mortality and morbidity (Baguley et al., 2000; Frieden et al., 2015; Heegaard & Biros, 2007; Maas et al., 2008, 2017; Tagliaferri et al., 2006) and has the highest incidence of all common neurological conditions (Maas et al., 2022). For many decades, TBI has also been associated with an increased risk of later development of neurodegenerative disease (NDD) such as Alzheimer's disease (AD) (Fleminger, 2003; Graves et al., 1990; Molgaard et al., 1990) and is now acknowledged as the strongest environmental risk factor for development of numerous NDDs (Collins et al., 2020; Fann et al., 2018; Li et al., 2017; Livingston et al., 2020; LoBue et al., 2018; Maas et al., 2022; Nordström & Nordström, 2018; D. Smith et al., 2013b). However, a complex series of pathologies develop in the hours and months after TBI and there is a need for greater understanding of the driving forces behind this neurodegeneration.

Astrocytes are the most abundant cells within the CNS and act as specialised glial cells, involved in may complex supportive roles such as within the BBB, where astrocytic end foot processes maintain homeostatic balance and blood flow (Abbott, 2005; Abbott et al., 1992; Cabezas et al., 2014; Hayashi et al., 1997). Further to this, they are key supporters of mechanical strains within the brain; where upon exposure to stressors, astrocytes will become reactive and undergo a morphological change where they rapidly proliferate, hypertrophy and their dendrites become more branched, resulting in intertwined cellular processes (X. Cheng et al., 2019; Sofroniew, 2015). This is coupled with an increase in expression of protein markers such as glial fibrillary acidic protein (GFAP). A chronic and more severe astrocytic response can lead to glial scar formation (Burda et al., 2016; D'Ambrosi & Apolloni, 2020; Dossi et al., 2018; Sofroniew, 2009), characterised by over expression of neuroinflammatory modulators and involving glia, neurons and other cells of the parenchyma to form a barrier around tissue lesions. Expression GFAP and hypertrophy of astrocytes observed proximal to Aß plaques (Griffin et al., 1989; Kashon et al., 2004; Simpson et al., 2010) and a correlation between Braak staging and increased GFAP expression is noted in AD

patients (Simpson et al., 2010). Astrocytic endfeet are a key architectural and intercellular signalling element of the BBB, participating in ionic, amino acid and water homeostasis within the brain (Abbott et al., 2006; Ballabh et al., 2004; Heithoff et al., 2021). Aquaporin 4 (AQP4) is the major, bidirectional water channel in the brain, predominantly localised on astrocytic endfeet (Nielsen et al., 1997; Rash et al., 1998; Venero et al., 2001) and has been observed in astrocytes colocalised with cerebral amyloid angiopathy (CAA) in AD patients (Hoshi et al., 2012) and is associated with Aß- clearance in animal models of AD (Iliff et al., 2012; A. Smith et al., 2019).

Neuroinflammation is a central factor in the development of degeneration following TBI, where it has largely been characterised by the microglial response (Hernandez-Ontiveros et al., 2013; Loane et al., 2014; Loane & Byrnes, 2010; Loane & Kumar, 2016; Mannix & Whalen, 2012; Ramlackhansingh et al., 2011; Witcher et al., 2021). Microglia are quickly activated and proliferate within hours of injury (Loane et al., 2014), a process which can continue for weeks and months after injury (Gentleman et al., 2004; Johnson, et al., 2013; Loane et al., 2014). However, astrocytes are also a central factor in initiating and mediating the neuroinflammatory response to TBI (Burda et al., 2016; Karve et al., 2016; Laird et al., 2008). From post-mortem tissue cases of human TBI, regional GFAP-immunoreactive astrogliosis has also been shown to occur at the interface zones of the subpial layer and at grey-white matter junctions in survivors of blast injury (Shively et al., 2016) and localised in the sulcal depths of cases demonstrating p-tau immunoreactivity, in a case of CTE pathology observed after single severe TBI (Shively et al., 2017). This sulcal astrocytic p-tau pathology – ageing-related tau astrogliopathy (ARTAG) is distinct from other tau pathology and a proposed hallmark of CTE (Kovacs et al., 2016; Lace et al., 2012; Lõpez-González et al., 2013; C. McKee & Lukens, 2016).

The BBB is disrupted following injury (Hay et al., 2015) and may be therapeutic targets of both BBB protection and recovery after injury (Michinaga et al., 2021; Michinaga & Koyama, 2019). Malfunction of aquaporin water channels such as AQP4, may play a role in dysregulation of water transport within the CNS after injury due to their involvement in the balance of extracellular fluid osmolarity and extracellular space volume (Nagelhus et al., 2004; Papadopoulos & Verkman,

2007, 2013). Contusional tissue excised following TBI demonstrated co-expression AQP1, AQP4 and vascular endothelial growth factor (VEGF) in proximity to cerebral blood vessels within 72 hours of injury (Suzuki et al., 2006), while survival of up to 30 days elicited an increase in both AQP4 and GFAP paired with increased oedema (Neri et al., 2018) suggesting involvement in astrocytic AQP4 activation and regulation of water content following injury. AQP4 KO mice have demonstrated exacerbated neurofibrillary tau pathology and neurodegeneration in a mouse model of CTE (Iliff et al., 2014), and that clearance of p-tau may be affected by changes in perivascular AQP4 in astrocytes of mice exposed to CCI model of TBI contributing to cognitive decline after TBI (Z. A. Zhao et al., 2017).

Previous studies indicate that the astrogliotic response to injury encompasses many aspects that propagate neurodegeneration, however the roles of astrocytes in progression of TBI pathology, both across time frames and injury type, remains poorly understood. This study aims to examine multiple astrocytic markers to characterise the response to injury across survival periods and TBI sub-cohorts.

Aim: To characterise astroglial response to injury in cohorts of both sTBI and rTBI and across survival timeframes, examining association of GFAP, AQP4 and NQO1 expression.

4.2 Specific methods

4.2.1 Case selection

All tissue was selected from the Glasgow Traumatic Brain Injury Archive of the Department of Neuropathology, Glasgow, UK. All material was obtained following routine diagnostic autopsy examination at the same institution and approved for use in this study by the Greater Glasgow and Clyde Bio-repository Governance Committee.

Material from patients aged 60 years or younger at death and exposed to a single, moderate to severe TBI was selected to include patients who survived acutely following injury (n=20; survival < 2 weeks; mean survival 66 hours [range 11 hours – 11 days]; mean age 44.1 [range 18-60]); patients who survived into the long-term phase after injury (n=20; survival ≥1 year; mean survival 9.3 years [range 1 – 47 years]; mean age 46.9 [range 19-60]); and age-matched control patients who were aged under 60 years or younger at time of death and with no known history of TBI or neurological disease (n=23; mean age 43.7 [range 20-60]). Also selected from the archive was material from patients who were professional sports players (rugby, football or boxing, **Table 4-1**) and who donated their tissue after a diagnosis of neurodegenerative disease in life (n=14, mean age 68.5 [range 28-86]) alongside material from control patients who had no known history of TBI or neurological disease and were individually age-matched to each of the professional sports players (n=14; average age 67.9 [range 26-85]).

Comprehensive diagnostic neuropathological and forensic reports were available for all cases, with all single TBI cases fulfilling standard definitions of moderate or severe TBI by Glasgow Coma Scale. Full clinical and demographic information, including causes of death are listed in **Table 4-1.**

4.2.2 Brain tissue preparation

As stated previously, whole brains were immersion fixed in 10% formal saline at autopsy for a minimum of 3 weeks prior to dissection, sampling following standardised block selection and processing to paraffin using standard techniques. For this study, paraffin tissue blocks from a coronal slice of the cerebral hemispheres at the level of the lateral geniculate nucleus were selected to comprise the medial temporal lobe, including the inferior temporal gyrus and the cingulate gyrus with adjacent corpus callosum.

Table 4-1 Demographic and clinical information of chapter 4 cohorts

	sTBI Controls (n=20)	sTBI Acute Survival (n=20)	sTBI Long-Term Survival (n=20)	rTBI Controls (n=14)	Contact Sports Players (rTBI) (n=14)
Mean age (range), years	43.7 (20-60)	44.1 (18-60)	46.9 (19-60)	67.9 (26-85)	68.5 (28-86)
Males, n (%)	13 (65)	12 (60)	19 (95)	14 (100)	14 (100)
Mean post-mortem delay (range), hou	63.0 (12-168)	45.9 (3-120)	67.0 (3-120)	108.0 (12-552)	166.5 (24-672)
Mean survival interval (range)		92.8 hours (11-264 hours)	9.3 years (1-47 years)		
Cause of sTBI, n (%)					
Fall		8 (40)	9 (45%)		
RTA	N/A	8 (40)	4 (20)	N/A	N/A
Assault	(No History of sTBI)	3 (15)	5 (25)	(No History of sTBI)	(No History of sTBI)
Unknown		1 (5)	2 (10)		
Professional Sport Participation, n (%)					
Football					7 (50)
Rugby	n/a	n/a	n/a	n/a	4 (28.6)
Boxing					2 (14.3)
PE Teacher					1 (7.1)
Cause of death, n (%)					
Head injury	0	18 (90)	0	0	0
AD	0	0	0	0	2 (14.3)
ARDS	0	0	0	0	1 (7.1)
Bronchopneumonia	1 (5)	1 (5)	3 (15)	1 (7.1)	3 (21.4)
Cancer	0	0	0	3 (21.4)	0
Corticobasal degeneration	0	0	0	0	1 (7.1)
Chronic traumatic encephalopathy	0	0	0	0	2 (14.3)
Dementia	0	0	0	0	1 (7.1)

	sTBI Controls (n=20)	sTBI Acute Survival (n=20)	sTBI Long-Term Survival (n=20)	rTBI Controls (n=14)	Contact Sports Players (rTBI) (n=14)
Cause of death, n (%)					
Drug overdose	2 (10)	0	0	0	0
FTLD-Tau (PSP)	0	0	0	0	1 (7.1)
GIT haemorrhage	0	0	1 (5)	0	0
Hanging	0	0	0	1 (7.1)	0
Heart disease	6 (30)	0	8 (40)	4 (28.6)	0
Hypovolemic Shock	1 (5)	0	0	0	0
Inhalation of gastric contents	1 (5)	0	0	2 (14.3)	0
Laceration of liver and rib fractures	0	0	1 (5)	0	0
Liver failure	0	0	1 (5)	0	0
Liver Haemorrhage	1 (5)	0	0	0	0
Myasthenia Gravis	0	0	0	1 (7.1)	0
Myotonic Dystrophy	1 (5)	0	0	0	0
Normal pressure hydrocephalus	0	0	0	0	1 (7.1)
Pulmonary Thromboembolism	1 (5)	0	0	0	0
Renal Failure	0	0	1 (5)	0	0
Septicaemia	1 (5)	1 (5)	0	1 (7.1)	1 (7.1)
SUDEP	4 (20)	0	5 (25)	0	0
Unknown	0	0	0	1 (7.1)	0
Vascular dementia	0	0	0	0	1 (7.1)
TBI pathologies, n (%)					
Skull fracture	0	12 (60)	3 (15)	0	0
Contusions	0	16 (80)	20 (100)	0	0
DAI	0	6 (30)	1 (5)	0	0
Brain swelling	0	11 (55)	1 (5)	0	0

	sTBI Controls (n=20)	sTBI Acute Survival (n=20)	sTBI Long-Term Survival (n=20)	rTBI Controls (n=14)	Contact Sports Players (rTBI) (n=14)
TBI pathologies, n (%)					
SDH	0	14 (70)	6 (30)	0	2 (14.3)
EDH	0	2 (10)	0	0	0
ICH	0	8 (40)	7 (35)	0	0
SAH	0	8 (40)	1 (5)	0	0
Dementia Diagnosis, n (%)					
AD	0	0	0	0	4 (28.5)
Vascular dementia	0	0	0	0	1 (7)
CTE	0	0	0	0	6 (42.3)
Corticobasal degeneration	0	0	0	0	1 (7)
FTLD (PSP)	0	0	0	0	1 (7)
Parkinson's disease	0	0	0	0	1 (7)

AD, Alzheimer's disease; ARDS, acute respiratory distress syndrome; CTE, chronic traumatic encephalopathy; DAI, diffuse axonal injury; EDH, extra dural haematoma; FTLD (PSP), frontotemporal lobar degeneration (progressive supranuclear palsy); FTLD- Tau, frontotemporal lobar degeneration-tau; ICH, intracraniam haematoma; RTA, road traffic accident; SAH, subarachnoid haematoma; SDH, subdural haematoma; SUDEP, sudden unexplained death in epilepsy

4.2.3 Immunohistochemistry

From each tissue block, 8µm-thick sections were prepared for immunohistochemistry. Sections were deparaffinised in xylene, rehydrated to water and then immersed in aqueous solution of 3% hydrogen peroxide for 15 minutes to quench endogenous peroxidases. Antigen retrieval via microwave pressure cooker was performed for 8 minutes in preheated 0.1M tris buffer, followed by blocking in 50□L of normal horse serum (Vector Laboratories, Peterborough, UK) per 5 mL of Optimax buffer (BioGenex, San Ramon, CA) for 30 minutes. Once blocked, overnight incubation with primary antibodies was performed at 4°C for 20 hours.

Primary antibodies were selected to reveal glial fibrillary acidic protein (GFAP; 1:250; clone GA5; Leica Biosystems, Newcastle-upon-Tyne, UK), aquaporin-4 protein (AQP4; 1:200; AB3594; Merck, Darmstadt, Germany) and NAD(P)H quinone oxidoreductase 1 (NQO1; 1:1000; A180; ThermoFisher Scientific, San Diego, CA, US). Following overnight incubation, biotinylated secondary antibody was then applied for 30 minutes (IgG, 1:200), followed by avidin-biotin complex as per the manufacturer's instructions (1:50; Vectastain Universal Elite kit, Vector Laboratories). Visualisation was achieved using 3,3'-diaminobenzidine (DAB) peroxidase substrate kit (Vector Laboratories) followed by counterstaining with haematoxylin. Known positive tissue sections were run in parallel with test sections in all antibody runs in addition to sections with primary antibody omitted as standard controls for antibody specificity.

All sections were viewed using a Leica DMRB light microscope (Leica Microsystems, UK) and digitized by scanning at 20x using a Hamamatsu Nanozoomer 2.0-HT slide scanner (Hamamatsu Photonics, UK), with the resultant images viewed via the SlidePath Digital Image Hub application (Leica Microsystems, UK) and NDP.view 2.0 viewing software (Hamamatsu Photonics, UK).

4.2.4 Analysis of immunohistochemistry

All sections were reviewed and analysed blind to demographic and clinical data and analyses were performed on multiple anatomic regions within each block. Specifically, analyses were performed in the corpus callosum, crest of cingulate gyrus, depth of cingulate sulcus and the subcortical white matter of the cingulate gyrus within the callosal block.

For sections stained for GFAP and AQP4, the extent of astrogliosis was measured using the ruler tool of the Hamamatsu View.2 digital image hub application, at the superficial glia limitans and the boundary between the neocortical grey matter and the superficial white matter (**Figure 4-1**). This was carried out at both the crest of the cingulate gyrus and the depth of the cingulate sulcus. Three measurements were taken for each region of interest, with the average value taken as the datapoint for that section.

Assessment of GFAP immunoreactive astroglial extent was calculated as percentage area of GFAP immunostain. Using Hamamatsu View.2 digital image hub application, the relevant ROI was defined, and area measured, and an exported image uploaded to ImageJ (NIH, Bethesda, MD) where background was subtracted, and the colour Deconvolution plugin applied using the installed haematoxylin/DAB vector (H/DAB) to produce separate colour channels for the haematoxylin counterstain and specific DAB immunostaining. The DAB-specific image was subsequently thresholded and the percentage of positive staining in the ROI calculated using the standardised algorithms in ImageJ.

Sections stained for NQO1, the relevant ROI was defined, and area measured using the Hamamatsu View.2 digital image hub application and then manual cell counts of NQO1-immunoreactive astrocytes performed.

4.2.1 Statistical analysis

All data were analysed using SPSS (Version 27; IBM, Inc). The Mann-Whitney U Test and Student's t-test were used to assess the differences in data between and within cohorts where applicable. Pearson's correlation coefficient was used to measure the linear correlation between 2 sets of data. All effects were significant where $p < 0.05$.

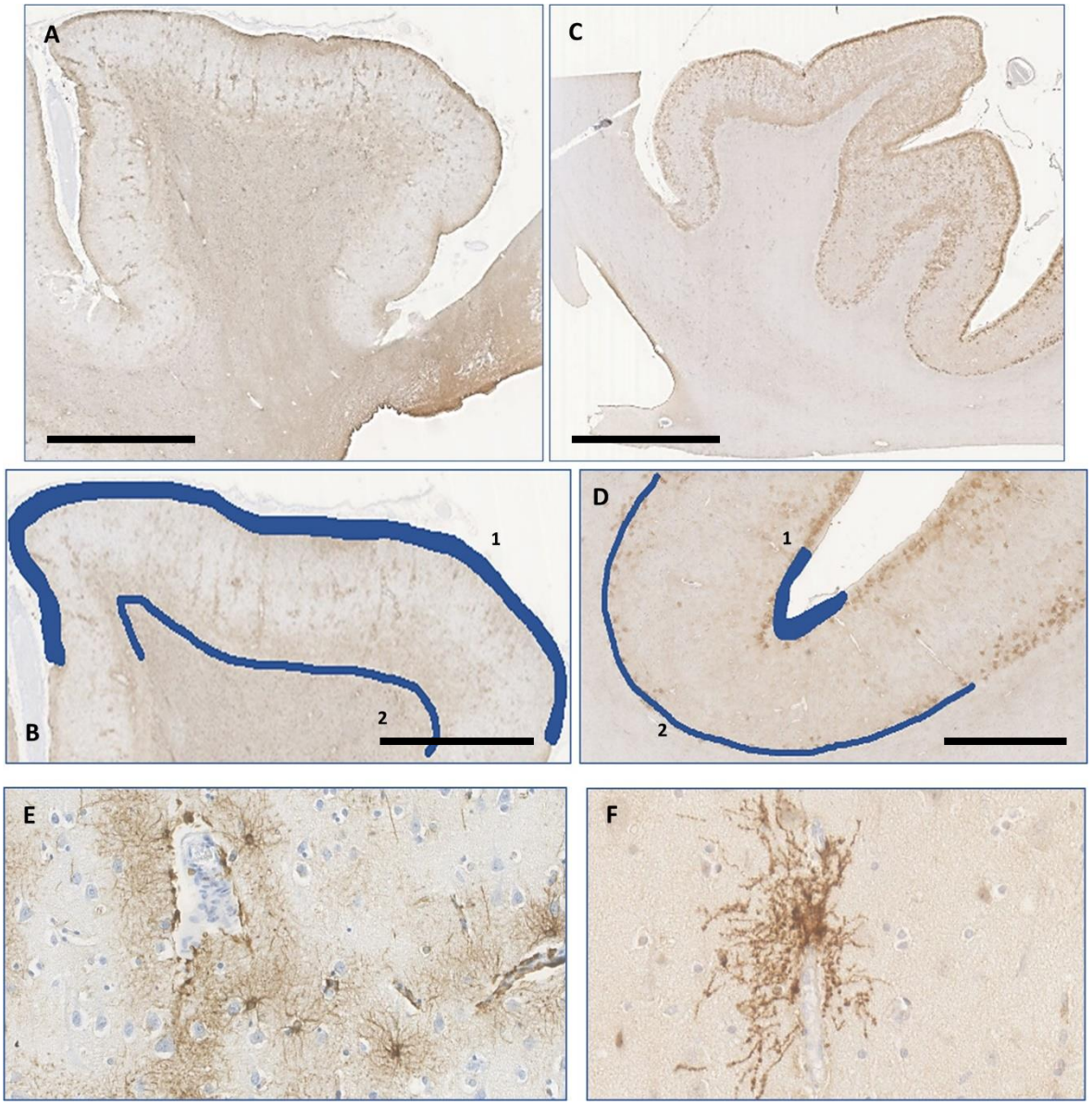

Figure 4-1 **Representative measurements of GFAP and AQP4 interface immunoreactivity.** (**A/B**) Extent of cingulate crest GFAP-immunoreactive astrogliosis at the SGL (**1**) and WMI (**2**) in a 29-year-old male who survived 7.5 years following an assault. (**C/D**) Cingulate sulcus AQP4-immunoreactive astrogliosis at the SGL (**1**) and WMI (**2**) in a 31-year-old female with no history of TBI. (**E**) Perivascular GFAP immunoreactive astrocytes in the cingulate gyrus of a 29-year-old male who survived 7.5 years following an assault. (**F**) Perivascular AQP4-immunoreactive astrocyte in the cingulate gyrus of a 43-year-old female with no history of TBI. Scale bar 5mm, 2.5mm and 250µm respectively.

4.3 Results

4.3.1 Ageing results in an expansion of interface GFAP-immunoreactive profiles

In non-injured sTBI controls, GFAP-immunoreactive astrocytic profiles with fine and widely ramified cellular processes were distributed throughout the cortex, localised around penetrating blood vessels and concentrated at both the superficial glial limitans (SGL), immediately beneath the pia, and the white matter interface (WMI), between subcortical white matter and the overlying neocortical grey (**Figure 4-2**). GFAP-immunoreactive astrocytes were also present within the superficial white matter, again preferentially localised to penetrating blood vessels. Typically, GFAP-immunoreactive astrocytes were distributed as a thin interface band at the SGL and WMI and sporadically throughout the neocortex, with little overlap between individual cell domains (**Figure 4-2**). There was significant correlation between age and extent of GFAP-immunoreactive interface astrogliosis across the entire cohort, at the SGL ($r(81) = 0.28$, $p = 0.02$; Pearson's correlation) and WMI ($r(81) = 0.31$, $p = 0.029$) at the crests of cingulate gyri, and at the WMI at the depths of the cingulate sulci ($r(82) = 0.44$, $p < 0.001$; **Figure 4-3**), but not at the SGL of the cingulate sulcus (NS).

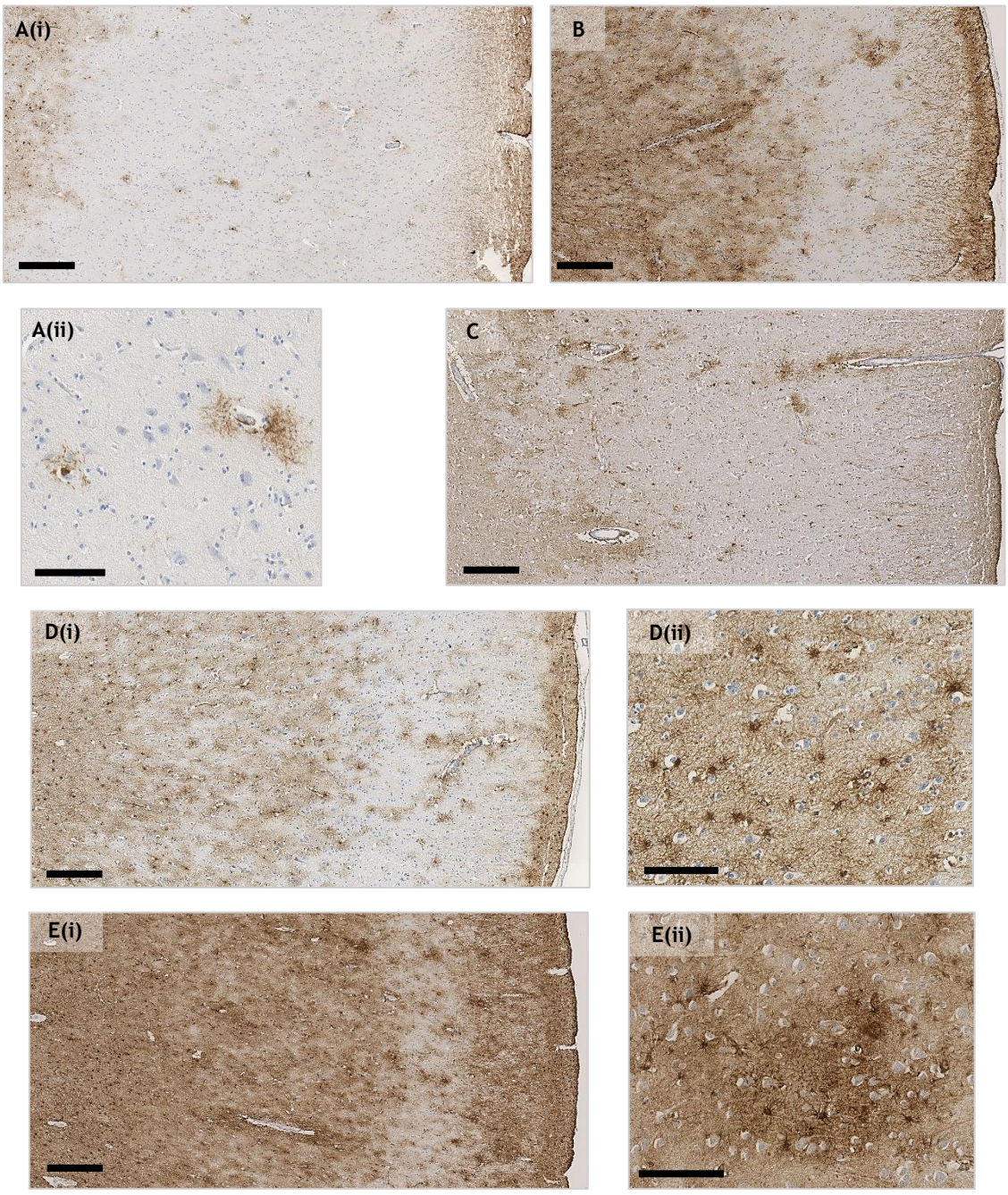

Figure 4-2 Representative images of extent of GFAP-immunoreactivity in age-matched, uninjured controls after sTBI and rTBI. (**A**) 36-year-old Female with no history of TBI, with (**i**) localised GFAP-immunoreactive astrocytes at the SGL and WMI and (**ii**) individual perivascular astrocytes. (**B**) 74-year-old male with no history of TBI or neurological disease, demonstrating expansion of interface GFAP-immunoreactive astrogliosis at the WMI and SGL. (**C**) 43-year-old male who survived 11 days after a single moderate to severe TBI, with GFAP-immunoreactive astrocytes largely isolated to the WMI border and SGL. (**D**) 47-year-old male who survived 1 year after single moderate to severe TBI, showing (**i**) expansion of GFAP-immunoreactive interface zone astrogliosis and (**ii**) an increase in activated astrocytes with overlapping of cellular domains. (**E**) 75-year-old male former professional football player with a history of multiple TBIs, with (**i**) a similar expansion of GFAP-immunoreactivity at interface zones and (**ii**) astrogliosis. Scale bar = 500/250μm.

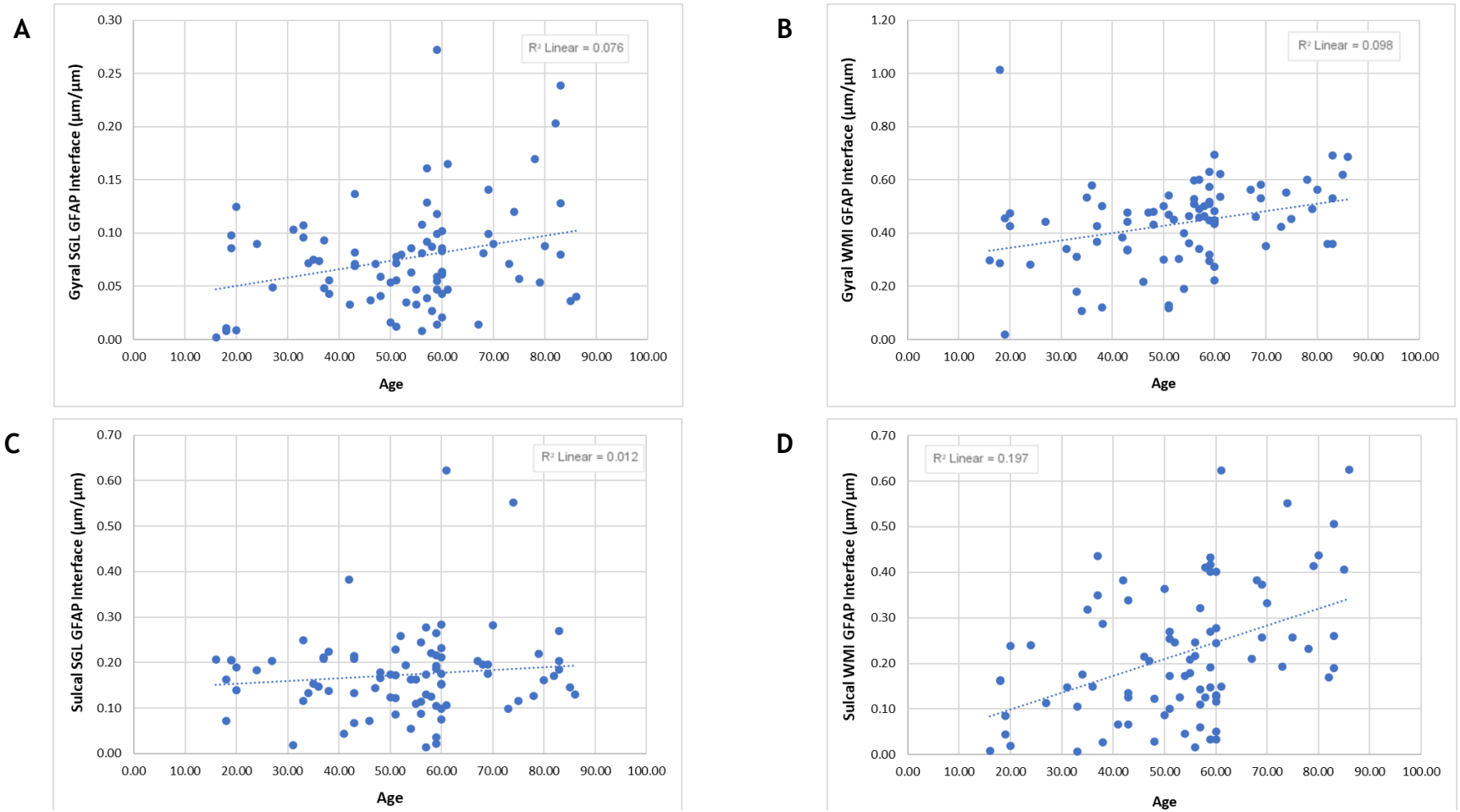

Figure 4-3 Correlation of age and interface GFAP-immunoreactivity in TBI compared to uninjured controls. Positive correlation between age and GFAP-immunoreactivity within the cingulate gyrus at (**A**) the SGL (p=0.02), and (**B**) the WMI (p=0.029), and within the cingulate sulcus at (**D**) the WMI (p<0.001; Pearson's correlation). No correlation was observed between age and GFAP immunoreactive astrogliosis in the cingulate sulcus at (**C**) the SGL.

4.3.2 Long-term survival from single to moderate severe TBI but not repetitive mild TBI results in GFAP-immunoreactive interface astrogliosis

Examining material from patients who died in the acute phase (<2 weeks post injury) following sTBI revealed essentially similar pattern and distribution of interface GFAP-positive astrocytes as in age-matched, non-injured controls (**Figure 4-2**). Specifically, GFAP-immunoreactive astrocytes were distributed as a thin interface band at the SGL and WMI, with no measurable increase in interface astrogliosis among acute sTBI survivors when compared to age matched, non-injured sTBI controls (**Figure 4-4**). In contrast, for patients with late survival (≥ 1 year) from sTBI, there was an increase in morphologically activated astrocytes, with expansion of cellular processes and greater overlap between cellular domains (**Figure 4-2**). This was accompanied by expansion of GFAP-immunoreactivity at multiple interface zones. Specifically, compared to age-matched, uninjured sTBI controls, those surviving more than a year from sTBI showed expansion of GFAP-immunoreactive interface astrogliosis at the WMI in the cingulate gyrus (0.465 µm/µm vs 0.377 µm/µm; p=0.012; Mann-Whitney U Test; Cohen's d = -1.094). This was also observed at the SGL (0.194 µm/µm vs 0.141 µm/µm; p=0.008; Cohen's d = -0.93) and WMI (0.201 µm/µm vs 0.125 µm/µm; p=0.039; Cohen's d = -0.768) of the cingulate sulcus (**Figure 4-4**). Further, there was associated reactive astrogliosis in the adjacent corpus callosal white matter of late sTBI survivors (45.65% ± 16.28%; mean ± standard deviation area staining) compared to their age-matched, non-injured controls (28.42% ± 13.52%; t(38) = 3.64, p=0.006, Student's t-test) (**Figure 4-6**). In contrast, when comparing individuals exposed to rTBI to age-matched, uninjured rTBI controls, there was no expansion of GFAP-immunoreactivity within the interface zones of the cingulate gyrus or cingulate sulcus (**Figure 4-2**), or in the adjacent white matter of the corpus callosum (**Figure 4-5**).

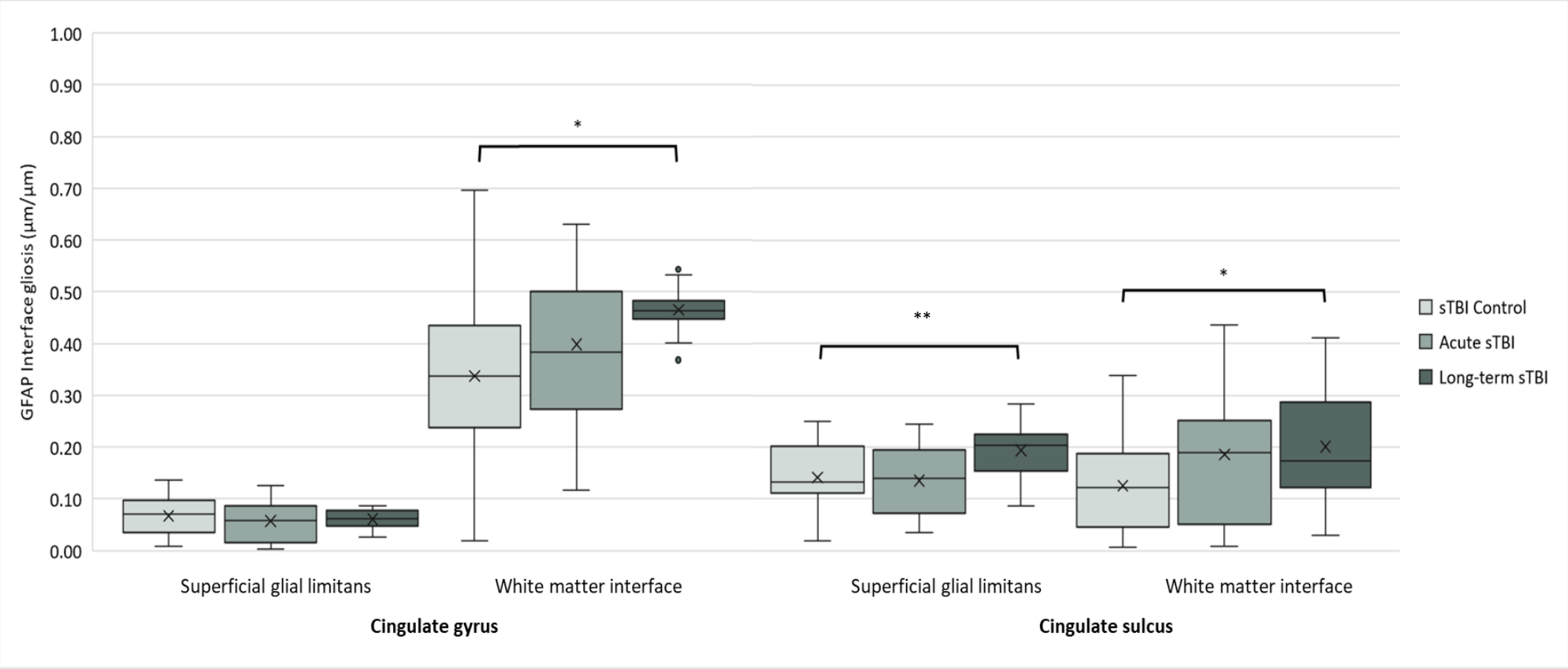

Figure 4-4 Regional distribution of GFAP interface measurements following sTBI vs sTBI Control. In acute sTBI survivals there was evidence of increased astrogliosis at the SGL and WMI, defined by a higher proportion of long-term sTBI survivors than age-matched, uninjured controls in material from the cingulate gyrus and the cingulate sulcus (* $p<0.05$; ** $p<0.01$; Mann-Whitney U Test).

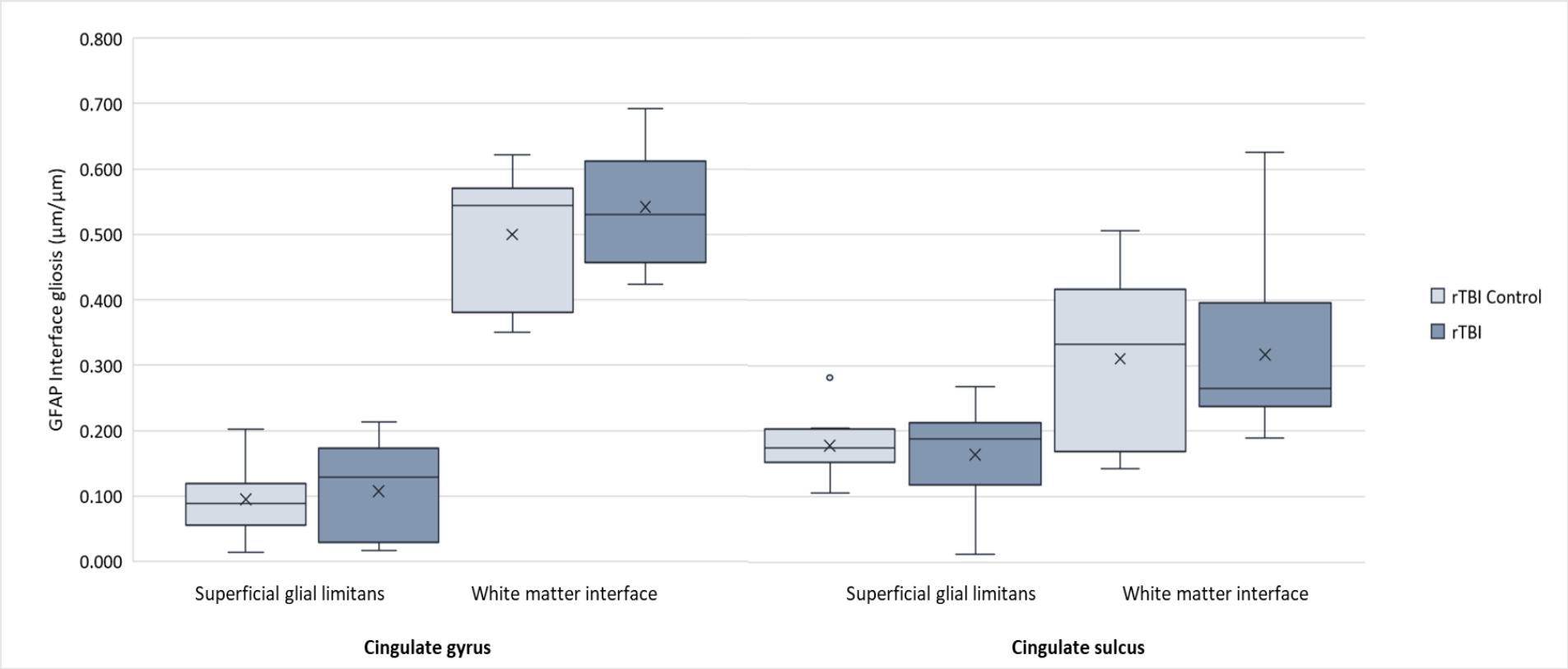

Figure 4-5 Regional distribution of GFAP interface measurements following rTBI vs rTBI Control. In rTBI survivals there was no evidence of increased astrogliosis at the SGL and WMI, (NS; Mann-Whitney U Test).

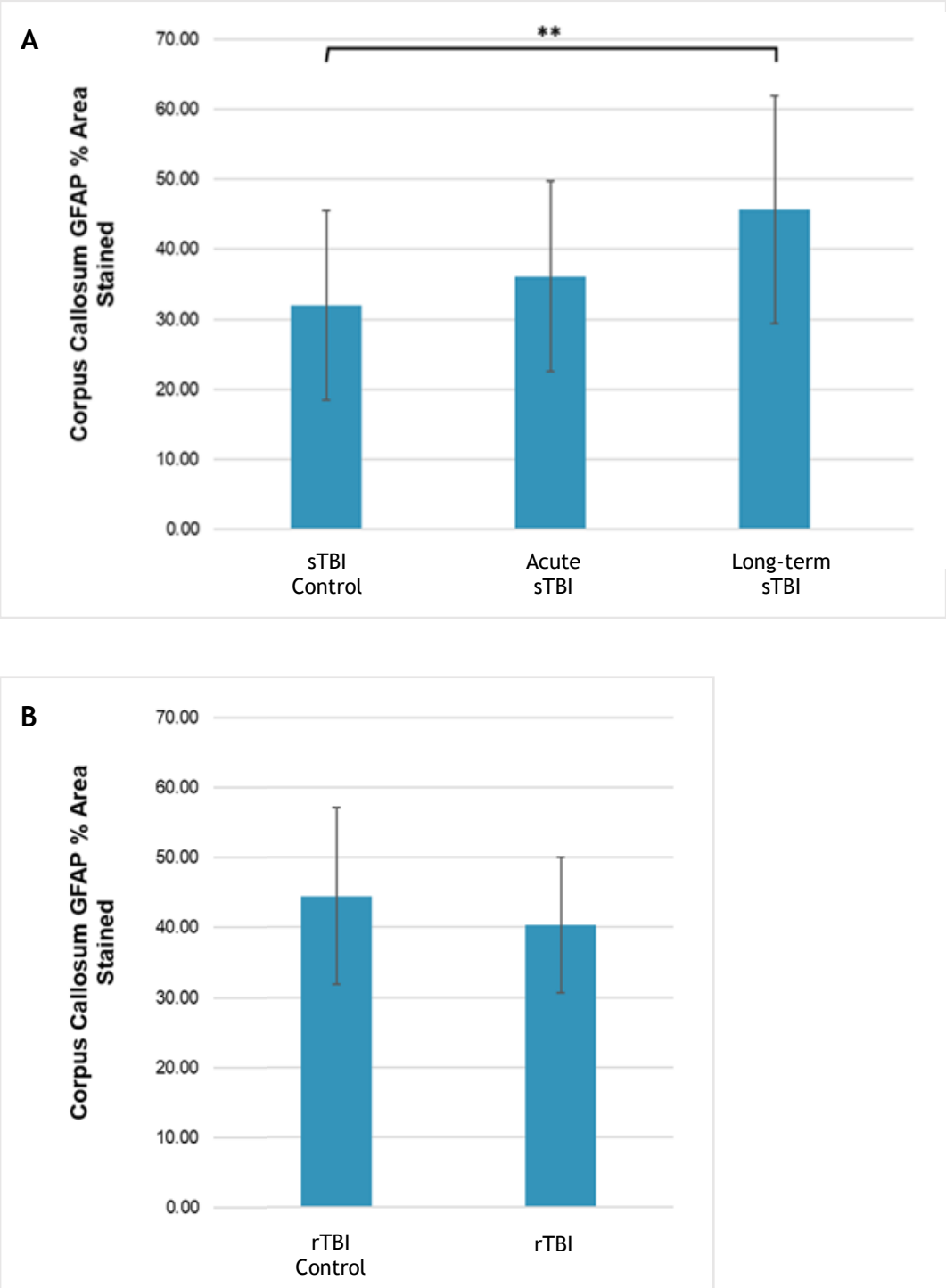

Figure 4-6 Percentage area staining of GFAP immunoreactivity in the corpus callosum. There was evidence of increased astrogliosis in long-term survivors of sTBI compared to sTBI controls, defined by a higher percentage GFAP-immunoreactivity (** $p<0.01$; Student's t-test).

4.3.3 Ageing results in an expansion of interface AQP4-immunoreactive profiles

In sections from age-matched, non-injured controls prepared for APQ4-immunoreactivity, staining was predominantly localised to astrocytic processes, highlighted at end feet, with minimal AQP4-immunoreactivity within cell bodies. Distribution of AQP4-immunoreactive profiles showed the same characteristic WMI pattern, at the boundary between neocortical grey matter and immediately underlying subcortical white matter, and at the SGL, below the pia mater (**Figure 4-7**). AQP4-immunoreactivity was also present within white matter regions of the cingulate, with immunoreactive profiles predominantly located around blood vessels. Similar to GFAP-immunoreactive interface astrogliosis, there was correlation between age and extent of interface AQP4 expression, with increasing age of the individual associated with expansion of AQP4-immunoreactivity at the SGL ($r(84) = 0.23$, $p = 0.019$; Pearson's correlation) of the cingulate gyrus and WMI ($r(84) = 0.19$, $p = 0.023$; **Figure 4-8**) in the cingulate sulcus. There was no correlation between age and AQP4-immunorective astrogliosis at the WMI of the cingulate gyrus or SGL of the cingulate sulcus (NS).

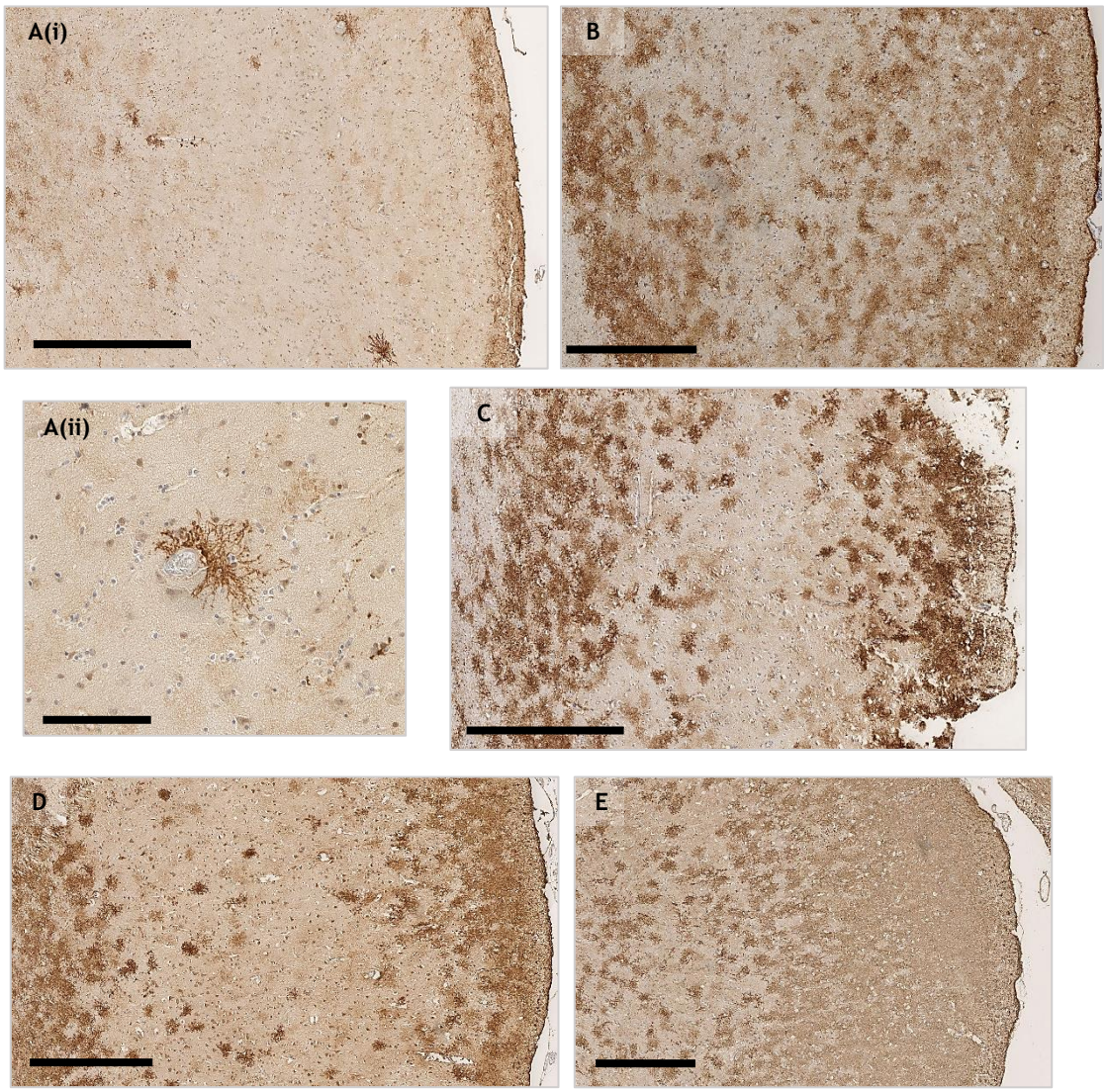

Figure 4-7 Representative images of extent of AQP4-immunoreactivity in age-matched, uninjured controls after and sTBI and rTBI. (**A**) 43-year-old female with no history of TBI, with (**i**) localised GFAP-immunoreactive astrocytes at the SGL and WMI and (**ii**) individual perivascular astrocytes. (**B**) 69-year-old male with no history of TBI or neurodegenerative disease, demonstrating expansion of the AQP4-immunoreactive, interface astrogliosis at the WMI and SGL. (**C**) A 56-year-old male who survived 11 days after moderate to severe sTBI, with expansion of AQP4-immunreactive astrocytes at the interface zones of the SGL and WMI. (**D**) 51-year-old male who survived 5 years following moderate to severe sTBI showing lesser AQP-immunoreactive astrogliosis at interface zones. (**E**) 83-year-old male, former professional footballer exposed to rTBI demonstrating large expansion of AQP4-immunoreactive astrogliosis at the SGL interface region and an increase in the WMI also. Scale bar = 125/500 μm.

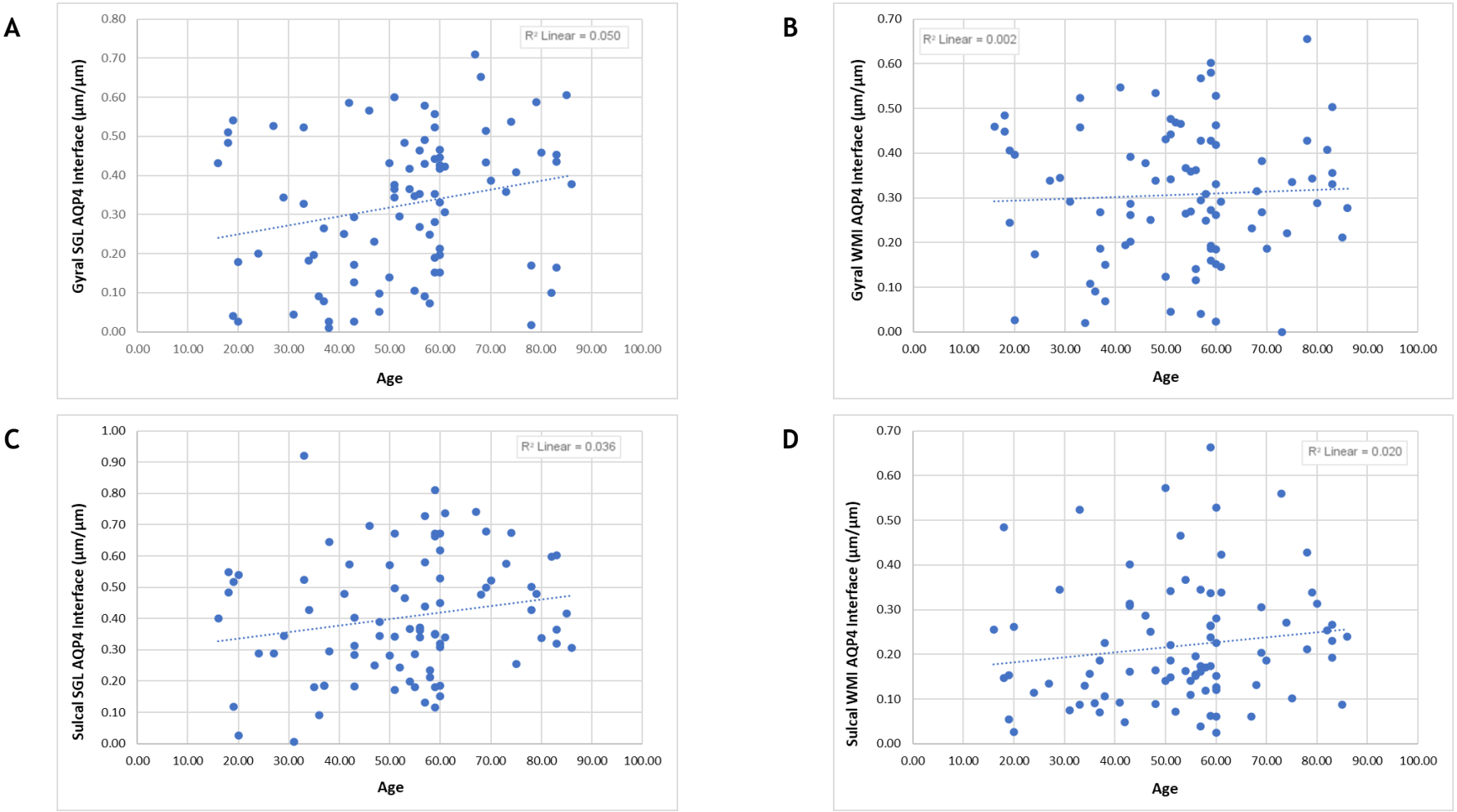

Figure 4-8 Correlation of age and interface AQP4-immunoreactivity in TBI compared to uninjured controls. Positive correlation between age and AQP4-immunoreactivity within the cingulate gyrus at (A) the SGL (p=0.019; Pearson's correlation), and at (D) the WMI within the cingulate sulcus (p=0.023). No correlation was observed between age and AQP4 immunoreactive astrogliosis at (B) the WMI of the cingulate gyrus, or at (C) the SGL within the cingulate sulcus (NS).

4.3.4 Acute moderate or severe TBI leads to AQP4-immunoreactve interface astrogliosis

In contrast to the relatively confined zones of AQP4-immunoractivity observed among their age-matched, non-injured controls, material from patients dying in the acute phase (<14 days) after moderate to severe TBI demonstrated a marked increase in the number of AQP4-immunoreactive astrocytes within the parenchyma resulting in difficulty distinguishing between individual cellular domains, and astrocytes no longer localised to perivascular spaces (**Figure 4-7**). Further, there was expansion of AQP4-immunoractivity at both the SGL (0.412 µm/µm vs. 0.181 µm/µm; $p<0.001$; Mann-witney U Test) and WMI (0.354 µm/µm vs. 0.235 µm/µm; $p=0.019$) of the cingulate gyrus crest, and the SGL (0.522 µm/µm vs. 0.365 µm/µm; $p=0.015$) and WMI (0.202 µm/µm vs. 0.138 µm/µm; $p=0.02$) of the cingulate sulcus depths, compared to the uninjured, age-matched sTBI controls (**Figure 4-9**).

In contrast, for with late (≥ 1 year) survival from sTBI there was no significant increase when compared to uninjured, age-matched sTBI controls (**Figure 4-9**). Similarly, there was no difference in AQP4-immunoractivity at SGL and WMI zones in material from patients exposed to rTBI, and their uninjured, age-matched rTBI controls (**Figure 4-10**).

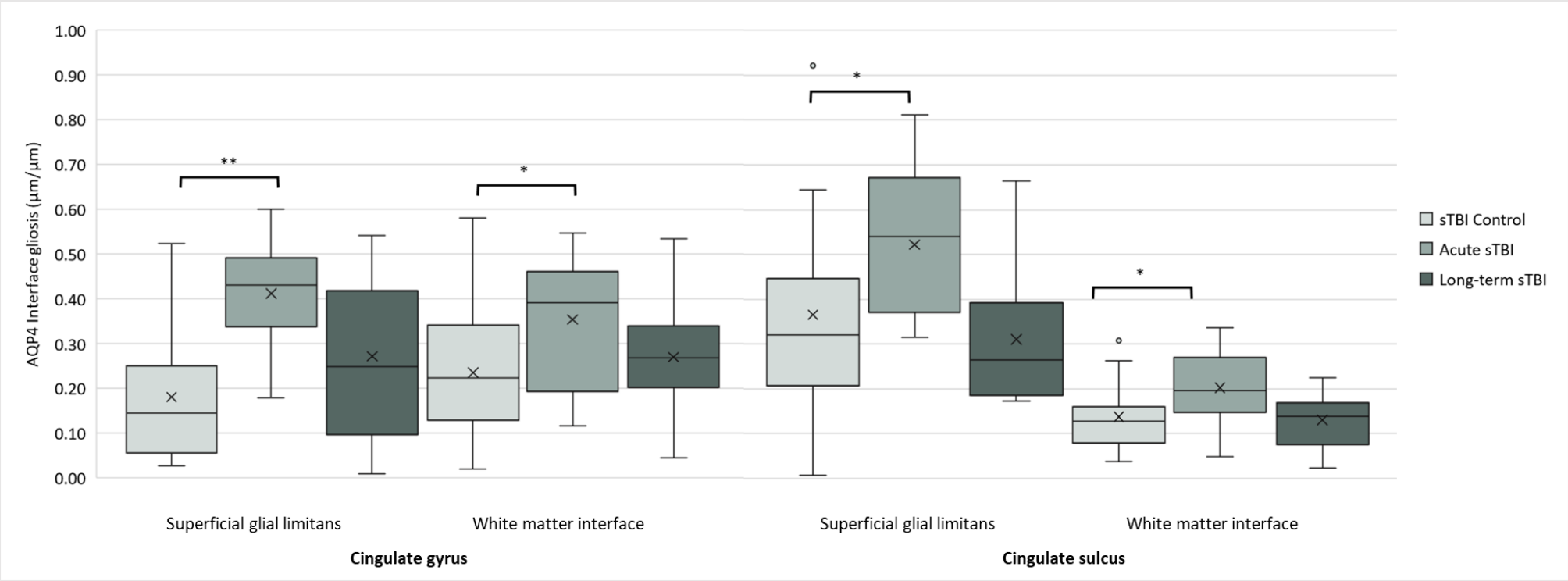

Figure 4-9 Regional distribution of AQP4 interface measurements following sTBI vs sTBI Control. In acute sTBI survivals there was evidence of increased astrogliosis at the SGL and WMI, defined by a higher proportion of sTBI survivors than age-matched, uninjured controls in material from the cingulate gyrus and the cingulate sulcus (* $p<0.05$; ** $p<0.01$; Mann-Whitney U Test).

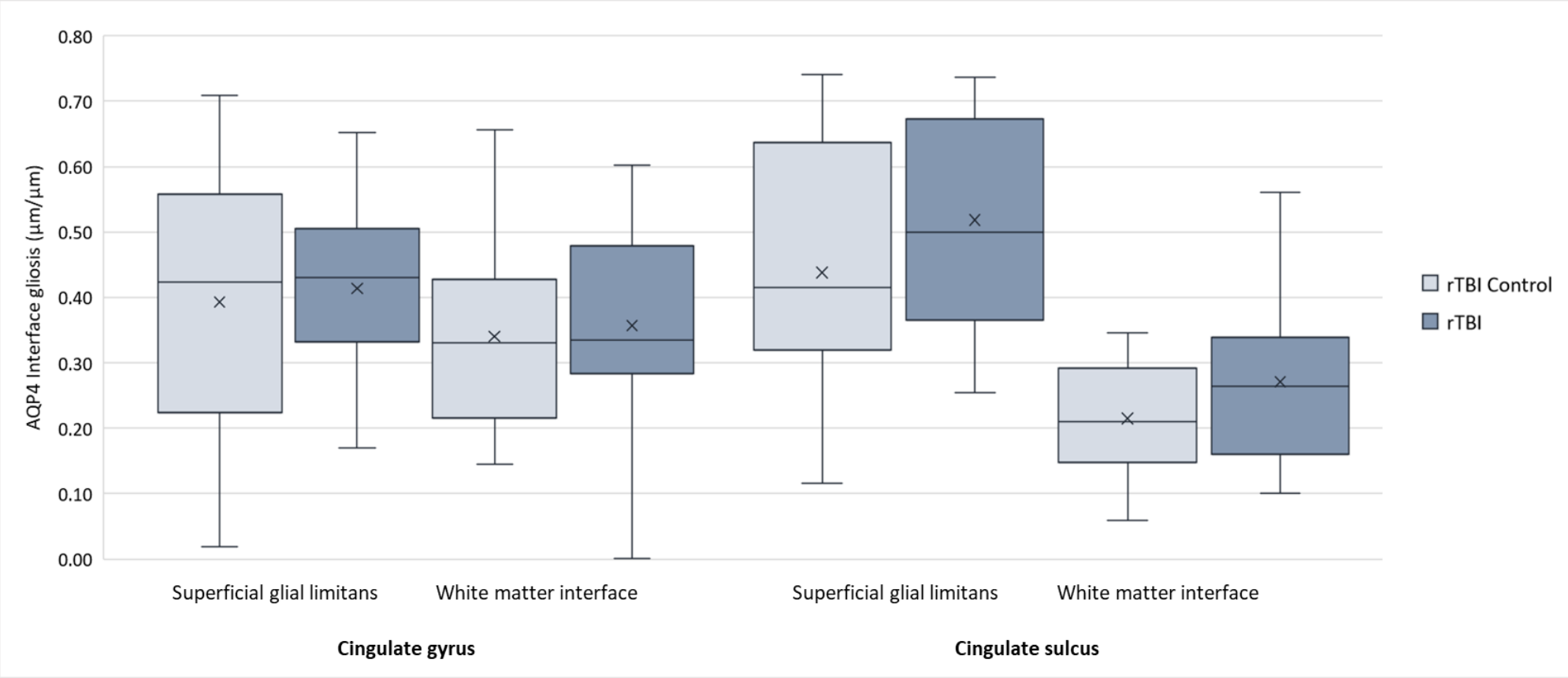

Figure 4-10 Regional distribution of AQP4 interface measurements following rTBI vs rTBI Control. In acute sTBI survivals there was no evidence of increased astrogliosis at the SGL and WMI, defined by a higher proportion of rTBI survivors than age-matched, uninjured controls in material from the cingulate gyrus and the cingulate sulcus (NS Mann-Whitney U Test).

4.3.5 An increase in NQO1-immunoreactivity in rTBI cohort compared to rTBI controls

NQO1 astrocytic immunoreactivity was observed to some extent across all cases within both the rTBI and age-matched, uninjured rTBI control cohorts, typically localised to the cingulate sulcus. NQO1-immunoreactivity progressed from limited staining confined to the cell body of astrocytes within the external granular (II) and external pyramidal (III) layers of the cortex, secondarily observed within cellular processes - sporadically within the parenchyma of the neocortex, and finally with the appearance of fully reactive astrocytes additionally within the multiform (VI) layer of the neocortex in those cases most affected (**Figure 4-11**). When examining patients exposed to rTBI, there was an increase in the number of NQO1-immunoreactive astrocytes within the sulcal depths of the cingulate (4.2 cells/mm^2 vs. 2.2 cells/mm^2, p=0.046; Student's *t*-test) compared to uninjured, age-matched rTBI controls (**Figure 4-12**). There was no increase in astrocytic NQO1 immunoreactivity within the cingulate gyrus or within either the superficial white matter or corpus callosum.

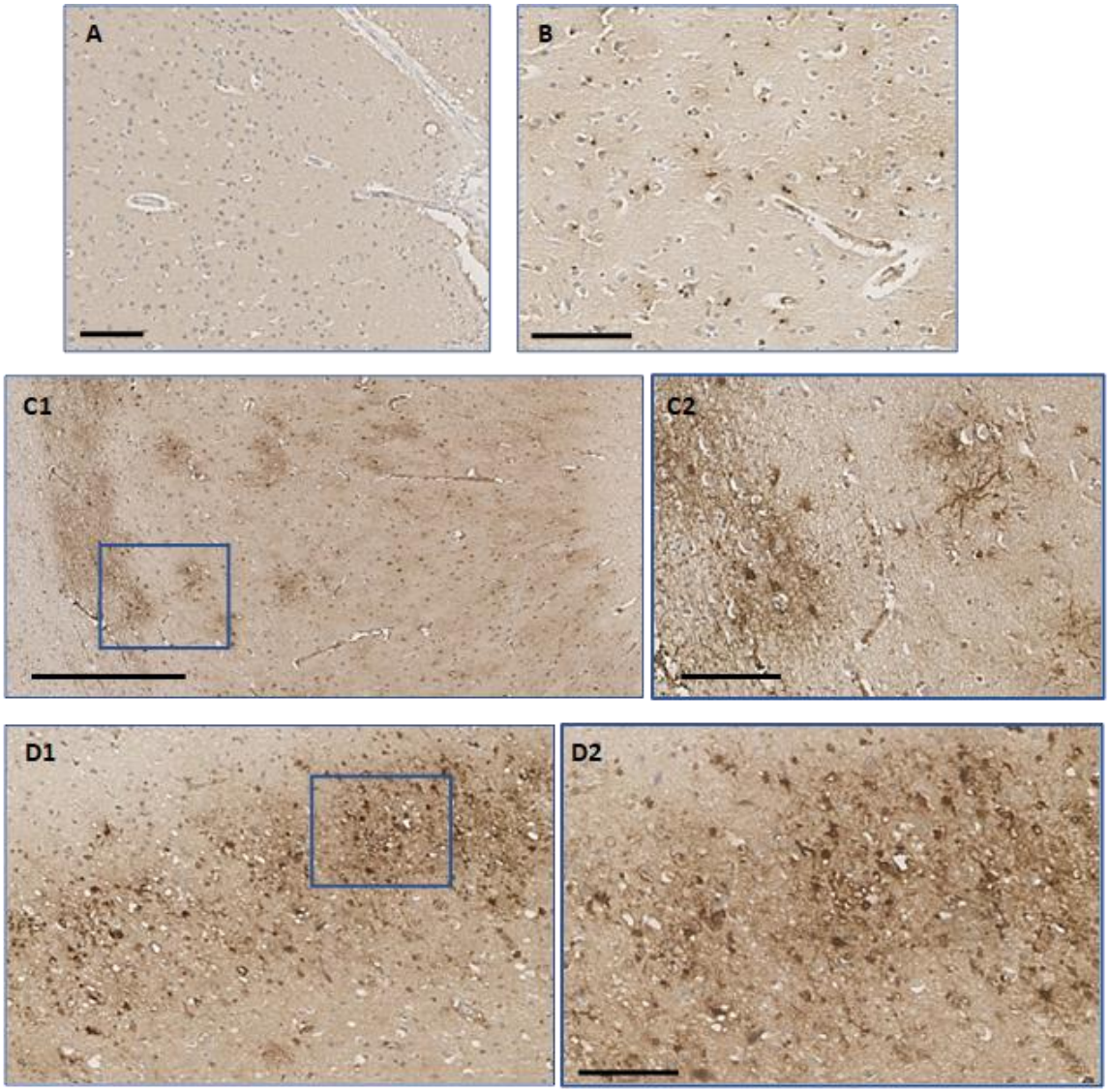

Figure 4-11 Representative images of astrocytic NQO1-immunoreactivity at the cingulate sulcus of rTBI and age-matched, uninjured controls. (**A**) 83-year-old male with no history of TBI scale bar = 125um, (**B**) 60-year-old male with no history of TBI scale bar = 125um, (**C1 & C2**) 78-year-old former rugby player scale bar = 1mm/250µm respectively. (**D1 & D2**) 73-year-old former rugby player scale bar = 500/250µm respectively.

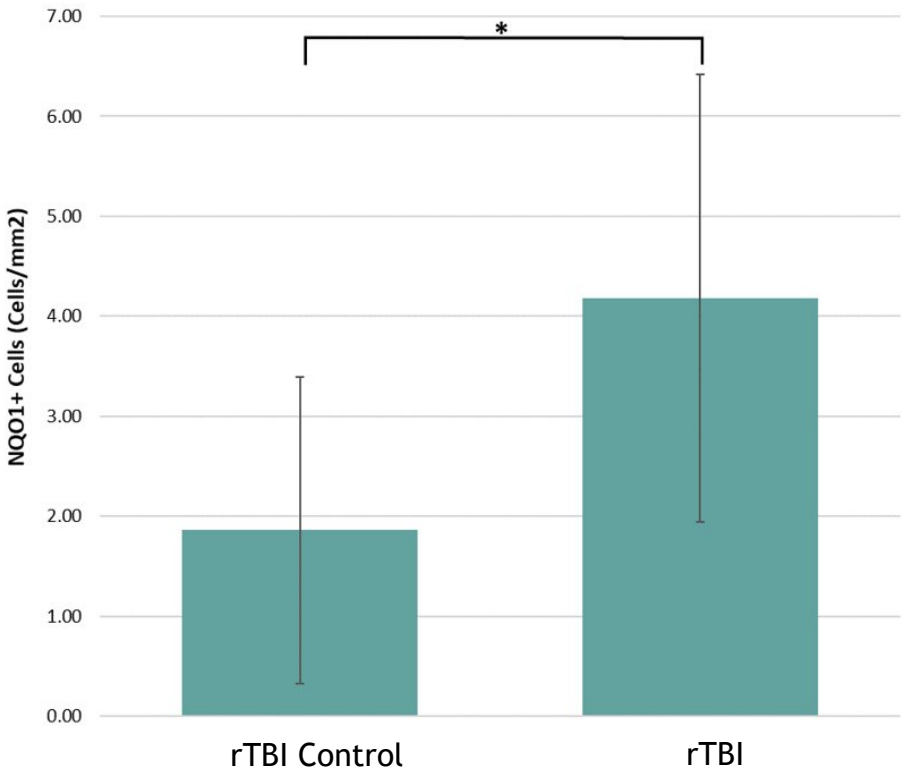

Figure 4-12 Distribution of NQO1 immunoreactivity within the cingulate sulcus. An increase in NQO1 immunoreactivity within the corpus callosum of rTBI patients compared to age-matched, uninjured rTBI controls (* $p < 0.05$ cells/mm^2; Student's *t*-test).

4.4 Discussion

This study demonstrates histological evidence of age-associated changes in interface astrocytes, together with specific time and region dependent responses of astrocytes to TBI. Specifically, in comparison to material from the region of the cingulate gyrus in age-matched, uninjured controls, material from patients dying in the acute period following moderate to severe sTBI shows increased AQP4-immunoreactivity at stereotypical interface zones of the superficial glial limitans (SGL) and the interface between the neocortex and the underlying white matter (WMI). Notably, this pathological expansion of interface AQP4-immunoreactivity was not observed in material from patients surviving a year or more from sTBI. In contrast, sections stained for GFAP, a marker of reactive astrocytes, demonstrated no measurable differences between age-matched controls and individuals dying in the acute phase post sTBI, while there was clear expansion of interface astrogliosis in those surviving a year or more from sTBI. In respect of rTBI although there was evidence of ageing related increases in GFAP and AQP4 expression, these were not in excess of those seen in their appropriately age-matched, uninjured controls. Observed in rTBI cases was an increase in NQO1-immunoreactive astrocytes compared to age-matched rTBI controls.

GFAP expression is recognised as upregulated in a variety of CNS disease, including neurodegenerative diseases (NDD) such as AD (Beach et al., 1989; Beach & Mceer, 1988; Blasko & Grubeck-Loebenstein, 2003; Itagaki et al., 1989; Perez-Nievas & Serrano-Pozo, 2018). In relation to TBI, previous studies have revealed rapid and reported evidence of a GFAP-immunoreactive interface astrogliosis at grey-white matter zones in material from individuals with history of blast (Shively et al., 2016) and rTBI (Babcock et al., 2022) compared to controls. In contrast, in a single study, no evidence of similar interface expansion in GFAP was reported in individuals with purported sTBI history. This current work appears to contradict these previous observations by showing interface zone expansion in GFAP-immunoreactivity is apparently isolated to material from individuals with history of sTBI and late survival, and not seen in individuals with history of rTBI. Notably, the single, previous descriptive study describing no evidence of interface astrogliosis following sTBI considered only limited case numbers, with inconsistent injury definition, wide-ranging survivals and age ranges and inclusion of

inadequate, non-injured controls (Shively et al., 2016). In this present study we employ quantitative methodologies to evaluate pathology in a relatively large sample of individuals with consistent and standardised sTBI history in comparison to a suitably sized cohort of appropriately age matched, non-injured controls. As such, differences observed between the two studies might reflect the more rigorous methodologies employed in the current study.

As regards the apparent contradiction in our findings related to interface astrogliosis in those with histories of rTBI and a previous study (Babcock et al., 2022) again this might reflect methodological differences. In particular, the individuals included in the present study are typically of older age (mean age around 68 years) than those in that previous study (mean age ~40years). Our data on controls with no history of TBI provide evidence that the process of 'normal' ageing is associated with an increase in interface astrogliosis. As such, it is conceivable that there might be a 'ceiling' effect whereby a maximal interface astrogliosis is reached, with our older rTBI patients and their age matched controls both having reached this ceiling, resulting in no measurable difference. Studies to across the ages are therefore required to explore further the relationship between rTBI and associated reactive interface astrogliosis.

GFAP is a recognised biomarker for glial pathology in NDD (FDA Authorizes Marketing First Blood Test Aid Evaluation Concussion Adults, 2018; Petzold, 2015), and serum levels are elevated acutely following both moderate to severe single TBI (Nylén et al., 2006) and mild to moderate injury (Papa et al., 2012), it is also predictive of an unfavourable outcome (Vos et al., 2010) and correlated with clinical severity and extent of pathology (Czeiter et al., 2020). However, whilst we do not see a measurable rise in GFAP immunoreactivity at interface zones in the acute period after injury, this is supported by studies which demonstrate that raised GFAP levels are more associated with focal compared to diffuse pathology (Blennow et al., 2011; Mondello et al., 2011; Pelinka et al., 2004)). Age is also indicated to affect diagnostic efficacy of GFAP as a biomarker for intracranial trauma (Gardner et al., 2018) which supports the observations from this study of age blinding differences in GFAP expression between rTBI patients and age-matched uninured controls.

The role of astrocytes in maintaining the balance of water ions within the brain has been examined here by scrutinising the expression of AQP4, the most abundant aquaporin water channel within the CNS (Nielsen et al., 1996; Papadopoulos et al., 2004; Papadopoulos & Verkman, 2007; Rash et al., 1998; Venero et al., 2001). AD is characterised by the build-up of amyloid-ß (Aß) within the brain, and studies suggest a connection between the failure of Aß-clearance and activation of astrocytes/BBB disruption (Fukuda & Badaut, 2012; Hoshi et al., 2012). Both animal models of TBI (Ren et al., 2013) and studies of human brain injury patients (Neri et al., 2018) suggest that AQP4 may be involved in reducing oedema following sTBI. This study demonstrates there is an immediate, increase in AQP4 in interface astrocytes following sTBI, which is no longer detectable in material from patients surviving a year or more from injury. This suggests that there is a rapid astrocytic response to maintain water-homeostasis following mechanical brain injury, which would correlate previously described BBB disruption that is known to occur acutely following injury (Hay et al., 2015) . When examining AQP4 expression in cases of rTBI, there is again no local expansion of AQP4-immunoreactivity at the typical interface zones, when compared to age-matched, uninjured rTBI controls. This may once more be due to the fact that both of these cohorts are older in age and so any alteration in the expression of AQP4 in astrocytes is masked by the confounding effects of age, which you can see positively influences AQP4 expression in uninjured cohorts.

The brain consumes approximately 20% of all oxygen within the body to maintain neuronal activity through intensive ATP generation (Goyal et al., 2014; Magistretti & Allaman, 2015; Mink et al., 1981), which makes the brain particularly susceptible to oxidative stress (Cobley et al., 2018). Instigated by an imbalance of reactive oxygen species (ROS) and antioxidants (Halliwell, 2012; Ray et al., 2012), oxidative stress is a key factor for progression of AD (L. Chen et al., 2008; X. Chen et al., 2012; G. Kim et al., 2015; Y. Zhao & Zhao, 2013) and normal ageing-associated neurodegeneration (Beal, 1995; Mecocci et al., 2018; Urano et al., 1998; Williams, 1995). Astrocytes are involved in regulation of oxidative stress following TBI, via activation of endogenous antioxidant pathways, expressing upregulated enzymes such as NQO1 to counter the elevated levels of ROS produced by neuroinflammatory processes (Chen, Liang, et al., 2020; Z.-G. Cheng et al., 2013; Cherry et al., 2018; Ross & Siegel, 2018). NQO1 immunoreactivity was

examined in both rTBI cohort and respective controls, with repetitive, chronic exposure to mTBI demonstrating an increase in expression of this antioxidant enzyme within astrocytes. The NQO1 immunoreactivity was not expressed in the same localised manner as GFAP and AQP4 with a lack of expression within the SGL and positively stained cells found predominantly in the depths of the cingulate sulcus. The increase in NQO1 expression was present within astrocytes in the cases of patients exposed to rTBI compared to age-matched, uninjured controls, despite both cohorts being of an older mean age, suggesting that the astrocytic response to oxidative stress is not as influenced by increased age as by injury. This NQO1 pathology draws parallels with the sulcal astrocytic p-tau – ageing-related tau astrogliopathy (ARTAG) which is a hallmark of CTE (Kovacs et al., 2016; Lace et al., 2012; Lõpez-González et al., 2013; C. McKee & Lukens, 2016), due to the specific location of NQO1 within the sulcal depths examined in these rTBI

Limitations of this study included that due to its retrospective nature examining archival tissue, there was limited access to patient's entire clinical record such as imageing, family history, cognitive assessments or any treatments they were undergoing. It was not possible to compare sTBI and rTBI cases, as they had such different age demographics (45.5 ± 13.3 vs. 68.5 ± 15.1 years) that any effects would be unreliable as we showed that age has a significant effect on the expression of GFAP and AQP4 at interface zones. Further, NQO1 expression was only examined in a pilot study of rTBI cases where is has been identified as a possible marker from previous studies. Further work of interest would be to examine NQO1 expression across sTBI cohorts and in rTBI cohorts who are of a younger age to examine possible distinctions when older age is not a co-factor. Additionally, colocalization studies including other regions of interest such as the hippocampus using double-labelling or multiplex immunofluorescence (mIF) with platforms such as the Akoya Biosciences Phenocycler™ Protein Imaging System would allow us to examine how these markers interact within astrocytic communities and with other pathologies such as Aß.

Astrocytes serve multiple functions within the brain in response to injury and this study aimed to examine how each of these are altered across a spectrum of TBI mechanisms and survival time periods when compared to appropriate, age

matched, uninjured controls. Increased age appears to have a more of a manifest influence on the astrocytic functions examined in this chapter which may have reduced the effect of TBI being investigated. However, the observations made work to increase the understanding of how astrocytes are involved in the response to TBI and also provide a springboard for future studies which may examine how these processes are simultaneously occurring within the brain.

Chapter 5 – Amyloid-beta plaque pathology in elderly TBI

5.1 Introduction

Traumatic brain injury is a leading global cause of death and disability (Faul et al., 2010) and is acknowledged as a major risk-factor for neurodegenerative disease such as Alzheimer's (Collins et al., 2020; Fann et al., 2018; Livingston et al., 2020; LoBue et al., 2018; Nordström & Nordström, 2018; Schaffert et al., 2018). TBI is particularly problematic in older adults, with increased rates of TBI-related hospital admissions and mortality observed in persons aged 65 years and older (Marincowitz et al., 2019), accounting for approximately 50% of fall related deaths in the US (Thompson et al., 2006). Age also influences outcomes after injury (Frankel et al., 2006; Hukkelhoven et al., 2009; Ramanathan et al., 2012), resulting in increased injury severity, and lower rates of recovery and hospital discharge, whilst acting as an independent predictor of mortality and poorer functional outcome after similar injury (Mosenthal et al., 2002, 2004; Susman et al., 2002). However, underrepresentation of older patients in research cohorts (Gardner et al., 2015, 2017; Munro et al., 2002; Thompson et al., 2006) results in a lack of understanding of the relationship between comorbidities of age and the pathologies driving neurodegeneration in these vulnerable patients. Therefore, with an increasingly elderly global population, the understanding of whether head injury in later life hastens the onset or increases the risk of dementia is vitally important.

A hallmark of AD (Beyreuther & Masters, 1991; Hardy JA & GA., 1992; Ittner & Götz, 2011; Price & Morris, 1999; Sisodia & Price, 1995), progressive amyloid-beta (Aß) deposition, has long been considered one of the causative agents of AD pathogenesis (Selkoe & Hardy, 2016). The initial aggregation of Aß peptides into irregularly shaped, diffuse plaques is associated with the early stages of disease (Behrouz et al., 1991; Dickson & Vickers, 2001; Malek-Ahmadi et al., 2016; Morris, Storandt, Mckeel, et al., 1996), while the latter development of senile, neuritic plaques is considered a pathological correlate of clinical AD (Mirra et al., 1991). These neuritic plaques consist of a central zone of dense Aß with radiating fibrils,

commonly with neuritic elements and microglial involvement (DeTure and Dickson, 2019; Dickson and Vickers, 2001; Perl, 2010). Similarly, Aß accumulation within the brain is observed in normal brain ageing (Blumenthal, 2004; Jack et al., 2009; Quigley et al., 2011; K. M. Rodrigue et al., 2009) and is known to precede the initial signs of cognitive decline, with 29% of healthy, older controls showing Aß deposition (Jack et al., 2009)). Positron emission tomography imaging of Aß with Pittsburgh Compound B (C-PIB-PET) has been used to suggest a link between the presence of Aß and early memory changes in non-demented individuals (Pike et al., 2007), where post-mortem studies demonstrate diffuse plaque accumulation in non-cognitively impaired, normal ageing (Malek-Ahmadi et al., 2016; Morris, Storandt, McKeel, et al., 1996; Teissier et al., 2020a) and these diffuse plaques typically have a regional distribution correlating with earlier stages of neurodegenerative decline (Grothe et al., 2017; Teissier et al., 2020b; D. R. Thal et al., 2004).

Aß plaques are also observed following TBI, occurring in up to 30% of patients dying acutely following a moderate to severe head injury – even in younger adults (Hong et al., 2014; Roberts et al., 1994, 1991, 1990; Smith et al., 2003). Plaques seen acutely after injury can occur rapidly, having been noted in tissue surgically excised from TBI patients (DeKosky et al., 2007; Ikonomovic et al., 2004) and are often diffuse, similar to that seen in ageing brains and in the early stages of AD (Dickson & Vickers, 2001; Malek-Ahmadi et al., 2016; Morris, Storandt, McKeel, et al., 1996). Aß plaque is also found in patients who survive chronically after a moderate to severe brain injury, reappearing in the late phase of survival with a more often neuritic appearance (Johnson et al., 2012), similar to those seen in AD (Mirra et al., 1991). Experimental animal studies of TBI in aged mice demonstrate that older animals display worse overall recovery outcomes and slower reversal of oedema, alongside an increase in blood-brain barrier disruption and increased neuroinflammatory response in both the acute and long-term phase after injury, compared to uninjured, aged mice (Onyszchuk et al., 2008, 2009).

An additional hallmark of AD, hyperphosphorylated neurofibrillary tangles (NFTs) of tau protein within neurons, are also developed in normal ageing. The presence of NFTs has been detected in elderly subjects, correlated with age (Braskie et al., 2010; Pontecorvo et al., 2019; Price & Morris, 1999; Schöll et al., 2016) and

imaging studies using tau PET agents detect early deposition of both tangles and Aß plaques before any detectable changes to cortical structures (Braskie et al., 2010; Pontecorvo et al., 2019; Schöll et al., 2016), which follows the predicted path of Braak et al. (2006) staging of disease progression. The importance of tau pathology following TBI is becoming further understood and chronic traumatic encephalopathy (CTE) is commonly described as a tauopathy, with the pathognomonic lesion increasingly thought of as aggregates of tau within neurons and astrocytes located at sulcal depths (Arena et al., 2020). It is also seen following survival of a year or more after a single, moderate to severe TBI, with both a greater density and distribution of NFTs in up to 30% of cases compared to age-matched controls (Johnson et al., 2011) mirroring the distribution described in cases of repetitive mTBI and CTE (Stewart et al., 2016). However, similar tau pathology was not observed in post-mortem tissue from patients, who survived up to 4 weeks following single, moderate to severe TBI, in a cohort ranging in age from youth to elderly (C. Smith et al., 2003).

Whilst neurodegenerative patterns of change are known to occur in elderly individuals without associated cognitive decline, further investigation is required to fully understand the effects of TBI and any connection to resulting progression to neurodegenerative disease such as AD. Indeed, Aß plaque observed after acute injury in an elderly population may represent co-existing pathologies rather than TBI-associated phenomena. Transgenic animal models of AD have indicated that TBI accelerates the onset of AD-related pathology such as neuronal loss, gliosis, atrophy, increased phospho-tau immunoreactivity, Aß deposition, and greater cognitive impairment (Nakagawa et al., 2000; D. Tran et al., 2011; Uryu et al., 2002; Washington et al., 2014), compared to non-TBI mice. However, more research is required to fully assess the connection between age and neuropathological change post-injury in this vulnerable cohort. This chapter aims to examine Aß plaque and NFT pathology in an aged population of acute TBI survivors, with the hypothesis that we will observe increased Aß plaque deposition in the acute phase following injury when compared with age-matched, uninjured controls with no previous history of neurological disorder.

Aim:

To characterise Aß and tau pathology in an aged population of individuals in the acute period following exposure to moderate to severe sTBI.

5.2 Specific methods

5.2.1 Case selection

All tissue was selected from the holdings of the Glasgow Traumatic Brain Injury Archive of the Department of Neuropathology, Glasgow, UK. All material was obtained following routine diagnostic autopsy examination at the same institution and approved for use in this study by the Greater Glasgow and Clyde Bio-repository Governance Committee. Cases with a history of acute survival following a single, moderate, or severe TBI aged over 60 years at time of death (n=42) were selected from the archive, together with age-matched controls with no known history of TBI or neurological disease (n=42). The UN defines older persons as those aged 60 years and over (Raut, 2019), while a study of older trauma patients established 60 years as the data-driven definition of elderly in trauma (Campbell-Furtick et al., 2016). Detailed reports from the original diagnostic post-mortem evaluation were available for all cases, supplemented by forensic and clinical records, where necessary. All TBI cases had a confirmed history of a single, moderate or severe TBI, as defined by Glasgow Coma Scale at presentation. Full clinical and demographic information for each cohort is presented in **Table 5-1**.

5.2.2 Brain tissue preparation

Whole brains were immersion fixed in 10% formal saline at autopsy for a minimum of 3 weeks prior to dissection, sampling following standardised block selection and processing to paraffin using standard techniques. Paraffin tissue blocks from a coronal slice of the cerebral hemispheres at the level of the lateral geniculate nucleus were selected to include: the hippocampus and adjacent medial temporal lobe, including the inferior temporal gyrus; the cingulate gyrus and adjacent corpus callosum; the insular cortex; the thalamus; and the cerebellum at the dentate nucleus.

Table 5-1 Demographic and clinical information of chapter 5 cohorts

	Elderly TBI (n=42)	**Elderly Controls (n=42)**
Mean age (range) years	70.12 (60-89)	70.4 (60-86)
Males, n (%)	29 (69)	28 (67)
Mean post-mortem delay (range), hours	68.10 (4-264)	56.42 (4-288)
Mean survival interval (range), hours	86.29 (0.6-336)	Not applicable (No history of TBI)
Cause of TBI, n (%)		
Fall	24 (57.14)	
RTA	12 (28.57)	n/a
RTA ped	4 (9.52)	(No history of TBI)
Unknown	2 (4.76)	
Cause of death, n (%)		
Acute head injury	31 (73.81)	-
Unknown	1 (2.38)	9 (21.42%)
Bronchopneumonia	5 (11.90)	5 (11.90%)
Heart failure	-	4 (9.52%)
Multiple injuries	3 (7.14)	-
Myocardial infarction	-	3 (7.14%)
Septicaemia	-	3 (7.14%)
SUDEP	-	3 (7.14%)
Cancer	-	2 (4.76%)
COAD	-	2 (4.76%)
Organ failure	-	2 (4.76%)
Pulmonary congestion	-	2 (4.76%)
Pulmonary thromboembolism	2 (4.76)	-

	Elderly TBI (n=42)	Elderly Controls (n=42)
Cause of death, n (%)		
Inhalation gastric contents	-	1 (2.38%)
Liver haemorrhage	-	1 (2.38%)
Myelopathy	-	1 (2.38%)
Perforated viscus	-	1 (2.38%)
Polymyositis	-	1 (2.38%)
Renal failure	-	1 (2.38%)
Vasculitis	-	1 (2.38%)
TBI Pathologies, n (%)		
Skull fracture	31 (73.81)	-
DAI	24 (57.14)	-
Brain swelling	22 (52.38)	-
SDH	31 (73.81)	-
EDH	3 (7.14)	-
SAH	22 (52.38)	-

COAD, chronic obstructive airways disease; DAI, diffuse axonal injury; EDH, extradural haematoma; RTA, road traffic accident; RTA, road traffic accident - pedestrian; SAH, subarachnoid haematoma; SDH, subdural haematoma; SUDEP, sudden unexplained death in epilepsy

5.2.3 Immunohistochemistry

From each tissue block, 8µm-thick sections were prepared for immunohistochemistry. Sections were deparaffinised in xylene, rehydrated to water, and then immersed in aqueous solution of 3% hydrogen peroxide for 15 minutes to quench endogenous peroxidases. Antigen retrieval via microwave pressure cooker was performed for 8 minutes in preheated 0.1M citrate buffer, followed by blocking in 50µL of normal horse serum (Vector Laboratories, Peterborough, UK) per 5 mL of Optimax buffer (BioGenex, San Ramon, CA) for 30 minutes.

Once blocked, overnight incubation with primary antibodies was performed at 4°C for 20 hours. Primary antibodies were selected to reveal Aß (clone 6F3D; 1:75; Dako, Santa Clara, CA) and tau (PHF1; 1:1000; gift from P. Davies, Feinstein Institute for Medical Research, Manhasset, NY, USA). Following overnight incubation, biotinylated secondary antibody was then applied for 30 minutes (IgG, 1:200), followed by avidin-biotin complex as per the manufacturer's instructions (1:50; Vectastain Universal Elite kit, Vector Laboratories). Visualisation was achieved using 3,3'-diaminobenzidine (DAB) peroxidase substrate kit (Vector Laboratories) followed by counterstaining with haematoxylin. Known positive tissue sections were run in parallel with test sections in all antibody runs in addition to sections with primary antibody omitted as standard controls for antibody specificity.

5.2.4 Analysis of immunohistochemistry

Observations were made blind to demographic and clinical data for all cases. The frequency and distribution of Aß plaques was semi-quantitatively assessed using modifications of standardised, semi-quantitative scoring systems. Plaque density was scored using a modified version of the system set out by the "Consortium to Establish a Registry for Alzheimer's Disease" (CERAD) system (Mirra et al., 1991; G. W. Roberts et al., 1994) as: no plaques (score 0), sparse plaques (score 1), moderate plaques (score 2) or frequent plaques (score 3) (Figure 5-2). The extent of plaque density was calculated as the highest modified-CERAD score across all

regions for each case. Morphology of Aß plaque was defined as either fibrillar, neuritic plaque which consisted of a central beta-amyloid core surrounded by circular fibrillary extensions or diffuse plaque, which had a more amorphous, irregular shape and did not contain a central core of Aß (**Figure 5-1**). Diffuse and fibrillar neuritic plaque were assessed both independently and jointly. The regional distribution of Aß plaque pathology was assessed using a modified version of the scoring system reported by Thal et al (2002), whereby the hierarchical presence of plaques across brain regions was scored as: cingulate (grade 1), hippocampus (grade 2), thalamus (grade 3) and finally cerebellar (grade 4) (**Figure 5-2**).

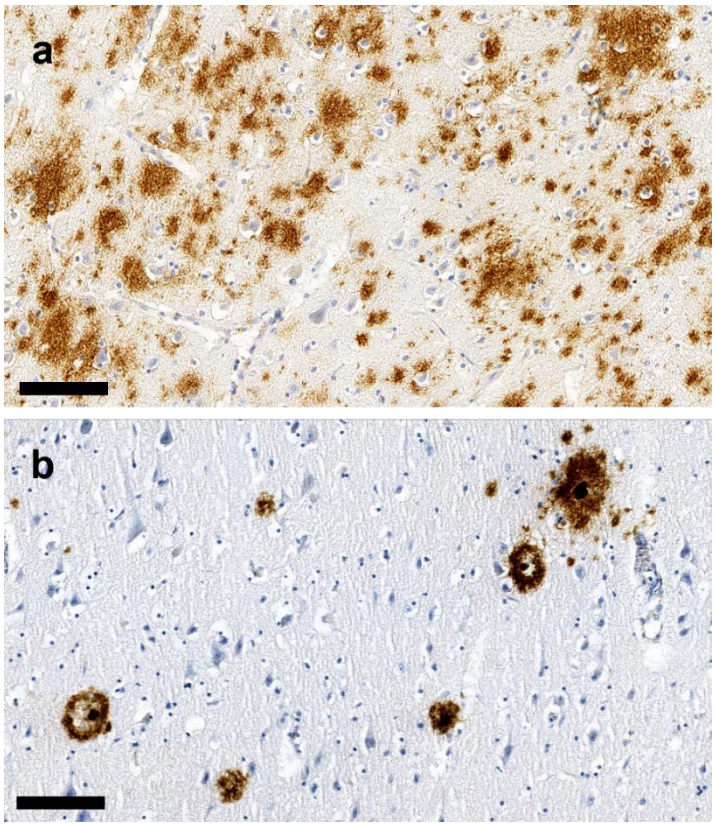

Figure 5-1 Representative images of diffuse and neuritic plaque stained with BA4 (Dako, 6F/3D). (**A**) diffuse Aβ plaque in the cingulate gyrus of a 79-year-old female who survived 8 days following an RTA, and (**B**) neuritic Aβ plaque in the cingulate gyrus of a 64-year-old male who survived 24 hours after a fall. Bar is 100µm.

Tau-immunoreactivity was assessed using a modified, standardized, semi-quantitative system of analysis (Braak et al., 2006; D. Smith et al., 2013b). PHF1-immunoreactive NFTs and neurites of sparse to moderate density in the transentorhinal cortex with or without small numbers in the CA1 sector of the hippocampus were defined as a score of 1. PHF1-immunoreactive NFTs and neurites as described in score 1, together with NFTs extending into the fusiform gyrus and sparse tangles in the neocortex denoted a score of 2, while PHF1-positive NFTs and neurites in widespread sectors of the hippocampal formation and subiculum, with extensive medial temporal, cingulate and insular cortical involvement indicated a score of 3 (**Figure 5-2**).

5.2.5 Statistical analysis

Statistical analysis comparing cohorts was performed using IBM SPSS Statistics Software (version 25; SPSS Inc., Chicago, Illinois, USA). The Mann-Whitney U test was used to compare medians between cohorts and Pearson's chi-squared test and Fisher's exact test were used to assess categorical data. Cramer's V and partial eta squared were used to determine effect size for Chi-squared and Mann-Whitney U tests respectively. All effects were considered statistically significant when $p < 0.05$.

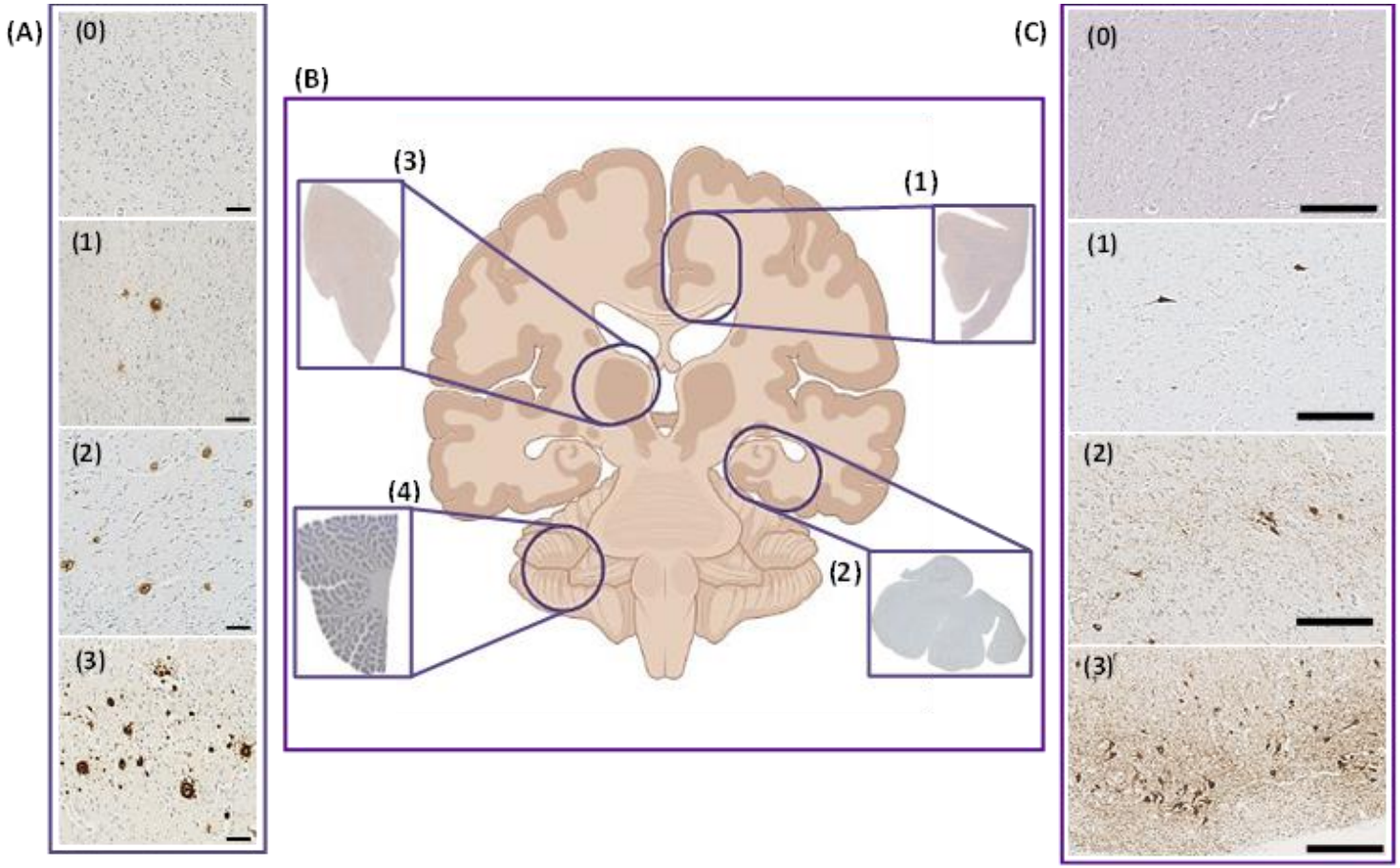

Figure 5-26 Representative images of modified, standardized, semi-quantitative scoring methods undertaking in this investigation. (A) CERAD Scoring method of BA4-immunoreactive amyloid-plaque demonstrating the extent of amyloid-beta plaque pathology across all brain regions examined. Score of (1) is zero plaques, Score (2) is sparse plaque, Score (3) is moderate plaques, and Score (4) is frequent plaques. (B) Modified Thal scoring method for the hierarchical regional distribution of BA4-immunoreactive amyloid-beta plaque across 4 ROI. Score (1) is amyloid-beta plaques limited to the cingulate, Score (2) is involvement of hippocampal areas, Score (3) is inclusion of thalamic areas, and Score (4) is involvement of the cerebellar cortex. (C) Modified Braak scoring method of PHF-1-immunoreactive NFTs. Score (1) sparse to moderate density in transentorhinal cortex with/without small numbers in hippocampus CA1. Score (2) is addition of NFTs extending into the fusiform gyrus and sparse tangles in the neocortex. Score (3) is widespread sectors of the hippocampal formation and subiculum, with extensive medial temporal, cingulate and insular cortical involvement. Created with BioRender.com.

5.3 Results

5.3.1 Presence of Aβ plaque

Aß plaques were observed in the majority of both control and TBI cases; 31 of 38 (81.5%) uninjured elderly control cases and 27 of 38 (71.1%) elderly TBI cases (NS, Chi-squared). Across both experimental groups, diffuse plaques were present in the majority of cases in both cohorts, with elderly controls demonstrating diffuse plaque in 30 of 38 (78.9%) cases, while they were present in 23 of 38 (60.5%) elderly TBI patients (NS, Chi-squared). However, when looking at the presence of neuritic plaque, there was a higher incidence in elderly TBI patients (20 of 38, 52.6%) compared to uninjured controls (11 of 38, 28.9%; p = 0.036, Cramer's V = 0.241, **Table 5-2** [supplementary], **Figure 5-3**). In both experimental groups, Aß plaque was typically observed in one of two patterns. Sporadic and isolated clusters of plaque within the grey matter regions, surrounded by plaque-free neuropil, predominantly located at the gyral crests in neocortical areas. Alternatively, extensive deposits of plaque occurred across cortical layers and grey matter bodies, expanding into white matter. In these cases, plaque frequently extended throughout gyral crests and sulcal depths.

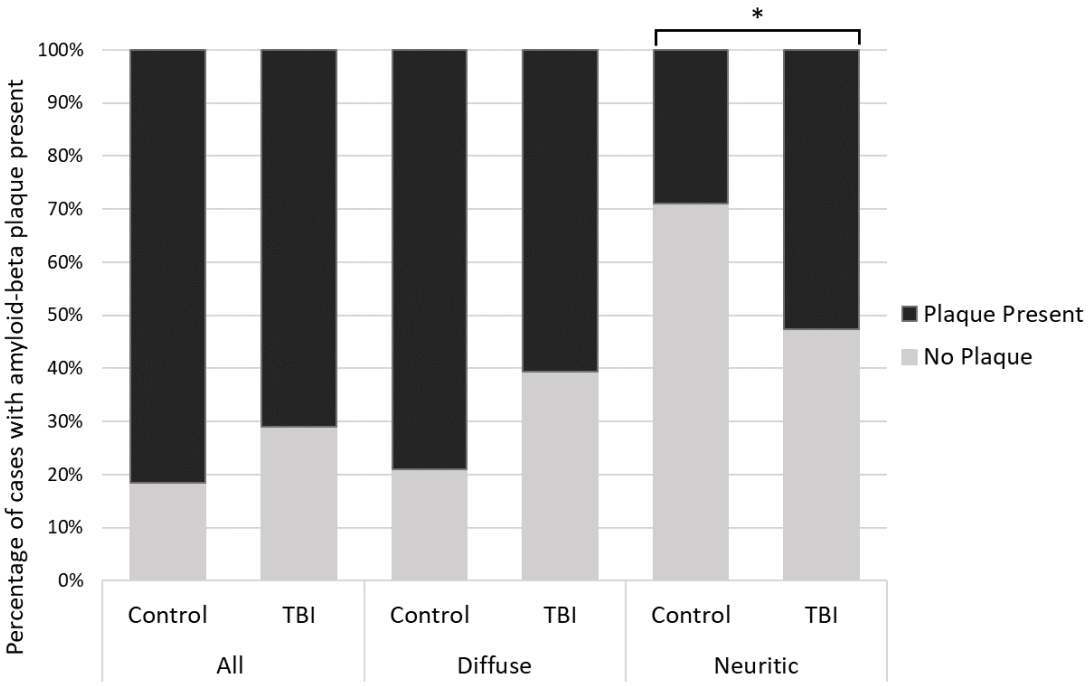

Figure 5-3 Proportion of cases with presence of overall, diffuse and neuritic Aβ plaque presence in both elderly uninjured controls and elderly TBI patients. An increase in the presence of neuritic Aβ plaque in elderly TBI patients (* $p < 0.05$, Chi-squared test).

5.3.2 Extent of Aβ plaque

The extent of Aß plaque pathology within our cohorts was examined by generating the mean of the CERAD score (Roberts et al., 1994) across the four ROI analysed for each case. When looking at the overall extent of Aß plaque pathology, there was no increase in the proportion of cases affected by sparse, moderate, or frequent plaque between uninjured elderly controls and elderly TBI patients (NS, Mann-Whitney U test). The same pattern was observed for simply diffuse Aß plaque (NS, Mann-Whitney U test), with a similar extent of diffuse plaque pathology in elderly TBI patients compared to uninjured elderly controls. However, there was an increase in the extent of neuritic Aß plaque pathology in elderly TBI patients compared to uninjured elderly controls ($p = 0.048$, $\eta_p^2 = 0.05$, Mann-Whitney U test, **Table 5-3** [supplementary]). This increase was driven by a higher level of elderly TBI patients demonstrating a moderate score for neuritic

Aß plaque deposition (8 of 38, 21%) compared to uninjured, age-matched controls (2 of 38, 5%; p = 0.042, Chi-squared, Cramer's V = 0.234).

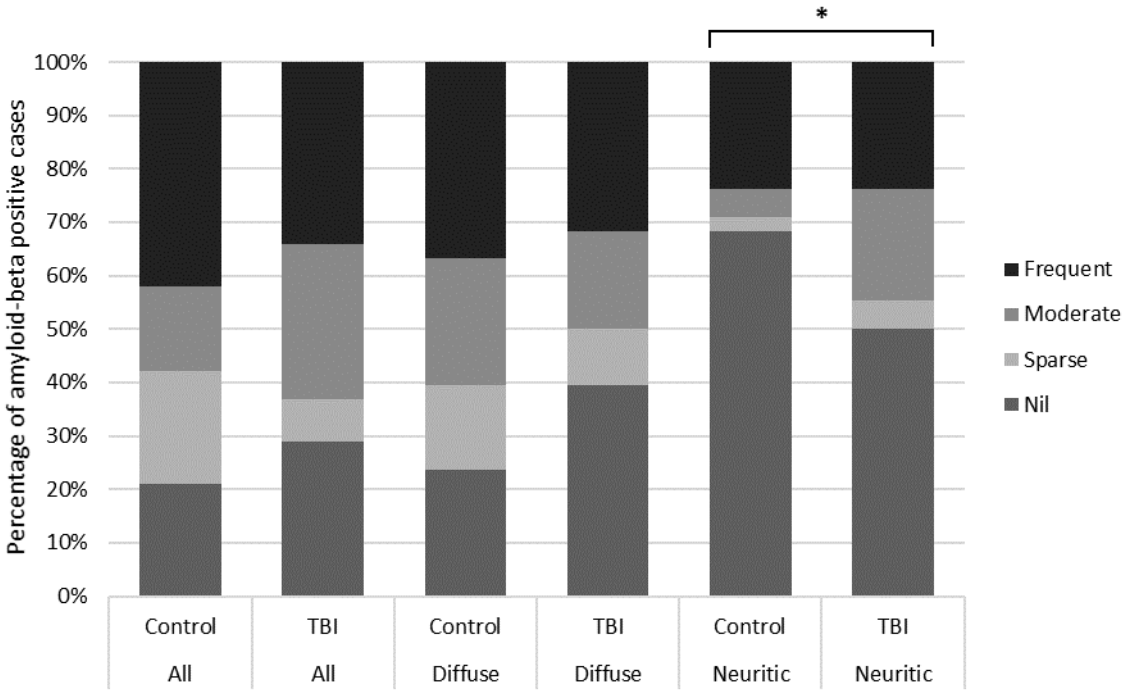

Figure 5-4 Graphical representation of the proportion of all, diffuse and neuritic Aβ plaque pathology within elderly-control and elderly TBI patients. An increase in the extent of neuritic plaque in elderly TBI patients compared to uninjured elderly-controls (* p <0.05, Mann-Whitney U test).

5.3.3 Regional differences in Aβ plaque

In both uninjured control and TBI cases, when present in the cingulate region, Aß plaques were found across cortical laminae and encroaching into superficial white matter in most extreme cases. Within hippocampal involvement, small aggregates of plaques were frequently observed in the inferior temporal gyrus, fusiform sulcus, and entorhinal cortex, whilst cases with more extensive plaques throughout the isocortex of the cingulate and level of the hippocampus plaques were also observed within the subiculum and hippocampal formation. Involvement

of the thalamic region saw sparse individual plaques distributed throughout the thalamic nuclei, largely surrounded by plaque-free neuropil. Sparse, diffuse plaques were located within both the molecular and granular layers of the cerebellar cortex.

The regional distribution of Aß plaque pathology was calculated using a modified version of the Thal *et al*. methodology (Thal 2002). When all plaque was analysed, this demonstrated an increase in the regional distribution of Aß plaque in elderly TBI patients compared to uninjured elderly-controls, with plaques observed in three or more regions examined in 15 of 38 elderly TBI cases (39.5%) compared to 5 of 38 (13.2%) elderly controls (p = 0.006; Chi-square test,). When diffuse Aß plaque alone was examined, there was a similar increase in the regional distribution of plaque, with plaques observed in 9 of the 38 elderly TBI patients (23.7%), and 4 of 38 (10.5%) of elderly, uninjured controls (p = 0.031; Chi-squared test). Lastly, the same pattern was also observed when examining only neuritic plaque, where plaques were seen in 3 or more regions examined in 7 of 38 elderly TBI cases (18.4%) compared to just 1 of the 38 uninjured elderly-controls (2.6%, p = 0.025, Chi-squared test, **Figure 5-5, Table 5-4**).

Table 5-4 Modified Thal score for regional distribution of Aß plaque within elderly controls and elderly TBI patients

	All plaque		**Diffuse plaque**		**Neuritic plaque**	
	Control	**TBI**	**Control**	**TBI**	**Control**	**TBI**
0 Regions	9	12	13	19	30	20
1-2 Regions	24	11	21	10	7	11
3-4 Regions	5	15	4	9	1	7
Chi-squared	**p = 0.006**		**p = 0.031**		**p = 0.025**	
Cramer's V	0.367		0.302		0.312	

This increase in the distribution of Aß plaque is driven by a hierarchical increase in plaque deposition in elderly TBI patients. Overall, Aß plaque was observed widely in the cingulate and hippocampal regions across cohorts, but deposits within the deeper thalamic regions were more frequently observed in elderly TBI (13 of 38, 34.2%) compared to elderly controls (5 of 38, 13.2%, p = 0.031 Chi-squared test, Cramer's V = 0.248). Aß plaques were also observed exclusively within the cerebellum of TBI survivors displaying extensive pathology across multiple other regions and were absent within this region in all uninjured, age-matched controls.

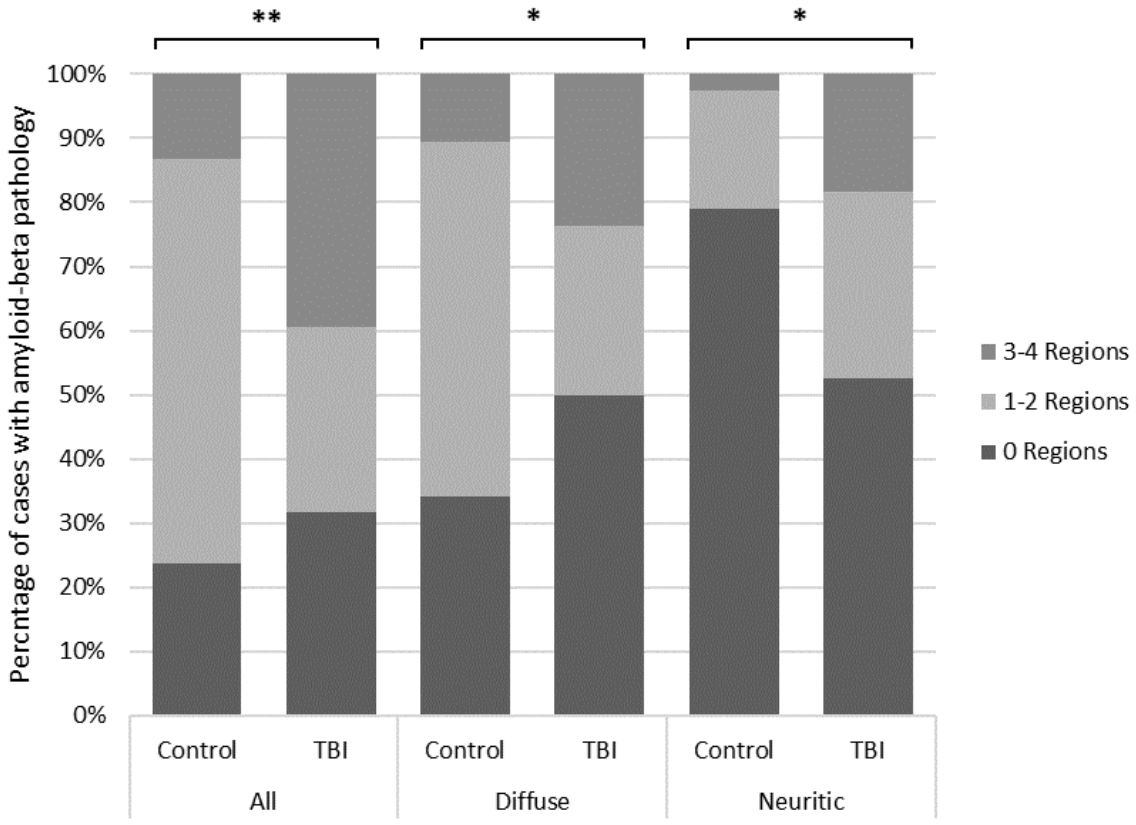

Figure 5-6 Graphical representation of the comparison of regional distribution of Aβ plaque for all, diffuse and neuritic plaque between elderly controls and elderly TBI patients. An increase in the proportion of elderly TBI cases with amyloid-beta plaque in 3-4 regions is present in all plaque subgroups, compared to uninjured elderly controls. (* $p < 0.05$, ** $p < 0.01$, Pearson's chi-squared).

5.3.4 Tau NFT pathology

The extent and distribution of NFTs across brain regions were examined using a modified version of the Braak et al (2006) method of semi-quantitative scoring (Johnson 2012). Both uninjured control and TBI cohorts demonstrated a similar extent and distribution of phospho-tau pathology, with NFTs present in 35 of 37 elderly uninjured control cases (95%) compared to 34 of 37 (92%) of elderly TBI patients (NS; Fisher's exact test, **Figure 5-6**).

Both elderly TBI and age-matched uninjured control cases demonstrated mild pathology, with occasional tau neurofibrillary tangles (NFTs) observed within the superficial layers of the transentorhinal cortex and sporadically within the CA1 region of the hippocampal formation. In elderly TBI and control cases with more severe NFT pathology, widespread tangles were observed throughout the hippocampal formation and subiculum, with comprehensive involvement of cortical laminae of the fusiform and entorhinal cortex as well as previously affected transentorhinal cortex. Additionally, in these cases, tau NFT pathology was observed throughout the crests of the cingulate gyrus, superficial frontal gyrus, and insular cortex, with clusters of tangles also observed at the sulcal depths.

Semi-quantitative analysis of density and distribution of tau NFT pathology demonstrated that TBI patients did not display more extensive pathology than age-matched, uninjured controls (NS, Mann-Whitney U test, **Figure 5-6**). In cases of uninjured elderly controls, 16 of 37 cases (43%) met the criteria for score 1 classification, with tangles in the transentorhinal cortex and CA1 of the hippocampus, while 19 of 37 (51%) of elderly patients who died acutely following TBI also scored 1. Score 2 classification for uninjured controls was 18 of 37 cases (49%) and 13 of 37 (35%) for TBI patients, with further extension of NFTs into the fusiform gyrus as well as equal pathology in the regions present for Score 1. Lastly, only 1 of 37 (3%) uninjured controls met the criteria of score 3 classification, with extensive NFTs throughout the hippocampus, subiculum, and greater involvement

of neocortical regions, whereas 2 of 37 TBI cases (5%) of cases were classed as Score 3 pathology.

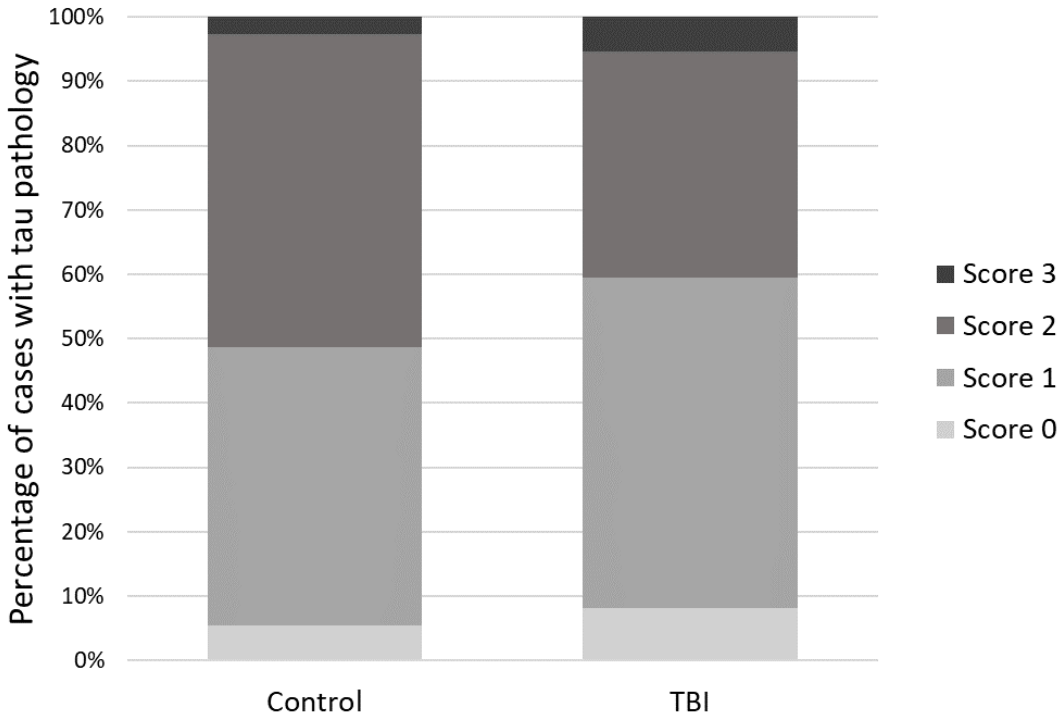

Figure 5-7 Graphical representation of extent and distribution of neurofibrillary tangles (NFTs) in elderly uninjured controls and elderly TBI patients. No increase in the extent or distribution of NFTs in elderly TBI patients compared to age-matched, elderly controls (NS; Fisher's exact test).

5.4 Discussion

This study demonstrates histological evidence of an increase in the extent of neuritic Aß plaque deposition in the acute period following moderate to severe single TBI, in elderly individuals compared to age-matched, uninjured controls. There was also a significant difference in the regional distribution of overall, diffuse and neuritic plaque, with an increase in the proportion of elderly TBI cases with Aß plaque pathology in three or more regions compared to uninjured elderly controls. Concurrently, there was no increase in the extent or distribution of NFTs in TBI patients compared to their uninjured counterparts.

Aß deposition is not only a hallmark and contributing driver of disease in AD (Ittner & Götz, 2011; Potter & Wisniewski, 2012; Selkoe & Hardy, 2016) but is also an age-associated pathology (Blumenthal, 2004; Price & Morris, 1999; Quigley et al., 2011; K. M. Rodrigue et al., 2009), known to precede any initial signs of cognitive decline. Estimates suggest that an interval of 20-30 years may occur between the primary development of Aß positivity and the onset of dementia (Jansen et al., 2015), while Aß deposition has been shown in 29% of healthy, older controls (Jack et al., 2009).

To this end, we would expect to observe Aß plaque pathology within both cohorts examined in this study, as they were pooled from across a spectrum of older patients. Our uninjured elderly controls were carefully selected to have no history of neurodegenerative disease and at post-mortem, any pathological changes were put down to normal ageing. However, one area where this study observed a difference, was in the extent of neuritic Aß plaque deposition in elderly TBI patients compared their age-matched, uninjured controls, where neuritic plaques were found in 53% of TBI patients compared to 29% of control participants. This is potentially substantial, as whilst diffuse plaque is known to accumulate in non-cognitively impaired normal ageing (Malek-Ahmadi et al., 2016; Morris, Storandt, McKeel, et al., 1996; Teissier et al., 2020b) and also in younger adult TBI patients in the acute period after moderate to severe TBI (Roberts 1994, Smith 2003, Ikonomovic 2004, DeKosky 2007), mature and densely-cored, neuritic plaques are related to later-stage clinical AD (Mirra et al., 1991) and long-term survival after moderate/severe sTBI in younger adults (Johnson et al., 2010, 2012).

The distribution of Aß plaque aggregates within regions of the brain is a diagnostic marker of AD, with a sequential development of plaque pathology in a hierarchical manner. The 2012 National Institute on Aging-Alzheimer's Association (NIA-AA) guidelines (Hyman 2012) utilises the system of grading disease progression set out by Thal et al., 2002, where Aß plaque deposition develops into regions which receive projections in an anterograde fashion, from areas which already display build-up of Aß plaques. Using a similar tiered method of grading the evolution of pathology within the brain, elderly TBI patients exhibited a pattern of Aß distribution which follows the model of disease of quantification set out by Thal et al for AD, whereby regional distribution increases with disease state and neuropathological decline.

Tau pathology is the other protein aggregate that we examined in this study, as it is again a major component for diagnosis of AD (Braak et al., 2006), seen to develop in typical ageing (Price & Morris, 1999)) as well as a pathology found in the chronic stages after TBI (Johnson et al., 2012) and in cases of repetitive TBI in younger-adult patients (Arena et al., 2020; Stewart et al., 2016). However, the changes in the extent and distribution of Aß plaques in the elderly TBI patients examined here was not paired with a similar increase in the extent or distribution of tau pathology compared to the elderly controls, similar to the lack of NFTs observed in the acute period following TBI in younger-adult patients (C. Smith et al., 2003). Therefore, age appears contribute to a greater extent on the development and progression of Aß pathology in the acute period following injury, as it seems to increase in isolation from other markers of disease such as NFTs.

Controlled cortical impact (CCI) models of TBI in aged mice demonstrate greater neurodegeneration and increased functional deficits compared to sham animals (Onyszchuk et al., 2008), while another study found an increase in thalamic pathology in aged mice following injury (Onyszchuk et al., 2009). This is akin to the increase in Aß pathology in the thalamic regions in elderly TBI patients we observed, compared to uninjured elderly controls ($p=0.031$, Chi-squared test). CCI models of TBI in transgenic AD mouse models have also been shown to rapidly develop amyloid-beta deposition within days of TBI (Washington et al., 2014), and while this has also been observed in correlation with increase in accumulation of NFTs (Tran et al., 2011), this was not observed in this study.

Interestingly, clearance of trauma-induced amyloid-beta deposits and reduction in cognitive deficits were observed in both Alzheimer's-transgenic (Washington et al., 2014) and wild-type mice (Shishido et al., 2019), suggesting TBI as a risk factor for acute cognitive impairment but that the transience of amyloid-beta deposition following TBI could limit the long-term contribution to neurodegeneration. Amyloid turnover and degradation of clearance pathways is believed to contribute to AD through a variety of mechanisms (Baranello et al., 2015; Cockerill et al., 2018; Hickman et al., 2008), pathways which may play a similarly important role in the clearance of Aß following TBI (Johnson et al., 2010). However, there is still little understanding of how the combination of TBI and age effects methods of amyloid turnover, but the acute development and distribution of neuritic, senile plaques observed in the elderly TBI cohort indicates that TBI could exacerbate the build-up of these proteins and result in a further backlog of clearance process.

This study observes a state of pathology of increased neuritic Aß plaque, which has developed within an acute timeframe of less than 2 weeks in these older TBI patients, similar to that seen in clinical Alzheimer's disease. One suggestion could be that these are patients who demonstrated an increase in the quantity of neuritic plaque and were exposed to a TBI due to the neurodegenerative processes which were already present within their brain, but which weren't demonstrating other cognitive changes which might have resulted in a clinical diagnosis of NDD. Aß pathology has long been thought of as an initial pathogenic event in AD development (Morris et al., 1996), and both post-mortem (Malek-Ahmadi et al., 2016) and imageing studies (Jack et al., 2009; Mintun et al., 2006; Pike et al., 2007; Rowe et al., 2007, 2010; Villemagne et al., 2021; Vlassenko et al., 2012) indicate that Aß pathology is present in approximately 25% portion of healthy older individuals aged over 75, whilst correlating with early memory changes in non-demented individuals (Lowe et al., 2009; Pike et al., 2007; Teissier et al., 2020b). Preclinical individuals are also at a higher risk of falls (Bollinger et al., 2021; Stark et al., 2013), while falls in cognitively normal individuals are associated with neurodegenerative markers such as Aß (Keleman et al., 2020). Therefore, if it is as thought, and Aß deposition is demonstrative of pre-clinical AD (Bäckman et al., 2005; Levey et al., 2006; Pike et al., 2007; Price & Morris, 1999; Small et al., 2007; D. R. Thal et al., 2004, 2014) and they are also at increased risk of TBI from falls, then these vulnerable individuals will benefit most widely from therapies

aimed at reducing amyloid burden (Panza et al., 2019; Shi et al., 2022; van Dyck et al., 2022)

The main limitation of this study is that it is a retrospective examination of a cohort of patients who have passed away following traumatic brain injury. The data available to us are from comprehensive pathology reports written by consultant pathologists, however we do not have access to a patient's entire clinical record. Information such as family history, post-injury treatment provision, cognitive assessment or any imaging examinations undergone would enable us to follow the progression of any neurodegenerative changes during their lifetime, and make this study more comparable to research into other neurodegenerative diseases such as AD. As such, it is not possible to link the observations in differences in the neuropathology with any clinical changes during the patient's lifetime as we do not have a record of each patient's pre-TBI functional status. These methodologies are increasingly being used in the field of human TBI research (PREVENT Football/Rugby), however this chapter considers purely the pathological changes observed in the brains of patients who were examined either following TBI or in age-matched, uninjured control subjects. Nevertheless, when stratifying by TBI severity and age, injury has been proven to sharply increase the risk of dementia across all ages (Gardner & Yaffe, 2014)

Cerebral ageing is a complex process, causing multiple age-related changes to brain size, vasculature, protein accumulation (Peters, 2006; Schöll et al., 2016), specifically the build of Aß deposits within the brain (Aizenstein et al., 2008; Gu et al., 2015; Malek-Ahmadi et al., 2016; K. Rodrigue et al., 2012), however it is not always associated with increased incidence of dementias. The relationship between the hallmarks of natural ageing and accelerated ageing of neurodegenerative disease such as AD are blurred, with the involvement of TBI-induced deposition and how it may relate to any resulting cognitive decline still an important question which highlights the importance of examining TBI in relation to appropriately age-matched uninjured controls. Roberts et al., 1994 observed an acute increase in the prevalence of plaque in their older cases, this study has gone further to examine the extent and distribution of amyloid-beta plaque and we demonstrate a similar increase in both, compared to uninjured controls. This

supports the theory that TBI is associated with an increase in the extent of neuritic plaque and change to the regional distribution of overall, diffuse and neuritic Aß plaque deposition in elderly patients.

Chapter 6 – Development of a protocol to analyse differences in proteomes of Alzheimer's disease, rTBI and uninjured controls

6.1 Introduction

Traumatic brain injury (TBI) is a major cause of morbidity and mortality globally with approximately 2.8 million people sustaining a TBI in the United States (US) each year (Taylor et al., 2017). TBI is also a leading environmental risk factor for the development of neurodegenerative disease later in life (Collins et al., 2020; Fleminger, 2003; Gardner & Yaffe, 2014; Gavett et al., 2010; Li et al., 2017; LoBue et al., 2018; Nordström & Nordström, 2018; Plassman & Grafman, 2015; Sivanandam & Thakur, 2012; Washington et al., 2016), in particular chronic traumatic encephalopathy (CTE). The chronic effects of TBI have been documented for almost 100 years, with the coinage of terms such as "traumatic encephalopathy" (Osnato & Giliberti, 1926) and "punch-drunk" symptoms (Martland 1928) leading to the use of the term CTE to describe the neuropathological changes observed following repetitive mild TBI (Edwards et al., 2017; McKee et al., 2009, 2013, 2015; Omalu et al., 2011; D. Smith et al., 2013b; Stewart et al., 2016) and in patients who survive in the long-term following a moderate to severe single TBI (Johnson et al., 2012; Kenney et al., 2018; Washington et al., 2016; Zanier et al., 2018). However, understanding of the cellular and molecular dynamics of both single and repeat TBI are lacking, and future work is required to provide insight into disease mechanisms and future therapeutic care.

Neuropathology observed after TBI is characterised not only by the initial primary pathology such as haemorrhagic damage and diffuse axonal injury, but also a secondary cascade of neurodegenerative processes associated with dementia, including cerebral atrophy (Bernick et al., 2020; Harris et al., 2018), neuroinflammation (Johnson, et al., 2013; Loane & Kumar, 2016) and proteinopathies. Misfolding and/or aggregation of proteins is a cornerstone pathology of neurodegenerative diseases, with Alzheimer's disease (AD) (Gamblin et al., 2003; Hardy & Selkoe, 2002; Ittner & Götz, 2011), frontotemporal dementia

(FTD) and amyotrophic lateral sclerosis (ALS) (Neumann et al., 2006), and Parkinson's disease (Polymeropoulos et al., 1997) all affected and defined by proteinopathies.

The abnormal accumulation of pathological proteins related to neurodegenerative disease is also seen both acutely and chronically following injury. In the acute phase after single moderate to severe TBI (sTBI), proteins such as alpha-synuclein (αsyn) (Ikonomovic et al., 2004; Newell et al., 1999), phospho-independent TAR DNA-binding protein 43 (TDP-43)(Johnson et al., 2011) and amyloid-beta (Aß) (DeKosky et al., 2007; Ikonomovic et al., 2004; G. W. Roberts et al., 1991, 1994; D. Smith et al., 2003) aggregate, while deposition of proteins is also observed in the chronic period following injury (Johnson et al., 2011, 2012; McKee et al., 2013). Patients exposed to repetitive mild TBI (rTBI) such as retired professional sports players, often demonstrate a differing phenotype of protein deposition to sTBI patients. Cytoplasmic phosphorylated, rather than TDP-43 contributes to a diagnosis of CTE (King et al., 2010; McKee et al., 2010, 2013, 2016), abundant diffuse Aß plaques (McKee et al., 2016; G. Roberts et al., 1990; Stein et al., 2015; Tokuda et al., 1991), and distinctive phosphorylated tau aggregates at depths of cortical sulci as neurofibrillary tangles (NFT) and glial tau inclusions (Arena et al., 2020; Kanaan et al., 2016; McKee et al., 2009, 2013; Mez et al., 2017; Saing et al., 2012; Schmidt. et al., 2001) are associated with CTE, and form a cornerstone of the disease staging in the current consensus diagnosis methodology (McKee et al., 2016).

Formalin fixed, paraffin embedded tissue (FFPE) has been used for decades to diagnose disease and evaluate tissue histology, but due to issues with protein extraction and peptide identification/quantification due to formaldehyde induced inter- and intra-molecular cross linking large archival FFPE tissue banks remain largely idle (Bedino, 2003; Tran et al., 2011). Quantitative proteomics of fresh post-mortem tissue of patients suffering from AD (Andreev et al., 2012; Butterfield & Castegna, 2003; Donovan et al., 2012; Sultana et al., 2007; Q. Wang et al., 2005) and PD (Basso et al., 2004; C. J. Werner et al., 2008) have identified proteins biochemically altered in disease, providing potential insight into key molecular pathways of neurodegeneration. Similarly, analysis of the proteome of frozen tissue from patients following TBI, highlight enrichment of proteins that are corelated with pathology staging (Abu Hamdeh, Shevchenko, et al., 2018; Cherry et al., 2018), with the hope that proteomic approaches may aid identification of

clinically useful biomarkers and advancement of therapeutic care (Lizhnyak & Ottens, 2015; Mi et al., 2014; Opii et al., 2007; K. Wang et al., 2004). Recent progress in methodologies of using FFPE tissue in proteomic research (Ostasiewicz & Wiśniewski, 2017; Tanca et al., 2012) has enabled recent studies to provide accurate and meaningful data, identifying novel disease associated proteins and pathways in AD (E. Drummond et al., 2017; E. S. Drummond et al., 2015).

The use of archival FFPE tissue from patients who have suffered a TBI would enable important comprehensive comparison of proteins aggregating within TBI and AD cohorts. The pathological changes driving post-TBI neurodegeneration and how they are related to other dementia diseases are still poorly understood, meaning that potential targets for intervention and specific therapies against development of dementia remain elusive. The opportunity to identify a unique marker of TBI pathology made possible by expanding the understanding the molecular changes following TBI could advance the field exponentially.

Aim: To develop a protocol for the successful identification of proteomes from archival FFPE tissue across a selection of cohorts including rTBI patients, individuals diagnosed with Alzheimer's disease and uninjured, age-matched controls.

6.2 Specific methods

6.2.1 Method 1: Laser microdissection of Aß plaques from FFPE tissue and downstream analysis

6.2.1.1 Case selection

All tissue was selected from the holdings of the Glasgow Traumatic Brain Injury Archive of the Department of Neuropathology, Glasgow, UK. All material was obtained following routine diagnostic autopsy examination at the same institution and approved for use in this study by the Greater Glasgow and Clyde Bio-repository Governance Committee.

A case with diagnosis of AD (n=1) and a case of a professional sports player with a history of rTBI (n=1) were selected from the archive. Detailed reports of diagnostic post-mortem evaluation were available. Full clinical and demographic information for each cohort in this overall study is presented in **Table 6-1**.

6.2.1.2 Brain tissue preparation

Whole brains underwent standard immersion fixation in 10% formal saline at autopsy for a minimum of 3 weeks prior to dissection, standardised sampling, block selection and processing to paraffin. For this portion of the study, paraffin tissue blocks from a coronal slice of the cerebral hemispheres at the level of the lateral geniculate nucleus were selected to include the cingulate gyrus and adjacent corpus callosum.

Table 6-1 Demographic and clinical information of chapter 6 cohorts

	Initial Methods Experiments		***Final Cohort***		
	AD (n=2)	**rTBI (n=4)**	**Controls (n=3)**	**AD (n=2)**	**rTBI (n=6)**
Mean age of tissue (range), years	31 (0)	7 (17)	23.3 (4)	31.0 (2)	2.5 (1-5)
Mean age (range), years	86 (6)	74 (10)	69.7 (7)	78.8 (20)	75.5 (14)
Males, n (%)	1 (50)	4 (100)	3 (100)	3 (100)	6 (100)
Mean post-mortem delay (range), hours	81 (0)	36 (12)	33.3 (52)	2.75 (0.5)	48 (0)
Professional Sport Participation, n (%)					
Football	n/a	*2 (50)*	n/a	n/a	*5 (83.3)*
Rugby	n/a	*1 (25)*	n/a	n/a	*1 (16.7)*
Boxing	n/a	*1 (25)*	n/a	n/a	*0*
Cause of death, n (%)					
Acute Cardiac Failure	-	-	*1(33.3)*	-	-
Alzheimer's disease	*1 (50)*	-	-	*2 (66.6)*	-
Bronchopneumonia	-	*1 (25)*	-	-	*1 (16.7)*
CTE	-	-	-	-	3 (50)
DLB	-	1 (25)	-	-	1 (16.7)
Normal pressure hydrocephalus	-	-	*1(33.3)*	-	-
Pulmonary ingestion	*1 (50)*	-	-	*1 (33.3)*	-
Respiratory Failure	-	-	*1(33.3)*	-	-
Sepsis	-	*1 (25)*	-	-	-
Unknown	-	-	n/a	-	-
Vascular dementia	-	*1 (25)*	-	-	*1 (16.7)*
Dementia Diagnosis					
AD	*2 (100)*	-	-	*3 (100)*	-

AD, Alzheimer's disease; CTE, Chronic traumatic encephalopathy: DLB, Dementia with Lewy Bodies; rTBI, repetitive TBI

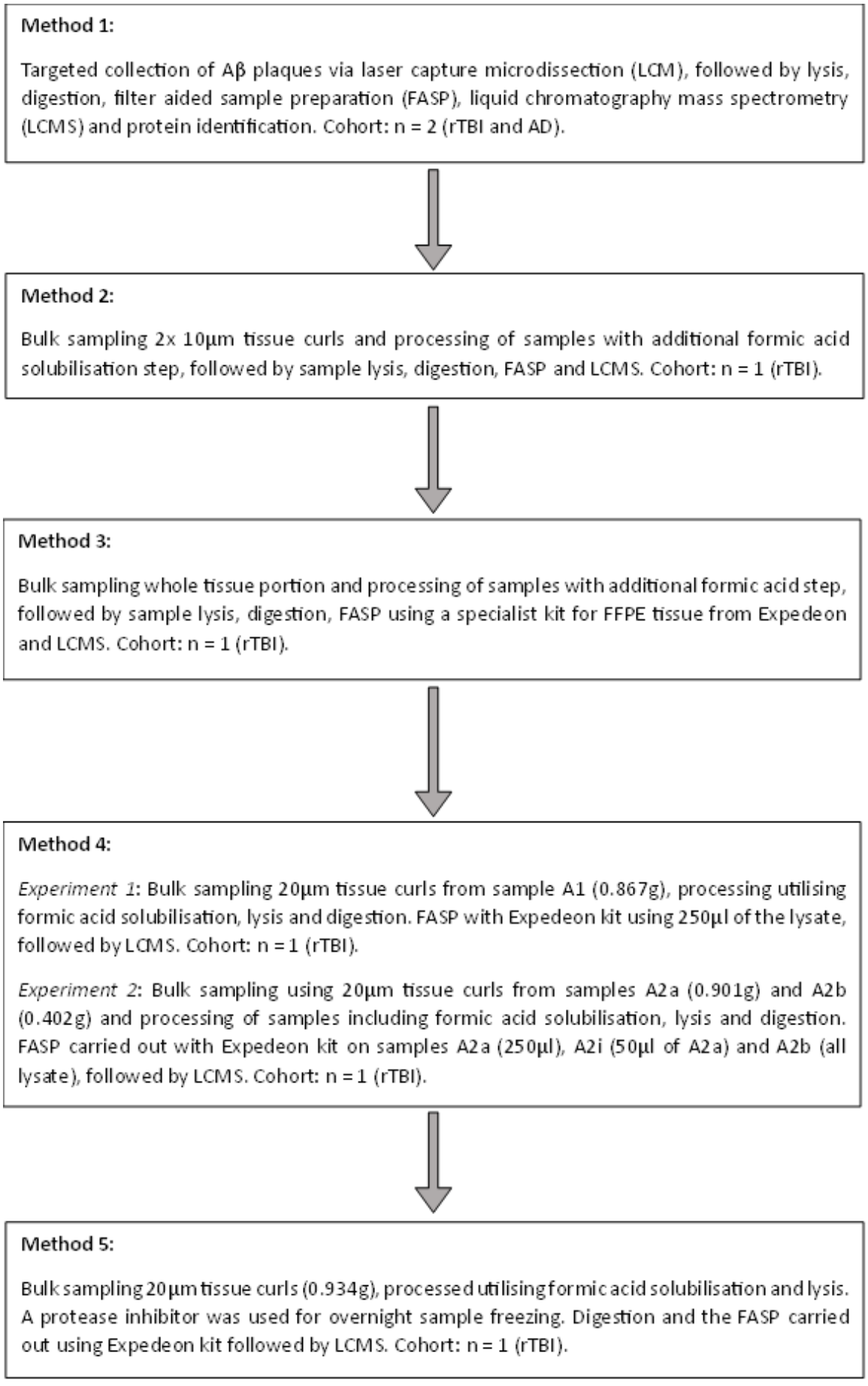

Figure 6-22 Representative structural outline of method development for proteomic analysis of archival FFPE

6.2.1.3 Immunohistochemistry

From the rTBI FFPE tissue block, 8µm-thick sections were prepared for immunohistochemistry. Sections were deparaffinised in xylene, rehydrated to water, and then immersed in aqueous solution of 3% hydrogen peroxide for 15 minutes to quench endogenous peroxidases. Antigen retrieval via microwave pressure cooker was performed for 8 minutes in preheated 0.1M citrate buffer, followed by blocking in 50µL of normal horse serum (Vector Laboratories, Peterborough, UK) per 5 mL of Optimax buffer (BioGenex, San Ramon, CA) for 30 minutes.

Once blocked, overnight incubation with primary antibodies was performed at 4°C for 20 hours. Primary antibody was selected to reveal Aß (clone 6F3D; 1:75; Dako, Santa Clara, CA). Following overnight incubation, biotinylated secondary antibody was then applied for 30 minutes (IgG, 1:200), followed by avidin-biotin complex as per the manufacturer's instructions (1:50; Vectastain Universal Elite kit, Vector Laboratories). Visualisation was achieved using 3,3'-diaminobenzidine (DAB) peroxidase substrate kit (Vector Laboratories) followed by counterstaining with haematoxylin. Sections were then left to air dry for 10 minutes.

6.2.1.4 Laser capture microdissection (LCM)

Microdissection of Aß plaques was undertaken using the Arcturus® XT system and CapSure® Macro LCM caps. Once the slide had been appropriately set up on the Arcturus, with a cap placed onto the relevant area of the section and set up for the infra-red (IR) laser with the relevant testing undertaken, targeted microdissection of Aß plaques was undertaken with the cap replaced upon the slide to capture approximately 300 plaques per cap. Caps were then moved to the QC station of the Arcturus and placed within a sterile microcentrifuge tube to be stored at -80°C until 30 caps had been collected.

6.2.1.5 Whole tissue section curl collection and dewaxing

From both tissue blocks, 2 10µm-thick sections were cut and placed into a sterile 1.5ml microcentrifuge tube using sterile disposable forceps until each sample had a total weight of 0.3g. A sterile environment was maintained at all times and between each sample.

To each microcentrifuge tube of a whole tissue section, 1ml of analar xylene was added and vortexed for 1 minute before being centrifuged at 13000rpm for 5 minutes. The xylene was decanted taking care to retain the section and 1ml of analar ethanol added, the tube vortexed for 1 minute and centrifuged at 13000rpm for 5 minutes. This step was repeated with a second wash of 1ml of ethanol and the waste ethanol decanted. Each microcentrifuge tube was covered with a layer of Parafilm and pierced several times and the samples dried in a heat block at 55-60℃ for 1-3 hours. Samples were then stored at -80℃ with the samples collected by LCM.

6.2.1.6 Sample lysis, digestion and filter aided sample preparation (FASP)

SDS lysis buffer was made up with 50ml of pH7.6 Tris, 2g 4% SDS and 0.75g of DTT (100mM) and cells lysed using a 1:10 sample to buffer ratio. All samples were thawed to room temperature. For the whole tissue samples 200µl of SDS lysis buffer was added and sample homogenised utilising a micro-pestle. For the LCM samples on the CapSure caps, each was placed on a flat, clean surface, film side up. 15µl of buffer was placed onto the surface of the cap film and incubated for 1 minute. The buffer was aspirated and dispensed up and down with a pipette several times to solubilise the plaques, being careful not to scrape the polymer surface of the cap. The extraction buffer was then collected in a microcentrifuge tube and samples from all caps collated into the one tube, reusing the SDS buffer so that a maximum of 200µl of buffer is used. Both whole tissue sample and collated LCM sample were then incubated at 95ºC for 5 minutes before being centrifuged at 16000xg for 5 minutes.

Urea buffer A (UA) was made up using 20ml of 100mM tris (pH 8.5) and 9.6g of urea (8M) and Urea buffer B (UB) using 10ml of 100mM tris (pH 8.0) and 4.8g of urea (8M). Iodoacetamide (IAA) was made up using 10mls of UA and 0.09g of IAA,

it must be kept in the dark. Ammonium bicarbonate solution was made using 50mls of dH_2O and 0.175g of ammonium bicarbonate.

Up to 30µl of protein extract was placed in the filter unit along with 200ul of UA and centrifuged at 14000xg for 40 minutes with this step repeated again. The flow-through from the collection tube was discarded and 100ul of IAA solution placed in the filter unit, mixed at 600rpm for 1 minute before incubating without movement for 20 minutes. 100ul of UB was placed in the filter unit and centrifuged at 14000xg for 40 minutes. 40ul of UB with endoproteinase Lys-C (at an enzyme to protein ratio of 1:50) was placed in the filter unit, mixed at 600 rpm for 1 minute before incubation in a wet chamber overnight. Samples in the filter units were transferred to a new collection tube and 120ul of ammonium bicarbonate solution with trypsin (at an enzyme to protein ratio of 1:100) was added to each filter unit, mixed at 600rpm for 1 minute and incubated at room temperature for 4 hours. The filter units were spun at 14000xg for 40 minutes. 50ul of 0.5M sodium chloride in 10% acetyl nitrate was added to each spin filter unit and centrifuged at 14000xg for 20 minutes. Samples were now in the final collection tube and acidified with 1% trifluoracetic acid.

6.2.1.7 Liquid-chromatography mass-spectrometry (LCMS) and protein identification

Dry peptides residues were solubilized by 5% acetonitrile with 0.5% formic acid using the auto-sampler of a nanoflow uHPLC system (Thermo Scientific RSLCnano). Online detection of peptide ions was by electrospray ionisation (ESI) mass spectrometry MS/MS with an Orbitrap Elite MS (Thermo Scientific).

Ionisation of LC eluent was performed by interfacing the LC coupling device to an NanoMate Triversa (Advion Bioscience) with an electrospray voltage of 1.8 kV. An injection volume of 1-2 µL of the reconstituted protein digest were desalted and concentrated for 10 min on trap column (0.3 × 5 mm) using a flow rate of 25 ▫l / min with 1 % acetonitrile with 0.1 % formic acid. Peptide separation were performed on a Pepmap C18 reversed phase column (50 cm × 75 µm, particle size 3 µm, pore size 100 Å, Thermo Scientific) using by a solvent gradient at a fixed solvent flow rate of 0.3 ▫l / min for the analytical column. The solvent composition was A) 5 % DMSO, 0.1 % formic acid in water B) 5 % DMSO, 0.1 % formic acid in acetonitrile. The solvent gradient was 4 % B for 10 min, 4 to 32 % for 170 min, 32

to 80 % for 15 min, held at 80 % for 5 min. A further 10 minutes at initial conditions for column re-equilibration was used before the next injection.

The Orbitrap Elite acquired full-scan MS in the range 300 to 2000 m/z for a high-resolution precursor scan at 30,000 RP (at 400 m/z), while simultaneously acquiring up to the top 20 precursors were isolated at 0.7 m/z width and subjected to CID fragmentation (35 % NCE) in the linear ion trap using rapid scan mode. Singly charged ions are excluded from selection, while selected precursors are added to a dynamic exclusion list for 30s.

Protein identifications were assigned using the Mascot search engine (v2.6.2, Matrix Science) to interrogate protein sequences in the NCBI Genbank database, allowing a mass tolerance of 10 ppm for the precursor and 0.3 Da MS/MS matching.

6.2.1.8 Repeat sample preparation for second samples

Certain steps in this methodology were repeated for a second cohort (**Table 6.1**), where LCM was undertaken on sections taken through IHC for Aβ, from 1 case with a history of rTBI and 2 cases with a diagnosis of AD, and Aβ plaques collected using the Arcturus® XT system and CapSure® Macro LCM caps. These samples then went through the same sample lysis, digestion and FASP followed by LCMS and protein identification.

6.2.2 Method 2: Proteomic analysis of FFPE whole tissue section with additional formic acid solubilisation

6.2.2.1 Case selection

All tissue was selected from the holdings of the Glasgow Traumatic Brain Injury Archive of the Department of Neuropathology, Glasgow, UK. All material was obtained following routine diagnostic autopsy examination at the same institution and approved for use in this study by the Greater Glasgow and Clyde Bio-repository Governance Committee.

A case of a professional sports player with a history of rTBI (n=1) was selected from the archive. Detailed reports of diagnostic post-mortem evaluation were available. Full clinical and demographic information for each cohort in this overall study is presented in **Table 6.1**.

6.2.2.2 Brain tissue preparation

This was carried out as seen in **6.2.1.2**

6.2.2.3 Whole tissue section curl collection and dewaxing

From the tissue block, 2x 10µm-thick sections were cut and placed into a sterile 1.5ml centrifuge tube using sterile disposable forceps until each sample had a total weight of 0.3g. Two samples were collected from this case for comparison of downstream proteomics with additional formic acid solubilization step and without. A sterile environment was maintained at all times and between each sample.

To each microcentrifuge tube of a whole tissue section, 1ml of analar xylene was added and vortexed for 1 minute before being centrifuged at 13000xg for 5 minutes. The xylene was decanted taking care to retain the section and 1ml of analar ethanol added, the tube vortexed for 1 minute and centrifuged at 13000xg for 5 minutes. This step was repeated with a second wash of 1ml of ethanol and the waste ethanol decanted. Each microcentrifuge tube was covered with a layer of Parafilm and pierced several times and the samples dried in a heat block at 55-60℃ for 1-3 hours and samples stored at -80℃.

6.2.2.4 Formic acid solubilisation

Formic acid (FA) solution was made up at 70% using LCMS-grade FA and LCMS-grade dH_2O. 100mM ammonium bicarbonate, 20% acetyl nitrate was made up using 0.395g of ammonium bicarbonate in 40ml of dH_2O and 10ml of ACN.

Each sample was thawed to room temperature and 150ul of the 100mM ammonium bicarbonate, 20% acetyl nitrate added to each sample and centrifuged at 14000xg for 5 minutes. Both samples were incubated at 95ºC for 1 hour and then 65ºC for 2 hours in preheated heat blocks with each sample wrapped in parafilm to keep the microcentrifuge tubes closed. The samples were cooled to room temperature and spun at 14500xg for 3 minutes before being placed in the SpeedVac vacuum centrifuge to dry out for approximately an hour. 90ul of the formic acid was placed into one sample, vortexed well and both samples incubated at room temperature overnight.

Both samples were then sonicated for 5 minutes using a water bath sonicator and vortexed 3 times in that 5 minutes before the formic acid sample was dried in the SpeedVac vacuum centrifuge. The samples were then resuspended in 200ul of SDS lysis buffer made up with 50ml of pH7.6 Tris, 2g 4% SDS and 0.75g of DTT (100mM) and homogenised with a micro-pestle.

6.2.2.5 Sample lysis, digestion, FASP, LCMS and protein identification

This was carried out using the same protocol as **6.2.1.6** and **6.2.1.7**

6.2.3 Method 3: Proteomic analysis of FFPE whole tissue portion with specialised FFPE FASP kit

6.2.3.1 Case selection

All tissue was selected from the holdings of the Glasgow Traumatic Brain Injury Archive of the Department of Neuropathology, Glasgow, UK. All material was obtained following routine diagnostic autopsy examination at the same institution and approved for use in this study by the Greater Glasgow and Clyde Bio-repository Governance Committee.

A case of a professional sports player with a history of rTBI (n=1) was selected from the archive. This case was selected due to the abundance of tissue available for this methodology. Detailed reports of diagnostic post-mortem evaluation were

available. Full clinical and demographic information for each cohort in this overall study is presented in **Table 6.1**.

6.2.3.2 Brain tissue preparation

Whole brains underwent standard immersion fixation in 10% formal saline at autopsy for a minimum of 3 weeks prior to dissection, standardised sampling, block selection and processing to paraffin. For this portion of the study, a paraffin tissue block from a coronal slice of the cerebral hemispheres at the level of the lateral geniculate nucleus were selected to include the frontal cortex.

6.2.3.3 Lysis, digestion, FASP using FFPE-FASP kit

The selected paraffin block was melted, and tip of gyrus removed to the weight of 0.693g, divided into smaller pieces and placed in a 15ml centrifuge tube. To the sample, 1ml of xylene was added and it was incubated with gentle agitation for 5 minutes. The sample was then centrifuged at 5,000xg for 5 minutes and excess xylene removed before repeating the process. To the sample, 1ml of absolute ethanol was added, centrifuged at 5000xg for 5 minutes and waste ethanol removed before repeating this process. The sample was then divided between two sterile 1.5ml microcentrifuge tubes before placed in a centrifugal vacuum for 30 minutes to dry the sample out. The tube was then weighed to enable accurate calculation of trypsin dilution required in later steps. The sample was then homogenised with universal protein extraction buffer (UPX - FFPE FASP Kit, Expedeon, San Diego, CA, US) using a dounce homogenizer and each sample tube covered with Parafilm whilst was incubated at 150°C for 30 minutes with agitation. The sample was then cooled to room temperature and pelleted at 14,000xg for 15 minutes. The lysate for was then collated from the two microcentrifuge tubes.

50µl of lysate was placed in the spin filter unit with 200µl of urea solution (FFPE FASP Kit, Expedeon, San Diego, CA, USA) and centrifuged at 15000xg for 30 minutes. This was repeated a total of 5 times to use all of the lysate in the same sin filter tube with waste from the collection tube removed when full. At the same

time a control tube with only urea underwent the same process. The sample was then vortexed with 90µl of urea solution and 10 µl of 10x iodoacetamide solution (FFPE FASP Kit, Expedeon, San Diego, CA, USA) for 1 minute before incubation in the dark for 20 minutes at room temperature. This was then centrifuged at 15000xg for 10 minutes. 100µl of urea solution was added and centrifuged for 15 minutes, this was repeated twice. The collection tube was emptied of waste at this point. 100µl of 50mM ammonium bicarbonate (FFPE FASP Kit, Expedeon, San Diego, CA, USA) was added to the spin filter and the sample centrifuged for 10 minutes at 15000xg, this stage was also repeated twice. The sample was moved to a new collection tube and 75µl of the trypsin solution (made up to a ratio of 1:100 of enzyme to protein at 0.05µg/µl in 50mM ammonium bicarbonate) and incubated in a heat block at 37ºC for 18 hours with the tubes covered in parafilm to minimise evaporation.

The spin filter was placed into a new collection tube and spun at 14,000 x g for 10 minutes. To the spin filter, 50µl of 50mM ammonium bicarbonate was added and the sample spun at 14, 000 x g for 10 minutes before 50µl of acetyl nitrile was added and the sample spun again at 14,000 x g for 10 minutes. Lastly, 1µl of trifluoroacetic acid was added to the collection tube and vortexed to produce the final protein digest. 100µl of the sample was then placed into a multiwell liquid chromatography-mass spectrometry tray and transferred to the centrifugal vacuum dryer to dry before repeating this process to utilise all of the protein digest sample.

6.2.3.4 LCMS and protein identification

This was performed as in **6.2.1.7**.

6.2.4 Method 4: Proteomic analysis of FFPE whole tissue section to optimise amount of lysate used with specialised FFPE-FASP kit

6.2.4.1 Case selection

All tissue was selected from the holdings of the Glasgow Traumatic Brain Injury Archive of the Department of Neuropathology, Glasgow, UK. All material was obtained following routine diagnostic autopsy examination at the same institution and approved for use in this study by the Greater Glasgow and Clyde Bio-repository Governance Committee.

A case of a professional sports player with a history of rTBI (n=1) was selected from the archive. Detailed reports of diagnostic post-mortem evaluation were available. Full clinical and demographic information for each cohort in this overall study is presented in **Table 6.1**.

6.2.4.2 Brain tissue preparation and whole tissue section curl collection

Brain tissue preparation was performed as in **6.2.3.2**.

From the tissue block, 20µm-thick sections were cut and placed into a sterile 1.5ml centrifuge tube using sterile disposable forceps. Two samples were collected from this case for comparison of downstream proteomics with to optimise the amount of lysate used with the following total weights for each sample: A2 weighed 0.9g, A2b weighed 0.4g.

6.2.4.3 Lysis, digestion, FASP using FFPE-FASP kit

To each sample, 2ml of xylene was added and it was incubated with gentle agitation for 5 minutes. The sample was then centrifuged at 5,000xg for 5 minutes and excess xylene removed before repeating the process. To the sample, 2ml of absolute ethanol was added, centrifuged at 5000xg for 5 minutes and waste ethanol removed before repeating this process. The sample was divided between two sterile 1.5ml microcentrifuge tubes before placed in a centrifugal vacuum for

30 minutes to dry the sample out. The sample pellet was weighed to enable accurate calculation of trypsin dilution required in later steps. The sample was homogenised with universal protein extraction buffer (UPX - FFPE FASP Kit, Expedeon, San Diego, CA, USA) using a dounce homogenizer and each sample tube covered with Parafilm whilst was incubated at 150°C for 30 minutes with agitation. The sample was then cooled to room temperature and pelleted at 14,000xg for 15 minutes. The lysate for was then collated from the two microcentrifuge tubes.

To optimise the amount of lysate utilised and reduce the number of times the sample has to be spun through the spin filter unit, there were three samples which went through the FFPE-FASP protocol. Sample A2i was 50ul of the lysate from sample A2 (original weight 0.9g of FFPR tissue), sample A2 was the remainder of the lysate from the 0.9g sample and sample A2b was all the lysate from the smaller FFPE whole tissue curls with an original weight of 0.4g.

50µl of lysate was placed in the spin filter unit with 200µl of urea solution (FFPE FASP Kit, Expedeon, San Diego, CA, USA) at any one time and centrifuged at 15000xg for 30 minutes. This was repeated for samples A2 and A2b to use all of the lysate in their respective spin filter units, with waste from the collection tube removed when full. At the same time a control tube with only urea underwent the same process.

The samples were then vortexed with 90µl of urea solution and 10 µl of 10x iodoacetamide solution (FFPE FASP Kit, Expedeon, San Diego, CA, USA) for 1 minute before incubation in the dark for 20 minutes at room temperature. These were then spun at 15000xg for 10 minutes. 100µl of urea solution was added and centrifuged for 15 minutes, this was repeated twice. The collection tubes were emptied of waste at this point. 100µl of 50mM ammonium bicarbonate (FFPE FASP Kit, Expedeon, San Diego, CA, USA) was added to the spin filters and the samples centrifuged for 10 minutes at 15000xg, this stage was also repeated twice. The samples in the spin filter unit were moved to a new collection tube and 75µl of the trypsin solution (made up to a ratio of 1:100 of enzyme to protein at 0.05µg/µl in 50mM ammonium bicarbonate relative to the weight of each sample) and incubated in a heat block at 37 C for 18 hours with the tubes covered in parafilm to minimise evaporation.

The spin filter was placed into a new collection tube and spun at 14,000 x g for 10 minutes. To the spin filter, 50µl of 50mM ammonium bicarbonate was added and the sample spun at 14, 000 x g for 10 minutes before 50µl of acetyl nitrile was added and the sample spun again at 14,000 x g for 10 minutes. Lastly, 1µl of trifluoroacetic acid was added to the collection tube and vortexed to produce the final protein digest. 100µl of the sample was then placed into a multiwell liquid chromatography-mass spectrometry tray and transferred to the centrifugal vacuum dryer to dry before repeating this process to utilise all of the protein digest sample.

6.2.4.4 LCMS and protein identification

This was performed as in **6.2.1.7**.

6.2.5 Method 5: Proteomic analysis of FFPE whole tissue section with specialised FFPE FASP kit and the use of a protease inhibitor to prepare for multiple samples

6.2.5.1 Case selection

All tissue was selected from the holdings of the Glasgow Traumatic Brain Injury Archive of the Department of Neuropathology, Glasgow, UK. All material was obtained following routine diagnostic autopsy examination at the same institution and approved for use in this study by the Greater Glasgow and Clyde Bio-repository Governance Committee.

A case of a professional sports player with a history of repetitive TBI (n=1) was selected from the archive. Detailed reports of diagnostic post-mortem evaluation were available. Full clinical and demographic information for each cohort in this overall study is presented in **Table 6.1**.

6.2.5.2 Brain tissue preparation and whole tissue section curl collection

Whole brains underwent standard immersion fixation in 10% formal saline at autopsy for a minimum of 3 weeks prior to dissection, standardised sampling, block selection and processing to paraffin. For this portion of the study, paraffin tissue blocks from a coronal slice of the cerebral hemispheres at the level of the lateral geniculate nucleus were selected to include the frontal cortex.

From the tissue block, 20µm-thick sections were cut and placed into a sterile 15ml centrifuge tube using sterile disposable forceps.

6.2.5.3 Lysis, digestion, FASP using a FFPE-FASP kit with protease inhibitor

To the sample in the 15ml centrifuge tube, 2ml of xylene was added and were incubated with gentle agitation for 5 minutes. The sample was centrifuged at 5,000xg for 5 minutes and the excess xylene removed before repeating the process. To the sample, 2ml of absolute ethanol was added, sample centrifuged at 5000xg for 5 minutes and waste ethanol removed before repeating this process. The sample was then divided between two sterile 1.5ml microcentrifuge tubes before placed in a centrifugal vacuum for 30 minutes to dry the sample out. The sample pellet was then weighed to enable accurate calculation of trypsin dilution required in later steps. The universal protein extraction buffer (UPX - FFPE FASP Kit, Expedeon, San Diego, CA, US) was then made up with protease inhibitor (Expedeon, San Diego, CA, US) to obtain a 1x concentration (5mM). Each sample was homogenised with UPX buffer/protease inhibitor solution using a dounce homogenizer and each sample tube covered with Parafilm whilst was incubated at 150°C for 30 minutes with agitation. The sample was then cooled to room temperature and pelleted at 14,000xg for 15 minutes. The lysate for the sample was then collated from the two microcentrifuge tubes - with care taken to not include any cellular debris or lipids, into one and placed in a freezer at -80°C overnight.

Once defrosted, the samples were spun at 14,000xg for 10 minutes to separate any cellular debris or lipids. Then 50µl of the sample was aliquoted into a spin

filter and the remainder of the sample placed into a -80°C freezer. Into the spin filter of each sample, 200µl of urea solution (1ml of Tris hydrochloride per tube of urea – FFPE FASP kit, Expedeon, San Diego, CA, US) was added and the sample spun at 14, 000 x g for 30 minutes. This was then repeated, and the sample spun for 20 minutes. The flow through from the collection tube was discarded and 90µl of urea solution and 10µl of 10x IAA solution (100µl of urea per black tube of IAA - FFPE FASP kit, Expedeon, San Diego, CA, US) added to the spin filter which was then incubated in the dark for 20 minutes without agitation. The spin filter was then spun at 14,000xg for 10 minutes. To the spin filter, 100µl of urea solution was added and all samples were spun at 14,000xg for 15 minutes, this was repeated twice. Subsequently, 100µl of 50mM ammonium bicarbonate (FFPE FASP kit, Expedeon, San Diego, CA, USA) was added to each spin filter which was spun at 14,000xg for 10 minutes, and this process repeated twice. The flow through from the collection tube was discarded.

Trypsin solution was then added to the spin filter (75µl made up to a 1µg trypsin: 100µg protein dilution in 50mM ammonium bicarbonate), vortexed for 1 minute and incubated at 37ºC for 18 hours with the spin filter wrapped in Parafilm to minimise the effects of evaporation of the digest.

Any sample which had condensed onto the lid of the spin filter was then pipetted back into the spin filter which was then placed into a new collection tube and spun at 14,000 x g for 10 minutes. To each spin filter, 50µl of 50mM ammonium bicarbonate was added and the samples spun at 14, 000 x g for 10 minutes before 50µl of acetyl nitrile was added and the sample spun again at 14,000 x g for 10 minutes. Lastly, 1µl of trifluoroacetic acid (TFA) was added to the collection tube and vortexed to produce the final protein digest.

To prepare the sample for LCMS, 100µl of the sample was then placed into a multiwell liquid chromatography-mass spectrometry tray and transferred to the centrifugal vacuum dryer to dry before repeating this process to utilise all of the protein digest sample.

6.2.5.4 Nanoflow HPLC electrospray tandem mass spectrometry (nLC-ESI-MS/MS) and protein identification

Dry peptides residues were solubilized in 20 µL 5 % acetonitrile with 0.5 % formic acid using the auto-sampler of a nanoflow uHPLC system (Thermo Scientific RSLCnano). Online detection of peptide ions was by electrospray ionisation (ESI) mass spectrometry MS/MS with an Orbitrap Elite MS (Thermo Scientific). Ionisation of LC eluent was performed by interfacing the stainless steel nanobore needle with an electrospray voltage of 2.0 kV. An injection volume of 5 µL of the reconstituted protein digest were desalted and concentrated for 12 min on trap column (0.3 × 5 mm) using a flow rate of 25 µl / min with 1 % acetonitrile with 0.1 % formic acid. Peptide separations were performed on a Pepmap C18 reversed phase column (75 cm × 75 µm, particle size 2 µm, pore size 100 Å, Thermo Scientific) using by a solvent gradient at a fixed solvent flow rate of 0.3 µl / min for the analytical column inside a thermostat column oven held at a constant 60°C. The solvent composition was A) 0.1 % formic acid in water B) 0.08 % formic acid in 80% acetonitrile 20% water. The solvent gradient was 4 % B for 12 min, 4 to 60 % for 102 min, 60 to 99 % for 14 min, held at 99 % for 5 min. A further 9 minutes at initial conditions for column re-equilibration was used before the next injection. The Orbitrap Elite acquired full-scan MS in the range 300 to 2000 m/z for a high-resolution precursor scan at 60,000 RP (at 400 m/z), while simultaneously acquiring up to the top 20 precursors were isolated at 0.7 m/z width and subjected to CID fragmentation (35 % NCE) in the linear ion trap using rapid scan mode. Singly charged ions are excluded from selection, while selected precursors are added to a dynamic exclusion list for 30s.

Protein identifications were assigned using the Mascot search engine (v2.6.2, Matrix Science) to interrogate protein sequences in the Swissprot database using human taxonomy, allowing a mass tolerance of 10 ppm for the precursor and 0.3 Da MS/MS matching.

6.2.6 Method 5 – Final Samples: Proteomic analysis of a cohort of FFPE whole tissue sections using FFPE-FASP kit and protease inhibitor to compare samples within TBI sub-cohorts and AD

6.2.6.1 Case selection

All tissue was selected from the holdings of the Glasgow Traumatic Brain Injury Archive of the Department of Neuropathology, Glasgow, UK. All material was obtained following routine diagnostic autopsy examination at the same institution and approved for use in this study by the Greater Glasgow and Clyde Bio-repository Governance Committee.

One case of a professional sports players with a history of rTBI was selected from the archive for the first experiment using this method, while 6 rTBI cases of professional sports players with a history of repetitive TBI, alongside cases with a known diagnosis of AD (n=3), and age-matched controls (n=3) with no known history of TBI or neurological disease were selected for the second experiment. Detailed reports of diagnostic post-mortem evaluation were available. Full clinical and demographic information for each cohort in this overall study is presented in **Table 6.1**.

6.2.6.2 Brain tissue preparation and whole tissue section curl collection

Whole brains underwent standard immersion fixation in 10% formal saline at autopsy for a minimum of 3 weeks prior to dissection, standardised sampling, block selection and processing to paraffin. For this portion of the study, paraffin tissue blocks from a coronal slice of the cerebral hemispheres at the level of the lateral geniculate nucleus were selected to include the frontal cortex.

For the first experiment, from the tissue block, 20µm-thick sections were cut to a weight of 0.9g and placed into a sterile 15ml centrifuge tube using sterile disposable forceps. For the second experiment, 20µm-thick sections were cut to a weight of 0.921g - 1.103g and placed into individual sterile 15ml centrifuge tube using sterile disposable forceps.

6.2.6.3 Lysis, digestion, FASP using FFPE-FASP kit with protease inhibitor

This was undertaken using the protocol in **6.2.5.3**.

6.2.6.4 Nanoflow HPLC electrospray tandem mass spectrometry (nLC-ESI-MS/MS)

This was undertaken using the protocol in **6.2.5.4**.

6.2.6.5 Protein identification

Protein identifications were assigned using the MaxQuant search engine (v1.6.5.0, Max Plank Institute, DE) to interrogate protein sequences in the UniProt database using human taxonomy (uniprot-proteome_UP000005640_human_22042020). Perseus software (v1.6.1.5, Max Plank Institute, DE) was subsequently used to process results to filter by: site, reverse, contaminants, identification by > 1 peptide, before being grouped into cohorts and filtered so as to only include proteins identified in ≥70% of cases within a cohort.

6.2.7 Statistical analysis

All data were analysed using SPSS (Version 27; IBM, Inc) and R Project (R Foundation for Statistical Computing, AT). In SPSS, one-way ANOVA tests with Tukey post hoc test, were used to assess the differences in data between and within cohorts where applicable. Using Searchlight in R Project (Cole et al., 2021), for principal component analysis and Student's t-test to compare protein expression between cohorts. All differences were significant where $p \leq 0.05$. Effect size was measured using the partial Eta squared (η_p^2); where 0.01 represents small effect size, 0.06 medium effect size, and > 0.14 large effect size.

6.3 Results

6.3.1 Method 1: Laser capture microdissection (LCM) of Amyloid-ß (Aß) plaques from FFPE tissue and downstream analysis.

LCM was used to identify and extract targeted Aß plaques from FFPE sections cut on to standard slides and stained for BA4 primary antibody. Aß plaques were observed using the microscope of the LCM and accurately removed from the tissue section using the infra=red (IR) target spot and adhered to the thermoplastic of the LCM caps (**Figure 6-1**).

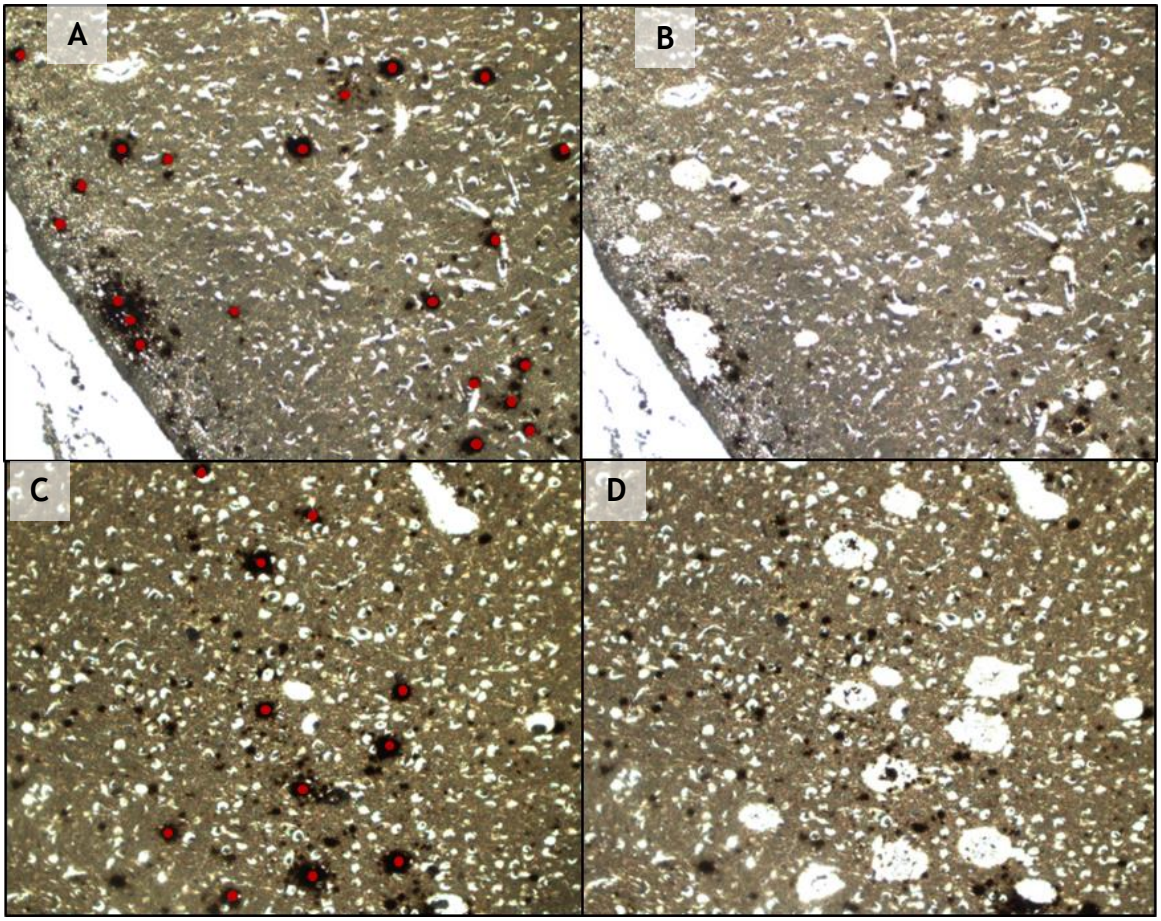

Figure 6-2 Representative images of targeted collection of amyloid-ß plaques gathered using laser capture microdissection (LCM). From the cingulate sulcus of a 79-year-old male former rugby player exposed to rTBI. (**A**) and (**C**) from before targeted collection, with red dots indicating the plaques to be captured and (**B**) and (**D**) of the same region after microdissection using an IR laser (Red dot). Scale bar = 500µm.

Once all appropriately sized plaques had been removed from the field of view of the LCM, the cap we repositioned to allow for further collection of Aß plaques until the necessary 300 had been collected and the cap was then frozen at -80°C in a microcentrifuge tube. On average, each cap was replaced onto the tissue slide 3 times.

Three samples were run for experiment 1 in this first methodology, 1 of Aß plaques selectively collected from the rTBI case using the LCM - Sample ID: 'AP'. Two samples prepared from 20µm whole section tissue curls – Sample ID: 'H' and 'C' (**Table 6-1**). This was carried out to assess the abundance of peptides present in each sample and to calculate whether the correct number of Aß plaques have been collected and whether whole section sample would produce too high a level of protein for the liquid chromatography–mass spectrometer (LCMS) to quantify.

The Spot Size of the IR laser had three settings which could be adjusted to allow for adequate power for collection of different sized Aß plaques. These were checked and modified depending on the appearance of the Aß plaques for each section. The LCM was carried out on non-coverslipped sections which air dried before being placed onto the stage of the LCM, this meant that sections could dry out and required careful attention to make sure that the sections were adequately but not overly dried out.

There was a large degree of variety in the number of protein hits observed in these samples (**Table 6-2**), but the sample processed using the LCM method (sample "AP") produced a far greater protein load of 543 than either of the samples so was decided to be the optimal protocol to move forward with. However, subsequent samples could not replicate this initial high output of proteins observed in sample "AP" (**Table 6-2**), so following experiments were derived with the aim of improving the protein read-out obtained from whole tissue curl samples, due to the time consuming and costly nature of collecting samples using LCM.

Table 6-2 Protein output for preliminary method experiments

Method 1 - Experiment 1					
Sample ID	**Case**	**Cohort**	**Sample type**	**Sample weight**	**Protein hits**
AP	A150016	rTBI	LCM Amyloid Plaque	n/a	543
H	A150016	rTBI	Whole tissue curl	n/a	4
C	A890001	AD	Whole tissue curl	n/a	90
Method 1 - Experiment 2					
Sample ID	**Case**	**Cohort**	**Sample type**	**Sample weight**	**Protein hits**
rTBI 2	A010103	rTBI	LCM Amyloid Plaque	n/a	4
AD1	A890001	AD	LCM Amyloid Plaque	n/a	5
AD2	A890362	AD	LCM Amyloid Plaque	n/a	8
Method 2					
Sample ID	**Case**	**Cohort**	**Sample type**	**Sample weight**	**Protein hits**
FA	A150016	rTBI	Whole tissue curl	n/a	273
No FA	A150016	rTBI	Whole tissue curl	n/a	147
Method 3					
Sample ID	**Case**	**Cohort**	**Sample type**	**Sample weight**	**Protein hits**
FFPE_tissue	A180017	rTBI	FFPE tissue wedge	n/a	326
Method 4 - Experiment 1					
Sample ID	**Case**	**Cohort**	**Sample type**	**Sample weight**	**Protein hits**
A1	A180090	rTBI	Tissue curls	0.867g	150
Control Blank	-	-	-	-	320
Method 4 - Experiment 2					
Sample ID	**Case**	**Cohort**	**Sample type**	**Sample weight**	**Protein hits**
A2a	A180017	rTBI	Tissue curls	0.901g	494
A2i	A180017	rTBI	Tissue curls - 50ul lysate from A2a	n/a	419
A2b	A180017	rTBI	Tissue curls	0.402g	542
Control Blank	-	-	-	-	214
Method 5 - Experiment 1					
A2	A180017	rTBI	Tissue curls - 50ul lysate from A2a	0.934g	431
Control blank	-	-	-	-	34

6.3.2 Method 2: Proteomic analysis of FFPE whole tissue section with additional formic acid solubilisation

An additional formic acid (FA) step was added to the protocol using LCMS grade FA in an adaptation of the protocol from Drummond et al (2015) to aid identification of insoluble proteins. This additional pre-processing step came before FASP before standard LCMS. Two samples were processed using this method (**Table 6-1**), one with added FA and another from the sample with no FA. This sample pre-treated with FA generated a higher protein load of 273 (**Table 6-2**) than the one with no additional FA step, 147 proteins.

6.3.3 Method 3: Proteomic analysis of FFPE whole tissue portion with specialised FFPE-FASP kit

A specialised kit was identified for the processing of FFPE tissue (UPX - FFPE FASP Kit, Expedeon, San Diego, CA, USA). This kit was optimised for use with FFPE tissue which is notoriously difficult to process, removing some small individual steps and producing a protein digest which is ready for downstream analysis. The kit also allows for greater consistency in tissue processing and the possibility of processing multiple samples simultaneously with greater ease.

For this experiment it was suggested in the user guide that a small portion of FFPE tissue could be used, rather than needing to cut tissue curls. The optimum weight described by the kit manufacturers was between 0.5-1.0g, so 0.693g was sectioned from the tip of a cortical gyrus. Dewaxing and pre-processing of the sample proved difficult in the form of a larger block of tissue as the FFPE tissue is quite firm and so was difficult to get the xylene and ethanol to penetrate the tissue, subsequently the sample was divided between two microcentrifuge tubes to allow for adequate combining of the reagents with the sample. Once the sample had been homogenised and the lysate was taken through the spin filter the later steps followed as per the previous methodology.

Despite the difficulty with sample pre-processing the use of the kit in this method produced a comparable protein load of 326 (**Table 6-2**). It was decided however to return to using tissue curls cut from the whole block for this protocol

development so as to streamline the initial processes before attempting more targeted sampling.

6.3.4 Method 4: Proteomic analysis of FFPE whole tissue section to optimise the amount of lysate used with specialised FFPE-FASP kit

This method used to calculate the optimal starting sample weight and optimal amount of lysate to be used within the spin filter column stage of the protocol, as previous experiments generated a considerable volume of lysate that required to be run through the spin filter column. A1 weighed 0.867g and was processed with a blank sample of kit reagents as a control again generating 250µl of lysate – resulting in 4 repeats of the spin filter column stage to maximise the number of peptides collected. This A1 sample produced a reasonable if perhaps slightly low protein load of 150 and unfortunately the control sample was contaminated, producing a protein load of 320 (**Table 6-2**).

Subsequently, sample A2a (weight 0.901g), sample A2b – taken from the same case but a smaller starting weight (0.402g) and sample A2i - a 50µl volume of lysate acquired from sample A2a (**Table 6-2**), were taken through the FFPE-FASP kit methodology to examine whether the starting weight should be reduced or whether the lysate volume from a larger sample could be limited to just 50µl. A control sample was included, again just including the FFPE-FASP kit reagents and no original sample. This experiment showed the sample with the highest number of proteins identified was A2b with 542 (**Table 6-2**) but using a larger sample weight with only 50µl lysate at the spin column stage still produced a reasonable number of protein hits without needing to repeat the spin column step multiple times. It was therefore decided to use the protocol for sample A2i with a starting sample weight of between 0.3-0.5g for the processing of multiple samples in the final protocol, so as to increase time efficiency.

6.3.5 Method 5 - Proteomic analysis of a cohort of FFPE whole tissue sections using an FFPE-FASP kit and protease inhibitor, initial experiment

This methodology involved the addition of a protease inhibitor step which meant that multiple samples could be prepared in one day and then frozen overnight before the trypsin digestion stage was begun, allowing us to run as comparable an experiment as possible, running multiple samples simultaneously on the same LC-MS run. In the initial experiment, the rTBI sample produced a comparable number of proteins to previous runs (431) while the blank control sample came back with just 34 protein hits indicating minimal contamination (**Table 6-2**), suggesting that the samples would not be degraded by overnight storage at -80ºC.

6.3.6 Method 5 - Label-free quantification of 12 samples, to compare proteins within TBI sub-cohorts and AD

The final experiment examining the protein load produced from the whole tissue section taken from 12 samples from a cohort of patients with: a diagnosis of AD, patients exposed to rTBI and uninjured, age-matched controls with no history of neurodegenerative disease (**Table 6-1**). There was a significant difference in the age of the archival, FFPE brain tissue used, with an increase in age of tissue from 2.5 ± 1.4 years in rTBI cases, to 23.3 ± 2.1 years in Control cases (95% CI 17.9 to 23.8; $p < 0.0005$) and to 31.0 ± 1.0 years in AD cases (95% CI 25.5 to 31.5; $F(2,9) = 5.7$, $p < 0.0005$; one-way ANOVA, $\eta_p^2 = 0.990$)

A strong protein load was obtained for each sample (**Figure 6-3**), with a higher number of proteins identified in rTBI cases (341.0 ± 57.9) compared to Alzheimer's cases (209.3 ± 73.9, 95% CI, 19.7 to 243.6; $F(2,9) = 4.4$, $p = 0.023$; one-way ANOVA, $\eta_p^2 = 0.551$).

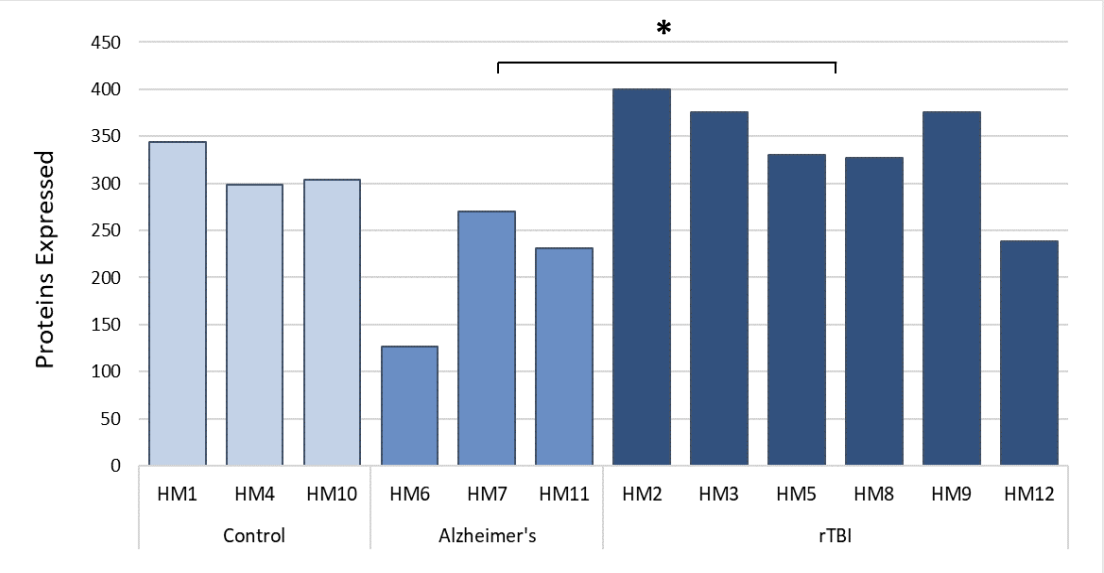

Figure 6-3 Representative image of protein hits within each of the 12 cases examined from Alzheimer's, rTBI and age-matched uninjured controls with no history of neurodegenerative disease prior to filtration. There was significantly higher protein load for rTBI cases compared to Alzheimer's cases ($p = 0.023$; one-way ANOVA).

Once the samples had been suitably filtered and grouped into cohorts, 267 proteins were identified across the 12 samples analysed (**Table 6-3** [supplementary]) with relative abundance for each protein calculated, followed by imputation and normalisation by log2 transformation.

Principal component analysis (PCA – **Figure 6-4**) demonstrates that samples within cohorts are largely distinct, with minimal overlap and high conformity within cohorts when comparing (**Figure 6-4A**) control to AD cohorts, and (**Figure 6-4C**) rTBI and AD cohorts. Slight overlap of one control sample (**Figure 6-4B)** when compared to rTBI cohorts indicates slight similarity but these two cohorts are largely distinct.

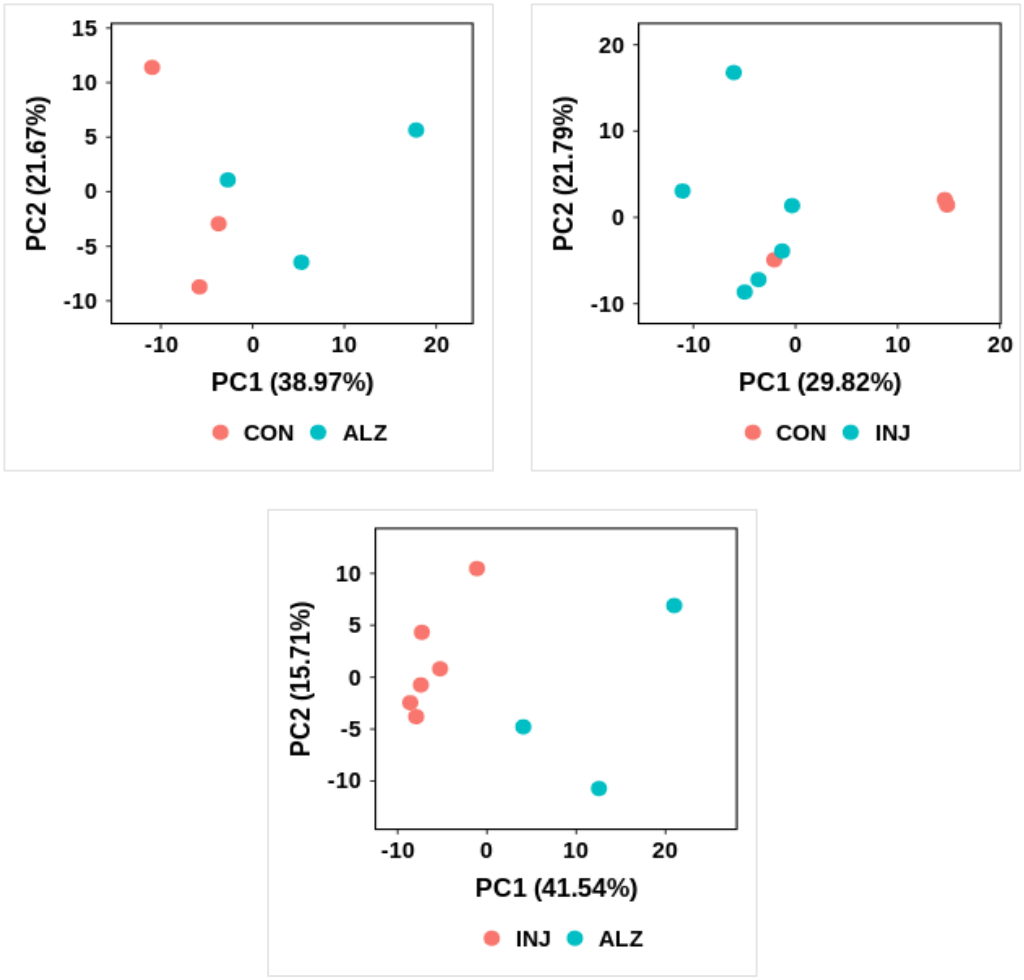

Figure 6-4 PCA of protein expression for AD, rTBI and uninjured controls cohorts. (A) Clustering of control and AD samples demonstrates no overlap for either cohort on PC1 (38.97%) or PC2 (21.67%). (B) Clustering of control and rTBI samples shows one control sample related to rTBI grouped samples with cohorts principally grouped along PC1 (29.82%) and PC2 (21.79%). (C) Samples for rTBI and AD cohorts are clustered into highly distinct groups for PC1 (41.5%) and PC2 (15.71%).

Of these the 267 proteins identified, significant differences in expression were observed in 19 proteins when comparing controls and AD cases (**Figure 6-5**), control and rTBI cases (**Figure 6-6**) and rTBI and AD cases (**Figure 6-7**; **Table 6-3** [supplementary], Student's *t*-test).

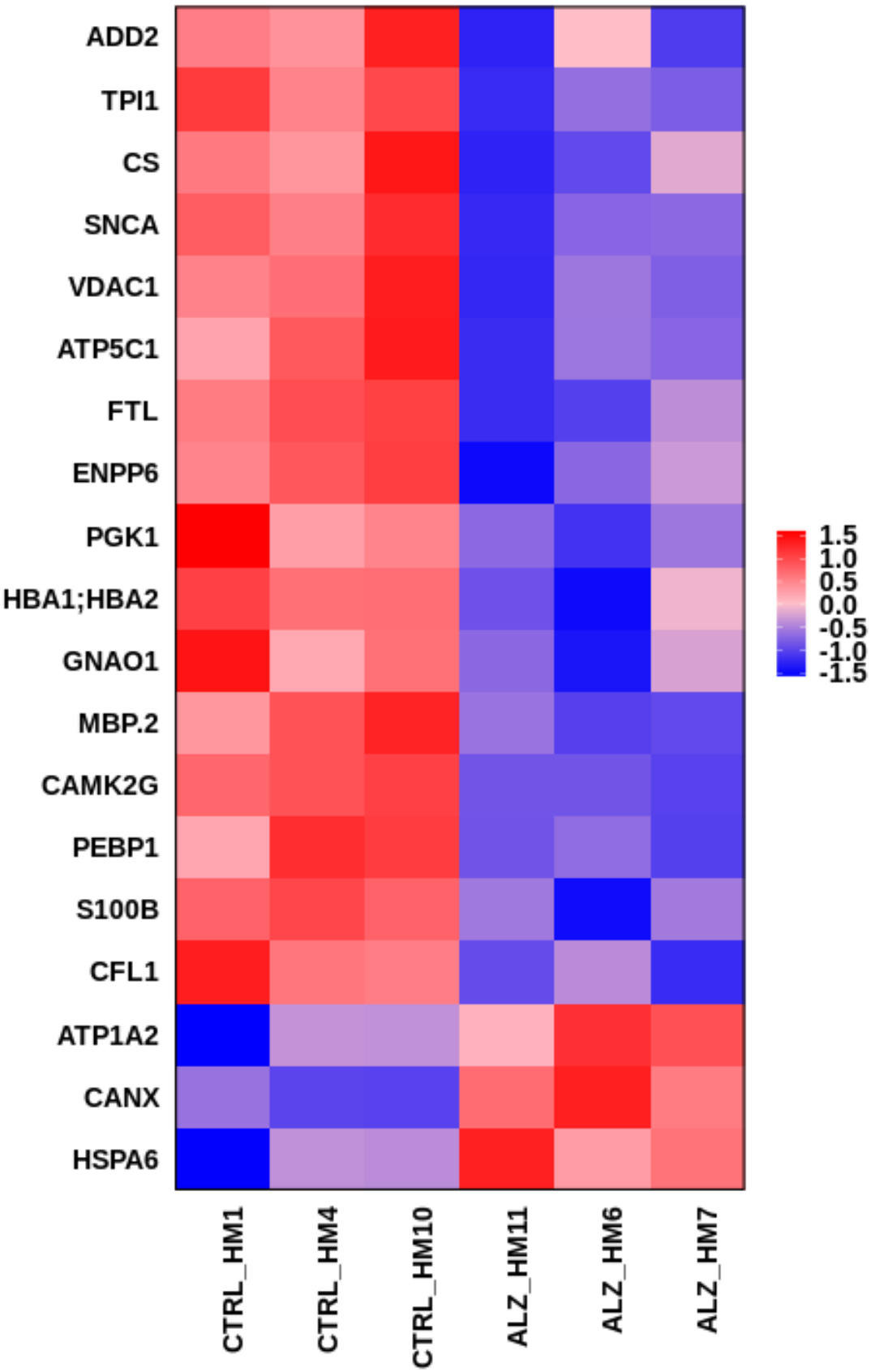

Figure 6-55 Heatmap of LFQ intensity (log2) for significantly differently expressed proteins in control (CTRL) and AD (ALZ) cohorts. 19 proteins were differentially expressed in control and AD cases (Student's t-test, $p < 0.05$), red indicating positive log2fold change and blue negative log2fold change. HSPA6, ATP1A2 and CANX proteins were expressed higher in AD cases, while HBA1;HBA2, S100B, PEBP1, MBP, CFL1, TPI1, ENPP6, CAMK2G, SNCA, VDAC1, GNAO1, PGK1, CS, ADD2, FTL and ATP5C1 showed higher expression in uninjured, age-matched controls.

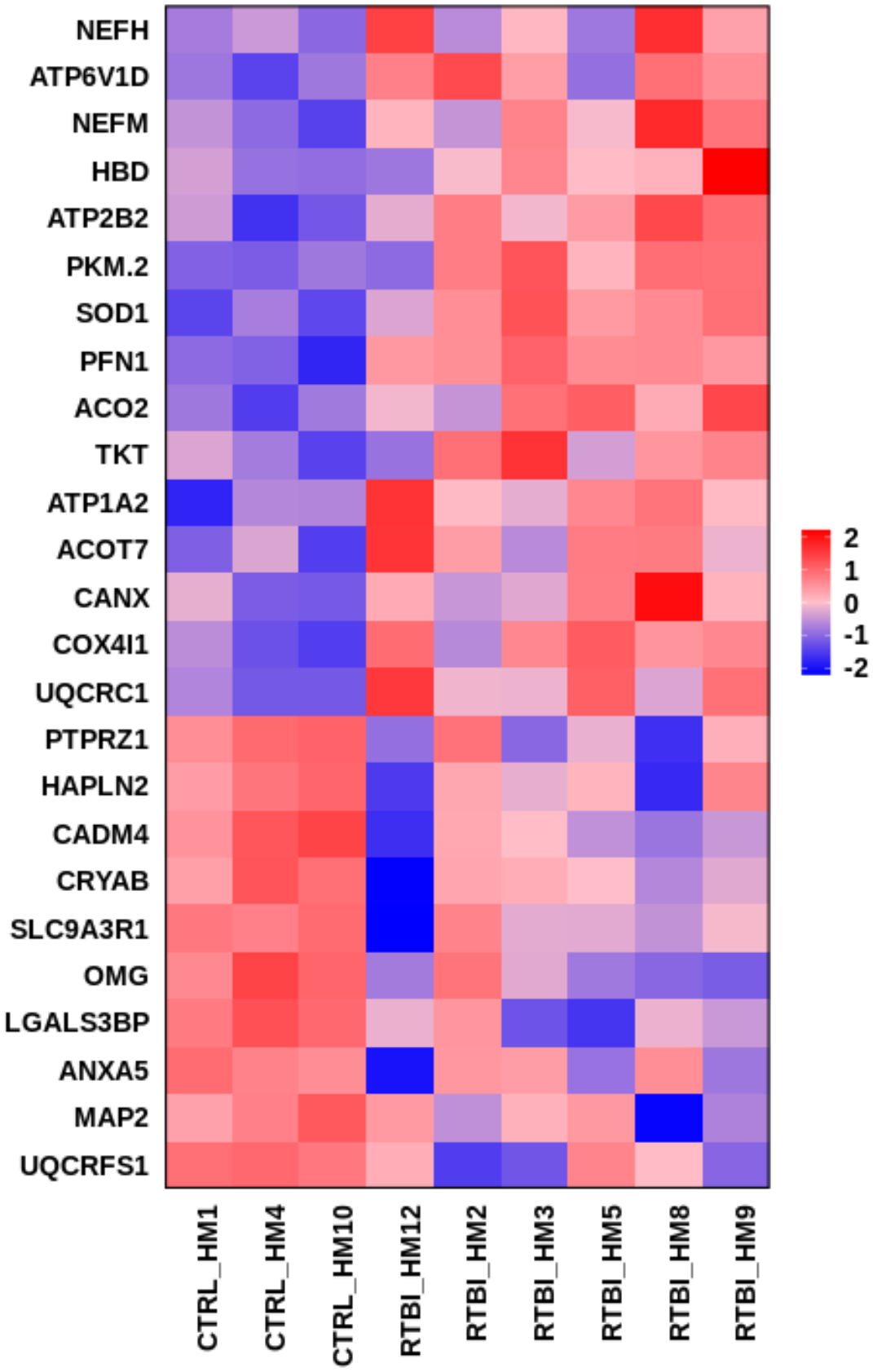

Figure 6-6 Heatmap of LFQ intensity (log2) for significantly differently expressed proteins in control (CTRL) and rTBI (RTBI) cohorts. 25 proteins were differentially expressed in control and rTBI cases (Student's t-test, $p < 0.05$), red indicating positive log2fold change and blue negative log2fold change. NEFM, ATP6V1D, NEFH, HBD, ATP2B2, PKM, SOD1, PFN1, ACO,2 TKT, ATP1A2, ACOT7, CANX, COX4I1 and UQCRC1 proteins were expressed higher in rTBI cases, while PTPRZ1, HAPLN2, CADM4, CRYAB, SLC9A3R1, OMG, LGALS3BP, ANXA5, MAP2 and UQCRFS1 showed higher expression in uninjured, age-matched controls.

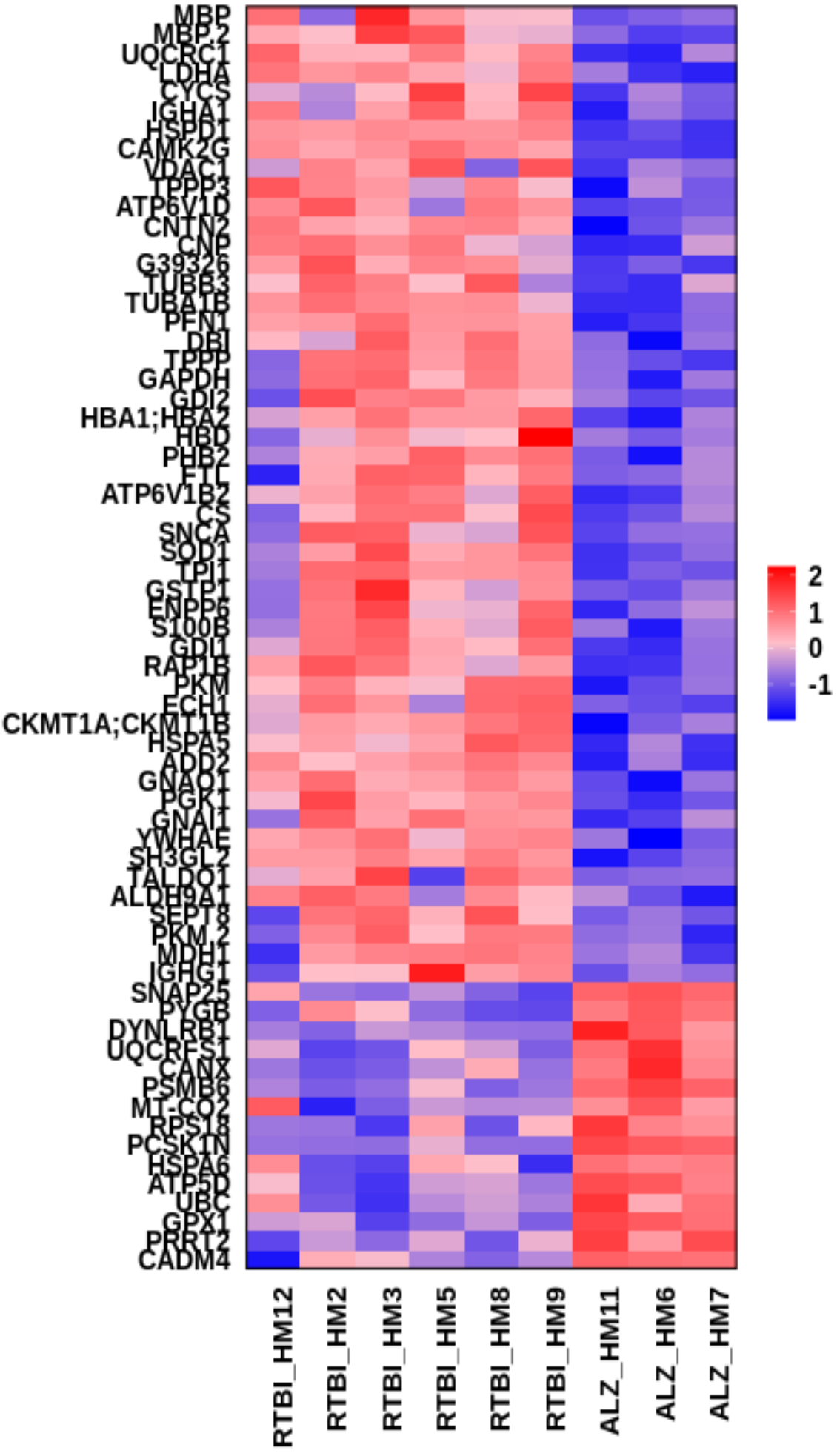
MBP
MBP2
UQCRC1
LDHA
CYCS
IGHA1
HSPD1
CAMK2G
VDAC1
TPPP3
ATP6V1D
CNTN2
CNP
G39326
TUBB3
TUBA1B
PFN1
DBI
TPPP
GAPDH
GDI2
HBA1;HBA2
HBD
PHB2
FTL
ATP6V1B2
CS
SNCA
SOD1
TPI1
GSTP1
ENPP6
S100B
GDI1
RAP1B
PKM
ECH1
CKMT1A;CKMT1B
HSPA5
ADD2
GNAO1
PGK1
GNAI1
YWHAE
SH3GL2
TALDO1
ALDH9A1
SEPT8
PKM.2
MDH1
IGHG1
SNAP25
PYGB
DYNLRB1
UQCRFS1
CANX
PSMB6
MT-CO2
RPS18
PCSK1N
HSPA6
ATP5D
UBC
GPX1
PRRT2
CADM4
RTBI_HM12
RTBI_HM2
RTBI_HM3
RTBI_HM5
RTBI_HM8
RTBI_HM9
ALZ_HM11
ALZ_HM6
ALZ_HM7
2
1
0
-1

Figure 6-7 Heatmap of LFQ intensity (log2) for significantly differently expressed proteins in rTBI (RTBI) and AD (ALZ) cohorts. 64 proteins were differentially expressed in rTBI and AD cases (Student's t-test, $p < 0.05$), red indicating positive log2fold change and blue negative log2fold change. MBP, UQCRC1, LDHA, CYCS, IGHA1, HSPD1, CAMK2G, VDAC1, TPPP3, ATP6V1D, CNTN2, CNP, SEPTIN7, TUBB3, TUBA1B, PFN1, DBI, TPPP, GAPDH, GDI2, HBA1;HBA2, HBD, PHB2, FTL, ATP6V1B2, CS, SNCA, SOD1, TPI1, GSTP1, ENPP6, S100B, GDI1, RAP1B, PKM, ECH1, CKMT1A;CKMT1B, HSPA5, ADD2, GNAO1, PGK1, GNAI1, YWHAE, SH3GL2, TALDO1, ALDH9A1, SEPT8, MDH1 and IGHG1 proteins were all expressed higher in rTBI cases, while SNAP25, PYGB, DYNLRB1, UQCRFS1, CANX, PSMB6, MT-CO2, RPS18, PCSK1N, HSPA6, ATP5D, UBC, GPX1, PRRT2 and CADM4 proteins showed higher expression in AD cases.

6.4 Discussion

This study has shown that it is possible to identify proteins from archival FFPE samples from across distinct cohorts, utilising a standardisable protocol and high throughput LCMS to make comparisons across cohorts and identify common and unique proteins across all 3 cohorts examined. This opens the door to potentially accessing data from thousands of samples which have until recently had limited viability for downstream proteomic analysis.

The majority of previous proteomic studies have utilised fresh-frozen (FF) post-mortem tissue or samples such as CSF for examining NDD such as AD (Andreev et al., 2012; Butterfield & Castegna, 2003; Donovan et al., 2012; Sultana et al., 2007; Q. Wang et al., 2005) and PD (Basso et al., 2004; Fountoulakis & Kossida, 2006; C. Werner & Engelhard, 2007). Furthermore, FF tissue has previously been used in the identification of possible CSF biomarkers for AD (Korolainen et al., 2010; Lista et al., 2013) and contributed to the identification potential treatment options including the demonstration of cytoprotective proteomic changes after the administration of the histone deacetylase inhibitor (HDACi) valproic acid (VPA), resulting in modulation of injury response after TBI in a swine model of injury (Pumiglia et al., 2021). However, most tissue archive collections consist of large banks of FFPE samples and concerns have long remained that there may be a much wider variation in quality of FFPE samples (Gaffney 2018) for example due to variation in processing protocols and also because of the modification of proteins by formalin during fixation (Giusti & Lucacchini, 2013). Recent developments in mass spectrometry techniques of analysing proteins from FFPE samples (Ostasiewicz et al., 2010; Wiśniewski et al., 2012) have made inroads into producing a practical, robust, and reproducible methodology for FFPE proteomics with the goal of comparable results to FF tissue. Rigorous comparative studies between the two tissue types have been carried out, one examining The *ProCOC* prostate cancer cohorts (Umbehr 2008) with a comparison of clinical standards and identification of a potential panel of biomarkers, for prostate cancer (Zhu et al., 2019). Additionally, the temporal stability of FFPE samples is a major benefit in its utilisation in diagnostic histopathology and research. This stability has been expounded by research identifying novel prognostic markers and even highlighting

the superior practically of FFPE tissue over FF (Drummond & Wisniewski, 2019). This study's continuation of the recent expansion in the use of FFPE tissue for proteomic analysis (Ostasiewicz & Wiśniewski, 2017; Tanca et al., 2012) demonstrates the potential wealth of future research available to us by accessing the proteome of our archived FFPE tissue.

TBI is widely recognised as the leading environmental risk factor for the development of neurodegenerative disease (NDD), seen to affect approximately 69 million individuals each year (Dewan et al., 2019) across the globe, responsible for approximately 3% of dementia in the general population. This study has provided a small insight into the possibilities for examination of the heterogeneity amongst different cohorts of injury mechanism and survival periods. The study by (Abu Hamdeh, et al., 2018), compared the proteome of cortical FFPE tissue taken from patients exposed to severe TBI compared to patients with idiopathic normal pressure hydrocephalus (iNPH) and were able to demonstrate a striking difference in the molecular profile between the two cohorts. Animal models of rTBI can further understanding of the chronic neurodegeneration that occurs in the years after injury. Comparison of a model of mild rTBI over a wide time frame, with a proteome of CTE-diagnosed patients to examine dysregulation between pathways observed 39 common upregulated proteins between species and 24 common pathways when compared to controls (Morin, 2022). Those relatively small number of human samples is comparable to the numbers examined in this study, however both form a springboard for future examination of larger cohorts of TBI subtypes and survival groups.

From the final experiment to compare cohorts of pathology, 267 proteins were successfully identified, with 84 of these significantly differentiated across the three cohorts. Several protein functions were represented in the proteins identified and differentially expressed in the 12 samples; including biomarkers for both widely understood and emerging NDD processes, as well as proteins identified in oxidative stress processes - increasingly aligned with neurodegeneration observed following TBI.

Neurofilaments are a structural component maintaining structural integrity comprising four subunits, light, middle and heavy weight chains and α-internexin or peripherin and are sensitive to neurodegeneration across NDD (Yuan et al., 2017; Yuan & Nixon, 2021), thus making them a promising biomarker for both disease and injury. An increase in CFS and plasma levels of neurofilament heavy chain (NEFH) subunit is observed in patients diagnosed with MND/ALS (Ganesalingam et al., 2013; Reijn et al., 2009; Steinacker et al., 2016; Zucchi et al., 2020). Alike, CCI animal models of TBI (Anderson et al., 2008) and acute survivors of moderate sTBI show an increase in serum NEFH compared to uninjured controls, correlated with injury severity (Shibahashi et al., 2016). This is reflected in a higher expression of NEFH in rTBI patients compared to uninjured controls ($p = 0.049$; Student's t-test) and further indicates NEFH as a potential diagnostic and prognostic biomarker for both NDD and TBI.

ProSAAS is a small endocrine and neuroendocrine chaperone protein expressed largely in the brain (Chaplot et al., 2020; Lanoue & Day, 2001). It has been observed co-localized with aggregates of Tau in Pick's disease (Kikuchi et al., 2003) and Alzheimer's disease and parkinsonism-dementia complex on Guam (Wada et al., 2004), Aß plaques in AD (Hoshino et al., 2014) and Lewy bodies in Parkinson's Disease (Jarvela et al., 2016) - where it is involved in reducing fibrillation and neurotoxicity of proteins such as alpha-synuclein. ProSAAS has also been identified as a potential differentially expressed biomarker in multiple studies of the CSF proteome of AD patients (Abdi et al., 2006; Choi et al., 2013; Davidsson et al., 2002; Hölttä et al., 2015; Jahn et al., 2011; Van Steenoven et al., 2020; Wang et al., 2016) and is associated with disease progression in AD (Mathys et al., 2019). Within this study, ProSAAS demonstrates a significantly higher expression in AD patients compared to rTBI cases ($p > 0.0001$).

Alpha-synuclein (α-syn) is a presynaptic protein involved in the release of neurotransmitters such as dopamine (Butler et al., 2015, 2017) and accumulation of aggregates is associated with Lewy bodies, the main neuropathological characteristic of PD (Bloem et al., 2021; Braak H; Braak E, 2000; Spillantini et al., 1997) and LBD (Hashimoto & Masliah, 1999; Lee et al., 2014; McKeith et al., 2017). Accumulation of α-syn is also observed in AD (Hashimoto & Masliah, 1999; Mikolaenko et al., 2005; Trojanowski & Virginia M-Y.L, 1998), which is supported by the higher expression of α-syn observed in AD patients compared to uninjured controls ($p = 0.003$) in this study. Chronic survival of a CCI model TBI in rats also

establishes increased α-syn accumulation in substantia nigra (Acosta et al., 2015), the region vulnerable to neurodegeneration in PD; and in patients exposed to severe TBI compared to healthy controls, elevation of CSF α-syn, where it is correlated with survival outcomes (Mondello et al., 2013), suggesting a pathological link between TBI and PD. This is strengthened further by the higher expression of α-syn in rTBI cases compared to uninjured controls ($p = 0.013$) demonstrated within this study.

Glyceraldehyde-3-phosphate dehydrogenase (GAPDH) is a redox-sensitive enzyme, that catalyses the first step of the glycolysis pathway, generating Adenosine Triphosphate (ATP) (Cumming & Schubert, 2005; Itakura et al., 2015; Tisdale, 2002). GAPDH undergoes nuclear translocation upon exposure to oxidative stress (Hara et al., 2005) and instigates transcription of apoptotic genes leading to cell death. It also forms Aß-like aggregates (Nakajima et al., 2007), which promote cell death and have been shown to accelerate Aß amyloidogenesis and subsequent cell death in in vitro and in vivo models of AD (Itakura et al., 2015) and are also observed in Huntington's disease and ALS (Lazarev et al., 2013). GAPDH is also thought to modulate secondary neurodegeneration after TBI and pharmaceutical inhibition in a weight-drop model of TBI results in better memory and motor function outcomes as well as reduction in GAPDH aggregates observed after injury (Dutysheva et al., 2023). GAPDH-targeted therapy has been identified as a possible therapeutic avenue for TBI patients (Lazarev et al., 2018) further supported by the higher expression of GAPDH in rTBI patients compared to AD patients ($p = 0.02$) in this study.

Superoxide dismutase [Cu-Zn] (SOD1) is an important antioxidant enzyme that functions in detoxifying superoxide free radicals (Branco et al., 2006), with mutations in SOD1 gene associated with neurodegenerative diseases ALS (Deng et al., 1993; Kiernan et al., 2011; Rosen et al., 1993) and PD (Helferich et al., 2015; Trist et al., 2017). In ALS, SOD1 mutations are largely believed to result in toxic gain of function, mediated by promotion of ROS and RNS molecules, where build up eventually leads to cell injury and death (Bruijn et al., 1997, 1998, 2004; Liu et al., 1998), or by accumulation of SOD1 aggregates – a confirmed pathology in the spinal cord of ALS patients (Forsberg et al., 2010; Kerman et al., 2010; Poon et al., 2005). SOD1-mutant mice exposed to a CCI model of TBI present with CTE-like tauopathy and associated motor impairment and white matter pathology and develop an earlier onset of ALS phenotype (Thomsen et al., 2016). TBI is also a

known environmental risk factor for ALS (H. Chen et al., 2007; X.-C. Chen et al., 2022; Wright et al., 2017), with professional football (Mackay et al., 2019) and rugby (Russell et al., 2022) players at higher risk of MND than age matched population controls. Therefore, the noted higher expression of SOD1 in rTBI cases compared to AD patients ($p = 0.001$) indicates involvement of oxidative stress on post traumatic neurodegenerative processes and further highlights the association between TBI and ALS neurodegenerative processes.

The protein loads for the samples examined in this study were potentially comparatively low compared to other proteomic studies from examining TBI and neurodegeneration in human FFPM and even FFPE tissue, however as a proof of principal pilot study we have been able to demonstrate that it is possible to obtain identifiable proteins from archival FFPE tissue from a range of time points. This included proteins which have been identified as potential biomarkers of NDD such as ProSAAS.

One step to build from this initial study could be to perform western blots to validate the differences observed here, but to obtain a truer understanding of the differences in protein expression, the next stage would be to move to undertake a labelling protocol such as Tandem Mass Tag protein labelling mass spectroscopy. The application of isotope labels to individual samples would allow us to run our samples simultaneously in the same test and reduce the batch effect of running multiple samples through the LCMS, allowing for a broader and more accurate analysis of the proteome across a multiplexed sample. This would remove the limitation of not being able to directly quantify differences in protein abundance between the samples created by running the samples sequentially as we did in this experiment, which inevitably leads to qualitative and/or quantitative differences between signals for the same peptide in different samples.

Additional studies could also increase the cohort size to include a more comprehensive number of samples, but the most wide-ranging investigations could be performed using new digital pathology technology such as the Nanostring © GeoMx™ Digital Spatial Profiling (DSP) platform. Antibodies which have

photocleavable oligonucleotide tags are hybridized to protein targets within a slide, counted and mapped to an image of the tissue and generate a spatial analysis of a panel of proteins, to truly assess the proteomic signature within a sample.

As the leading environmental factor for NDD, the increasing worldwide exposure to TBI presents a risk which means better understanding of current driving factors as well as that novel identification of future treatment targets is key to better understanding of this complex polypathology. The results found in this study demonstrate that possibility of proteomic analysis of vast archives of human tissue will hopefully aid in the development of effective strategies for how to tackle all aspects of TBI-induced neurodegeneration.

Chapter 7 – General discussion

7.1 Summary

The work presented in this thesis provides insight into the neuropathological changes which occur following single, moderate to severe TBI and rTBI. TBI affects approximately 69 million individuals globally each year and is the strongest environmental risk factor for the development of neurodegenerative disease. To date there is a limited understanding of the processes which drive an acute biomechanical injury to progressive, ongoing neurodegenerative disease. This thesis examines the processes which have the potential to influence progression of neurodegeneration following traumatic brain injury. No evidence of central adaptive immune system cellular response was observed across survival from acute to late time periods following moderate or severe sTBI. In contrast, multiple markers of astroglial activation were upregulated for both acute and long-term survivors of moderate to severe single TBI (sTBI) as well as individuals exposed to repetitive TBI (rTBI) through contact sport. The importance of examining TBI and proteinopathies in the context of age demonstrated that TBI at an older age leads to an increase in the extent and distribution of amyloid-ß (Aß) plaque, particularly neuritic plaque, compared to uninjured, age-matched controls, demonstrating the importance of examining TBI and proteinopathies in the context of age. Lastly, by developing a protocol and examining the proteome of rTBI, Alzheimer's disease (AD), and age-matched uninjured controls with no history of neurodegenerative disease (NDD), it was demonstrated that robust and reliable comparisons can be drawn from archival FFPE tissue.

7.2 TBI and neurodegenerative disease

Both single and repetitive TBI have been shown to contribute to the risk of developing neurodegenerative disease later in life, with the estimates suggesting that at least 3% of dementia in the general population are attributable to TBI (Livingston et al., 2020). The link between repeated mild TBI has existed for almost 100 years, initial (Brandenburg & Hallervorden, 1954; Corsellis et al., 1973; Martland, 1928; Millspaugh, 1937; G. W. Roberts et al., 1990; Spillane, 1962) it is

now recognised as a consequent of exposure to rTBI through various contact sports including American football (Gavett et al., 2010; McKee et al., 2009; Omalu et al., 2005, 2006, 2011; Omalu, Fitzsimmons, et al., 2010; Omalu, Hamilton, et al., 2010), Rugby (Russell et al., 2022; Stewart et al., 2016), association football (Mackay et al., 2019) and non-sports related injures such as blast injury (Goldstein et al., 2012). However, whilst TBI is recognised as the strongest environmental factor for development of NDD (Fann et al., 2018; LoBue et al., 2018; Nordström & Nordström, 2018), the complex and heterogeneous neurodegeneration observed following TBI means further research is required to understand the mechanisms underlying disease progression.

7.3 The adaptive and innate cellular immune response to TBI

Neuroinflammation is a central aspect to TBI, where it is involved in triggering a rapid multicellular cascade, but also for the development of neurodegenerative diseases like AD (Griffin et al., 1998; Perry et al., 2010). Much of the literature explores the acute and chronic microglial response to injury, characterised by morphological changes (Johnson, Stewart, Begbie, et al., 2013; Loane & Byrnes, 2010; Walker et al., 2014) and expression of pro-inflammatory mediators (Rodney et al., 2018; Thelin et al., 2017; Ziebell & Morganti-Kossmann, 2010) resulting in neuron damage and propagation of the inflammatory cycle. However, increasingly, research is looking beyond microglia to other innate cellular responses, such as that of astrocytes, and that of the adaptive immune system within the central nervous system (CNS).

Limited previous studies of human TBI indicate an influx of lymphocytes after severe TBI (Hausmann et al., 1999; Holmin et al., 1998; Kossmann et al., 1995) - across a BBB which is disrupted after injury (Dardiotis et al., 2012; Hay et al., 2015). This finding was not replicated in this study suggesting that the cellular arm of the adaptive immune response may not affect progression of neuropathology after TBI. However, it does not rule out the effect of pro- and anti-inflammatory cytokines released by peripherally circulating immune cells after injury. This study was limited by the nature of using immunohistochemistry

to examine a snapshot of the response by circulating peripheral lymphocytes in FFPE tissue. A larger cohort may have reduced this issue however, examination of peripheral blood samples from patients across injury time frames using flow cytometry, might provide further insight into the peripheral immune cells and their influence on the homeostatic balance after TBI.

Astrocytes exert multiple roles within the brain, both as supportive cells, but also as central figures in the neuroinflammatory response to disease (Beach et al., 1989; Beach & Mcgeer, 1988; Blasko & Grubeck-Loebenstein, 2003; Itagaki et al., 1989; Perez-Nievas & Serrano-Pozo, 2018) and trauma (Burda et al., 2016; Karve et al., 2016; Laird et al., 2008), where they exhibit both neuroprotective and neurotoxic roles. Reactive astrogliosis is a known driver of AD (Blasko & Grubeck-Loebenstein, 2003; Itagaki et al., 1989; Kashon et al., 2004; Perez-Nievas & Serrano-Pozo, 2018; Simpson et al., 2010) and also a response to sTBI (Burda et al., 2016; Karve et al., 2016; Laird et al., 2008), but further examination of the effect of rTBI on the astroglial response is required.

In this study, the stereotypical, localized proliferation and morphological reactive astrogliosis was observed by an increase in GFAP-immunoreactivity at the neocortical interface zones of the superficial glial limitans (SGL) and white matter interface (WMI) between the neocortex and superficial white matter. Long-term survivors of sTBI demonstrated an expansion of GFAP-immunoreactivity at the interface zones in comparison to age-matched, uninjured sTBI controls. There was no significant increase in GFAP-immunoreactive astrogliosis at interface zones in acute survivors of TBI as had been observed in previous studies (Hay, 2018), a difference which may have been affected by cohort size. Also, there was no significant difference in expression of GFAP when examining sTBI and rTBI cohorts, a result predisposed by the effect of increased age. Where there was a significant correlation between age and GFAP expression in the uninjured controls there was not going to be a significant difference in GFAP expression between sTBI and rTBI cases as they too had a large age difference.

The astrocytic role in water and ion homeostasis through activation of AQP4 channels on the astrocytic end food processes, was also examined and found that acute survivors of sTBI demonstrated a rapid increase in AQP4-immunoreactive astrocytes at the stereotypical interface zones when compared to uninjured, age-

matched sTBI controls. This AQP4-immunoreactive astrogliosis had diminished in long-term survivors and was not significantly different to tat observed in uninjured sTBI controls. Also, there was no significant difference in expression of AQP4-immunoreactive astrocytes when comparing sTBI and rTBI due to the increased age of the rTBI cases compared to sTBI and the effect of age on AQP4 expression in cases examined.

Lastly, oxidative stress in astrocytes was examined through assessing antioxidant enzyme NQO1 in a pilot cohort of rTBI cases, with an increase in NQO1-immunoreactive astrocytes observed in the depths of the cingulate sulcus in rTBI when compared to age matched rTBI controls. This finding indicates that oxidative stress processes are not as influenced by age and highlights a key avenue of research for both rTBI cohorts but also future examination of sTBI cohorts.

This examination of the astrocytic response was limited by a smaller cohort size which did not allow for comparison of sTBI and rTBI cohorts due to the effect of age on pathology observed. Future studies involving the inclusion of younger rTBI cases would allow for accurate comparisons but also, incorporating older survivors of aTBI and cTBI, age-matched to rTBI cases would provide insight into the pathology across a broader cohort of society, further understanding of how these cells respond to injury. Examination of how these markers colocalise within these and additional regions of interest such as the hippocampus and amygdala would also provide insight into how the multiple roles played by astrocytes plays out within the cellular environments and expand understanding of how neuropathological changes affect symptomatic changes for individuals affected.

7.4 Examination of Aß proteinopathy and sample proteomes in a selection of cohorts

TBI is particularly problematic amongst older populations (Thompson 2006, Gardner 2014, 2018, Marincowitz 2019) and there is a lack of understanding of the relationship between the root pathologies driving neurodegeneration and the effect of age. Aß deposition is a hallmark pathology of AD (Selkoe and Hardy 2016), normal ageing (Price 1999, Peters 2006), and also TBI (Roberts 1990, 1991 & 1994, Smith 2003, Hong 2014), however the morphology of Aß plaque is distinct between neurodegenerative processes, with neuritic plaque observed in AD and chronically after sTBI, while diffuse plaque is found in normal ageing and in the acute period following TBI. This study discovered that acute survival following single, moderate to severe TBI resulted in an increase in the extent of neuritic Aß plaque deposition compared to uninjured, age-matched older controls with no history of neurodegeneration. There was also an increase in the regional distribution of overall, diffuse and neuritic plaque, with an increase in the proportion of elderly TBI cases with Aß plaque pathology in three or more regions compared to uninjured elderly controls. This difference in Aß plaque pathology was not matched by a relative change in Tau NFT pathology in TBI patients – a pathology which is only observed in long-term survivors of TBI and not in acute survivors. This indicates that the differences seen in Aß pathology may be more than just age associated pathology.

The change in abundance of established, neuritic plaque indicates older individuals exposed to a fall or RTA potentially already have an amount of plaque deposited within the brain. These deposits then rapidly develop to the pathology observed in diagnosed AD patients. Alternatively, these patients may have already had elevated levels of Aß deposits which subsequently led to their TBI. Further work could lead to a greater understanding of the complex timeframe of neurodegenerative changes that occur with age. The findings of this study highlight the importance of using properly age-matched uninjured controls.

Lastly, proteomic analysis of vast archives of FFPE tissue has been limited due to issues with protein extraction and peptide identification/quantification because of formaldehyde induced crosslinking inherent to formalin fixation. This study aimed to develop a protocol for processing FFPE samples for downstream analysis

of peptides using liquid chromatography mass spectrometry (LCMS), initially using targeted samples collected via LCM and then whole tissue curls. This study demonstrates that it is possible to produce identifiable proteins and to undertake basic comparisons of their relative abundances for samples from across a range of cohorts and tissue ages. Whilst protein loads for the samples may be lower than for experiments utilizing fresh-frozen tissue, this proof of principal study examining a small cohort also identified proteins that are already recognized as potential biomarkers of NDD (ProSAAS). Imbalance of ROC and antioxidants contributes to neurodegeneration in disease through oxidative stress in NDD (X. Chen et al., 2012; G. Kim et al., 2015; Zhao & Zhao, 2013) and ageing (Grimm & Eckert, 2017; López-Otín et al., 2013; Mecocci et al., 2018).

Limitations of this study were that it was not possible to develop a protocol for analysis of targeted samples from LCM and that it is only possible to perform partial analysis on these non-labelled samples as this was truly a snapshot of what could be identified form these cohorts from these specific, individual samples. Labelling and pooling of samples through Tandem Mass Tag protein labelling mass spectroscopy would be a future avenue for this research and enable us to expand the cohort even further and utilise FFPE to identify potential therapeutic targets.

7.5 Conclusion

In summary, this work demonstrated a broad spectra of neuropathological changes observed following TBI across a range of cohorts representing various injury mechanisms, survival periods and age groups. TBI is not restricted to a certain demographic but is a unique public health issue in that it can and does affect all corners of society; and those deemed most vulnerable, the elderly and the young are also the most commonly exposed to the damage of TBI. This is why it has been vital to examine the effects of TBI across such a broad range of individuals within our cohorts available within the GBIRG archive. The largest limitation to this work has been that all tissue examined has been collected retrospectively, with limited clinical data available at times and cohorts necessarily small. It would be advantageous to work with cohorts gathered prospectively, where we could investigate the breadth of pathology observed after TBI in real time and with full

knowledge of the clinical outcomes, family background and any clinical interventions and therapeutics. Larger cohort numbers would also be advantageous, allowing for comparisons between groups for key factors such age and sex. Importantly, this work is now underway with both the COllaborative Neuropathology NEtwork Characterizing ouTcomes of TBI (CONNECT-TBI) and HEalth And Dementia outcomes following Traumatic Brain Injury (HEAD-TBI). Both projects aim to analyse the risk of dementia and other NDD in individuals with a broad range of TBI injury subtypes and survivals, importantly compared to the general population using prospective patient cohorts and tissue. This thesis has advanced our understanding of how the underlying neurodegenerative mechanisms come together to influence underlying TBI pathology.

Table 7-1 Summary of aims findings and possible future investigations

Hypothesis	Aims	Findings	Future Work
sTBI results in acute and long-lasting influx of adaptive immune cells	To characterise the pattern and timeframe of the adaptive immune cell response across a variety of survival time points after TBI	No histological evidence of a significant cellular response from the adaptive immune system following exposure to moderate to severe, single TBI in patients surviving acutely or long-term after injury, with no increase in T- or B-lymphocytes.	Examination of peripheral markers of the adaptive immune response across TBI timeframes and sub-cohorts such as rTBI or aged groups.
sTBI and rTBI result in an increase in reactive astrogliosis associated with increase in expression of the relevant markers GFAO, APQ4 and NQO1	To characterise astroglial response to injury in cohorts of both sTBI and rTBI, across survival timeframes and the association with GFAP, AQP4 and NQO1 expression	Increase in reactive astrogliosis following TBI exposure, with increase in AQP4-immunoreactive astrocytes in the acute period, increase in GFAP-immunoreactive astrocytes in long-term survivors and increase in NQO1 immunoreactivity in rTBI cases compared to age-matched controls. There was also an increase in AQP4 and GFAP in correlation with age across cases.	Examination of NQO1 in sTBI cohorts across survival timeframes and in younger rTBI patients. Study of colocalization of astrocytic markers through double labelling and multiplexed IF techniques.
In aged individuals, sTBI results in an acute Aß plaque deposition but no increase in hyperphosphorylated tau	To characterise Aß and tau pathology in an aged population of individuals	An increase in both presence neuritic Aß plaque and an increase in regional expression of all plaque compared to age-matched uninjured controls, but no increase in NFT pathology	Examination of Aß plaque in patients with comprehensive clinical work up and inclusion in imageing and serum/plasma biomarker studies
Identification of peptides is possible from across TBI and NND cohorts from FFPE archival tissue	To generate a protocol for the successful identification of a proteome from archival tissue	A protocol was developed for processing FFPE tissue and 267 proteins were identified with 84 differentially expressed across AD, rTBI and control cohorts	Expansion of the cohorts and inclusion of sTBI, as well as further techniques such as TMT-LCMS or spatial proteomics

Appendix 2 – Full cohorts and demographics

	Controls (n=32)	**Elderly Controls** (n=48)	**Acute sTBI** (n=32)	**Elderly Acute sTBI** (n=42)	**Long-term sTBI** (n=27)	**Alzheimer's** (n=4)	**rTBI** (n=15)
Mean age (range), years	40.8 (46)	71.3 (16)	42.4 (51)	70.1 (19)	47.7 (41)	79.8 (13)	74.4(58)
Males, n (%)	20 (62.5)	34 (71)	21 (66)	29 (69)	26 (96)	3 (75)	15 (100)
Mean post-mortem delay (range), hours	71.6 (180)	52.9 (548)	54.6 (236)	60.4 (242)	58.7 (181)	28.8(78.5)	36 (480)
Mean survival interval (range), hours	-	-	89.8 (258)	86.3 (335)	77088 (402960)	-	-
Cause of TBI, n (%)							
Fall	-	-	15 (47)	24 (57)	13 (46)	-	-
RTA	-	-	12 (38)	16 (38)	5 (18)	-	-
Assault	-	-	3 (9)	-	7 (25)	-	-
Unknown	-	-	2 (6)	2 (5)	3 (11)	-	-
Football	-	-	-	-	-	-	8 (53)
Rugby	-	-	-	-	-	-	4 (27)
Boxing	-	-	-	-	-	-	2 (13)
PE teacher	-	-	-	-	-	-	1 (7)
Cause of death, n (%)							
Acute fatty degeneration of liver	-	-	-	-	1 (4)	-	-
Acute purulent meningitis	-	-	-	-	1 (4)	-	-
Allergic reaction	-	1 (2)	-	-	-	-	-
AD	-	-	-	-	-	2 (50)	2 (13)
ARDS	-	-	-	-	-	-	1 (7)
Aspiration pneumonitis	-	3 (6)	-	-	1 (4)	-	-
Bronchopneumonia	1 (3)	3 (6)	2 (6)	5 (12)	2 (7)	2 (50)	3 (30)
Carcinoma of lung and pitauitary gland	-	1 (2)	-	-	-	-	-
CBD	-	-	-	-	-	-	1 (7)

	Controls (n=32)	Elderly Controls (n=48)	Acute sTBI (n=32)	Elderly Acute sTBI (n=42)	Long-term sTBI (n=27)	Alzheimer's (n=4)	rTBI (n=15)
Cause of death, n (%)							
Cirosis of liver	-	-	-	-	1 (4)	-	-
COAD	-	2 (4)	-	-	-	-	-
Complications of paraplegia due to myolopathy.	-	1 (2)	-	-	-	-	-
Coronary artery atheroma	-	-	-	-	1 (4)	-	-
CTE	-	-	-	-	-	-	3 (20)
DLB	-	-	-	-	-	-	1 (7)
Epilepsy	1 (3)	-	-	-	1 (4)	-	-
FTLD-PSP	-	-	-	-	-	-	1 (7)
GI Haemorrhage	-	-	-	-	1 (4)	-	-
Haemorrhage	1 (3)	-	-	-	-	-	-
Head Injury	-	-	28 (88)	31 (74)	-	-	-
Heart disease	2 (6)	-	-	-	6 (21)	-	-
Heart Failure	1 (3)	2 (4)	-	-	1 (4)	-	-
Heart transplant	-	1 (2)	-	-	-	-	-
Hepatic encephalopathy	-	-	-	-	1 (4)	-	-
Hepatic Failure	-	1 (2)	-	-	-	-	-
Hypothermia	1 (3)	-	-	-	-	-	-
Inhalation of gastric contents	2 (6)	-	-	-	-	-	-
Laceration of liver	-	-	-	-	1 (4)	-	-
Liver haemorrhage	1 (3)	1 (2)	-	-	-	-	-
Myasthenia Gravis	-	1 (2)	-	-	-	-	-
Myocardial infarction	2 (6)	3 (6)	1 (3)	-	-	-	-
Myotonic dystrophy	1 (3)	-	-	-	-	-	-

	Controls (n=32)	Elderly Controls (n=48)	Acute sTBI (n=32)	Elderly Acute sTBI (n=42)	Long-term sTBI (n=27)	Alzheimer's (n=4)	rTBI (n=15)
Cause of death, n (%)							
Multiple Injuries	-	-	-	3 (7)	-	-	-
Non hodgkins lymphoma	1 (3)	1 (2)	-	-	-	-	-
Normal pressure hydrocephalus	-	-	-	-	-	-	1 (7)
Overdose	4 (13)	1 (2)	-	-	-	-	-
Perforated Viscus	-	1 (2)	-	-	-	-	-
Polymyositis	-	1 (2)	-	-	-	-	-
PTE	-	-	-	-	1 (4)	-	-
Pulmonary congestion and oedema	-	2 (4)	-	-	-	-	-
Pulmonary Thromboembolism	1 (3)	-	-	1(2)	-	-	-
Pyelonephritis	-	-	-	-	1 (4)	-	-
Renal Failure	-	1 (2)	-	-	1 (4)	-	-
Respiratory failure	-	1 (2)	-	-	-	-	-
Sepsis	2 (6)	4 (8)	1(3)	-	-	-	1 (7)
Squamous cell carcinoma / bronchopneumonia	-	1 (2)	-	-	-	-	-
Stomach carcinoma/liver and adrenal metastes	-	1 (2)	-	-	-	-	-
Sudden death of cardiac origin	2 (6)	-	-	-	-	-	-
SUDEP	7 (22)	3 (6)	-	-	4 (14)	-	-
Suicide	1 (3)	-	-	-	-	-	-
Unknown	-	8 (17)	-	2 (5)	-	-	-
Vasculitis	-	1 (2)	-	-	-	-	-
Vascular dementia	-	-	-	-	-	-	1 (7)

	Controls (n=32)	Elderly Controls (n=48)	Acute sTBI (n=32)	Elderly Acute sTBI (n=42)	Long-term sTBI (n=27)	Alzheimer's (n=4)	rTBI (n=15)
TBI pathologies, n (%)							
Brain swelling	-	-	14 (44)	21 (50)	1(4)	-	-
Contusions	-	-	24 (75)	30 (71)	27 (96)	-	-
DAI	-	-	12 (38)	25 (60)	4 (14)	-	-
EDH	-	-	2 (6)	3 (7)	2 (7)	-	-
HBD	-	-	21 (66)	41 (98)	13 (46)	-	-
ICH	-	-	20 (63)	25 (60)	9 (32)	-	-
RIP	-	-	26 (81)	37 (88)	8 (29)	-	-
SAH	-	-	17 (53)	22 (52)	1(4)	-	-
SDH	-	-	23 (72)	31 (74)	13 (46)	-	-
Skull fracture	-	-	22 (69)	31 (74)	14 (50)	-	-

AD, Alzheimer's disease; ARDS, Acute respiratory distress syndrome; CBD, Corticobasal degeneration; COAD, Chronic obstructive airways disease; CTE, Chronic traumatic encephalopathy; DAI, Diffuse axonal injury; DLB, Dementia with Lewy bodies; EDH, Extradural haematoma; FTLD-PSP, Frontotemporal lobular degeneration - progressive supranuclear palsy; GIT, Gasterointestinal tract; HBD, Hypoxic brain damage; ICH, Intracranial haematoma; PTE, Post-traumatic epilepsy; RIP, Raised intracranial pressure; RTA, Road traffic accident; SAH, Subarachnoid haematoma; SDH, Subdural haematoma; SUDEP, Sudden unexplained death in epilepsy.

Appendix 3 – List of antibodies

Antigen	Clone/description	Antibody Source	Method of Antigen Retrieval	Concentration
CD3	SP7, Monoclonal Mouse Anti-CD3.	ThermoFisher Scientific, San Diego,CA	Microwave pressure cooker in 0.1M Citrate buffer (pH6)	1:100
CD20	L26, Monoclonal Mouse Anti-CD20.	Leica Biosystems, Newcastle-upon-Tyne, UK	Microwave pressure cooker in 0.1M Citrate buffer (pH6)	1:200
GFAP	GA 5, Monoclonal mouse anti-GFAP	Leica Biosystems, Newcastle-upon-Tyne, UK	Microwave pressure cooker and 0.1M Tris Buffer (pH8)	1:250
AQP4	AB3594, Polyclonal Rabbit Anti-AQP4	Merck, Darmstadt, Germany	Microwave pressure cooker and 0.1M Tris Buffer (pH8)	1:200
NQO1	A180, Monoclonal Mouse Anti-NQO1	Thermo Fisher Scientific, San Diego,CA	Microwave pressure cooker and 0.1M Tris Buffer (pH8)	1:1000
BA4	6F/3D, Monoclonal Mouse Anti BA4.	Dako/Agilent, Santa Clara, California, US	Formic acid (10%) for 5 minutes with wash, before Microwave pressure cooker in 0.1M Citrate buffer (pH6)	1:75
PHF-1	Gift from P. Davies, Paired helical filament	Feinstein Institute for Medical Research, Manhasset, NY, USA)	Microwave pressure cooker in 0.1M Citrate buffer (pH6)	1:1000

Appendix 4 – Supplementary tables

Supplementary 33 - (Table 3-3) Mean density of CD3- and CD20-immunoreactive profiles

(A) **CD3-immunoreactive Cells/mm²**

		Corpus callosum	Cingulate gyrus	Superficial white matter	Internal capsule	Thalamic nucleus
Control	Median	0.844	0.246	1.378	1.063	0.527
	SD	*0.720*	*0.395*	*1.038*	*0.749*	*0.353*
Acute	Median	0.837	0.262	1.464	0.862	0.443
	SD	*0.851*	*0.243*	*1.500*	*0.684*	*0.498*
	Mann-Whitney Test	0.842	0.601	0.874	0.151	0.212
Long-term	Median	1.139	0.103	0.981	0.465	0.209
	SD	*1.963*	*0.183*	*0.678*	*1.096*	*0.412*
	Mann-Whitney Test	0.755	**0.008**	0.074	**0.014**	**0.020**

(B) **CD20-immunoreactive Cells/mm²**

		Corpus callosum	Cingulate gyrus	Superficial white matter	Internal capsule	Thalami nucleus
Control	Median	0.000	0.014	0.014	0.014	0.043
	SD	*0.020*	*0.030*	*0.042*	*0.046*	*0.038*
Acute	Median	0.000	0.017	0.039	0.000	0.013
	SD	*0.019*	*0.038*	*0.084*	*0.027*	*0.017*
	Mann-Whitney Test	0.751	0.259	0.071	0.074	0.191
Long-term	Median	0.000	0.013	0.025	0.000	0.009
	SD	*0.057*	*0.055*	*0.050*	*0.016*	*0.022*
	Mann-Whitney Test	0.260	0.606	0.423	0.059	0.081

Supplementary 81 – (**Table 5-2**) Presence of Aß plaque

A	**All plaque**		**Diffuse plaque**		**Neuritic plaque**	
	Control	TBI	Control	TBI	Control	TBI
No Plaque present	7	11	8	15	27	18
Plaque Present	31	27	30	23	11	20
Chi-squared	*0.280*		*0.08*		***0.036***	
Cramer's V	0.124		0.2		0.241	

Supplementary 153 - (**Table 5-3**) CERAD score for extent of amyloid-beta pathology in elderly controls and elderly TBI patients

B	**All plaque**		**Diffuse plaque**		**Neuritic plaque**	
	Control	**TBI**	**Control**	**TBI**	**Control**	**TBI**
Nil	8	11	9	15	26	19
Sparse	8	3	6	4	1	2
Moderate	6	11	9	7	2	8
Frequent	16	13	14	12	9	9
Median	*2.0*	*2.0*	*2.0*	*1.5*	*0.0*	*0.5*
Mann-Whitney test	*0.704*		*0.288*		***0.048***	
η^2	*0.002*		*0.01*		*0.05*	

Supplementary 197 - (**Table 6-3**) – Label free quantification (LFQ) data for protein expression in control, AD and rTBI cohorts (log2). Peptides identified and sequence coverage (%), Student's *t*-test and log2fold change for cohort comparisons.

LFQ Intensity (log2)																							
	Control (C)				Alzheimer's (AD)				rTBI										Student's t-test					
Protein Names	HM1	HM4	HM10	*Mean*	HM11	HM6	HM7	*Mean*	HM12	HM2	HM3	HM5	HM8	HM9	*Mean*	Peptides	Unique peptides	Seq coverage [%]	ADvsC	ADvs rTBI	rTBIvsC	ADvsC log2fold	rTBIvsC log2fold	ADvsrTBI log2fold
ACO2	17.10	16.67	17.12	*16.96*	16.63	17.17	17.52	*17.11*	17.57	17.31	18.22	18.36	17.79	18.53	*17.96*	8	8	15.3	0.666	0.054	0.005	0.14	1	-0.86
ACOT7	15.80	16.10	15.66	*15.85*	16.52	16.23	16.32	*16.36*	16.83	16.37	15.99	16.51	16.52	16.16	*16.40*	3	3	11.6	0.041	0.799	0.027	0.5	0.54	-0.04
ACTG1	22.99	22.80	22.84	*22.88*	22.17	20.87	22.54	*21.86*	22.35	22.95	23.05	22.87	22.71	22.99	*22.82*	26	10	67.2	0.182	0.195	0.659	-1.01	-0.06	-0.96
ACTN1	15.99	14.94	14.56	*15.16*	14.57	15.54	15.97	*15.36*	16.80	15.77	14.95	15.76	16.48	14.94	*15.78*	4	2	5.4	0.758	0.456	0.302	0.2	0.62	-0.42
ADD2	15.23	15.11	15.76	*15.37*	13.97	14.87	14.11	*14.32*	15.92	15.46	15.73	15.89	16.13	15.95	*15.84*	2	1	3.3	0.042	0.022	0.120	-1.05	0.48	-1.53
ALDH2	16.48	14.53	15.37	*15.46*	15.41	14.68	16.34	*15.48*	17.38	17.65	17.25	16.57	17.72	17.14	*17.29*	5	5	13	0.981	0.050	0.073	0.02	1.83	-1.81
ALDH5A1	15.77	15.36	14.70	*15.28*	15.97	16.45	16.27	*16.23*	15.03	16.16	14.15	16.00	15.42	16.23	*15.50*	2	2	5.2	0.073	0.083	0.638	0.96	0.22	0.73
ALDH7A1	18.26	16.81	17.05	*17.37*	15.20	15.84	17.21	*16.08*	17.20	18.62	16.82	16.56	17.57	17.27	*17.34*	5	5	11.7	0.163	0.153	0.956	-1.29	-0.03	-1.26
ALDH9A1	16.21	14.60	15.22	*15.34*	15.34	14.85	14.39	*14.86*	16.25	16.52	16.32	15.20	16.19	15.80	*16.04*	6	6	16	0.438	0.024	0.271	-0.48	0.7	-1.18
ALDOA	18.94	18.14	18.51	*18.53*	19.16	18.66	19.16	*18.99*	19.27	19.50	19.11	19.37	19.63	19.53	*19.40*	17	16	50.8	0.190	0.115	0.052	0.46	0.87	-0.41
ALDOC	20.19	20.12	20.73	*20.34*	20.08	19.87	20.32	*20.09*	20.71	20.33	20.38	20.56	20.40	20.18	*20.43*	15	14	37.9	0.341	0.104	0.722	-0.26	0.08	-0.34
ANXA5	18.28	18.17	18.11	*18.19*	18.68	18.87	17.86	*18.47*	16.95	18.06	18.03	17.45	18.11	17.48	*17.68*	7	7	15.9	0.455	0.102	0.044	0.28	-0.51	0.79
ANXA6	17.37	14.84	17.42	*16.54*	15.28	16.26	15.00	*15.51*	15.11	17.85	17.59	14.52	17.71	17.35	*16.69*	15	15	20.4	0.357	0.144	0.898	-1.03	0.14	-1.17
ARHGDIA	16.64	14.95	15.61	*15.74*	15.37	16.23	14.31	*15.30*	15.30	16.94	16.87	16.58	15.87	16.76	*16.39*	2	2	15.7	0.590	0.177	0.321	-0.43	0.65	-1.09
ARPC4	16.05	14.52	16.84	*15.80*	16.54	14.62	16.11	*15.76*	15.71	15.80	16.12	16.51	15.85	16.00	*16.00*	2	2	13.7	0.962	0.722	0.802	-0.05	0.2	-0.24
ATP1A1	16.97	14.91	15.53	*15.81*	15.25	15.45	16.99	*15.89*	17.47	17.51	15.24	16.97	18.26	17.66	*17.19*	20	10	22.4	0.919	0.128	0.137	0.09	1.38	-1.29
ATP1A2	14.74	15.98	15.95	*15.56*	16.46	17.55	17.27	*17.09*	18.41	16.73	16.44	17.36	17.60	16.75	*17.21*	11	3	14.1	0.045	0.794	0.028	1.54	1.66	-0.12
ATP1A3	20.21	19.12	19.39	*19.57*	19.57	20.34	20.30	*20.07*	21.27	20.54	19.83	20.48	20.76	20.41	*20.55*	21	10	25.7	0.297	0.194	0.071	0.5	0.98	-0.48
ATP1B1	19.29	16.98	18.99	*18.42*	17.91	14.45	17.94	*16.77*	18.64	19.23	18.42	19.83	17.06	19.92	*18.85*	7	7	21.8	0.305	0.206	0.641	-1.65	0.43	-2.08
ATP2B2	14.97	14.32	14.55	*14.61*	15.89	14.66	14.61	*15.05*	15.08	15.61	15.14	15.43	15.94	15.71	*15.49*	3	2	3.9	0.411	0.414	0.019	0.44	0.87	-0.43
ATP5A1	20.55	20.86	21.38	*20.93*	21.73	21.80	20.98	*21.50*	20.66	20.49	21.18	20.97	20.42	21.18	*20.82*	33	33	56.1	0.183	0.097	0.713	0.57	-0.11	0.69
ATP5B	20.65	20.61	21.49	*20.92*	21.23	21.31	20.79	*21.11*	20.55	20.68	21.36	21.25	20.93	21.48	*21.04*	27	27	70.3	0.596	0.778	0.721	0.19	0.13	0.07
ATP5C1	15.40	15.64	15.83	*15.62*	14.85	15.08	15.03	*14.99*	14.64	15.47	16.15	15.78	14.86	17.09	*15.66*	5	5	25.2	0.020	0.127	0.922	-0.63	0.04	-0.67
ATP5D	17.18	19.21	20.02	*18.80*	20.52	20.34	19.67	*20.17*	18.58	16.84	16.37	18.06	18.16	17.46	*17.58*	4	4	20.2	0.241	0.001	0.281	1.37	-1.22	2.6
ATP5I	14.37	13.91	16.40	*14.89*	17.19	15.22	14.53	*15.65*	16.91	14.66	16.37	17.53	17.91	16.76	*16.69*	3	3	34.8	0.532	0.330	0.123	0.75	1.8	-1.04
ATP5O	18.05	18.10	19.48	*18.54*	19.00	18.24	18.53	*18.59*	18.30	18.03	18.72	18.95	18.16	19.15	*18.55*	10	10	59.6	0.931	0.897	0.986	0.05	0.01	0.04
ATP6V1A	17.63	17.47	17.82	*17.64*	17.85	16.56	17.96	*17.46*	17.24	18.02	18.01	17.46	17.81	17.90	*17.74*	14	14	26.6	0.730	0.600	0.557	-0.18	0.1	-0.28
ATP6V1B2	18.28	17.70	18.51	*18.16*	17.56	17.62	17.93	*17.70*	18.13	18.31	18.52	18.45	18.08	18.58	*18.34*	14	14	31.7	0.185	0.009	0.539	-0.46	0.18	-0.64
ATP6V1D	14.62	14.04	14.63	*14.43*	13.84	14.00	14.20	*14.01*	16.17	16.78	15.83	14.53	16.35	16.02	*15.95*	4	4	16.2	0.158	0.001	0.004	-0.41	1.52	-1.93
ATP6V1E1	19.27	15.15	20.24	*18.22*	20.90	15.13	19.83	*18.62*	19.07	19.65	19.45	19.46	19.17	20.26	*19.51*	7	7	30.5	0.874	0.665	0.495	0.4	1.29	-0.89
BASP1	17.91	18.40	20.06	*18.79*	20.88	14.35	19.08	*18.10*	18.85	15.20	13.89	18.01	17.05	18.19	*16.87*	5	5	51.1	0.765	0.602	0.105	-0.69	-1.92	1.24
BCAN	18.02	19.07	18.96	*18.68*	18.93	18.53	18.03	*18.50*	17.08	18.02	17.97	17.72	17.31	17.99	*17.68*	7	6	7.9	0.686	0.061	0.074	-0.18	-1	0.82

LFQ Intensity (log2)																								
	Control (C)				Alzheimer's (AD)				rTBI										Student's t-test					
Protein Names	HM1	HM4	HM10	*Mean*	HM11	HM6	HM7	*Mean*	HM12	HM2	HM3	HM5	HM8	HM9	*Mean*	Peptides	Unique peptides	Seq coverage [%]	ADvsC	ADvs rTBI	rTBIvsC	ADvsC log2fold	rTBIvsC log2fold	ADvsrTBI log2fold
BIN1	18.00	18.10	16.66	*17.59*	17.86	16.04	15.65	*16.52*	13.61	18.17	16.47	15.12	17.11	16.55	*16.17*	6	5	14.8	0.271	0.726	0.121	-1.07	-1.42	0.35
CA2	17.64	17.36	17.20	*17.40*	17.36	15.18	17.34	*16.63*	17.89	17.63	17.60	17.62	17.73	17.61	*17.68*	3	3	13.5	0.397	0.283	0.150	-0.77	0.28	-1.05
CADM4	17.50	17.96	18.09	*17.85*	17.84	17.77	17.74	*17.79*	16.03	17.33	17.17	16.79	16.58	16.83	*16.79*	4	4	12.1	0.754	0.003	0.007	-0.07	-1.06	1
CALM3	16.89	18.48	19.04	*18.14*	19.97	17.21	19.30	*18.83*	15.58	17.70	16.26	16.81	15.17	17.11	*16.44*	5	5	40.9	0.551	0.083	0.095	0.69	-1.7	2.39
CAMK2A	18.17	18.03	17.99	*18.07*	18.08	15.91	18.26	*17.42*	17.37	17.91	17.63	18.05	18.77	16.86	*17.76*	7	4	18.6	0.479	0.698	0.312	-0.65	-0.3	-0.35
CAMK2G	16.40	16.61	16.77	*16.59*	14.52	14.52	14.34	*14.46*	16.78	16.48	16.72	17.19	16.80	16.51	*16.75*	4	1	7.9	0.000	0.000	0.343	-2.14	0.15	-2.29
CANX	14.54	14.16	14.14	*14.28*	15.87	16.52	15.75	*16.05*	14.72	14.43	14.52	14.94	15.47	14.68	*14.79*	2	2	4.1	0.007	0.014	0.041	1.77	0.52	1.25
CAPZA1	17.20	16.35	16.98	*16.84*	16.94	14.99	14.47	*15.47*	16.47	16.42	16.75	16.94	16.72	16.53	*16.64*	2	1	8.4	0.202	0.260	0.506	-1.38	-0.21	-1.17
CAPZA2	17.13	16.80	17.08	*17.01*	17.10	16.73	17.68	*17.17*	17.35	17.44	17.20	17.19	17.45	17.17	*17.30*	3	2	14.7	0.628	0.680	0.081	0.16	0.29	-0.13
CBR1	19.61	19.62	18.64	*19.29*	19.21	19.10	18.84	*19.05*	18.44	19.79	18.99	18.55	18.53	17.84	*18.69*	9	7	51.3	0.542	0.257	0.216	-0.24	-0.6	0.36
CBR3	17.73	17.57	16.66	*17.32*	16.47	14.42	16.74	*15.88*	17.22	17.71	16.37	16.76	16.34	15.99	*16.73*	3	1	13.4	0.179	0.367	0.230	-1.44	-0.59	-0.85
CFL1	18.02	16.94	16.83	*17.26*	14.64	15.41	14.24	*14.76*	15.39	17.87	14.46	14.34	17.09	18.01	*16.19*	3	3	20.5	0.008	0.106	0.213	-2.5	-1.07	-1.43
CKB	19.74	19.98	19.29	*19.67*	19.38	19.87	19.54	*19.60*	19.27	19.99	19.21	19.51	18.83	18.63	*19.24*	13	13	44.6	0.800	0.184	0.184	-0.07	-0.43	0.36
CKMT1A;CKMT1B	17.38	16.19	17.02	*16.86*	14.53	15.76	16.26	*15.52*	16.86	17.73	17.50	17.77	18.24	18.48	*17.76*	9	9	24.5	0.106	0.031	0.103	-1.34	0.9	-2.24
CLU	16.24	17.06	16.39	*16.56*	16.42	14.74	16.64	*15.93*	14.42	16.66	16.66	16.48	16.28	16.40	*16.15*	3	3	8.9	0.412	0.770	0.375	-0.63	-0.41	-0.22
CNDP2	16.64	16.37	15.05	*16.02*	16.42	15.58	16.75	*16.25*	17.02	17.54	16.09	16.32	16.22	16.30	*16.58*	6	5	14.5	0.724	0.473	0.378	0.23	0.56	-0.33
CNP	18.63	17.70	17.08	*17.80*	14.68	14.75	16.88	*15.44*	18.82	19.08	18.46	18.91	17.32	16.97	*18.26*	15	9	41.3	0.060	0.038	0.469	-2.37	0.46	-2.82
CNTN1	18.91	18.45	18.82	*18.73*	18.46	18.10	18.58	*18.38*	17.00	19.25	18.89	18.74	18.23	18.46	*18.43*	14	14	16	0.161	0.895	0.425	-0.35	-0.3	-0.05
CNTN2	16.03	14.65	14.07	*14.92*	13.93	14.72	15.06	*14.57*	16.55	16.09	15.95	16.36	16.43	16.06	*16.24*	3	3	4.2	0.640	0.030	0.148	-0.35	1.32	-1.67
CNTNAP1	17.71	17.34	16.86	*17.30*	16.62	17.17	17.05	*16.95*	16.85	17.53	16.49	16.94	16.35	16.85	*16.83*	11	11	10	0.306	0.655	0.192	-0.36	-0.47	0.11
COX4I1	15.92	14.98	14.68	*15.19*	14.35	15.38	17.41	*15.71*	18.00	15.87	17.60	18.29	17.40	17.58	*17.46*	2	2	12.4	0.635	0.181	0.006	0.52	2.26	-1.74
COX5A	16.29	16.95	18.36	*17.20*	14.73	15.40	17.39	*15.84*	17.18	15.58	17.02	17.17	16.87	17.71	*16.92*	4	4	22	0.251	0.308	0.705	-1.36	-0.28	-1.08
COX5B	15.69	15.31	17.41	*16.14*	14.97	14.86	17.36	*15.73*	17.54	15.88	17.53	18.35	17.83	17.67	*17.47*	4	4	30.2	0.717	0.153	0.161	-0.41	1.33	-1.74
CRYAB	19.29	20.81	20.28	*20.12*	19.34	15.56	19.69	*18.20*	14.80	19.18	19.00	18.66	17.51	18.19	*17.89*	13	13	73.1	0.279	0.849	0.027	-1.93	-2.23	0.31
CRYM	17.56	17.56	17.86	*17.66*	18.13	14.46	17.80	*16.80*	17.10	17.73	17.87	17.55	16.72	17.94	*17.48*	5	5	18.8	0.540	0.619	0.459	-0.86	-0.17	-0.69
CS	15.92	15.72	16.58	*16.07*	14.36	14.62	15.28	*14.75*	14.80	16.02	16.82	16.83	15.89	17.27	*16.27*	5	5	11.6	0.025	0.013	0.671	-1.32	0.2	-1.52
CTSD	15.83	16.49	17.23	*16.52*	15.22	14.35	16.07	*15.21*	16.12	16.37	16.46	16.29	15.12	16.66	*16.17*	4	4	15.5	0.115	0.183	0.502	-1.31	-0.35	-0.96
CYCS	15.39	14.84	16.42	*15.55*	14.84	15.63	15.22	*15.23*	15.98	15.70	16.27	17.49	16.31	17.44	*16.53*	3	3	25.7	0.588	0.012	0.154	-0.31	0.98	-1.3
DBI	19.32	17.52	18.95	*18.60*	18.78	18.14	18.84	*18.59*	19.37	19.14	19.95	19.57	19.84	19.54	*19.57*	3	3	41.4	0.985	0.026	0.216	-0.01	0.97	-0.98
DDAH1	20.60	19.67	19.87	*20.05*	19.74	19.72	20.33	*19.93*	20.14	20.21	20.45	20.24	20.46	20.03	*20.26*	6	6	34	0.757	0.242	0.539	-0.11	0.21	-0.32
DLST	16.93	16.60	16.93	*16.82*	17.22	17.61	16.72	*17.18*	17.48	16.81	16.51	17.22	17.12	17.13	*17.04*	3	3	7.7	0.291	0.662	0.242	0.36	0.22	0.14
DNM1	15.95	17.44	16.12	*16.50*	16.97	15.87	16.93	*16.59*	16.91	16.76	16.56	16.45	18.09	15.47	*16.71*	11	11	13	0.889	0.825	0.743	0.09	0.2	-0.12

LFQ Intensity (log2)																							
	Control (C)				Alzheimer's (AD)				rTBI										Student's t-test					
Protein Names	HM1	HM4	HM10	*Mean*	HM11	HM6	HM7	*Mean*	HM12	HM2	HM3	HM5	HM8	HM9	*Mean*	Peptides	Unique peptides	Seq coverage [%]	ADvsC	ADvs rTBI	rTBIvsC	ADvsC log2fold	rTBIvsC log2fold	ADvsrTBI log2fold
DPYSL2	21.48	20.60	20.16	*20.75*	20.06	19.38	20.84	*20.09*	20.55	21.67	21.25	21.03	21.27	20.84	*21.10*	24	21	53.3	0.319	0.126	0.467	-0.65	0.35	-1.01
DPYSL3	15.83	14.72	14.24	*14.93*	14.32	14.26	15.54	*14.71*	15.42	17.60	17.63	14.87	16.77	14.51	*16.13*	10	7	24	0.738	0.082	0.148	-0.23	1.2	-1.43
DYNC1H1	15.86	15.76	15.23	*15.61*	15.38	14.99	15.97	*15.45*	16.52	16.22	16.01	15.73	16.75	14.11	*15.89*	6	6	1.9	0.657	0.389	0.546	-0.17	0.27	-0.44
DYNLRB1	17.59	18.44	18.41	*18.15*	19.73	19.16	18.54	*19.14*	17.46	17.20	17.72	17.59	17.35	17.33	*17.44*	2	2	21.9	0.090	0.034	0.117	1	-0.7	1.7
ECH1	15.98	15.07	14.12	*15.06*	14.86	14.69	14.55	*14.70*	15.62	16.60	16.21	15.18	16.66	16.74	*16.17*	3	3	9.5	0.580	0.002	0.159	-0.35	1.11	-1.46
ECHS1	15.14	14.66	15.81	*15.20*	15.61	16.01	15.10	*15.57*	15.96	15.82	15.19	15.87	15.65	16.03	*15.75*	2	2	11.4	0.437	0.571	0.233	0.37	0.55	-0.19
EEF1A1	17.79	18.14	13.89	*16.61*	18.54	19.58	18.51	*18.88*	18.38	17.88	18.33	18.83	18.40	17.46	*18.21*	2	2	5.4	0.233	0.190	0.359	2.27	1.61	0.66
EFHD2	15.90	15.83	15.96	*15.90*	14.17	16.09	15.69	*15.31*	13.87	16.05	16.32	15.82	15.26	15.90	*15.54*	5	4	22.5	0.425	0.764	0.369	-0.58	-0.36	-0.22
EIF4A2	15.52	16.13	16.08	*15.91*	16.46	15.26	16.57	*16.10*	16.43	15.50	15.45	16.35	16.61	14.99	*15.89*	4	4	13.5	0.715	0.704	0.959	0.19	-0.02	0.21
EIF4H	14.80	17.10	16.56	*16.15*	17.79	14.67	17.12	*16.53*	15.51	14.72	15.81	15.85	16.38	15.18	*15.58*	2	2	9.7	0.766	0.422	0.499	0.38	-0.58	0.95
ENO1	19.16	18.40	18.64	*18.73*	18.01	16.23	17.88	*17.37*	18.10	19.40	19.40	18.61	18.55	19.48	*18.92*	23	21	64.1	0.128	0.097	0.585	-1.36	0.19	-1.55
ENO2	21.21	20.73	20.99	*20.98*	20.98	20.31	20.67	*20.65*	20.52	21.22	20.89	20.91	20.36	21.19	*20.85*	21	19	57.6	0.258	0.462	0.550	-0.32	-0.13	-0.19
ENPP6	16.38	16.87	17.16	*16.80*	13.74	14.77	15.31	*14.61*	14.82	17.04	17.77	15.84	15.77	17.33	*16.43*	6	6	20.5	0.025	0.033	0.488	-2.2	-0.38	-1.82
EPB41L3	16.60	17.04	16.98	*16.87*	16.94	16.47	16.52	*16.65*	16.37	17.16	16.18	16.78	15.87	16.07	*16.41*	6	6	8	0.330	0.364	0.095	-0.23	-0.47	0.24
ETFA	14.77	14.87	15.78	*15.14*	15.23	14.73	14.77	*14.91*	15.29	15.14	15.40	15.28	14.84	15.84	*15.30*	4	4	18.3	0.577	0.125	0.679	-0.22	0.16	-0.38
FABP3	16.78	17.43	17.51	*17.24*	17.81	14.75	17.83	*16.80*	15.95	14.13	14.06	17.03	17.35	16.77	*15.88*	2	2	16.5	0.710	0.490	0.076	-0.44	-1.36	0.91
FTH1	19.71	20.16	19.23	*19.70*	18.98	14.46	18.81	*17.41*	18.06	19.93	19.97	19.55	19.31	19.54	*19.39*	11	11	59.6	0.261	0.312	0.461	-2.28	-0.31	-1.98
FTL	19.52	19.70	19.75	*19.66*	18.71	18.79	19.08	*18.86*	18.19	19.72	20.34	20.29	19.63	20.13	*19.72*	6	6	34.3	0.007	0.048	0.862	-0.8	0.06	-0.86
GAPDH	19.73	19.08	19.55	*19.45*	19.05	18.42	19.10	*18.86*	19.00	20.16	20.23	19.66	20.09	19.87	*19.83*	25	25	71.9	0.112	0.019	0.212	-0.6	0.38	-0.98
GDI1	19.33	19.09	18.36	*18.93*	18.14	18.04	18.50	*18.22*	18.83	19.46	19.57	19.15	19.03	19.51	*19.26*	12	6	33.3	0.120	0.003	0.378	-0.71	0.33	-1.04
GDI2	16.28	15.20	15.14	*15.54*	15.09	14.64	14.77	*14.83*	14.75	16.53	16.14	16.22	15.93	15.75	*15.89*	10	4	27	0.188	0.008	0.480	-0.7	0.35	-1.05
GFAP	22.07	21.16	19.75	*20.99*	20.04	19.51	21.23	*20.26*	20.79	22.09	21.61	20.94	21.85	21.25	*21.42*	44	42	67.1	0.437	0.134	0.598	-0.73	0.43	-1.16
GLIPR2	16.39	16.49	16.86	*16.58*	14.95	14.75	16.17	*15.29*	17.04	16.07	16.21	15.88	16.75	15.74	*16.28*	2	2	16.9	0.088	0.137	0.278	-1.29	-0.3	-0.99
GLUD1	18.59	17.28	18.30	*18.06*	17.24	15.68	16.66	*16.53*	14.93	19.00	18.34	17.92	17.20	18.52	*17.65*	15	15	32.6	0.065	0.180	0.587	-1.53	-0.41	-1.12
GNAI1	17.17	15.28	16.10	*16.19*	14.20	14.45	15.28	*14.64*	14.98	16.85	16.15	16.67	16.31	16.25	*16.20*	4	1	11.3	0.087	0.015	0.979	-1.54	0.02	-1.56
GNAO1	20.13	18.54	19.13	*19.27*	17.34	16.44	17.97	*17.25*	19.47	20.19	19.31	19.48	19.89	19.57	*19.65*	14	11	40.7	0.035	0.024	0.498	-2.01	0.39	-2.4
GNB1	18.82	17.86	18.31	*18.33*	18.53	17.96	17.92	*18.14*	17.42	19.19	17.37	17.43	17.62	17.58	*17.77*	6	6	18.5	0.613	0.322	0.211	-0.19	-0.56	0.37
GNB2	18.87	17.77	17.62	*18.09*	18.49	18.14	18.36	*18.33*	17.11	19.02	17.87	17.78	18.40	17.57	*17.96*	3	3	8.8	0.609	0.249	0.799	0.24	-0.13	0.37
GOT1	19.21	19.30	19.90	*19.47*	19.54	18.80	19.49	*19.28*	19.61	19.51	19.35	19.30	19.41	19.43	*19.44*	17	17	40.7	0.581	0.573	0.896	-0.19	-0.03	-0.16
GOT2	17.30	18.05	18.39	*17.91*	17.60	17.16	17.35	*17.37*	17.19	17.57	16.34	18.04	16.36	17.80	*17.22*	6	6	20.7	0.230	0.653	0.171	-0.54	-0.69	0.15
GPI	18.43	17.83	17.42	*17.89*	17.40	16.10	17.97	*17.16*	17.72	18.85	17.90	17.38	18.18	17.38	*17.90*	7	7	17.6	0.321	0.309	0.987	-0.74	0.01	-0.74
GPX1	15.14	16.40	14.92	*15.49*	16.96	16.75	16.51	*16.74*	15.19	15.29	14.18	14.67	15.12	14.51	*14.83*	2	2	11.8	0.103	0.000	0.285	1.25	-0.66	1.91

LFQ Intensity (log2)																							
	Control (C)				Alzheimer's (AD)				rTBI										Student's t-test					
Protein Names	HM1	HM4	HM10	*Mean*	HM11	HM6	HM7	*Mean*	HM12	HM2	HM3	HM5	HM8	HM9	*Mean*	Peptides	Unique peptides	Seq coverage [%]	ADvsC	ADvs rTBI	rTBIvsC	ADvsC log2fold	rTBIvsC log2fold	ADvsrTBI log2fold
GSTP1	16.51	15.77	14.32	*15.53*	14.61	14.48	14.92	*14.67*	14.82	16.32	17.02	15.69	15.25	16.05	*15.86*	6	6	37.1	0.310	0.013	0.682	-0.86	0.32	-1.18
H1.4	18.74	18.70	18.55	*18.66*	18.18	15.23	18.34	*17.25*	17.66	19.10	18.25	19.40	18.09	19.53	*18.67*	10	3	30.1	0.296	0.291	0.980	-1.42	0.01	-1.42
H2AC18	16.50	17.57	17.96	*17.34*	18.38	14.60	17.46	*16.81*	14.90	16.99	16.05	16.94	15.25	16.90	*16.17*	6	2	35.4	0.697	0.638	0.099	-0.53	-1.17	0.64
H2BC15	21.73	21.79	21.84	*21.78*	22.96	20.99	22.61	*22.19*	21.19	21.34	21.81	21.90	21.10	21.44	*21.47*	7	1	53.6	0.574	0.356	0.062	0.4	-0.32	0.72
H3-7	18.40	19.94	19.89	*19.41*	21.43	14.98	20.42	*18.94*	18.24	18.15	18.04	19.25	17.70	18.66	*18.34*	4	4	22.1	0.839	0.794	0.155	-0.47	-1.07	0.6
HADHA	14.45	15.61	14.69	*14.92*	14.70	15.58	15.66	*15.31*	15.54	15.02	15.24	14.08	15.31	15.09	*15.05*	2	2	4.7	0.445	0.516	0.765	0.4	0.13	0.26
HADHB	15.94	14.22	15.12	*15.09*	15.06	15.98	14.87	*15.30*	14.59	15.64	16.31	15.31	15.83	15.60	*15.55*	3	3	8	0.746	0.592	0.472	0.21	0.45	-0.24
HAGH	15.93	16.18	14.63	*15.58*	14.51	15.39	16.44	*15.45*	15.19	16.05	16.48	16.50	16.80	16.15	*16.20*	2	2	5.8	0.866	0.313	0.334	-0.13	0.62	-0.75
HAPLN2	18.64	19.66	20.06	*19.45*	18.75	18.90	18.30	*18.65*	14.18	18.33	17.23	17.99	13.76	19.23	*16.79*	10	10	28.8	0.190	0.102	0.037	-0.8	-2.66	1.86
HBA1;HBA2	21.65	20.69	20.74	*21.03*	16.82	15.35	18.85	*17.01*	19.83	21.83	23.29	22.07	22.04	23.63	*22.12*	10	6	69.7	0.048	0.018	0.128	-4.02	1.09	-5.11
HBB	23.36	23.01	22.77	*23.05*	22.51	23.06	22.70	*22.76*	22.32	23.40	23.92	23.44	23.54	25.10	*23.62*	13	7	85.7	0.283	0.071	0.203	-0.29	0.57	-0.86
HBD	18.41	17.93	17.89	*18.07*	18.19	17.86	18.20	*18.08*	17.98	18.70	19.34	18.79	18.89	20.75	*19.07*	8	2	55.1	0.963	0.048	0.050	0.01	1	-0.99
HINT1	17.29	17.61	17.53	*17.47*	17.43	15.45	17.34	*16.74*	14.48	17.83	18.13	17.61	17.31	17.62	*17.17*	2	2	32.5	0.375	0.639	0.601	-0.73	-0.31	-0.42
HIST1H2AC	21.30	22.63	22.21	*22.05*	23.23	21.27	22.81	*22.44*	20.80	21.36	20.52	21.79	20.41	21.47	*21.06*	6	2	35.4	0.617	0.133	0.108	0.39	-0.99	1.38
HIST1H4A	18.10	19.52	19.72	*19.11*	19.71	17.84	18.37	*18.64*	17.57	18.24	18.19	18.60	17.80	18.80	*18.20*	8	8	64.1	0.565	0.519	0.208	-0.47	-0.91	0.44
HK1	17.05	15.85	14.85	*15.92*	16.22	17.51	15.94	*16.56*	17.41	17.58	16.78	17.81	17.64	17.94	*17.53*	11	11	11.8	0.470	0.171	0.118	0.64	1.61	-0.97
HPRT1	16.53	17.04	17.49	*17.02*	16.68	15.50	17.05	*16.41*	15.39	17.40	16.88	16.81	15.79	17.12	*16.57*	4	4	17	0.338	0.798	0.323	-0.61	-0.46	-0.16
HSP90AA1	18.04	16.93	16.13	*17.03*	16.67	15.64	17.04	*16.45*	16.91	18.26	17.94	16.86	17.34	15.30	*17.10*	12	8	14.8	0.455	0.320	0.925	-0.58	0.07	-0.65
HSPA1A	18.11	16.70	14.94	*16.58*	15.80	14.63	16.60	*15.68*	14.52	18.26	17.42	16.49	17.60	17.83	*17.02*	14	7	24.5	0.458	0.146	0.705	-0.9	0.44	-1.34
HSPA5	16.04	14.23	16.40	*15.56*	13.98	14.96	14.07	*14.34*	15.52	15.90	15.46	15.87	16.62	16.42	*15.96*	7	6	13.3	0.204	0.015	0.612	-1.22	0.41	-1.63
HSPA6	17.24	17.79	17.77	*17.60*	18.58	18.11	18.26	*18.32*	17.97	14.57	14.27	17.39	16.92	13.84	*15.83*	6	1	12.6	0.037	0.019	0.061	0.72	-1.77	2.49
HSPA8	19.89	19.63	19.57	*19.70*	18.01	18.23	19.38	*18.54*	19.36	20.29	20.35	20.05	20.21	20.24	*20.08*	25	17	37.8	0.106	0.055	0.071	-1.15	0.39	-1.54
HSPA9	17.07	14.62	15.35	*15.68*	14.95	15.99	16.73	*15.89*	17.05	17.51	15.88	17.66	17.85	17.11	*17.18*	10	10	17.7	0.827	0.109	0.162	0.21	1.5	-1.29
HSPB1	15.93	17.54	15.91	*16.46*	17.24	16.14	17.44	*16.94*	14.93	17.61	17.69	17.40	16.30	16.65	*16.76*	5	5	29.8	0.518	0.773	0.681	0.48	0.3	0.18
HSPD1	17.85	14.88	14.71	*15.81*	14.41	14.93	14.36	*14.57*	18.20	18.06	18.39	18.21	18.21	18.55	*18.27*	13	13	25.7	0.345	0.001	0.137	-1.25	2.45	-3.7
HSPE1	15.20	16.48	19.32	*17.00*	18.36	13.87	18.15	*16.79*	17.48	15.94	18.14	18.08	18.16	18.52	*17.72*	10	10	85.3	0.919	0.596	0.622	-0.21	0.72	-0.92
IGHA1	15.96	15.94	13.99	*15.30*	14.76	15.79	15.42	*15.32*	17.28	15.90	16.89	17.57	16.68	17.36	*16.95*	4	4	16.1	0.970	0.010	0.113	0.03	1.65	-1.62
IGHG1	15.85	17.45	17.42	*16.91*	14.68	15.31	15.06	*15.02*	14.69	16.19	16.14	18.34	16.62	16.89	*16.48*	2	2	9.4	0.057	0.029	0.573	-1.89	-0.43	-1.46
IGKC	14.74	17.73	17.86	*16.77*	15.11	14.93	17.28	*15.78*	17.22	16.46	16.29	17.93	14.96	17.39	*16.71*	2	2	32.7	0.478	0.353	0.957	-1	-0.07	-0.93
IGLC3	14.62	15.98	15.80	*15.47*	14.84	14.74	15.28	*14.95*	15.48	14.60	15.24	16.26	14.10	15.75	*15.24*	2	2	30.2	0.356	0.456	0.691	-0.51	-0.23	-0.28
IGSF8	17.42	17.82	18.08	*17.77*	18.71	17.80	18.20	*18.23*	17.65	17.54	17.50	17.32	17.66	18.08	*17.62*	10	10	18.9	0.238	0.133	0.545	0.46	-0.15	0.61
IMPA1	16.37	15.66	16.49	*16.17*	15.97	15.13	15.86	*15.66*	14.95	16.18	15.72	16.02	15.99	16.18	*15.84*	3	3	13.7	0.236	0.600	0.359	-0.52	-0.33	-0.18

LFQ Intensity (log2)																							
	Control (C)				Alzheimer's (AD)				rTBI										Student's t-test					
Protein Names	HM1	HM4	HM10	*Mean*	HM11	HM6	HM7	*Mean*	HM12	HM2	HM3	HM5	HM8	HM9	*Mean*	Peptides	Unique peptides	Seq coverage [%]	ADvsC	ADvs rTBI	rTBIvsC	ADvsC log2fold	rTBIvsC log2fold	ADvsrTBI log2fold
INA	17.76	18.58	17.54	*17.96*	17.09	16.40	18.88	*17.45*	19.05	17.99	17.91	18.63	19.66	17.91	*18.52*	20	17	35.7	0.579	0.282	0.244	-0.5	0.56	-1.07
L1CAM	17.31	14.41	16.79	*16.17*	16.98	14.68	17.19	*16.28*	16.92	17.28	16.70	17.00	17.24	16.44	*16.93*	3	3	3.2	0.928	0.509	0.485	0.12	0.76	-0.65
LDHA	17.65	14.82	14.76	*15.74*	16.21	15.49	15.35	*15.68*	17.57	17.25	17.41	17.08	16.75	17.53	*17.26*	5	4	20.5	0.957	0.013	0.249	-0.06	1.53	-1.58
LDHB	19.75	18.34	19.13	*19.07*	18.23	16.16	19.17	*17.85*	20.05	19.81	19.10	19.51	19.45	19.62	*19.59*	11	10	34.1	0.307	0.187	0.330	-1.22	0.52	-1.73
LGALS1	16.50	14.82	15.14	*15.48*	14.79	14.83	15.55	*15.05*	15.17	16.55	16.75	14.30	16.17	15.98	*15.82*	4	4	35.6	0.508	0.133	0.625	-0.43	0.34	-0.77
LGALS3BP	16.01	16.51	16.22	*16.25*	15.68	14.68	14.57	*14.98*	14.99	15.69	13.86	13.50	15.00	14.69	*14.62*	3	3	6.7	0.053	0.493	0.003	-1.27	-1.62	0.35
MAG	18.21	17.06	18.13	*17.80*	17.06	16.59	16.01	*16.55*	18.32	17.33	16.27	17.38	17.85	17.84	*17.50*	6	6	10.2	0.063	0.068	0.553	-1.25	-0.3	-0.95
MAP1A	15.73	16.20	15.13	*15.69*	15.00	15.91	15.30	*15.40*	15.45	16.85	15.83	15.20	15.52	15.34	*15.70*	7	6	3.1	0.523	0.447	0.977	-0.28	0.01	-0.3
MAP1B	17.86	17.36	16.48	*17.24*	16.54	16.49	17.58	*16.87*	17.28	17.93	17.00	16.48	17.79	16.51	*17.17*	11	10	5.3	0.533	0.535	0.889	-0.37	-0.07	-0.29
MAP1LC3B	17.28	17.94	17.38	*17.53*	18.08	14.52	17.71	*16.77*	15.08	16.29	17.48	16.52	17.45	16.65	*16.58*	3	2	20.8	0.573	0.881	0.055	-0.76	-0.96	0.2
MAP2	16.01	16.27	16.58	*16.29*	14.08	14.23	16.62	*14.97*	16.07	15.40	15.88	16.08	14.30	15.29	*15.50*	4	4	2.4	0.249	0.593	0.046	-1.31	-0.78	-0.53
MAP6	17.76	18.05	17.87	*17.89*	17.69	14.33	18.24	*16.76*	17.51	17.59	17.49	18.06	17.10	17.34	*17.52*	4	4	9.2	0.450	0.598	0.045	-1.14	-0.38	-0.76
MAPK1	18.63	18.26	17.83	*18.24*	18.48	18.26	18.73	*18.49*	18.77	18.60	18.36	13.94	18.95	13.83	*17.07*	4	4	14.7	0.406	0.222	0.308	0.25	-1.16	1.42
MAPT	18.53	17.60	18.34	*18.16*	16.48	15.57	17.79	*16.61*	18.21	18.54	18.39	18.72	18.04	18.22	*18.35*	6	6	9.9	0.124	0.110	0.566	-1.54	0.2	-1.74
MBP	21.45	20.65	22.95	*21.68*	20.98	21.13	21.24	*21.12*	22.59	21.20	23.21	22.27	21.89	21.90	*22.18*	21	1	52.5	0.491	0.012	0.550	-0.56	0.5	-1.06
MBP	20.47	21.34	21.93	*21.25*	18.98	18.34	18.45	*18.59*	20.55	20.24	22.10	21.73	20.08	19.99	*20.78*	22	2	41.8	0.013	0.001	0.445	-2.66	-0.46	-2.19
MDH1	16.65	14.54	17.07	*16.09*	15.28	15.57	14.37	*15.07*	14.25	16.93	17.29	17.36	17.48	17.26	*16.76*	5	5	21	0.329	0.031	0.510	-1.01	0.68	-1.69
MDH2	18.86	18.29	19.30	*18.82*	18.01	16.34	18.47	*17.61*	19.05	19.06	19.08	19.46	19.01	19.46	*19.19*	18	18	59.8	0.195	0.133	0.336	-1.21	0.37	-1.58
MIF	18.35	18.32	17.56	*18.07*	17.67	17.08	18.25	*17.67*	17.94	17.62	17.64	17.99	17.87	17.05	*17.68*	2	2	17.4	0.393	0.967	0.267	-0.41	-0.39	-0.02
MOG	19.00	19.76	20.02	*19.60*	19.64	20.70	19.70	*20.01*	18.27	19.31	19.28	19.63	18.85	19.28	*19.10*	8	8	30.4	0.417	0.095	0.249	0.42	-0.49	0.91
MT-CO2	17.59	19.69	17.00	*18.09*	19.26	19.75	19.16	*19.39*	19.71	17.45	17.99	18.50	18.38	18.38	*18.40*	2	2	7.5	0.250	0.028	0.749	1.3	0.31	0.99
MYL6	16.71	16.68	16.93	*16.77*	14.49	13.97	17.19	*15.22*	15.00	16.89	16.92	17.27	16.73	16.56	*16.56*	2	2	19.2	0.259	0.309	0.553	-1.56	-0.21	-1.34
NCAM1	17.93	16.57	17.45	*17.31*	17.16	15.61	17.22	*16.66*	14.34	17.96	17.31	17.15	17.39	17.73	*16.98*	5	5	6.9	0.384	0.690	0.635	-0.65	-0.33	-0.32
NCAM1	14.94	15.66	15.84	*15.48*	17.05	15.53	17.00	*16.53*	15.03	15.09	14.96	14.52	15.05	15.02	*14.95*	3	3	10.5	0.159	0.082	0.186	1.05	-0.53	1.58
NCAN	17.85	18.97	19.57	*18.79*	18.50	15.98	17.25	*17.24*	16.75	17.56	17.34	17.58	17.13	17.94	*17.38*	8	7	6.6	0.163	0.864	0.095	-1.55	-1.41	-0.14
NDRG2	16.17	16.96	16.63	*16.58*	14.37	15.34	16.59	*15.43*	16.14	16.37	16.39	16.18	15.58	15.31	*16.00*	3	3	16.2	0.208	0.476	0.106	-1.15	-0.59	-0.56
NDUFA13	15.46	14.69	16.93	*15.69*	16.38	16.87	16.33	*16.53*	14.06	16.07	16.54	16.95	16.24	16.63	*16.08*	3	3	22.9	0.330	0.363	0.646	0.84	0.39	0.45
NDUFB7	14.92	15.96	16.72	*15.87*	15.07	14.74	15.72	*15.17*	16.57	15.46	14.55	16.65	14.62	16.53	*15.73*	2	2	12.4	0.326	0.301	0.844	-0.69	-0.14	-0.55
NDUFS1	16.83	16.42	17.32	*16.86*	16.49	14.26	16.41	*15.72*	17.06	16.84	16.45	16.90	16.35	16.81	*16.74*	7	7	11.7	0.257	0.299	0.700	-1.13	-0.12	-1.01
NEFH	17.83	18.07	17.67	*17.86*	15.63	16.09	18.33	*16.68*	19.48	17.96	18.47	17.79	19.65	18.67	*18.67*	16	14	15.8	0.294	0.126	0.049	-1.18	0.81	-1.99
NEFL	19.05	19.47	18.77	*19.10*	15.61	14.63	19.17	*16.47*	19.54	18.96	19.83	19.17	20.48	20.23	*19.70*	31	29	48.4	0.195	0.140	0.100	-2.63	0.6	-3.23
NEFM	17.71	17.12	16.54	*17.12*	15.03	14.92	18.72	*16.22*	18.51	17.73	19.22	18.27	20.53	19.44	*18.95*	28	25	35.9	0.550	0.150	0.012	-0.9	1.83	-2.73

LFQ Intensity (log2)																								
	Control (C)				Alzheimer's (AD)				rTBI										Student's t-test					
Protein Names	HM1	HM4	HM10	*Mean*	HM11	HM6	HM7	*Mean*	HM12	HM2	HM3	HM5	HM8	HM9	*Mean*	Peptides	Unique peptides	Seq coverage [%]	ADvsC	ADvs rTBI	rTBIvsC	ADvsC log2fold	rTBIvsC log2fold	ADvsrTBI log2fold
NEGR1	14.87	16.98	17.48	*16.44*	16.27	15.81	17.48	*16.52*	16.83	17.42	16.80	16.93	17.11	16.92	*17.00*	2	2	8.2	0.936	0.439	0.557	0.08	0.56	-0.48
NFASC	18.31	18.35	17.86	*18.17*	18.10	15.28	18.26	*17.21*	17.87	18.88	18.35	17.81	17.20	18.20	*18.05*	16	3	18.4	0.427	0.480	0.681	-0.96	-0.12	-0.84
NIPSNAP1	16.37	16.07	16.93	*16.45*	14.53	14.74	16.37	*15.21*	16.47	15.61	16.33	16.20	16.51	16.93	*16.34*	2	2	7	0.153	0.183	0.735	-1.24	-0.11	-1.13
NME2	18.49	19.58	19.12	*19.06*	18.81	17.54	18.58	*18.31*	18.06	18.88	18.81	17.94	14.94	19.12	*17.96*	4	4	31.6	0.211	0.654	0.165	-0.75	-1.1	0.35
NPEPPS	15.42	15.21	15.90	*15.51*	14.37	15.00	14.95	*14.77*	14.88	15.98	15.97	15.47	14.15	15.84	*15.38*	7	7	10.3	0.063	0.139	0.724	-0.74	-0.13	-0.61
NSF	15.98	14.75	14.74	*15.15*	14.92	15.15	16.40	*15.49*	17.66	16.48	14.62	16.05	17.67	14.55	*16.17*	9	9	14.1	0.614	0.383	0.189	0.34	1.02	-0.68
OMG	17.03	18.19	17.63	*17.62*	18.01	15.02	17.33	*16.79*	14.93	17.38	15.73	14.89	14.60	14.41	*15.32*	2	2	4.1	0.465	0.242	0.005	-0.83	-2.29	1.47
PARK7	18.74	19.28	19.33	*19.12*	19.54	20.58	19.27	*19.80*	18.88	18.76	18.67	18.57	18.93	18.95	*18.79*	5	5	34.9	0.226	0.125	0.221	0.68	-0.32	1
PCBP1	15.83	15.40	15.22	*15.48*	14.83	16.15	15.35	*15.44*	15.13	16.43	15.40	15.71	14.84	14.16	*15.28*	2	1	6.7	0.926	0.759	0.593	-0.04	-0.2	0.16
PCMT1	17.43	17.50	17.40	*17.44*	17.44	17.23	17.85	*17.51*	17.57	17.45	17.81	17.28	17.34	17.16	*17.44*	5	5	33	0.772	0.756	0.932	0.06	-0.01	0.07
PCSK1N	17.91	19.14	19.47	*18.84*	20.69	20.47	20.33	*20.50*	18.02	17.97	17.95	18.85	17.97	17.96	*18.12*	10	10	38.5	0.067	0.000	0.265	1.66	-0.72	2.38
PDHB	16.86	16.45	17.34	*16.88*	16.68	14.58	17.05	*16.10*	17.71	16.76	17.46	17.10	17.66	17.54	*17.37*	3	3	12.8	0.422	0.239	0.190	-0.78	0.49	-1.27
PEBP1	16.77	18.35	18.16	*17.76*	15.03	15.35	14.77	*15.05*	15.15	14.58	17.53	17.43	16.14	16.33	*16.19*	7	7	52.9	0.023	0.067	0.068	-2.71	-1.57	-1.14
PFN1	15.03	14.94	14.20	*14.72*	14.02	14.34	15.02	*14.46*	16.57	16.67	17.22	16.72	16.73	16.57	*16.75*	3	3	32.9	0.544	0.010	0.009	-0.26	2.02	-2.29
PGK1	17.70	16.43	16.63	*16.92*	15.46	15.02	15.57	*15.35*	16.85	18.52	17.41	17.10	17.47	17.67	*17.50*	13	13	37.2	0.042	0.000	0.280	-1.57	0.59	-2.15
PHB	16.72	17.27	17.86	*17.28*	17.12	16.53	17.05	*16.90*	17.60	17.07	17.85	17.46	17.53	17.50	*17.50*	6	6	35.3	0.385	0.058	0.579	-0.38	0.22	-0.6
PHB2	16.52	14.73	17.29	*16.18*	14.80	13.74	15.45	*14.66*	15.36	16.50	16.70	17.54	16.97	17.33	*16.73*	9	9	34.1	0.181	0.028	0.554	-1.52	0.55	-2.07
PHGDH	16.49	16.56	16.04	*16.36*	14.24	14.23	16.19	*14.89*	16.65	17.02	16.63	16.72	15.76	16.01	*16.47*	3	3	6.6	0.144	0.126	0.704	-1.48	0.1	-1.58
PIN1	16.62	17.36	17.07	*17.02*	15.73	15.02	16.76	*15.84*	16.75	16.86	17.23	17.09	17.21	16.80	*16.99*	3	3	22.1	0.131	0.146	0.922	-1.18	-0.02	-1.15
PKM	20.84	20.09	20.08	*20.34*	19.97	20.23	20.43	*20.21*	20.80	21.10	20.85	20.76	21.21	21.21	*20.99*	26	0	60	0.685	0.010	0.110	-0.13	0.65	-0.78
PKM	14.17	14.08	14.59	*14.28*	14.53	14.78	13.16	*14.16*	14.32	17.20	17.99	16.18	17.50	17.45	*16.77*	26	2	58.2	0.837	0.012	0.005	-0.12	2.5	-2.62
PLEC	16.72	14.55	14.12	*15.13*	14.91	15.48	17.14	*15.85*	14.95	17.39	16.55	14.38	16.98	11.93	*15.37*	18	18	4.9	0.533	0.669	0.846	0.72	0.24	0.48
PLIN3	16.08	15.26	15.18	*15.51*	15.89	15.95	15.35	*15.73*	14.74	16.12	15.81	14.60	14.76	14.96	*15.17*	3	3	13.1	0.556	0.123	0.421	0.23	-0.34	0.57
PMP2	14.91	17.89	18.31	*17.03*	14.97	15.28	15.70	*15.32*	15.09	16.07	17.03	17.50	14.90	17.60	*16.36*	6	6	43.2	0.247	0.092	0.610	-1.72	-0.67	-1.05
PPIA	19.72	19.35	19.43	*19.50*	19.14	15.63	19.54	*18.10*	19.34	19.82	20.35	19.68	19.99	19.56	*19.79*	12	12	77.6	0.378	0.307	0.157	-1.4	0.29	-1.69
PPP3CA	17.94	16.61	17.07	*17.21*	16.91	17.21	17.89	*17.34*	16.97	18.13	16.74	15.92	16.71	17.37	*16.97*	9	7	21.1	0.809	0.419	0.654	0.13	-0.24	0.36
PRDX1	17.87	16.53	17.18	*17.19*	14.40	15.50	17.39	*15.76*	17.61	18.51	19.07	18.33	18.62	18.54	*18.45*	8	7	42.7	0.240	0.085	0.061	-1.43	1.26	-2.69
PRDX2	19.06	18.67	19.48	*19.07*	16.53	16.54	18.78	*17.28*	18.01	19.29	19.93	19.12	19.03	20.22	*19.27*	13	12	40.9	0.129	0.100	0.636	-1.79	0.19	-1.99
PRDX5	16.14	17.05	17.12	*16.77*	16.59	17.40	17.19	*17.06*	17.27	16.12	14.17	17.00	17.13	16.72	*16.40*	3	3	16.8	0.508	0.260	0.540	0.29	-0.37	0.66
PRDX6	16.96	16.31	14.97	*16.08*	17.16	14.71	16.93	*16.27*	16.53	17.08	16.86	16.41	16.52	16.53	*16.66*	3	3	18.8	0.858	0.669	0.430	0.19	0.58	-0.39
PRRT2	16.88	16.29	16.78	*16.65*	17.69	17.01	17.59	*17.43*	15.84	16.44	16.09	16.55	15.94	16.62	*16.25*	2	2	3.5	0.051	0.011	0.143	0.78	-0.41	1.18
PSMB1	15.94	16.32	16.04	*16.10*	14.42	16.14	16.11	*15.56*	15.28	16.05	15.61	15.96	15.74	16.36	*15.83*	2	2	10	0.443	0.681	0.208	-0.54	-0.27	-0.27

LFQ Intensity (log2)																							
	Control (C)				Alzheimer's (AD)				rTBI										Student's t-test					
Protein Names	HM1	HM4	HM10	*Mean*	HM11	HM6	HM7	*Mean*	HM12	HM2	HM3	HM5	HM8	HM9	*Mean*	Peptides	Unique peptides	Seq coverage [%]	ADvsC	ADvs rTBI	rTBIvsC	ADvsC log2fold	rTBIvsC log2fold	ADvsrTBI log2fold
PSMB6	16.01	17.39	17.34	*16.91*	17.86	18.27	17.93	*18.02*	16.38	15.99	16.15	16.93	16.02	16.25	*16.29*	3	3	13.4	0.125	0.000	0.296	1.1	-0.63	1.73
PTGDS	17.17	18.00	17.67	*17.61*	17.36	15.40	15.48	*16.08*	15.31	16.98	17.62	16.30	16.04	17.77	*16.67*	2	2	17.4	0.127	0.481	0.080	-1.53	-0.94	-0.59
PTPRZ1	17.72	18.00	18.05	*17.92*	17.99	15.67	17.25	*16.97*	16.73	17.93	16.67	17.22	16.24	17.47	*17.04*	5	5	2.2	0.299	0.929	0.016	-0.95	-0.88	-0.07
PYGB	16.33	15.31	15.38	*15.67*	16.64	17.08	16.74	*16.82*	14.50	16.43	15.73	14.65	14.23	14.18	*14.95*	2	2	2.4	0.058	0.003	0.196	1.15	-0.72	1.87
QDPR	18.20	18.66	18.36	*18.41*	17.94	14.26	17.19	*16.46*	16.74	18.52	18.43	18.23	17.62	18.75	*18.05*	6	6	42.2	0.224	0.290	0.321	-1.95	-0.36	-1.59
RAB6A	14.59	17.10	16.73	*16.14*	17.40	15.04	16.67	*16.37*	15.05	16.00	15.87	15.79	16.01	15.85	*15.76*	5	3	32.7	0.839	0.475	0.675	0.23	-0.38	0.61
RAB7A	16.70	16.36	16.28	*16.45*	16.11	14.73	14.48	*15.11*	16.02	16.49	16.00	16.10	16.35	16.45	*16.24*	2	2	13	0.110	0.152	0.251	-1.34	-0.21	-1.13
RALA	15.64	14.80	16.29	*15.58*	14.33	14.42	15.31	*14.69*	15.12	16.11	15.46	15.63	15.33	16.09	*15.63*	4	4	25.7	0.177	0.071	0.923	-0.89	0.05	-0.94
RAP1B	15.37	14.40	14.67	*14.82*	14.32	14.34	14.69	*14.45*	15.33	15.73	15.57	15.26	15.00	15.36	*15.38*	3	3	13.6	0.337	0.002	0.181	-0.36	0.56	-0.92
RPL11	15.54	15.69	15.07	*15.43*	14.94	15.73	14.80	*15.16*	14.41	14.96	15.63	15.64	16.08	14.34	*15.18*	2	2	16.3	0.477	0.956	0.496	-0.27	-0.25	-0.02
RPS18	15.39	17.00	16.87	*16.42*	16.99	16.29	16.15	*16.48*	14.99	14.97	14.40	15.98	14.65	15.78	*15.13*	2	2	13.2	0.929	0.011	0.110	0.06	-1.29	1.35
RPSA	16.79	17.66	17.38	*17.28*	17.25	17.32	17.40	*17.32*	16.95	17.26	16.45	16.92	14.88	16.68	*16.52*	4	4	18.3	0.873	0.069	0.125	0.05	-0.75	0.8
RTN1	16.21	17.23	14.66	*16.03*	17.57	14.00	17.23	*16.27*	15.99	16.25	16.26	16.18	16.23	14.43	*15.89*	2	2	3.6	0.873	0.777	0.873	0.23	-0.14	0.38
S100B	19.00	19.45	19.02	*19.16*	16.49	14.78	16.50	*15.92*	16.66	19.04	19.49	18.07	17.37	19.54	*18.36*	2	2	21.3	0.024	0.023	0.169	-3.23	-0.8	-2.43
SEPTIN2	16.32	15.34	15.38	*15.68*	15.68	14.21	16.25	*15.38*	14.96	16.90	17.30	16.58	17.14	16.26	*16.52*	5	5	19.1	0.690	0.190	0.123	-0.3	0.84	-1.14
SEPTIN7	16.40	15.07	14.90	*15.46*	14.87	15.09	14.86	*14.94*	15.92	16.36	15.81	16.07	16.01	15.57	*15.96*	3	3	9.8	0.388	0.000	0.405	-0.52	0.5	-1.02
SEPT8	14.51	14.03	15.46	*14.67*	14.81	15.01	14.77	*14.86*	14.66	16.07	16.17	15.63	16.31	15.55	*15.73*	3	3	8.1	0.696	0.015	0.105	0.19	1.06	-0.87
SFXN1	15.93	15.60	17.37	*16.30*	16.28	15.88	16.90	*16.35*	17.59	15.81	16.64	17.35	17.09	17.26	*16.96*	4	4	14.9	0.936	0.186	0.356	0.05	0.66	-0.6
SH3GL2	17.24	16.10	16.29	*16.55*	14.78	15.36	15.78	*15.30*	17.23	17.23	17.53	17.12	17.58	17.27	*17.33*	4	4	16.8	0.055	0.015	0.153	-1.24	0.78	-2.02
SIRPA	19.06	19.15	19.79	*19.33*	20.03	19.61	19.75	*19.80*	19.76	19.18	18.61	19.52	19.74	18.68	*19.25*	9	9	23.2	0.171	0.059	0.797	0.46	-0.08	0.55
SIRT2	17.60	16.86	16.27	*16.91*	16.81	17.73	15.66	*16.73*	17.38	17.56	17.05	16.94	17.20	15.92	*17.01*	3	3	6.9	0.814	0.699	0.841	-0.18	0.1	-0.28
SLC25A12	14.74	15.55	15.67	*15.32*	14.92	14.99	16.29	*15.40*	14.55	15.76	16.60	16.94	16.84	17.04	*16.29*	4	4	8.1	0.887	0.196	0.091	0.08	0.97	-0.89
SLC9A3R1	16.92	16.85	17.02	*16.93*	16.82	14.25	14.63	*15.24*	14.84	16.83	16.19	16.18	15.99	16.30	*16.06*	3	3	15.6	0.168	0.416	0.022	-1.69	-0.87	-0.82
SNAP25	20.48	21.12	21.07	*20.89*	21.13	21.20	21.12	*21.15*	20.91	20.53	20.49	20.64	20.47	20.35	*20.56*	15	15	55.8	0.332	0.000	0.248	0.26	-0.33	0.59
SNCA	16.66	16.32	17.15	*16.71*	14.20	14.80	14.83	*14.61*	14.77	17.40	17.34	15.78	15.57	17.51	*16.40*	7	6	54.3	0.003	0.012	0.575	-2.1	-0.32	-1.78
SOD1	14.11	15.10	14.16	*14.46*	14.74	15.11	15.52	*15.12*	15.80	17.09	18.12	16.89	17.16	17.60	*17.11*	3	3	58.4	0.175	0.001	0.001	0.66	2.65	-1.99
SPTAN1	18.06	16.97	16.71	*17.24*	17.32	17.08	18.05	*17.48*	18.16	18.83	17.92	17.50	18.88	17.47	*18.13*	36	36	17.6	0.666	0.156	0.151	0.24	0.88	-0.64
SPTBN1	18.56	17.55	17.87	*17.99*	16.68	15.80	18.51	*17.00*	18.51	18.84	17.99	17.98	19.01	17.95	*18.38*	25	25	13.9	0.339	0.221	0.343	-1	0.39	-1.38
STMN1	19.18	18.50	18.80	*18.83*	18.24	15.29	18.26	*17.26*	17.81	19.08	18.73	18.13	18.05	18.42	*18.37*	6	6	38.3	0.251	0.379	0.148	-1.57	-0.46	-1.11
STX1A	17.69	16.73	16.67	*17.03*	15.66	14.91	17.43	*16.00*	17.34	18.02	16.78	17.28	17.60	16.93	*17.33*	6	6	22.6	0.303	0.212	0.489	-1.03	0.3	-1.33
STX1B	17.39	17.36	17.13	*17.29*	17.10	16.04	17.75	*16.96*	17.69	17.72	17.34	17.21	18.05	17.82	*17.64*	8	8	30.2	0.574	0.305	0.055	-0.33	0.34	-0.68
STXBP1	19.10	18.48	17.84	*18.47*	18.51	18.04	19.25	*18.60*	19.84	19.38	19.26	19.21	19.96	18.33	*19.33*	12	12	23.7	0.818	0.162	0.125	0.13	0.86	-0.73

LFQ Intensity (log2)																							
	Control (C)				Alzheimer's (AD)				rTBI										Student's t-test					
Protein Names	HM1	HM4	HM10	*Mean*	HM11	HM6	HM7	*Mean*	HM12	HM2	HM3	HM5	HM8	HM9	*Mean*	Peptides	Unique peptides	Seq coverage [%]	ADvsC	ADvs rTBI	rTBIvsC	ADvsC log2fold	rTBIvsC log2fold	ADvsrTBI log2fold
SYN1	18.57	17.97	18.13	*18.22*	17.92	14.99	17.92	*16.94*	18.28	18.93	18.41	18.85	19.16	17.61	*18.54*	12	11	27.7	0.318	0.239	0.314	-1.28	0.32	-1.6
SYN2	17.71	16.75	16.66	*17.04*	16.94	14.79	17.40	*16.38*	14.71	17.82	16.50	16.76	16.89	15.98	*16.45*	4	3	13.2	0.507	0.944	0.310	-0.66	-0.6	-0.07
TAGLN3	17.02	16.45	15.19	*16.22*	14.75	16.59	15.05	*15.46*	17.05	16.28	15.17	17.06	17.16	16.85	*16.60*	3	3	15.1	0.387	0.171	0.587	-0.76	0.37	-1.14
TALDO1	16.61	14.21	15.25	*15.36*	15.02	15.16	15.19	*15.12*	15.92	16.53	17.61	14.66	17.19	16.82	*16.46*	6	6	18.1	0.771	0.026	0.256	-0.23	1.1	-1.33
THY1	16.29	17.38	17.48	*17.05*	17.94	14.60	17.23	*16.59*	14.59	17.06	17.68	16.56	16.27	17.28	*16.58*	4	4	26.1	0.705	0.991	0.447	-0.46	-0.47	0.01
TKT	17.06	16.64	16.08	*16.59*	16.82	17.04	17.10	*16.99*	16.55	18.12	18.72	16.98	17.73	17.91	*17.67*	14	14	26.3	0.296	0.088	0.044	0.4	1.08	-0.68
TMSB10	17.59	17.32	17.25	*17.39*	18.86	16.50	18.11	*17.82*	13.86	16.74	17.83	14.11	17.43	14.95	*15.82*	3	3	68.2	0.595	0.092	0.078	0.44	-1.57	2.01
TNR	19.22	18.66	17.94	*18.60*	18.94	18.09	19.04	*18.69*	17.46	19.35	19.03	18.49	19.17	18.82	*18.72*	12	12	11.1	0.866	0.941	0.811	0.09	0.12	-0.03
TPI1	17.40	16.63	17.25	*17.09*	14.41	15.14	14.96	*14.84*	15.60	18.06	18.15	17.35	17.38	17.53	*17.34*	12	12	55.6	0.002	0.001	0.589	-2.25	0.25	-2.51
TPM1	18.15	15.88	17.17	*17.07*	17.37	17.13	18.34	*17.61*	18.54	18.90	18.35	18.12	18.73	18.12	*18.46*	9	6	36.7	0.519	0.137	0.163	0.55	1.39	-0.85
TPM3	17.39	17.25	14.97	*16.54*	17.98	15.07	18.18	*17.08*	18.39	17.79	17.92	17.51	18.85	17.46	*17.98*	8	4	33	0.695	0.464	0.201	0.54	1.45	-0.91
TPM4	16.31	14.61	14.94	*15.29*	15.04	14.89	16.53	*15.49*	17.10	16.04	15.68	16.34	17.25	16.13	*16.42*	5	1	24.6	0.796	0.205	0.143	0.2	1.14	-0.94
TPP1	16.65	16.54	16.86	*16.68*	15.07	15.20	16.92	*15.73*	14.88	16.67	17.26	16.50	16.71	16.14	*16.36*	3	3	7.5	0.249	0.417	0.387	-0.95	-0.32	-0.63
TPPP	17.98	14.56	14.72	*15.75*	15.36	14.61	14.14	*14.71*	15.17	18.77	18.89	17.86	18.70	17.91	*17.88*	6	6	32.4	0.451	0.002	0.184	-1.05	2.13	-3.18
TPPP3	17.71	16.66	16.46	*16.94*	14.87	16.22	15.68	*15.59*	17.75	17.30	17.10	16.35	17.29	16.65	*17.07*	2	2	15.9	0.070	0.041	0.787	-1.36	0.13	-1.48
TUBA1A	15.83	15.70	13.84	*15.12*	14.69	15.15	15.31	*15.05*	14.38	14.74	14.14	14.71	15.15	13.58	*14.45*	20	1	51.7	0.926	0.079	0.409	-0.07	-0.67	0.6
TUBA1B	22.49	22.23	21.26	*21.99*	20.73	20.72	21.21	*20.88*	22.16	22.44	22.27	22.18	22.20	21.74	*22.16*	21	0	54.5	0.080	0.004	0.698	-1.11	0.17	-1.28
TUBA4A	18.31	18.20	14.89	*17.13*	17.23	15.37	14.92	*15.84*	17.00	18.19	17.64	13.85	17.66	16.74	*16.85*	21	6	55.4	0.395	0.337	0.838	-1.29	-0.28	-1.01
TUBB	19.25	18.33	13.81	*17.13*	14.44	14.99	18.68	*16.04*	19.20	19.36	18.88	18.55	19.73	17.95	*18.94*	19	2	47.5	0.639	0.157	0.394	-1.09	1.81	-2.9
TUBB2A	22.43	22.53	21.31	*22.09*	21.25	21.22	21.83	*21.43*	21.61	22.59	22.33	21.93	22.15	21.63	*22.04*	23	2	58.4	0.234	0.065	0.917	-0.65	-0.05	-0.61
TUBB3	17.64	17.98	15.60	*17.07*	15.50	15.34	16.67	*15.84*	16.92	17.94	17.63	16.93	18.05	16.27	*17.29*	20	7	45.8	0.239	0.046	0.807	-1.24	0.22	-1.45
TUBB4A	19.68	18.30	18.77	*18.92*	19.06	15.19	18.93	*17.73*	20.51	19.47	19.78	18.66	18.92	18.96	*19.38*	20	4	48.4	0.452	0.320	0.395	-1.19	0.47	-1.66
TUBB4B	22.27	22.13	20.84	*21.75*	20.70	20.35	22.04	*21.03*	22.47	22.27	21.84	21.93	22.25	21.03	*21.97*	22	2	52.4	0.357	0.202	0.691	-0.71	0.22	-0.93
UBA1	16.70	16.66	16.48	*16.61*	16.61	15.02	16.57	*16.07*	16.16	17.53	16.37	15.68	16.29	14.36	*16.06*	6	6	7.9	0.407	0.996	0.251	-0.55	-0.55	0
UBC	19.58	20.73	20.57	*20.29*	21.61	20.49	21.04	*21.04*	20.75	19.31	18.93	19.79	19.97	19.70	*19.74*	9	9	72.3	0.196	0.029	0.276	0.75	-0.55	1.3
UBE2V2	19.03	15.18	16.62	*16.95*	16.22	14.32	17.65	*16.06*	18.52	16.90	18.29	17.78	18.42	17.56	*17.91*	2	2	17.9	0.585	0.189	0.484	-0.88	0.96	-1.85
UCHL1	18.52	17.43	17.43	*17.79*	16.98	14.72	18.12	*16.60*	17.71	18.89	18.02	17.62	18.80	17.44	*18.08*	9	9	42.2	0.359	0.275	0.552	-1.19	0.29	-1.47
UQCRC1	16.59	16.29	16.30	*16.39*	14.88	14.71	16.02	*15.20*	17.84	16.89	16.88	17.58	16.80	17.47	*17.24*	5	5	13.3	0.094	0.023	0.004	-1.19	0.85	-2.04
UQCRC2	16.87	16.13	17.68	*16.89*	15.63	15.30	17.48	*16.14*	18.17	16.88	17.91	18.26	18.25	18.28	*17.96*	7	7	21	0.412	0.103	0.121	-0.76	1.07	-1.83
UQCRFS1	18.76	18.80	18.69	*18.75*	19.38	19.99	19.04	*19.47*	18.35	17.37	17.53	18.61	18.25	17.64	*17.96*	2	2	8	0.120	0.010	0.012	0.72	-0.79	1.51
VAMP1	15.74	15.92	16.23	*15.96*	16.73	15.11	14.30	*15.38*	16.26	15.30	16.35	16.02	15.93	16.39	*16.04*	3	1	23.7	0.503	0.453	0.724	-0.58	0.08	-0.66
VAMP2	18.12	17.56	18.13	*17.94*	18.60	16.88	18.44	*17.97*	17.30	18.54	18.68	18.75	18.65	18.71	*18.44*	5	3	39.7	0.961	0.494	0.140	0.03	0.5	-0.47

LFQ Intensity (log2)																							
	Control (C)				Alzheimer's (AD)				rTBI										Student's t-test					
Protein Names	HM1	HM4	HM10	*Mean*	HM11	HM6	HM7	*Mean*	HM12	HM2	HM3	HM5	HM8	HM9	*Mean*	Peptides	Unique peptides	Seq coverage [%]	ADvsC	ADvs rTBI	rTBIvsC	ADvsC log2fold	rTBIvsC log2fold	ADvsrTBI log2fold
VAPB	15.63	16.11	15.64	*15.79*	16.54	15.28	14.33	*15.38*	15.98	15.65	16.28	15.86	14.42	15.93	*15.69*	2	1	11.5	0.591	0.694	0.740	-0.41	-0.11	-0.3
VCAN	21.26	21.12	21.24	*21.21*	20.96	15.45	17.87	*18.10*	19.07	21.72	21.57	20.16	21.02	21.49	*20.84*	14	14	5.4	0.191	0.223	0.427	-3.11	-0.37	-2.74
VCP	17.11	16.17	16.28	*16.52*	17.22	14.47	17.24	*16.31*	16.81	17.28	17.31	17.18	17.52	17.35	*17.24*	11	11	15.5	0.848	0.419	0.123	-0.21	0.72	-0.93
VDAC1	16.33	16.51	17.32	*16.72*	14.18	14.98	14.75	*14.64*	15.23	16.25	15.90	16.71	14.67	16.72	*15.91*	4	4	19.8	0.007	0.018	0.125	-2.08	-0.81	-1.27
VDAC2	16.67	16.46	17.42	*16.85*	14.99	14.90	16.66	*15.52*	17.38	16.64	17.21	17.84	17.49	17.72	*17.38*	5	5	21.8	0.130	0.071	0.203	-1.33	0.53	-1.86
VIM	16.69	15.20	15.82	*15.90*	15.09	14.23	16.68	*15.33*	14.53	16.90	18.50	17.54	17.76	17.05	*17.05*	17	15	35.8	0.542	0.125	0.150	-0.57	1.14	-1.71
YWHAE	18.96	19.16	19.10	*19.07*	18.55	17.78	18.38	*18.24*	19.17	19.33	19.52	18.95	19.34	19.39	*19.28*	11	9	39.2	0.062	0.034	0.073	-0.84	0.21	-1.05
YWHAG	20.26	19.73	20.12	*20.04*	19.91	14.18	19.95	*18.01*	20.44	20.18	20.36	20.38	19.86	20.32	*20.26*	8	5	34.8	0.402	0.362	0.308	-2.02	0.22	-2.24
YWHAH	19.83	18.58	18.91	*19.11*	19.23	18.62	19.69	*19.18*	19.79	19.13	18.74	19.07	19.71	18.42	*19.14*	5	3	23.2	0.887	0.920	0.943	0.07	0.03	0.04
YWHAQ	17.11	15.33	16.09	*16.18*	15.25	14.94	17.15	*15.78*	18.45	16.20	14.62	16.90	18.37	16.86	*16.90*	5	3	17.6	0.672	0.272	0.388	-0.4	0.72	-1.12
YWHAZ	17.95	14.16	17.16	*16.42*	15.04	14.91	17.09	*15.68*	18.88	17.96	17.63	17.67	18.11	18.17	*18.07*	9	7	41.6	0.618	0.068	0.288	-0.74	1.65	-2.39

List of References

Abbott. (2005). Dynamics of CNS barriers: Evolution, differentiation, and modulation. *Cellular and Molecular Neurobiology*, *25*(1), 5–23. https://doi.org/10.1007/s10571-004-1374-y

Abbott, Revest, P. A., & Romero, I. A. (1992). Glial Symposium Astrocyte-endothelial interaction: physiology and pathology. *Neuropathology and Applied Neurobiology*, *18*, 424–433.

Abbott, Rönnbäck, L., & Hansson, E. (2006). Astrocyte-endothelial interactions at the blood-brain barrier. *Nature Reviews Neuroscience*, *7*(1), 41–53. https://doi.org/10.1038/nrn1824

Abdi, F., Quinn, J. F., Jankovic, J., McIntosh, M., Leverenz, J. B., Peskind, E., Nixon, R., Nutt, J., Chung, K., Zabetian, C., Samii, A., Lin, M., Hattan, S., Pan, C., Wang, Y., Jin, J., Zhu, D., Li, G. J., Liu, Y., … Zhang, J. (2006). Detection of biomarkers with a multiplex quantitative proteomic platform in cerebrospinal fluid of patients with neurodegenerative disorders. *Journal of Alzheimer's Disease*, *9*(3), 293–348. https://doi.org/10.3233/JAD-2006-9309

Abu Hamdeh, S., Waara, E. R., Möller, C., Söderberg, L., Basun, H., Alafuzoff, I., Hillered, L., Lannfelt, L., Ingelsson, M., & Marklund, N. (2018). Rapid amyloid-ß oligomer and protofibril accumulation in traumatic brain injury. *Brain Pathology*, *28*(4), 451–462. https://doi.org/10.1111/bpa.12532

Abu Hamdeh, Shevchenko, G., Mi, J., Musunuri, S., Bergquist, J., & Marklund, N. (2018). Proteomic differences between focal and diffuse traumatic brain injury in human brain tissue. *Scientific Reports*, *8*(1), 1–15. https://doi.org/10.1038/s41598-018-25060-0

Acosta, S. A., Tajiri, N., de la Pena, I., Bastawrous, M., Sanberg, P. R., Kaneko, Y., & Borlongan, C. V. (2015). Alpha-Synuclein as a pathological link between chronic traumatic brain injury and parkinson's disease. *Journal of Cellular Physiology*, *230*(5), 1024–1032. https://doi.org/10.1002/jcp.24830

Adams, J. H., Doyle, D., Ford, I., Gennarelli, T. A., Graham, D. I., & Mclellan, D. R. (1989). Diffuse axonal injury in head injury: Definition, diagnosis and grading. *Histopathology*, *15*(1), 49–59. https://doi.org/10.1111/j.1365-2559.1989.tb03040.x

Adams, J. H., Graham, D. I., Murray, L. S., & Scott, G. (1982). Diffuse axonal injury due to nonmissile head injury in humans: an analysis of 45 cases. *Annals of Neurology*, *12*(6), 557–563. https://doi.org/10.1002/ana.410120610

Adams, J. W., Alvarez, V. E., Mez, J., Huber, B. R., Tripodis, Y., Xia, W., Meng, G., Kubilus, C. A., Cormier, K., Kiernan, P. T., Daneshvar, D. H., Chua, A. S., Svirsky, S., Nicks, R., Abdolmohammadi, B., Evers, L., Solomon, T., Cherry, J. D., Aytan, N., … Stein, T. D. (2018). Lewy Body Pathology and Chronic Traumatic Encephalopathy Associated with Contact Sports. *Journal of Neuropathology and Experimental Neurology*, *77*(9), 757–768. https://doi.org/10.1093/jnen/nly065

Aizenstein, H. J., Nebes, R. D., Saxton, J. A., Price, J. C., Mathis, C. A., Tsopelas, N. D., Ziolko, S. K., James, J. A., Snitz, B. E., Houck, P. R., Bi, W., Cohen, A. D., Lopresti, B. J., Dekosky, S. T., Halligan, E. M., & Klunk, W. E. (2008). Frequent Amyloid Deposition Without Significant Cognitive Impairment Among the Elderly. *Arch Neurol*, *65*(11), 1509–1517. www.fil.ion.ucl.ac.uk/spm/software/spm5/

Akiyama, H., Barger, S., Barnum, S., Bradt, B., Bauer, J., Cole, G. M., Cooper, N. R., Eikelenboom, P., Emmerling, M., Fiebich, B. L., Finch, C. E., Frautschy, S., Griffin, W. S. T., Hampel, H., Hull, M., Landreth, G., Lue, L. F., Mrak, R., MacKenzie, I. R., … Wyss-Coray, T. (2000). Inflammation and Alzheimer's disease. In *Neurobiology of Aging* (Vol. 21, Issue 3). https://doi.org/10.1016/S0197-4580(00)00124-X

Allsop, D., Haga, S., Bruton, C., lshii, T., & Roberts, G. W. (1990). Rapid Communication Neurofibrillary Tangles in Some Cases of Dementia Pugilistica Share Antigens with Amyloid fl-Protein of Alzheimer's Disease. In *American journal ofPathology* (Vol. 136, Issue 2).

Alosco, M. L., Stein, T. D., Tripodis, Y., Chua, A. S., Kowall, N. W., Huber, B. R., Goldstein, L. E., Cantu, R. C., Katz, D. I., Palmisano, J. N., Martin, B., Cherry, J. D., Mahar, I., Killiany, R. J., McClean, M. D., Au, R., Alvarez, V., Stern, R. A., Mez, J., & McKee, A. C. (2019). Association of White Matter Rarefaction, Arteriolosclerosis, and Tau with Dementia in Chronic Traumatic Encephalopathy. *JAMA Neurology*, *76*(11), 1298–1308. https://doi.org/10.1001/jamaneurol.2019.2244

Anderson, Scheff, S. W., Miller, K. M., Roberts, K. N., Gilmer, L. K., Yang, C., & Shaw, G. (2008). The phosphorylated axonal form of the neurofilament subunit NF-H (pNF-H) as a blood biomarker of traumatic brain injury. *Journal of Neurotrauma*, *25*(9), 1079–1085. https://doi.org/10.1089/neu.2007.0488

Andreev, V. P., Petyuk, V. A., Brewer, H. M., Karpievitch, Y. V., Xie, F., Clarke, J., Camp, D., Smith, R. D., Lieberman, A. P., Albin, R. L., Nawaz, Z., El Hokayem, J., & Myers, A. J. (2012). Label-free quantitative LC-MS proteomics of alzheimer's disease and normally aged human brains. *Journal of Proteome Research*, *11*(6), 3053–3067. https://doi.org/10.1021/pr3001546

Ankeny, D. P., Guan, Z., & Popovich, P. G. (2009). B cells produce pathogenic antibodies and impair recovery after spinal cord injury in mice. *The Journal of Clinical Investigation*, *119*(10), 2990. https://doi.org/10.1172/JCI39780DS1

Ankeny, D. P., Lucin, K. M., Sanders, V. M., McGaughy, V. M., & Popovich, P. G. (2006). Spinal cord injury triggers systemic autoimmunity: Evidence for chronic B lymphocyte activation and lupus-like autoantibody synthesis. *Journal of Neurochemistry*, *99*(4), 1073–1087. https://doi.org/10.1111/j.1471-4159.2006.04147.x

Ankeny, D. P., & Popovich, P. G. (2009). Mechanisms and implications of adaptive immune responses after traumatic spinal cord injury. *Neuroscience*, *158*(3), 1112–1121. https://doi.org/10.1016/j.neuroscience.2008.07.001

Aoki-Yoshino, K., Uchihara, T., Duyckaerts, C., Nakamura, A., Hauw, J. J., & Wakayama, Y. (2005). Enhanced expression of aquaporin 4 in human brain with inflammatory diseases. *Acta Neuropathologica*, *110*(3), 281–288. https://doi.org/10.1007/s00401-005-1052-2

Arena, J. D., Smith, D. H., Lee, E. B., Gibbons, G. S., Irwin, D. J., Robinson, J. L., Lee, V. M. Y., Trojanowski, J. Q., Stewart, W., & Johnson, V. E. (2020). Tau immunophenotypes in chronic traumatic encephalopathy recapitulate those of ageing and Alzheimer's disease. *Brain : A Journal of Neurology*, *143*(5), 1572–1587. https://doi.org/10.1093/brain/awaa071

Areza-Fegyveres, Rosemberg, S., Castro, R. M. R. P. S., Porto, C. S., Santoro Bahia, V., Caramelli, P., Nitrini, R., & Renata, D. (2007). Dementia

Pugilistica with CliniCal Features oF alzheimer's Disease. *Arq Neuropsiquiatr*, *65*(3-B), 830–833.

Ariza, M., Serra-Grabulosa, J. M., Junqué, C., Ramírez, B., Mataró, M., Poca, A., Bargalló, N., & Sahuquillo, J. (2006). Hippocampal head atrophy after traumatic brain injury. *Neuropsychologia*, *44*(10), 1956–1961. https://doi.org/10.1016/j.neuropsychologia.2005.11.007

Armstrong, M. J., & Okun, M. S. (2020). Diagnosis and Treatment of Parkinson Disease: A Review. In *JAMA - Journal of the American Medical Association* (Vol. 323, Issue 6, pp. 548–560). American Medical Association. https://doi.org/10.1001/jama.2019.22360

Baba, M., Nakajo, S., Tu, P.-H., Tomita, T., Nakaya, K., M-Y Lee, V., Trojanowski, J. Q., Iwatsubo, T., & M-Y Lee or John Trojanowski, V. Q. (1998). Short Communication Aggregation of a-Synuclein in Lewy Bodies of Sporadic Parkinson's Disease and Dementia with Lewy Bodies. In *Amercan Journal ofPathology* (Vol. 152, Issue 4).

Babcock, K. J., Abdolmohammadi, B., Kiernan, P. T., Mahar, I., Cherry, J. D., Alvarez, V. E., Goldstein, L. E., Stein, T. D., McKee, A. C., & Huber, B. R. (2022). Interface astrogliosis in contact sport head impacts and military blast exposure. *Acta Neuropathologica Communications*, *10*(1). https://doi.org/10.1186/s40478-022-01358-z

Bäckman, L., Jones, S., Berger, A. K., Laukka, E. J., & Small, B. J. (2005). Cognitive impairment in preclinical Alzheimer's disease: A meta-analysis. *Neuropsychology*, *19*(4), 520–531. https://doi.org/10.1037/0894-4105.19.4.520

Baguley, I., Slewa-Younan, S., Lazarus, R., & Green, A. (2000). Long-term mortality trends in patients with traumatic brain injury. *Brain Injury*, *14*(6), 505–512. https://doi.org/10.1080/026990500120420

Baldwin, S., Fugaccia, I., Brown, D., Brown, L., & Scheff, S. (1996). Blood-brain barrier breach following cortical contusion in the rat. *Journal of Neurosurgery*, *85*, 476–481.

Ballabh, P., Braun, A., & Nedergaard, M. (2004). The blood-brain barrier: An overview: Structure, regulation, and clinical implications. *Neurobiology of Disease*, *16*(1), 1–13. https://doi.org/10.1016/j.nbd.2003.12.016

Baranello, R. J., Bharani, K. L., Padmaraju, V., Chopra, N., Lahiri, D. K., Greig, N. H., Pappolla, M. A., & Sambamurti, K. (2015). Amyloid-Beta Protein Clearance and Degradation (ABCD) Pathways and their Role in Alzheimer's Disease HHS Public Access Author manuscript. *Curr Alzheimer Res*, *12*(1), 32–46.

Bardehle, S., Krüger, M., Buggenthin, F., Schwausch, J., Ninkovic, J., Clevers, H., Snippert, H. J., Theis, F. J., Meyer-Luehmann, M., Bechmann, I., Dimou, L., & Götz, M. (2013). Live imaging of astrocyte responses to acute injury reveals selective juxtavascular proliferation. *Nature Neuroscience*, *16*(5), 580–586. https://doi.org/10.1038/nn.3371

Baskaya, M. K., Rao, A. M., Dogan, A., Donaldson, D., & Dempsey, R. J. (1997). The biphasic opening of the blood-brain barrier in the cortex and hippocampus after traumatic brain injury in rats. *Neuroscience Letters*, *226*, 33–36.

Basso, M., Giraudo, S., Corpillo, D., Bergamasco, B., Lopiano, L., & Fasano, M. (2004). Proteome analysis of human substantia nigra in Parkinson's disease. *Proteomics*, *4*(12), 3943–3952. https://doi.org/10.1002/pmic.200400848

Beach, T. G., & Mcgeer, E. G. (1988). Lamina-specific arrangement of astrocytic gliosis and senile plaques in Alzheimer's disease visual cortex. In *Brain Research* (Vol. 463).

Beach, T. G., Walker, R., & McGeer, E. G. (1989). Patterns of gliosis in alzheimer's disease and aging cerebrum. *Glia*, *2*(6), 420–436. https://doi.org/10.1002/glia.440020605

Beal. (1995). Aging, energy, and oxidative stress in neurodegenerative diseases. *Annals of Neurology*, *38*(3), 357–366. https://doi.org/10.1002/ana.410380304

Becher, B., Prat, A., & Antel, J. P. (2000). *Brain-Immune Connection : Immuno-Regulatory Properties of CNS-Resident Cells*. *304*(October 1999), 293–304.

Bedino, J. H. (2003). Embalming chemistry: glutaraldehyde versus formaldehyde. *Champion Expanding Encyclopedia of Mortuary Practices*, *649*, 2614–2632.

Beers, D. R., Zhao, W., Wang, J., Zhang, X., Wen, S., Neal, D., Thonhoff, J. R., Alsuliman, A. S., Shpall, E. J., Rezvani, K., & Appel, S. H. (2017). ALS patients' regulatory T lymphocytes are dysfunctional, and correlate with disease progression rate and severity. *JCI Insight*, *2*(5). https://doi.org/10.1172/jci.insight.89530

Behrouz, N., Defossez, A., Delacourte, A., & Mazzuca, M. (1991). The Immunohistochemical Evidence of Amyloid Diffuse Deposits as a Pathological Hallmark in Alzheimer's Disease. In *Journal ofGeronwlogv: BIOLOGICAL SCIENCES* (Vol. 46, Issue 6). https://academic.oup.com/geronj/article/46/6/B209/633985

Bell, R. D., & Zlokovic, B. V. (2009). Neurovascular mechanisms and blood-brain barrier disorder in Alzheimer's disease. In *Acta Neuropathologica* (Vol. 118, Issue 1, pp. 103–113). https://doi.org/10.1007/s00401-009-0522-3

Berg, D., Postuma, R. B., Adler, C. H., Bloem, B. R., Chan, P., Dubois, B., Gasser, T., Goetz, C. G., Halliday, G., Joseph, L., Lang, A. E., Liepelt-Scarfone, I., Litvan, I., Marek, K., Obeso, J., Oertel, W., Olanow, C. W., Poewe, W., Stern, M., & Deuschl, G. (2015). MDS research criteria for prodromal Parkinson's disease. In *Movement Disorders* (Vol. 30, Issue 12, pp. 1600–1611). John Wiley and Sons Inc. https://doi.org/10.1002/mds.26431

Bergold. (2016). Treatment of traumatic brain injury with anti-inflammatory drugs. *Experimental Neurology*, *275*(3), 367–380. https://doi.org/10.1016/j.expneurol.2015.05.024

Bernick, C., Shan, G., Zetterberg, H., Banks, S., Mishra, V. R., Bekris, L., Leverenz, J. B., & Blennow, K. (2020). Longitudinal change in regional brain volumes with exposure to repetitive head impacts. *Neurology*, *94*(3), e232–e240. https://doi.org/10.1212/WNL.0000000000008817

Beyreuther, K., & Masters, C. L. (1991). Amyloid Precursor Protein (APP) and BZA4 Amyloid in the Etiology of Alzheimer's Disease: Precursor-Product Relationships in the Derangement of Neuronal Function. *Brain Pathology*, *1*(4), 241–251. https://doi.org/10.1111/j.1750-3639.1991.tb00667.x

Bieniek, K. F., Cairns, N. J., Crary, J. F., Dickson, D. W., Folkerth, R. D., Keene, C. D., Litvan, I., Perl, D. P., Stein, T. D., Vonsattel, J. P., Stewart, W., Dams-O'connor, K., Gordon, W. A., Tripodis, Y., Alvarez, V. E., Mez, J., Alosco, M. L., Mckee, A. C., Babcock, D., … Koroshetz, W. (2021). The Second NINDS/NIBIB Consensus Meeting to Define Neuropathological Criteria for the Diagnosis of Chronic Traumatic Encephalopathy. *Journal of Neuropathology and Experimental Neurology*, *80*(3), 210–219. https://doi.org/10.1093/jnen/nlab001

Blasko, I., & Grubeck-Loebenstein, B. (2003). Role of the immune system in the pathogenesis, prevention and treatment of Alzheimer's disease. *Drugs Aging*, *20*(2), 101–113. https://doi.org/200202 [pii]

Blennow, Jonsson, M., Andreasen, N., Rosengren, L., Wallin, A., Hellström, P. A., & Zetterberg, H. (2011). No neurochemical evidence of brain injury after blast overpressure by repeated explosions or firing heavy weapons. *Acta Neurologica Scandinavica*, *123*(4), 245–251. https://doi.org/10.1111/j.1600-0404.2010.01408.x

Blixt, J., Svensson, M., Gunnarson, E., & Wanecek, M. (2015). Aquaporins and blood-brain barrier permeability in early edema development after traumatic brain injury. *Brain Research*, *1611*, 18–28. https://doi.org/10.1016/j.brainres.2015.03.004

Block, M. L., & Hong, J. S. (2005). Microglia and inflammation-mediated neurodegeneration: Multiple triggers with a common mechanism. In *Progress in Neurobiology* (Vol. 76, Issue 2, pp. 77–98). https://doi.org/10.1016/j.pneurobio.2005.06.004

Bloem, B. R., Okun, M. S., & Klein, C. (2021). Parkinson's disease. In *The Lancet* (Vol. 397, Issue 10291, pp. 2284–2303). Elsevier B.V. https://doi.org/10.1016/S0140-6736(21)00218-X

Blumenthal, H. T. (2004). Amyloidosis: A Universal Disease of Aging? *The Journals of Gerontology Series A: Medical Sciences*, *59*(4), 361–369. https://doi.org/10.1093/gerona/59.4.m361

Blyth, B. J., Farhavar, A., Gee, C., Hawthorn, B., He, H., Nayak, A., Stö, V., & Bazarian, J. J. (2009). Validation of Serum Markers for Blood-Brain Barrier Disruption in Traumatic Brain Injury. *Journal of Neurotrauma*, *26*, 1497–1507.

Bogerts, B., Winopal, D., Schwarz, S., Schlaaff, K., Dobrowolny, H., Mawrin, C., Frodl, T., & Steiner, J. (2017). Evidence of neuroinflammation in subgroups of schizophrenia and mood disorder patients: a semiquantitative postmortem study of CD3 and CD20 immunoreactive lymphocytes in several brain regions. *Neurology, Psychiatry and Brain Research*, *23*, 2–9.

Bollinger, R. M., Keleman, A., Thompson, R., Westerhaus, E., Fagan, A. M., Benzinger, T. L. S., Schindler, S. E., Xiong, C., Balota, D., Morris, J. C., Ances, B. M., & Stark, S. L. (2021). Falls: A marker of preclinical Alzheimer disease: A cohort study protocol. *BMJ Open*, *11*(9). https://doi.org/10.1136/bmjopen-2021-050820

Bouzier-Sore, A.-K., Merle, M., Magistretti, P. J., & Pellerin, L. (2002). Feeding active neurons: (re)emergence of a nursing role for astrocytes. *Journal of Physiology*, *96*, 273–282. www.elsevier.com/locate/jphysparis

Braak, H., Alafuzoff, I., Arzberger, T., Kretzschmar, H., & Tredici, K. (2006). Staging of Alzheimer disease-associated neurofibrillary pathology using paraffin sections and immunocytochemistry. *Acta Neuropathologica*, *112*(4), 389–404. https://doi.org/10.1007/s00401-006-0127-z

Braak H; Braak E. (2000). Pathoanatomy of Parkinson's disease. *Journal of Neuro*, *247*(2), II3–II10.

Branco, R. J. F., Fernandes, P. A., & Ramos, M. J. (2006). Molecular dynamics simulations of the enzyme Cu, Zn superoxide dismutase. *Journal of Physical Chemistry B*, *110*(33), 16754–16762. https://doi.org/10.1021/jp056855l

Brandenburg, W., & Hallervorden, J. (1954). *Dementia pugilistica mit anatomischem Befund*. *325*, 680–709.

Braskie, M. N., Klunder, A. D., Hayashi, K. M., Protas, H., Kepe, V., Miller, K. J., Huang, S. C., Barrio, J. R., Ercoli, L. M., Siddarth, P., Satyamurthy, N., Liu,

J., Toga, A. W., Bookheimer, S. Y., Small, G. W., & Thompson, P. M. (2010). Plaque and tangle imaging and cognition in normal aging and Alzheimer's disease. *Neurobiology of Aging*, *31*(10), 1669–1678. https://doi.org/10.1016/j.neurobiolaging.2008.09.012

Brendon P. Boot, M., Carolyn F. Orr, Mbc., J. Eric Ahlskog, P. M., Tanis J. Ferman, P., Rosebud Roberts, Mbc., Vernon S. Pankratz, P., Dennis W. Dickson, M., Joseph Parisi, M., Jeremiah A. Aakre, Bs., Yonas E. Geda, M., David S. Knopman, M., Ronald C. Petersen, P., & Bradley F. Boeve, M. (2013). Risk factors for dementia with Lewy bodies A case-control study. *American Academy of Neurology*, *81*, 833–840. www.neurology.org

Bruijn, Beal, M. F., Becher, M. W., Schulz, J. B., Wong, P. C., Price, D. L., & Cleveland, D. W. (1997). through use of peroxynitrite or from peroxi-dation arising from elevated production of hydroxyl radicals through use of hydrogen peroxide as a substrate [Wiedau-Pazos. *Proc. Natl. Acad. Sci. USA*, *94*, 7606–7611. www.pnas.org.

Bruijn, Houseweart, M. K., Kato, S., Anderson, K. L., Anderson, S. D., Ohama, E., Reaume, A. G., Scott, R. W., & Cleveland, D. W. (1998). Aggregation and Motor Neuron Toxicity of an ALS-Linked SOD1 Mutant Independent from Wild-Type SOD1. *Science*, *281*, 1851–1853. www.sciencemag.org

Bruijn, L. I., Miller, T. M., & Cleveland, D. W. (2004). Unraveling the mechanisms involved in motor neuron degeneration in ALS. *Annual Review of Neuroscience*, *27*, 723–749. https://doi.org/10.1146/annurev.neuro.27.070203.144244

Bryson, K. J., & Lynch, M. A. (2016). Linking T cells to Alzheimer's disease: from neurodegeneration to neurorepair. *Current Opinion in Pharmacology*, *26*, 67–73.

Burda, J. E., Bernstein, A. M., & Sofroniew, M. V. (2016). Astrocyte roles in traumatic brain injury. *Experimental Neurology*, *375*, 305–315. https://doi.org/10.1016/j.expneurol.2015.03.020

Burda, J. E., & Sofroniew, M. V. (2017). Seducing astrocytes to the dark side. *Cell Research*, *27*(6), 726–727. https://doi.org/10.1038/cr.2017.37

Butler, Saha, K., Rana, T., Becker, J. P., Sambo, D., Davari, P., Goodwin, J. S., & Khoshbouei, H. (2015). Dopamine transporter activity is modulated by α-synuclein. *Journal of Biological Chemistry*, *290*(49), 29542–29554. https://doi.org/10.1074/jbc.M115.691592

Butler, Sambo, D., & Khoshbouei, H. (2017). Alpha-synuclein modulates dopamine neurotransmission. *Journal of Chemical Neuroanatomy*, *83–84*, 41–49. https://doi.org/10.1016/j.jchemneu.2016.06.001

Butterfield, D. A., & Castegna, A. (2003). Proteomic analysis of oxidatively modified proteins in Alzheimer's disease brain: insights into neurodegeneration. *Cellular and Molecular Biology (Noisy-Le-Grand, France)*, *49*(5), 747–751.

Cabezas, R., Ávila, M., Gonzalez, J., El-Bachá, R. S., Báez, E., García-Segura, L. M., Coronel, J. C. J., Capani, F., Cardona-Gomez, G. P., & Barreto, G. E. (2014). Astrocytic modulation of blood brain barrier: Perspectives on Parkinson's disease. In *Frontiers in Cellular Neuroscience* (Vol. 8, Issue AUG). Frontiers Research Foundation. https://doi.org/10.3389/fncel.2014.00211

Campbell-Furtick, M., Moore, B. J., Overton, T. L., Laureano Phillips, J., Simon, K. J., Gandhi, R. R., Duane, T. M., & Shafi, S. (2016). Post-trauma mortality increase at age 60: a cutoff for defining elderly? *American Journal of Surgery*, *212*(4), 781–785. https://doi.org/10.1016/j.amjsurg.2015.12.018

Candelario-Jalil, E., Yang, Y., & Rosenberg, G. A. (2009). Diverse roles of matrix metalloproteinases and tissue inhibitors of metalloproteinases in neuroinflammation and cerebral ischemia. In *Neuroscience* (Vol. 158, Issue 3, pp. 983–994). https://doi.org/10.1016/j.neuroscience.2008.06.025

Casili, G., Impellizzeri, D., Cordaro, M., Esposito, E., & Cuzzocrea, S. (2016). B-Cell Depletion with CD20 Antibodies as New Approach in the Treatment of Inflammatory and Immunological Events Associated with Spinal Cord Injury. *Neurotherapeutics*, *13*(4), 880–894. https://doi.org/10.1007/s13311-016-0446-2

Casson, I. R., Siegel, O., Sham, R., Campbell, E. A., Tarlau, M., & Didomenico, A. (1984). Brain Damage in Modern Boxers. *Journal of American Medical Association*, *251*(20), 2663–2667. https://jamanetwork.com/

Castellani, R. J., & Perry, G. (2017). Dementia Pugilistica Revisited. In *Journal of Alzheimer's Disease* (Vol. 60, Issue 4, pp. 1209–1221). IOS Press. https://doi.org/10.3233/JAD-170669

Chaplot, Jarvela, T. S., & Lindberg, I. (2020). Secreted Chaperones in Neurodegeneration. *Frontiers in Aging Neuroscience*, *12*. https://doi.org/10.3389/fnagi.2020.00268

Chen, H., Richard, M., Sandler, D., Umbach, D. M., & Kamel, F. (2007). Head injury and amyotrophic lateral sclerosis. *American Journal of Epidemiology*, *166*(7), 810–816. https://doi.org/10.1093/aje/kwm153

Chen, L., Na, R., Gu, M., Richardson, A., & Ran, Q. (2008). Lipid peroxidation up-regulates BACE1 expression in vivo: A possible early event of amyloidogenesis in Alzheimer's disease. *Journal of Neurochemistry*, *107*(1), 197–207. https://doi.org/10.1111/j.1471-4159.2008.05603.x

Chen, Liang, H., Xi, Z., Yang, Y., Shan, H., Wang, B., Zhong, Z., Xu, C., Yang, G. Y., Sun, Q., Sun, Y., & Bian, L. (2020). BM-MSC Transplantation Alleviates Intracerebral Hemorrhage-Induced Brain Injury, Promotes Astrocytes Vimentin Expression, and Enhances Astrocytes Antioxidation via the Cx43/Nrf2/HO-1 Axis. *Frontiers in Cell and Developmental Biology*, *8*. https://doi.org/10.3389/fcell.2020.00302

Chen, Qin, C., Huang, J., Tang, X., Liu, C., Huang, K., Xu, J., Guo, ang, Tong, A., & Zhou, L. (2020). The role of astrocytes in oxidative stress of central nervous system: A mixed blessing. *Cell Proliferation*, *53*(3). https://doi.org/10.1111/cpr.12781

Chen, X., Guo, C., & Kong, J. (2012). Oxidative stress in neurodegenerative diseases. *Neural Regeneration Research*, *7*(5), 376–385. https://doi.org/10.3969/j.issn.1673-5374.2012.05.009

Chen, X. H., Johnson, V. E., Uryu, K., Trojanowski, J. Q., & Smith, D. H. (2009). A lack of amyloid ß plaques despite persistent accumulation of amyloid ß in axons of long-term survivors of traumatic brain injury. *Brain Pathology*, *19*(2), 214–223. https://doi.org/10.1111/j.1750-3639.2008.00176.x

Chen, X. H., Siman, R., Iwata, A., Meaney, D. F., Trojanowski, J. Q., & Smith, D. H. (2004). Long-Term Accumulation of Amyloid-,-Secretase, Presenilin-1, and Caspase-3 in Damaged Axons Following Brain Trauma. *American Journal of Pathology*, *165*(2), 357–371.

Chen, X.-C., Douwes, J., van den Berg, L. H., Glass, B., McLean, D., & 't Mannetje, A. M. (2022). Sports and trauma as risk factors for Motor Neurone Disease: New Zealand case–control study. *Acta Neurologica Scandinavica*, *145*(6), 770–785. https://doi.org/10.1111/ane.13615

Chen, Y., & Swanson, R. A. (2003). Astrocytes and brain injury. In *Journal of Cerebral Blood Flow and Metabolism* (Vol. 23, Issue 2, pp. 137–149).

Lippincott Williams and Wilkins. https://doi.org/10.1097/01.WCB.0000044631.80210.3C

Cheng, X., Wang, J., Sun, X., Shao, L., Guo, Z., & Li, Y. (2019). Morphological and functional alterations of astrocytes responding to traumatic brain injury. *Journal of Integrative Neuroscience*, *18*(2), 203–215. https://doi.org/10.31083/j.jin.2019.02.110

Cheng, Z.-G., Zhang, G.-D., Shi, P.-Q., & Du, B.-S. (2013). Expression and antioxidation of Nrf2/ARE pathway in traumatic brain injury. *Asian Pacific Journal of Tropical Medicine*, 305–310. www.elsevier.com/locate/apjtm

Chen-Plotkin, A. S., Lee, V. M. Y., & Trojanowski, J. Q. (2010). TAR DNA-binding protein 43 in neurodegenerative disease. In *Nature Reviews Neurology* (Vol. 6, Issue 4, pp. 211–220). https://doi.org/10.1038/nrneurol.2010.18

Cherry, J. D., Meng, G., Daley, S., Xia, W., Svirsky, S., Alvarez, V. E., Nicks, R., Pothast, M., Kelley, H., Huber, B., Tripodis, Y., Alosco, M. L., Mez, J., McKee, A. C., & Stein, T. D. (2020). CCL2 is associated with microglia and macrophage recruitment in chronic traumatic encephalopathy. *Journal of Neuroinflammation*, *17*(1). https://doi.org/10.1186/s12974-020-02036-4

Cherry, J. D., Tripodis, Y., Alvarez, V. E., Huber, B., Kiernan, P. T., Daneshvar, D. H., Mez, J., Montenigro, P. H., Solomon, T. M., Alosco, M. L., Stern, R. A., McKee, A. C., & Stein, T. D. (2016). Microglial neuroinflammation contributes to tau accumulation in chronic traumatic encephalopathy. *Acta Neuropathologica Communications*, *4*(1), 112. https://doi.org/10.1186/s40478-016-0382-8

Cherry, J. D., Zeineddin, A., Dammer, E. B., Webster, J. A., Duong, D., Seyfried, N. T., Levey, A. I., Alvarez, V. E., Huber, B. R., Stein, T. D., Kiernan, P. T., McKee, A. C., Lah, J. J., & Hales, C. M. (2018). Characterization of detergent insoluble proteome in chronic traumatic encephalopathy. *Journal of Neuropathology and Experimental Neurology*, *77*(1), 40–49. https://doi.org/10.1093/jnen/nlx100

Choi, Hou, S., Choe, L. H., & Lee, K. H. (2013). Targeted human cerebrospinal fluid proteomics for the validation of multiple Alzheimer's disease biomarker candidates. *Journal of Chromatography B*, *930*, 129–135. https://doi.org/10.1016/j.jchromb.2013.05.003

Chongshan, B., Tham, D. K. L., Perronnet, C., Joshi, B., Nabi, I. R., & Moukhles, H. (2017). The oxidative stress-induced increase in the membrane expression of the water-permeable channel aquaporin-4 in astrocytes is regulated by caveolin-1 phosphorylation. *Frontiers in Cellular Neuroscience*, *11*. https://doi.org/10.3389/fncel.2017.00412

Chung, I. Y. (1990). TNF-alpha production by astrocytes, induction by lipopolysaccharide, IFN-gamma and IL-1beta. *Journal of Immunology*, *144*(8), 2999–3007. http://journals.aai.org/jimmunol/article-pdf/144/8/2999/1047437/2999.pdf

Clark, Joannides, A., Adeleye, A. O., Bajamal, A. H., Bashford, T., Biluts, H., Budohoski, K., Ercole, A., Fernández-Méndez, R., Figaji, A., Gupta, D. K., Härtl, R., Iaccarino, C., Khan, T., Laeke, T., Rubiano, A., Shabani, H. K., Sichizya, K., Tewari, M., … Ziga, M. (2022). Casemix, management, and mortality of patients receiving emergency neurosurgery for traumatic brain injury in the Global Neurotrauma Outcomes Study: a prospective observational cohort study. *The Lancet Neurology*, *21*(5), 438–449. https://doi.org/10.1016/S1474-4422(22)00037-0

Clark., Perreau, V. M., Shultz, S. R., Brady, R. D., Lei, E., Dixit, S., Taylor, J. M., Beart, P. M., & Boon, W. C. (2019). Inflammation in Traumatic Brain

Injury: Roles for Toxic A1 Astrocytes and Microglial–Astrocytic Crosstalk. *Neurochemical Research*, *44*(6), 1410–1424. https://doi.org/10.1007/s11064-019-02721-8

Cobley, Fiorello, M. L., & Bailey, D. M. (2018). 13 reasons why the brain is susceptible to oxidative stress. *Redox Biology*, *15*, 490–503. https://doi.org/10.1016/j.redox.2018.01.008

Cockerill, I., Oliver, J. A., Xu, H., Fu, B. M., & Zhu, D. (2018). Blood-brain barrier integrity and clearance of amyloid-ß from the BBB. In *Advances in Experimental Medicine and Biology* (Vol. 1097, pp. 261–278). Springer New York LLC. https://doi.org/10.1007/978-3-319-96445-4_14

Cole, Faydaci, B. A., McGuinness, D., Shaw, R., Maciewicz, R. A., Robertson, N. A., & Goodyear, C. S. (2021). Searchlight: automated bulk RNA-seq exploration and visualisation using dynamically generated R scripts. *BMC Bioinformatics*, *22*(1). https://doi.org/10.1186/s12859-021-04321-2

Cole, J. H., Jolly, A., De Simoni, S., Bourke, N., Patel, M. C., Scott, G., & Sharp, D. J. (2018). Spatial patterns of progressive brain volume loss after moderate-severe traumatic brain injury. *Brain*, *141*(3), 822–836. https://doi.org/10.1093/brain/awx354

Collins, J. M., Woodhouse, A., Bye, N., Vickers, J. C., King, A. E., & Ziebell, J. M. (2020). Pathological Links between Traumatic Brain Injury and Dementia: Australian Pre-Clinical Research. *Journal of Neurotrauma*, *37*(5), 782–791. https://doi.org/10.1089/neu.2019.6906

Collins-Praino, L. E., & Corrigan, F. (2017). Does neuroinflammation drive the relationship between tau hyperphosphorylation and dementia development following traumatic brain injury? In *Brain, Behavior, and Immunity* (Vol. 60, pp. 369–382). Academic Press Inc. https://doi.org/10.1016/j.bbi.2016.09.027

Conductier, G., Blondeau, N., Guyon, A., Nahon, J. L., & Rovère, C. (2010). The role of monocyte chemoattractant protein MCP1/CCL2 in neuroinflammatory diseases. In *Journal of Neuroimmunology* (Vol. 224, Issues 1–2, pp. 93–100). Elsevier. https://doi.org/10.1016/j.jneuroim.2010.05.010

Conte, V., Uryu, K., Fujimoto, S., Yao, Y., Rokach, J., Longhi, L., Trojanowski, J. Q., Lee, V. M. Y., McIntosh, T. K., & Praticò, D. (2004). Vitamin E reduces amyloidosis and improves cognitive function in Tg2576 mice following repetitive concussive brain injury. *Journal of Neurochemistry*, *90*(3), 758–764. https://doi.org/10.1111/j.1471-4159.2004.02560.x

Corrigan, F., Vink, R., Blumbergs, P. C., Masters, C. L., Cappai, R., & Van Den Heuvel, C. (2012). SAPPα rescues deficits in amyloid precursor protein knockout mice following focal traumatic brain injury. *Journal of Neurochemistry*, *122*(1), 208–220. https://doi.org/10.1111/j.1471-4159.2012.07761.x

Corsellis, J. A. N., Bruton, C. J., & Freeman-Browne, D. (1973). The aftermath of boxing. *Psychological Medicine*, *3*(3), 270–303. https://doi.org/10.1017/S0033291700049588

Cox, A. L., Coles, A. J., Nortje, J., Bradley, P. G., Chatfield, D. A., Thompson, S. J., & Menon, D. K. (2006). An investigation of auto-reactivity after head injury. *Journal of Neuroimmunology*, *174*(1–2), 180–186. https://doi.org/10.1016/j.jneuroim.2006.01.007

Crane, P. K., Gibbons, L. E., Dams-O'Connor, K., Trittschuh, E., Leverenz, J. B., Dirk Keene, C., Sonnen, J., Montine, T. J., Bennett, D. A., Leurgans, S., Schneider, J. A., & Larson, E. B. (2016). Association of traumatic brain injury with late-life neurodegenerative conditions and Neuropathologic

findings. *JAMA Neurology*, *73*(9), 1062–1069. https://doi.org/10.1001/jamaneurol.2016.1948

Critchley, M. (1957). Medical aspects of boxing, particularly from a neurological standpoint. *BRITISH MEDICAL JOURNAL*, 357–362.

Cumming, & Schubert, D. (2005). Amyloid-β induces disulfide bonding and aggregation of GAPDH in Alzheimer's disease. *The FASEB Journal*, *19*(14), 2060–2062. https://doi.org/10.1096/fj.05-4195fje

Czeiter, Amrein, K., Gravesteijn, B. Y., Lecky, F., Menon, D. K., Mondello, S., Newcombe, V. F. J., Richter, S., Steyerberg, E. W., Vyvere, T. V., Verheyden, J., Xu, H., Yang, Z., Maas, A. I. R., Wang, K. K. W., & Büki, A. (2020). Blood biomarkers on admission in acute traumatic brain injury: Relations to severity, CT findings and care path in the CENTER-TBI study. *EBioMedicine*, *56*. https://doi.org/10.1016/j.ebiom.2020.102785

Dale, G. E., Leigh, P. N., Luthert, P., Anderton, B. H., & Roberts, G. W. (1991). Neurofibrillary tangles in dementia pugilistica are ubiquitinated. *Journal of Neurology Neurosurgery and Psychiatry*, *54*(2), 116–118. https://doi.org/10.1136/jnnp.54.2.116

D'Ambrosi, N., & Apolloni, S. (2020). Fibrotic Scar in Neurodegenerative Diseases. *Frontiers in Immunology*, *11*. https://doi.org/10.3389/fimmu.2020.01394

Daneshvar, D. H., Mez, J., Alosco, M. L., Baucom, Z. H., Mahar, I., Baugh, C. M., Valle, J. P., Weuve, J., Paganoni, S., Cantu, R. C., Zafonte, R. D., Stern, R. A., Stein, T. D., Tripodis, Y., Nowinski, C. J., & McKee, A. C. (2021). Incidence of and Mortality from Amyotrophic Lateral Sclerosis in National Football League Athletes. *JAMA Network Open*, *4*(12). https://doi.org/10.1001/jamanetworkopen.2021.38801

Dardiotis, E., Karanikas, V., Paterakis, K., Fountas, K., & Hadjigeorgiou, G. (2012). Traumatic Brain Injury and Inflammation; Emerging role of Innate and Adaptive Immunity. In *Brain Injury* (pp. 23–38). https://doi.org/http://dx.doi.org/10.5772/46845

Das, M., Mohapatra, S., & Mohapatra, S. S. (2012). New perspectives on central and peripheral immune responses to acute traumatic brain injury. In *Journal of Neuroinflammation* (Vol. 9). BioMed Central. https://doi.org/10.1186/1742-2094-9-236

Davidsson, Sjogren, M., Andreasen, N., Lindbjer, M., Nilsson, C. L., Westman-Brinkmalm, A., & Blennow, K. (2002). Studies of the pathophysiological mechanisms in frontotemporal dementia by proteome analysis of CSF proteins. *Molecular Brain Research*, *109*, 128–133. www.elsevier.com/locate/molbrainres

DeKosky, S. T., Wisniewski, S. R., Clark, R. S. B., & Ikonomovic, M. D. (2007). *Association of Increased Cortical Soluble AB42 levles with Diffuse Plaques after severe TBI in humans*. *64*.

Dendrou, C. A., Fugger, L., & Friese, M. A. (2015). Immunopathology of multiple sclerosis. *Nature Reviews Immunology*, *15*(9), 545–558. https://doi.org/10.1038/nri3871

Deng, Hentati, A., Tainer, J. A., Iqbal, Z., Cayabyab, A., Hung, W.-Y., Getzoff, E. D., Hu, P., Herzfeldt, B., Roos, R. P., Warner, C., Deng, G., Soriano, E., Smyth, C., Parge, H. E., Ahmed, A., Roses, A. D., Hallewell, R. A., Pericak-Vance, M. A., & Siddique, T. (1993). ALS and structural defects in Cu,Zn Superoxide Dismutase. *Science*, *261*, 1047–1051.

Deture, M. A., & Dickson, D. W. (2019). The neuropathological diagnosis of Alzheimer's disease. In *Molecular Neurodegeneration* (Vol. 14, Issue 1). BioMed Central Ltd. https://doi.org/10.1186/s13024-019-0333-5

Dewan, M. C., Rattani, A., Gupta, S., Baticulon, R. E., Hung, Y. C., Punchak, M., Agrawal, A., Adeleye, A. O., Shrime, M. G., Rubiano, A. M., Rosenfeld, J. V., & Park, K. B. (2019). Estimating the global incidence of traumatic brain injury. *Journal of Neurosurgery*, *130*(4), 1080–1097. https://doi.org/10.3171/2017.10.JNS17352

Dickson, T. C., & Vickers, J. (2001). The morphological phenotype of ß-amyloid plaques and associated neuritic changes in Alzheimer's disease. *Neuroscience*, *105*(1), 99–107.

Donovan, Higginbotham, L., Dammer, E., Gearing, M., Rees, H., Xia, Q., Duong, D., Seyfried, N., Lah, J., & Levey, A. (2012). Analysis of a membrane entriched Proteome from Post-mortem human brain tissue in Alzheimer's Disease. *Proteomics Clin. Appl.*, *6*(3–4), 201–211. https://doi.org/10.1016/j.clinph.2008.06.019.Brain-Computer

Donovan, V., Kim, C., Anugerah, A. K., Coats, J. S., Oyoyo, U., Pardo, A. C., & Obenaus, A. (2014). Repeated mild traumatic brain injury results in long-term white-matter disruption. *Journal of Cerebral Blood Flow and Metabolism*, *34*(4), 715–723. https://doi.org/10.1038/jcbfm.2014.6

Dossi, E., Vasile, F., & Rouach, N. (2018). Human astrocytes in the diseased brain. *Brain Research Bulletin*, *136*, 139–156. https://doi.org/10.1016/j.brainresbull.2017.02.001

Drachman. (1999). Case 12 - 1999 : A 67-year-old man with three years of Dementia. *The New England Journal of Medicine*, *340*(16), 1269–1277.

Drummond, E., Nayak, S., Faustin, A., Pires, G., Hickman, R. A., Askenazi, M., Cohen, M., Haldiman, T., Kim, C., Han, X., Shao, Y., Safar, J. G., Ueberheide, B., & Wisniewski, T. (2017). Proteomic differences in amyloid plaques in rapidly progressive and sporadic Alzheimer's disease. *Acta Neuropathologica*, *133*(6), 933–954. https://doi.org/10.1007/s00401-017-1691-0

Drummond, E. S., Nayak, S., Ueberheide, B., & Wisniewski, T. (2015). Proteomic analysis of neurons microdissected from formalin-fixed, paraffin-embedded Alzheimer's disease brain tissue. *Scientific Reports*, *5*(September), 15456. https://doi.org/10.1038/srep15456

Drummond, & Wisniewski, T. (2019). Alzheimer's Disease. *Alzheimer's Disease*, 37–51. https://doi.org/10.15586/alzheimersdisease.2019

Dutysheva, Mikhaylova, E. R., Trestsova, M. A., Andreev, A. I., Apushkin, D. Y., Utepova, I. A., Serebrennikova, P. O., Akhremenko, E. A., Aksenov, N. D., Bon', E. I., Zimatkin, S. M., Chupakhin, O. N., Margulis, B. A., Guzhova, I. V., & Lazarev, V. F. (2023). Combination of a Chaperone Synthesis Inducer and an Inhibitor of GAPDH Aggregation for Rehabilitation after Traumatic Brain Injury: A Pilot Study. *Pharmaceutics*, *15*(7). https://doi.org/10.3390/pharmaceutics15010007

Edwards, & CRASH Trial Collaborators. (2005). Final results of MRC CRASH, a randomised placebo-controlled trial of intravenous corticosteroid in adults with head injury—outcomes at 6 months. *The Lancet*, *365*(9475), 1957–1959.

Edwards, G., Moreno-Gonzalez, I., & Soto, C. (2017). Amyloid-beta and tau pathology following repetitive mild traumatic brain injury. *Biochemical and Biophysical Research Communications*, *483*(4), 1137–1142. https://doi.org/10.1016/j.bbrc.2016.07.123

Engel, S., Schluesener, H., Mittelbronn, M., Seid, K., Adjodah, D., Wehner, H. D., & Meyermann, R. (2000). Dynamics of microglial activation after human traumatic brain injury are revealed by delayed expression of macrophage-related proteins MRP8 and MRP14. *Acta Neuropathologica*, *100*(3), 313–322. https://doi.org/10.1007/s004019900172

Faden, A. I., & Loane, D. J. (2015). Chronic Neurodegeneration After Traumatic Brain Injury: Alzheimer Disease, Chronic Traumatic Encephalopathy, or Persistent Neuroinflammation? *Neurotherapeutics*, *12*(1), 143–150. https://doi.org/10.1007/s13311-014-0319-5

Fann, J. R., Ribe, A. R., Pedersen, H. S., Fenger-Grøn, M., Christensen, J., Benros, M. E., & Vestergaard, M. (2018). Long-term risk of dementia among people with traumatic brain injury in Denmark: a population-based observational cohort study. *The Lancet Psychiatry*, *5*(5), 424–431. https://doi.org/10.1016/S2215-0366(18)30065-8

Farbota, K. D. M., Sodhi, A., Bendlin, B. B., McLaren, D. G., Xu, G., Rowley, H. A., & Johnson, S. C. (2012). Longitudinal volumetric changes following traumatic brain injury: A tensor-based morphometry study. *Journal of the International Neuropsychological Society*, *18*(6), 1006–1018. https://doi.org/10.1017/S1355617712000835

Faul, M., Xu, L., Wald, M. M., & Coronado, V. G. (2010). Traumatic brain injury in the United States: emergency department visits, hospitalizations, and deaths. *Centers for Disease Control and Prevention, National Center for Injury Prevention and Control*, 891–904. https://doi.org/10.1016/B978-0-444-52910-7.00011-8

FDA authorizes marketing first blood test aid evaluation concussion adults. (2018). FDA.

Fearnley, J. M., & Lees, A. J. (1991). AGEING AND PARKINSON'S DISEASE: SUBSTANTIA NIGRA REGIONAL SELECTIVITY. In *Brain* (Vol. 114). https://academic.oup.com/brain/article/114/5/2283/399854

Ferreira, D., Molina, Y., Machado, A., Westman, E., Wahlund, L. O., Nieto, A., Correia, R., Junqué, C., Díaz-Flores, L., & Barroso, J. (2014). Cognitive decline is mediated by gray matter changes during middle age. *Neurobiology of Aging*, *35*(5), 1086–1094. https://doi.org/10.1016/j.neurobiolaging.2013.10.095

Fleming, J. C., Norenberg, M. D., Ramsay, D. A., Dekaban, G. A., Marcillo, A. E., Saenz, A. D., Pasquale-Styles, M., Dietrich, W. D., & Weaver, L. C. (2006). The cellular inflammatory response in human spinal cords after injury. *Brain*, *129*(12), 3249–3269. https://doi.org/10.1093/brain/awl296

Fleminger, S. (2003). Head injury as a risk factor for Alzheimer's disease. *Journal of Neurology, Neurosurgery and Psychiatry*, *74*(6), 832–833.

Fletcher, J. M., Lalor, S. J., Sweeney, C. M., Tubridy, N., & Mills, K. H. G. (2010). T cells in multiple sclerosis and experimental autoimmune encephalomyelitis. In *Clinical and Experimental Immunology* (Vol. 162, Issue 1, pp. 1–11). https://doi.org/10.1111/j.1365-2249.2010.04143.x

Flügel, A., Willem, M., Berkowicz, T., & Wekerle, H. (1999). Gene transfer into CD4+ T lymphocytes: Green fluorescent protein- engineered, encephalitogenic T cells illuminate brain autoimmune responses. *Nature Medicine*, *5*(7), 843–847. https://doi.org/10.1038/10567

Forsberg, Jonsson, P. A., Andersen, P. M., Bergemalm, D., Graffmo, K. S., Hultdin, M., Jacobsson, J., Rosquist, R., Marklund, S. L., & Brännström, T. (2010). Novel antibodies reveal inclusions containing non-native SOD1 in

sporadic ALS patients. *PLoS ONE*, *5*(7). https://doi.org/10.1371/journal.pone.0011552

Fountoulakis, & Kossida, S. (2006). Proteomics-driven progress in neurodegeneration research. In *Electrophoresis* (Vol. 27, Issue 8, pp. 1556–1573). https://doi.org/10.1002/elps.200500738

Frakes, A. E., Ferraiuolo, L., Haidet-Phillips, A. M., Schmelzer, L., Braun, L., Miranda, C. J., Ladner, K. J., Bevan, A. K., Foust, K. D., Godbout, J. P., Popovich, P. G., Guttridge, D. C., & Kaspar, B. K. (2014). Microglia induce motor neuron death via the classical NF-κB pathway in amyotrophic lateral sclerosis. *Neuron*, *81*(5), 1009–1023. https://doi.org/10.1016/j.neuron.2014.01.013

Frankel, J. E., Marwitz, J. H., Cifu, D. X., Kreutzer, J. S., Englander, J., & Rosenthal, M. (2006). A follow-up study of older adults with traumatic brain injury: Taking into account decreasing length of stay. *Archives of Physical Medicine and Rehabilitation*, *87*(1), 57–62. https://doi.org/10.1016/j.apmr.2005.07.309

Frieden, T. R., Houry, D., & Baldwin, G. (2015). *Traumatic Brain Injury In the United States: Epidemiology and Rehabilitation*.

Fukuda, A. M., & Badaut, J. (2012). Aquaporin 4: A player in cerebral edema and neuroinflammation. *Journal of Neuroinflammation*, *9*(1), 1. https://doi.org/10.1186/1742-2094-9-279

Gamblin, T. C., Chen, F., Zambrano, A., Abraha, A., Lagalwar, S., Guillozet, A. L., Lu, M., Fu, Y., Garcia-Sierra, F., LaPointe, N., Miller, R., Berry, R. W., Binder, L. I., & Cryns, V. L. (2003). Caspase cleavage of tau: Linking amyloid and neurofibrillary tangles in Alzheimer's disease. *Proceedings of the National Academy of Sciences of the United States of America*, *100*(17), 10032–10037. https://doi.org/10.1073/pnas.1630428100

Ganesalingam, An, J., Bowser, R., Andersen, P. M., & Shaw, C. E. (2013). PNfH is a promising biomarker for ALS. *Amyotrophic Lateral Sclerosis and Frontotemporal Degeneration*, *14*(2), 146–149. https://doi.org/10.3109/21678421.2012.729596

Gardner, Burke, J. F., Nettiksimmons, J., Goldman, S., Tanner, C. M., & Yaffe, K. (2015). Traumatic brain injury in later life increases risk for Parkinson disease. *Annals of Neurology*, *77*(6), 987–995. https://doi.org/10.1002/ana.24396

Gardner, Hess, C., Possin, K., Cohn-Sheehy, B., Kramer, J., Berger, M., Miller, B., Yaffe, K., & Rabinovici, G. (2014). *Cavum Septum Pellucidum in Symptomatic Retired Pro-football Players (P6. 327)*. AAN Enterprises.

Gardner, R. C., Dams-O'Connor, K., Morrissey, M. R., & Manley, G. T. (2017). Geriatric Traumatic Brain Injury: Epidemiology, Outcomes, Knowledge Gaps, and Future Directions. *Journal of Neurotrauma*, *35*(7), 889–906. https://doi.org/10.1089/neu.2017.5371

Gardner, Rubenstein, R., Wang, K. K. W., Korley, F. K., Yue, J. K., Yuh, E. L., Mukherje, P., Valadka, A. B., Okonkwo, D. O., Diaz-Arrastia, R., & Manley, G. T. (2018). Age-Related Differences in Diagnostic Accuracy of Plasma Glial Fibrillary Acidic Protein and Tau for Identifying Acute Intracranial Trauma on Computed Tomography: A TRACK-TBI Study. *Journal of Neurotrauma*, *35*(20), 2341–2350. https://doi.org/10.1089/neu.2018.5694

Gardner, & Yaffe, K. (2014). Traumatic brain injury may increase risk of young onset dementia. *Annals of Neurology*, *75*(3), 339–341. https://doi.org/10.1002/ana.24121

Gavett, B. E., Nowinski, C. J., McKee, A. C., Stern, R. A., & Cantu, R. C. (2010). Mild traumatic brain injury: a risk factor for neurodegeneration. *Alzheimer's Research & Therapy*, *2*(18), 1–3. https://doi.org/10.1186/alzrt42

Geddes, J. F., Vowles, G. H., Beer, T. W., & Ellison, D. W. (1997). The diagnosis of diffuse axonal injury: implications for forensic practice. In *Neuropathology and Applied Neurobiology* (Vol. 23).

Geddes, J. F., Vowles, G. H., Nicoll, J. A. R., & Révész, T. (1999). Neuronal cytoskeletal changes are an early consequence of repetitive head injury. *Acta Neuropathologica*, *98*(2), 171–178. https://doi.org/10.1007/s004010051066

Gentleman, S. M., Leclercq, P. D., Moyes, L., Graham, D. I., Smith, C., Griffin, W. S. T., & Nicoll, J. A. R. (2004). Long-term intracerebral inflammatory response after traumatic brain injury. *Forensic Science International*, *146*(2–3), 97–104. https://doi.org/10.1016/j.forsciint.2004.06.027

Gentleman, S. M., Nash, M. J., Sweeting, C. J., Graham, D. I., & Roberts, G. W. (1993). ß-Amyloid precursor protein (ßAPP) as a marker for axonal injury after head injury. *Neuroscience Letters*, *160*(2), 139–144. https://doi.org/10.1016/0304-3940(93)90398-5

Geser, F., Martinez-Lage, M., Kwong, L. K., Lee, V. M. Y., & Trojanowski, J. Q. (2009). Amyotrophic lateral sclerosis, frontotemporal dementia and beyond: The TDP-43 diseases. In *Journal of Neurology* (Vol. 256, Issue 8, pp. 1205–1214). https://doi.org/10.1007/s00415-009-5069-7

Giraldo, E., Lloret, A., Fuchsberger, T., & Viña, J. (2014). Aß and tau toxicities in Alzheimer's are linked via oxidative stress-induced p38 activation: Protective role of vitamin E. *Redox Biology*, *2*(1), 873–877. https://doi.org/10.1016/j.redox.2014.03.002

Giusti, & Lucacchini, A. (2013). Proteomic studies of formalin-fixed paraffin-embedded tissues. *Expert Review of Proteomics*, *10*(2), 165–177.

Goldfinger, M. H., Ling, H., Tilley, B. S., Liu, A. K. L., Davey, K., Holton, J. L., Revesz, T., & Gentleman, S. M. (2018). The aftermath of boxing revisited: identifying chronic traumatic encephalopathy pathology in the original Corsellis boxer series. In *Acta Neuropathologica* (Vol. 136, Issue 6, pp. 973–974). Springer Verlag. https://doi.org/10.1007/s00401-018-1926-8

Goldstein, Fisher, A., Tagge, C., Zhang, X.-L., Velisek, L., Sullivan, J., Upreti, C., Kracht, J., Ericsson, M., Wojnarowicz, M., Goletiani, C., Maglakelidze, G., Casey, N., Moncaster, J., Minaeva, O., Cormier, K., Kubilus, C., Moir, R., Nowinski, C., … McKee, A. (2012). Chronic traumatic encephalopathy (CTE) in blast-exposed U.S. military veterans and a new blast neurotrauma mouse model. *Alzheimer's & Dementia*, *8*(4), P212–P213. https://doi.org/10.1016/j.jalz.2012.05.592

Goyal, Hawrylycz, M., Miller, J. A., Snyder, A. Z., & Raichle, M. E. (2014). Aerobic glycolysis in the human brain is associated with development and neotenous gene expression. *Cell Metabolism*, *19*(1), 49–57. https://doi.org/10.1016/j.cmet.2013.11.020

Graham, Adams, J. H., & Gennarelli, T. A. (1988). Mechanisms of non-penetrating head injury. *Progress in Clinical and Biological Research*, *264*, 159–168.

Graham, Gentleman, S. M., Lynch, A., & Roberts, G. W. (1995). Distribution of ß-amyloid protein in the brain following severe head injury. *Neuropathology and Applied Neurobiology*, *21*(1), 27–34. https://doi.org/10.1111/j.1365-2990.1995.tb01025.x

Graham, & Luntos. (2002). Greenfield's neuropathology. *European Journal of Neurology*, *9*(6), 705.

Graham, N., Zimmerman, K. A., Bertolini, G., Magnoni, S., Oddo, M., Zetterberg, H., Moro, F., Novelli, D., Heslegrave, A., Chieregato, A., Fainardi, E., Fleming, J. M., Garbero, E., Abed-Maillard, S., Gradisek, P., Bernini, A., & Sharp, D. J. (2020). Multicentre longitudinal study of fluid and neuroimaging BIOmarkers of AXonal injury after traumatic brain injury: The BIO-AX-TBI study protocol. *BMJ Open*, *10*(11). https://doi.org/10.1136/bmjopen-2020-042093

Grahmann, H., & Ule, G. (1957). Diagnosis of chronic cerebral symptoms in boxers (dementia pugilistica & traumatic encephalopathy of boxers). *Psychiatria et Neurologia*, *134*(3–4), 261–283.

Grammas, P., Martinez, J., & Miller, B. (2011). Cerebral microvascular endothelium and the pathogenesis of neurodegenerative diseases. In *Expert reviews in molecular medicine* (Vol. 13). https://doi.org/10.1017/S1462399411001918

Graves, M. C., Fiala, M., Dinglasan, L. A. V., Liu, N. Q., Sayre, J., Chiappelli, F., van Kooten, C., & Vinters, H. V. (2004). Inflammation in amyotrophic lateral sclerosis spinal cord and brain is mediated by activated macrophages, mast cells and t cells. *Amyotrophic Lateral Sclerosis and Other Motor Neuron Disorders*, *5*(4), 213–219. https://doi.org/10.1080/14660820410020286

Graves, White, E., Koepsell, T. D., Reifler, B. V, Belle, G. V. A. N., Larson, E. B., & Raskind, M. (1990). The association between head trauma and Alzheimer 's disease. *American Journal of Epidemiology*, *131*(3), 491–501. https://doi.org/10.1093/oxfordjournals.aje.a115523

Griffin, W. S. T., Sheng, J. G., Royston, M. C., Gentleman, S. M., McKenzie, J. E., Graham, D. I., Roberts, G. W., & Mrak, R. E. (1998). Glial-neuronal interactions in Alzheimer's disease: The potential role of a "cytokine cycle" in disease progression. *Brain Pathology*, *8*(1), 65–72. https://doi.org/10.1111/j.1750-3639.1998.tb00136.x

Griffin, W. S. T., Stanley, L. C., Ling, C., White, L., MacLeod, V., Perrot, L. J., White, C. L., & Araoz, C. (1989). Brain interleukin 1 and S-100 immunoreactivity are elevated in Down syndrome and Alzheimer disease. *Proceedings of the National Academy of Sciences of the United States of America*, *86*(19), 7611–7615. https://doi.org/10.1073/pnas.86.19.7611

Grimm, A., & Eckert, A. (2017). Brain aging and neurodegeneration: from a mitochondrial point of view. In *Journal of Neurochemistry* (Vol. 143, Issue 4, pp. 418–431). Blackwell Publishing Ltd. https://doi.org/10.1111/jnc.14037

Grothe, M. J., Barthel, H., Sepulcre, J., Dyrba, M., Sabri, O., & Teipel, S. J. (2017). In vivo staging of regional amyloid deposition From the German Center for Neurodegenerative Diseases (DZNE) (M. *Neurology*, *89*, 2031–2038.

Gu, Y., Razlighi, Q. R., Zahodne, L. B., Janicki, S. C., Ichise, M., Manly, J. J., Devanand, D. P., Brickman, A. M., Schupf, N., Mayeux, R., & Stern, Y. (2015). Brain amyloid deposition and longitudinal cognitive decline in nondemented older subjects: Results from a multi-ethnic population. *PLoS ONE*, *10*(7), 1–14. https://doi.org/10.1371/journal.pone.0123743

Guo, Z., Cupples, L. A., Kurz, A., Auerbach, S. H., Volicer, L., & Chui, H. (2000). Head injury and the risk of AD in the. *Neurology*.

Habbas, S., Santello, M., Becker, D., Stubbe, H., Zappia, G., Liaudet, N., Klaus, F. R., Kollias, G., Fontana, A., Pryce, C. R., Suter, T., & Volterra, A. (2015).

Neuroinflammatory TNFα Impairs Memory via Astrocyte Signaling. *Cell*, *163*(7), 1730–1741. https://doi.org/10.1016/j.cell.2015.11.023

Hafler, C. S. and D. A. (2009). T-Cells in Multiple Sclerosis. *Results and Problems in Cell Differentiation*, *48*(August 2009), 1–25. https://doi.org/10.1007/400

Halliwell. (2012). Free radicals and antioxidants: Updating a personal view. *Nutrition Reviews*, *70*(5), 257–265. https://doi.org/10.1111/j.1753-4887.2012.00476.x

Halliwell, B. (1992). Reactive Oxygen Species and the Central Nervous System. *Journal of Neurochemistry*, *59*(5), 1609–1623. https://doi.org/10.1111/j.1471-4159.1992.tb10990.x

Hansson, O., Zetterberg, H., Buchhave, P., Londos, E., Blennow, K., & Minthon, L. (2006). Association between CSF biomarkers and incipient Alzheimer's disease in patients with mild cognitive impairment: A follow-up study. *Lancet Neurology*, *5*(3), 228–234. https://doi.org/10.1016/S1474-4422(06)70355-6

Hara, M. R., Agrawal, N., Kim, S. F., Cascio, M. B., Fujimuro, M., Ozeki, Y., Takahashi, M., Cheah, J. H., Tankou, S. K., Hester, L. D., Ferris, C. D., Hayward, S. D., Snyder, S. H., & Sawa, A. (2005). S-nitrosylated GAPDH initiates apoptotic cell death by nuclear translocation following Siah1 binding. *Nature Cell Biology*, *7*(7), 665–674. https://doi.org/10.1038/ncb1268

Hardy, J., & Selkoe, D. J. (2002). The amyloid hypothesis of Alzheimer's disease: Progress and problems on the road to therapeutics. *Science*, *297*(5580), 353–356. https://doi.org/10.1126/science.1072994

Hardy JA, & GA., H. (1992). Alzheimer's disease: the amyloid cascade hypothesis. *Science*, *256*(5054), 184–185.

Harris, T. C., de Rooij, R., & Kuhl, E. (2018). The Shrinking Brain: Cerebral Atrophy Following Traumatic Brain Injury. *Annals of Biomedical Engineering*, *47*(9), 1941–1959. https://doi.org/10.1007/s10439-018-02148-2

Hashimoto, & Masliah, E. (1999). Alpha-synuclein in Lewy body disease and Alzheimer's disease. *Brain Pathology*, *9*(4), 707–720. https://doi.org/10.1111/j.1750-3639.1999.tb00552.x

Hausmann, R., Kaiser, A., Lang, C., Bohnert, M., & Betz, P. (1999). A quantitative immunohistochemical study on the time-dependent course of acute inflammatory cellular response to human brain injury. *International Journal of Legal Medicine*, *112*(4), 227–232. https://doi.org/10.1007/s004140050241

Hay. (2018). *Vascular and cellular responses to TBI*.

Hay, Johnson, V. E., Smith, D. H., & Stewart, W. (2016). Chronic Traumatic Encephalopathy: The Neuropathological Legacy of Traumatic Brain Injury. *Annual Review of Pathology: Mechanisms of Disease*, *11*, 21–45. https://doi.org/10.1146/annurev-pathol-012615-044116

Hay, Johnson, V. E., Young, A. M. H., Smith, D. H., & Stewart, W. (2015). Blood-Brain Barrier Disruption Is an Early Event That May Persist for Many Years After Traumatic Brain Injury in Humans. *Journal of Neuropathology & Experimental Neurology*, *74*(12), 1147–1157. https://doi.org/10.1097/NEN.0000000000000261

Hayakata, T., Shiozaki, T., Tasaki, O., Ikegawa, H., Inoue, Y., Toshiyuki, F., Hosotubo, H., Kieko, F., Yamashita, T., Tanaka, H., Shimazu, T., & Sugimoto, H. (2004). Changes in CSF S100B and cytokine concentrations in early-phase severe traumatic brain injury. *Shock*, *22*(2), 102–107. https://doi.org/10.1097/01.shk.0000131193.80038.f1

Hayashi, Y., Nomura, M., Yamagishi, S.-I., Harada, S.-I., Yamashita, J., & Yamamoto, H. (1997). Induction of Various Blood-Brain Barrier Properties in Non-Neural Endothelial Cells by Close Apposition to Co-Cultured Astrocytes. In *GLIA* (Vol. 19). Wiley-Liss, Inc.

Heegaard, W., & Biros, M. (2007). Traumatic brain injury. *Emergency Medicine Clinics of North America*, *25*(3), 655–678.

Hefter, D., & Draguhn, A. (2017). APP as a protective factor in acute neuronal insults. In *Frontiers in Molecular Neuroscience* (Vol. 10). Frontiers Media S.A. https://doi.org/10.3389/fnmol.2017.00022

Heithoff, George, K. K., Phares, A. N., Zuidhoek, I. A., Munoz-Ballester, C., & Robel, S. (2021). Astrocytes are necessary for blood–brain barrier maintenance in the adult mouse brain. *GLIA*, *69*(2), 436–472. https://doi.org/10.1002/glia.23908

Helferich, Ruf, W. P., Grozdanov, V., Freischmidt, A., Feiler, M. S., Zondler, L., Ludolph, A. C., McLean, P. J., Weishaupt, J. H., & Danzer, K. M. (2015). α-Synuclein interacts with SOD1 and promotes its oligomerization. *Molecular Neurodegeneration*, *10*(66). https://doi.org/10.1186/s13024-015-0062-3

Hely, M. A., Reid, W. G. J., Adena, M. A., Halliday, G. M., & Morris, J. G. L. (2008). The Sydney Multicenter Study of Parkinson's disease: The inevitability of dementia at 20 years. *Movement Disorders*, *23*(6), 837–844. https://doi.org/10.1002/mds.21956

Hemmer, B., Kerschensteiner, M., & Korn, T. (2015). Role of the innate and adaptive immune responses in the course of multiple sclerosis. In *The Lancet Neurology* (Vol. 14, Issue 4, pp. 406–419). Lancet Publishing Group. https://doi.org/10.1016/S1474-4422(14)70305-9

Henry-Feugeas, M. C., Azouvi, P., Fontaine, A., Denys, P., Bussel, B., Maaz, F., Samson, Y., & Schouman-Claeys, E. (2000). MRI-analysis of brain atrophy after severe closed-head injury: Relation to clinical status. *Brain Injury*, *14*(7), 597–604. https://doi.org/10.1080/02699050050043962

Hernandez-Ontiveros, Tajiri, N., Acosta, S., Giunta, B., Tan, J., & Borlongan, C. V. (2013). Microglia activation as a biomarker for traumatic brain injury. *Frontiers in Neurology*, *4*(30). https://doi.org/10.3389/fneur.2013.00030

Hickey, W. F. (1999). Leukocyte traffic in the central nervous system: The participants and their roles. *Seminars in Immunology*, *11*(2), 125–137. https://doi.org/10.1006/smim.1999.0168

Hickey, W. F. (2001). Basic principles of immunological surveillance of the normal central nervous system. *Glia*, *36*(2), 118–124. https://doi.org/10.1002/glia.1101

Hickey, W. F., & Kimura, H. (1987). Graft-vs.-host disease elicits expression of class I and class II histocompatibility antigens and the presence of scattered T lymphocytes in rat central nervous system. *Proceedings of the National Academy of Sciences of the United States of America*, *84*(7), 2082–2086. https://doi.org/10.1073/pnas.84.7.2082

Hickman, Allison, E. K., & El Khoury, J. (2008). Microglial dysfunction and defective ß-amyloid clearance pathways in aging alzheimer's disease mice. *Journal of Neuroscience*, *28*(33), 8354–8360. https://doi.org/10.1523/JNEUROSCI.0616-08.2008

Hickman, Izzy, S., Sen, P., Morsett, L., & El Khoury, J. (2018). Microglia in neurodegeneration. *Nature Neuroscience*, *21*(10), 1359–1369. https://doi.org/10.1038/s41593-018-0242-x

Ho, K. M., Honeybul, S., Yip, C. B., & Silbert, B. I. (2014). Prognostic significance of blood-brain barrier disruption in patients with severe

nonpenetrating traumatic brain injury requiring decompressive craniectomy. *Journal of Neurosurgery*, *121*(3), 674–679. https://doi.org/10.3171/2014.6.JNS132838

Hof, P. R., Bouras, C., Buée, L., Delacourte, A., Perl, D. P., & Morrison, J. H. (1992). Differential distribution of neurofibrillary tangles in the cerebral cortex of dementia pugilistica and Alzheimer's disease cases. *Acta Neuropathologica*, *85*(1), 23–30. https://doi.org/10.1007/BF00304630

Höglinger, G. U., Respondek, G., & Kovacs, G. G. (2018). New classification of tauopathies. *Revue Neurologique*, *174*(9), 664–668.

Holmin, S., & Mathiesen, T. (1999). Long-term intracerebral inflammatory response after experimental focal brain injury in rat. *Neuroreport*, *10*(9), 1889–1891. http://www.ncbi.nlm.nih.gov/pubmed/10501527%5Cnhttp://graphics.tx.ovid.com/ovftpdfs/FPDDNCJCHCDGFI00/fs024/ovft/live/gv013/00001756/00001756-199906230-00017.pdf

Holmin, S., Mathiesen, T., Shetye, J., & Biberfeld, P. (1995). Intracerebral inflammatory response to experimental brain contusion. *Acta Neurochirurgica*, *132*(1–3), 110–119. https://doi.org/10.1007/BF01404857

Holmin, S., Söderlund, J., Biberfeld, P., & Mathiesen, T. (1998). Intracerebral inflammation after human brain contusion. *Neurosurgery*, *42*(2), 291–299. https://doi.org/10.1097/00006123-199802000-00047

Hölttä, Minthon, L., Hansson, O., Holmén-Larsson, J., Pike, I., Ward, M., Kuhn, K., Rüetschi, U., Zetterberg, H., Blennow, K., & Gobom, J. (2015). An integrated workflow for multiplex CSF proteomics and peptidomics-identification of candidate cerebrospinal fluid biomarkers of alzheimer's disease. *Journal of Proteome Research*, *14*(2), 654–663. https://doi.org/10.1021/pr501076j

Hong, Y. T., Veenith, T., Dewar, D., Outtrim, J. G., Mani, V., Williams, C., Pimlott, S., Hutchinson, P. J. A., Tavares, A., Canales, R., Mathis, C. A., Klunk, W. E., Aigbirhio, F. I., Coles, J. P., Baron, J. C., Pickard, J. D., Fryer, T. D., Stewart, W., & Menon, D. K. (2014). Amyloid imaging with carbon 11 - Labeled pittsburgh compound B for traumatic brain injury. *JAMA Neurology*, *71*(1), 23–31. https://doi.org/10.1001/jamaneurol.2013.4847

Hong, Y., Zhang, J. M., Yan, W., Chen, S., & Sun, C. R. (2010). The role of Nrf2 signaling in the regulation of antioxidants and detoxifying enzymes after traumatic brain injury in rats and mice. *Acta Pharmacologica Sinica*, *31*(11), 1421–1430. https://doi.org/10.1038/aps.2010.101

Hoshi, A., Yamamoto, T., Shimizu, K., Ugawa, Y., Nishizawa, M., Takahashi, H., & Kakita, A. (2012). Characteristics of aquaporin expression surrounding senile plaques and cerebral amyloid angiopathy in Alzheimer disease. *Journal of Neuropathology and Experimental Neurology*, *71*(8), 750–759. https://doi.org/10.1097/NEN.0b013e3182632566

Hoshino, Helwig, M., Rezaei, S., Berridge, C., Eriksen, J. L., & Lindberg, I. (2014). A novel function for proSAAS as an amyloid anti-aggregant in Alzheimer's disease. *Journal of Neurochemistry*, *128*(3), 419–430. https://doi.org/10.1111/jnc.12454

Hsieh, H.-L., Lin, C.-C., Shih, R.-H., Hsiao, L.-D., & Yang, C.-M. (2012). NADPH oxidase-mediated redox signal contributes to lipoteichoic acid-induced MMP-9 upregulation in brain astrocytes. *Journal of Neuroinflammation*, *9*(110). http://www.jneuroinflammation.com/content/9/1/110

Hukkelhoven, C. W. P. M., Steyerberg, E. W., Rampen, A. J. J., Farace, E., Habbema, J. D. F., Marshall, L. F., Murray, G. D., & Maas, A. I. R. (2009).

Patient age and outcome following severe traumatic brain injury: an analysis of 5600 patients. *Journal of Neurosurgery*, *99*(4), 666–673. https://doi.org/10.3171/jns.2003.99.4.0666

Ii, M., Sunamoto, M., Ohnishi, K., & Ichimori, Y. (1996). B-Amyloid protein-dependent nitric oxide production from microglial cells and neurotoxicity. *Brain Research*, *720*, 93–100.

Ikonomovic, M. D., Uryu, K., Abrahamson, E. E., Ciallella, J. R., Trojanowski, J. Q., Lee, V. M.-Y., Clark, R. S., Marion, D. W., Wisniewski, S. R., & DeKosky, S. T. (2004). Alzheimer's pathology in human temporal cortex surgically excised after severe brain injury. *Experimental Neurology*, *190*(1), 192–203.

Iliff, J. J., Chen, M. J., Plog, B. A., Zeppenfeld, D. M., Soltero, M., Yang, L., Singh, I., Deane, R., & Nedergaard, M. (2014). Impairment of Glymphatic Pathway Function Promotes Tau Pathology after Traumatic Brain Injury. *The Journal of Neuroscience*, *34*(49), 16180–16193. https://doi.org/10.1523/JNEUROSCI.3020-14.2014

Iliff, Wang, M., Liao, Y., Plogg, B. A., Peng, W., Gundersen, G. A., Benveniste, H., Vates, G. E., Deane, R., Goldman, S. A., Nagelhus, E. A., & Nedergaard, M. (2012). A paravascular pathway facilitates CSF flow through the brain parenchyma and the clearance of interstitial solutes, including amyloid ß. *Science Translational Medicine*, *4*(147). https://doi.org/10.1126/scitranslmed.3003748

Itagaki, S., Mcgeer, P. L., Akiyama, H., Zhu, S., & Selkoe, D. (1989). Relationship of microglia and astrocytes to amyloid deposits of Alzheimer disease. In *Journal of Neuroimmunology* (Vol. 24).

Itakura, M., Nakajima, H., Kubo, T., Semi, Y., Kume, S., Higashida, S., Kaneshige, A., Kuwamura, M., Harada, N., Kita, A., Azuma, Y. T., Yamaji, R., Inui, T., & Takeuchi, T. (2015). Glyceraldehyde-3-phosphate dehydrogenase aggregates accelerate amyloid-ß amyloidogenesis in Alzheimer disease. *Journal of Biological Chemistry*, *290*(43), 26072–26087. https://doi.org/10.1074/jbc.M115.669291

Ittner, L. M., & Götz, J. (2011). Amyloid-ß and tau - A toxic pas de deux in Alzheimer's disease. *Nature Reviews Neuroscience*, *12*(2), 67–72. https://doi.org/10.1038/nrn2967

Jack, C. R., Lowe, V. J., Weigand, S. D., Wiste, H. J., Senjem, M. L., Knopman, D. S., Shiung, M. M., Gunter, J. L., Boeve, B. F., Kemp, B. J., Weiner, M., & Petersen, R. C. (2009). Serial PIB and MRI in normal, mild cognitive impairment and Alzheimers disease: Implications for sequence of pathological events in Alzheimers disease. *Brain*, *132*(5), 1355–1365. https://doi.org/10.1093/brain/awp062

Jackson, J. G., & Robinson, M. B. (2018). Regulation of mitochondrial dynamics in astrocytes: Mechanisms, consequences, and unknowns. In *GLIA* (Vol. 66, Issue 6, pp. 1213–1234). John Wiley and Sons Inc. https://doi.org/10.1002/glia.23252

Jafari, S., Etminan, M., Aminzadeh, F., & Samii, A. (2013). Head injury and risk of Parkinson disease: A systematic review and meta-analysis. *Movement Disorders*, *28*(9), 1222–1229. https://doi.org/10.1002/mds.25458

Jahn, Wittke, S., Zürbig, P., Raedler, T. J., Arlt, S., Kellmann, M., Mullen, W., Eichenlaub, M., Mischak, H., & Wiedemann, K. (2011). Peptide fingerprinting of Alzheimer's disease in cerebrospinal fluid: Identification and prospective evaluation of new synaptic biomarkers. *PLoS ONE*, *6*(10). https://doi.org/10.1371/journal.pone.0026540

James, S. L., Bannick, M. S., Montjoy-Venning, W. C., Lucchesi, L. R., Dandona, L., Dandona, R., Hawley, C., Hay, S. I., Jakovljevic, M., Khalil, I., Krohn, K. J., Mokdad, A. H., Naghavi, M., Nichols, E., Reiner, R. C., Smith, M., Feigin, V. L., Vos, T., Murray, C. J. L., … Zaman, S. B. (2019). Global, regional, and national burden of traumatic brain injury and spinal cord injury, 1990-2016: A systematic analysis for the Global Burden of Disease Study 2016. *The Lancet Neurology*, *18*(1), 56–87. https://doi.org/10.1016/S1474-4422(18)30415-0

Jansen, Ossenkoppele, R., Knol, D. L., Tijms, B. M., Scheltens, P., Verhey, F. R. J., Visser, P. J., Aalten, P., Aarsland, D., Alcolea, D., Alexander, M., Almdahl, I. S., Arnold, S. E., Baldeiras, I., Barthel, H., Van Berckel, B. N. M., Bibeau, K., Blennow, K., Brooks, D. J., … Zetterberg, H. (2015). Prevalence of cerebral amyloid pathology in persons without dementia: A meta-analysis. *JAMA - Journal of the American Medical Association*, *313*(19), 1924–1938. https://doi.org/10.1001/jama.2015.4668

Jarvela, Lam, H. A., Helwig, M., Lorenzen, N., Otzen, D. E., McLean, P. J., Maidment, N. T., & Lindberg, I. (2016). The neural chaperone proSAAS blocks α-synuclein fibrillation and neurotoxicity. *Proceedings of the National Academy of Sciences of the United States of America*, *113*(32), E4708–E4715. https://doi.org/10.1073/pnas.1601091113

Jin, X., Ishii, H., Bai, Z., Itokazu, T., & Yamashita, T. (2012). Temporal changes in cell marker expression and cellular infiltration in a controlled cortical impact model in adult male C57BL/6 mice. *PLoS ONE*, *7*(7), 1–13. https://doi.org/10.1371/journal.pone.0041892

Johnson, V. E., Stewart, J. E., Begbie, F. D., Trojanowski, J. Q., Smith, D. H., & Stewart, W. (2013). Inflammation and white matter degeneration persist for years after a single traumatic brain injury. *Brain*, *136*(1), 28–42. https://doi.org/10.1093/brain/aws322

Johnson, Stewart, & Smith, D. H. (2013). Axonal Pathology in Traumatic Brain Injury. *Experimental Neurology*, *246*, 35–43. https://doi.org/10.1002/ana.22528.Toll-like

Johnson, Stewart, W., Arena, J. D., & Smith, D. H. (2017). Traumatic brain injury as a trigger of neurodegeneration. In *Advances in Neurobiology* (Vol. 15, pp. 383–400). Springer New York LLC. https://doi.org/10.1007/978-3-319-57193-5_15

Johnson, Stewart, W., & Smith, D. (2010). Traumatic brain injury and amyloid-ß pathology: a link to Alzheimer's disease? *Nat Rev Neurosci.*, *11*(5), 361–370. https://doi.org/10.1038/nrn2808.Traumatic

Johnson, Stewart, W., & Smith, D. H. (2012). Widespread Tau and Amyloid-Beta pathology many years after a single traumatic brain injury. *Brain Pathology*, *22*(2), 142–149. https://doi.org/10.1111/j.1750-3639.2011.00513.x.Widespread

Johnson, Stewart, W., Trojanowski, J. Q., & Smith, D. H. (2011). Acute and chronically increased immunoreactivity to phosphorylation-independent but not pathological TDP-43 after a single traumatic brain injury in humans. *Acta*, *122*, 715–726. https://doi.org/10.1007/s00401-011-0909-9

Jordan, B. D., Jahre, C., Hauser, W. A., Zimmerman, R. D., & Peterson, M. (1992). Serial computed tomography in professional boxers. *Journal of Neuroimaging*, *2*(4), 181–185.

Kamat, Swarnkar, S., Rai, S., Kumar, V., & Tyagi, N. (2014). Astrocyte mediated MMP-9 activation in the synapse dysfunction: An implication in Alzheimer

disease. *Therapeutic Targets for Neurological Diseases*, *1*(1). https://doi.org/10.14800/ttnd.243

Kanaan, N. M., Cox, K., Alvarez, V. E., Stein, T. D., Poncil, S., & McKee, A. C. (2016). Characterization of early pathological tau conformations and phosphorylation in chronic traumatic encephalopathy. *Journal of Neuropathology and Experimental Neurology*, *75*(1), 19–34. https://doi.org/10.1093/jnen/nlv001

Kanemitsu, H., Tomiyama, T., & Mori, H. (2003). Human neprilysin is capable of degrading amyloid ß peptide not only in the monomeric form but also the pathological oligomeric form. *Neuroscience Letters*, *350*(2), 113–116.

Karve, I. P., Taylor, J. M., & Crack, P. J. (2016). The contribution of astrocytes and microglia to traumatic brain injury. *British Journal of Pharmacology*, *173*(4), 692–702. https://doi.org/10.1111/bph.13125

Kashon, M. L., Ross, G. W., O'Callaghan, J. P., Miller, D. B., Petrovitch, H., Burchfiel, C. M., Sharp, D. S., Markesbery, W. R., Davis, D. G., & Hardman, J. (2004). Associations of cortical astrogliosis with cognitive performance and dementia status. *Journal of Alzheimer's Disease*, *6*(6), 595–604.

Kawamata, T., Akiyama, H., Yamada, T., & Mcgeer, P. L. (1992). Immunologic Reactions in Amyotrophic Lateral Sclerosis Brain and Spinal Cord Tissue. In *American Journal of Pathology* (Vol. 140, Issue 3).

Keleman, A., Wisch, J. K., Bollinger, R. M., Grant, E. A., Benzinger, T. L., Morris, J. C., Ances, B. M., & Stark, S. L. (2020). Falls Associate with Neurodegenerative Changes in ATN Framework of Alzheimer's Disease. *Journal of Alzheimer's Disease*, *77*(2), 745–752. https://doi.org/10.3233/JAD-200192

Kenney, K., Iacono, D., Edlow, B. L., Katz, D. I., Diaz-Arrastia, R., Dams-O'Connor, K., Daneshvar, D. H., Stevens, A., Moreau, A. L., Tirrell, L. S., Varjabedian, A., Yendiki, A., van der Kouwe, A., Mareyam, A., McNab, J. A., Gordon, W. A., Fischl, B., McKee, A. C., & Perl, D. P. (2018). Dementia after moderate-severe traumatic brain injury: Coexistence of multiple proteinopathies. *Journal of Neuropathology and Experimental Neurology*, *77*(1), 50–63. https://doi.org/10.1093/jnen/nlx101

Kerman, A., Liu, H. N., Croul, S., Bilbao, J., Rogaeva, E., Zinman, L., Robertson, J., & Chakrabartty, A. (2010). Amyotrophic lateral sclerosis is a non-amyloid disease in which extensive misfolding of SOD1 is unique to the familial form. *Acta Neuropathologica*, *119*(3), 335–344. https://doi.org/10.1007/s00401-010-0646-5

Kiernan, Vucic, S., Cheah, B. C., Turner, M. R., Eisen, A., Hardiman, O., Burrell, J. R., & Zoing, M. C. (2011). Seminar Amyotrophic lateral sclerosis. *Lancet*, *377*, 942–955. https://doi.org/10.1016/S0140

Kikuchi, K., Arawaka, S., Koyama, S., Kimura, H., Ren, C. H., Wada, M., Kawanami, T., Kurita, K., Daimon, M., Kawakatsu, S., Kadoya, T., Goto, K., & Kato, T. (2003). An N-terminal fragment of ProSAAS (a granin-like neuroendocrine peptide precursor) is associated with tau inclusions in Pick's disease. *Biochemical and Biophysical Research Communications*, *308*(3), 646–654. https://doi.org/10.1016/S0006-291X(03)01391-3

Kim, G., Kim, J. E., Rhie, S. J., & Yoon, S. (2015). The Role of Oxidative Stress in Neurodegenerative Diseases. In *Experimental Neurobiology* (Vol. 24, Issue 4, pp. 325–340). Korean Society for Neurodegenerative Disease. https://doi.org/10.5607/en.2015.24.4.325

Kim, H., Leigh, J. H., Lee, Y. S., Choi, Y., Kim, Y., Kim, J. E., Cho, W. S., Seo, H. G., & Oh, B. M. (2020). Decreasing incidence and mortality in traumatic

brain injury in korea, 2008–2017: A population-based longitudinal study. *International Journal of Environmental Research and Public Health*, *17*(17), 1–13. https://doi.org/10.3390/ijerph17176197

King, A., Sweeney, F., Bodi, I., Troakes, C., Maekawa, S., & Al-Sarraj, S. (2010). Abnormal TDP-43 expression is identified in the neocortex in cases of dementia pugilistica, but is mainly confined to the limbic system when identified in high and moderate stages of Alzheimer's disease. *Neuropathology*, *30*(4), 408–419. https://doi.org/10.1111/j.1440-1789.2009.01085.x

Kirk, J., Plumb, J., Mirakhur, M., & McQuaid, S. (2003). Tight junctional abnormality in multiple sclerosis white matter affects all calibres of vessel and is associated with blood-brain barrier leakage and active demyelination. *Journal of Pathology*, *201*(2), 319–327. https://doi.org/10.1002/path.1434

Korolainen, Nyman, T. A., Aittokallio, T., & Pirttilä, T. (2010). An update on clinical proteomics in Alzheimer's research. *Journal of Neurochemistry*, *112*(6), 1386–1414. https://doi.org/10.1111/j.1471-4159.2009.06558.x

Kossmann, T., Hans, V. H., Imhof, H. G., Stocker, R., Grob, P., Trentz, O., & Morganti-Kossmann, C. (1995). Intrathecal and serum interleukin-6 and the acute-phase response in patients with severe traumatic brain injuries. *Shock (Augusta, Ga.)*, *4*(5), 311—317. http://europepmc.org/abstract/MED/8595516

Kovacs, Ferrer, I., Grinberg, L. T., Alafuzoff, I., Attems, J., Budka, H., Cairns, N. J., Crary, J., Duyckaerts, C., Ghetti, B., Halliday, G. M., Ironside, J. W., Love, S., Mackenzie, I. R., Munoz, D. G., Murray, M. E., Nelson, P. T., Takahashi, H., Trojanowski, J. Q., … Dickson, D. W. (2016). Aging-related tau astrogliopathy (ARTAG): harmonized evaluation strategy. *Acta Neuropathologica*, *131*(1), 87–102. https://doi.org/10.1007/s00401-015-1509-x

Kovacs, G. G. (2018). Tauopathies. *Handbook of Clinical Neurology*, *145*, 355–368.

Kumar, R. G., Boles, J. A., & Wagner, A. K. (2015). Chronic inflammation after severe traumatic brain injury: Characterization and associations with outcome at 6 and 12 months postinjury. *Journal of Head Trauma Rehabilitation*, *30*(6), 369–381. https://doi.org/10.1097/HTR.0000000000000067

Lace, Ince, P. G., Brayne, C., Savva, G. M., Matthews, F. E., De Silva, R., Simpson, J. E., & Wharton, S. B. (2012). Mesial temporal astrocyte tau pathology in the MRC-CFAS ageing brain cohort. *Dementia and Geriatric Cognitive Disorders*, *34*(1), 15–24. https://doi.org/10.1159/000341581

Laird, M. D., Vender, J. R., & Dhandapani, K. M. (2008). Opposing Roles for Reactive Astrocytes following Traumatic Brain Injury. *Neurosignals*, *16*, 154–164. https://doi.org/10.1159/000111560

Lanoue, & Day, R. (2001). Coexpression of Proprotein Convertase SPC3 and the Neuroendocrine Precursor ProSAAS*. *Endocrinology*, *142*(9), 4141–4149. https://academic.oup.com/endo/article/142/9/4141/2989590

Lazarev, Dutysheva, E. A., Komarova, E. Y., Mikhaylova, E. R., Guzhova, I. V., & Margulis, B. A. (2018). GAPDH-targeted therapy – A new approach for secondary damage after traumatic brain injury on rats. *Biochemical and Biophysical Research Communications*, *501*(4), 1003–1008. https://doi.org/10.1016/j.bbrc.2018.05.099

Lazarev, Sverchinskyi, D. V., Ippolitova, M. V., Stepanova, A. V., Guzhova, I. V., & Marguilis, B. A. (2013). Factors affecting aggregate formation in cell

models of Huntington's Disease and Amytrophic Lateral Sclerosis. *Acta Naturae*, *5*(2), 81–89.

Leaston, J., Qiao, J., Harding, I. C., Kulkarni, P., Gharagouzloo, C., Ebong, E., & Ferris, C. F. (2021). Quantitative Imaging of Blood-Brain Barrier Permeability Following Repetitive Mild Head Impacts. *Frontiers in Neurology*, *12*. https://doi.org/10.3389/fneur.2021.729464

Lecky, F. E., Otesile, O., Marincowitz, C., Majdan, M., Nieboer, D., Lingsma, H. F., Maegele, M., Citerio, G., Stocchetti, N., Steyerberg, E. W., Menon, D. K., Maas, A. I. R., Åkerlund, C., Amrein, K., Andelic, N., Andreassen, L., Anke, A., Antoni, A., Audibert, G., … Zoerle, T. (2021). The burden of traumatic brain injury from low-energy falls among patients from 18 countries in the CENTER-TBI Registry: A comparative cohort study. *PLoS Medicine*, *18*(9). https://doi.org/10.1371/journal.pmed.1003761

Lee, Bae, E.-J., & Lee, S.-J. (2014). Extracellular α-synuclein—a novel and crucial factor in Lewy body diseases. *Nature Reviews Neurology*, *10*(2), 92–98.

Lee, C. (2012). *Objective To review evidences on the management of patients with motor neuron disease. Reviewing evidences on the management of patients with motor neuron disease*. www.hkmj.org

Lee, E., Kinch, K., Johnson, V. E., Trojanowski, J. Q., Smith, D. H., & Stewart, W. (2019). Chronic traumatic encephalopathy is a common co-morbidity, but less frequent primary dementia in former soccer and rugby players. *Acta Neuropathologica*, *138*(3), 389–399. https://doi.org/10.1007/s00401-019-02030-y

Lee, Y., Hou, S. W., Lee, C. C., Hsu, C. Y., Huang, Y. S., & Su, Y. C. (2013). Increased Risk of Dementia in Patients with Mild Traumatic Brain Injury: A Nationwide Cohort Study. *PLoS ONE*, *8*(5). https://doi.org/10.1371/journal.pone.0062422

Leech, S., Kirk, J., Plumb, J., & McQuaid, S. (2007). Persistent endothelial abnormalities and blood-brain barrier leak in primary and secondary progressive multiple sclerosis. *Neuropathology and Applied Neurobiology*, *33*(1), 86–98. https://doi.org/10.1111/j.1365-2990.2006.00781.x

Lehman. (2013). *Epidemiology of neurodegeneration in American-style professional football players*. http://alzres.com/content/5/4/34

Levey, A., Lah, J., Goldstein, F., Steenland, K., & Bliwise, D. (2006). Mild cognitive impairment: An opportunity to identify patients at high risk for progression to Alzheimer's disease. In *Clinical Therapeutics* (Vol. 28, Issue 7, pp. 991–1001). https://doi.org/10.1016/j.clinthera.2006.07.006

Levin, H. S., Williams, D. H., Michael Valastro, M. A., Eisenberg, H. M., Crofford, M. J., & Handel, S. F. (1990). Corpus Callosum atrophy following closed head injury, detection with MRI. *Journal of Neurosurgery*, *73*, 77–81.

Li, Y., Li, Y., Li, X., Zhang, S., Zhao, J., Zhu, X., & Tian, G. (2017). Head injury as a risk factor for dementia and Alzheimer's disease: A systematic review and meta-analysis of 32 observational studies. *PLoS ONE*, *12*(1). https://doi.org/10.1371/journal.pone.0169650

Liddell, J. R. (2017). Are astrocytes the predominant cell type for activation of Nrf2 in aging and neurodegeneration? In *Antioxidants* (Vol. 6, Issue 3). MDPI. https://doi.org/10.3390/antiox6030065

Liddelow, S. A., Guttenplan, K. A., Clarke, L. E., Bennett, F. C., Bohlen, C. J., Schirmer, L., Bennett, M. L., Münch, A. E., Chung, W. S., Peterson, T. C., Wilton, D. K., Frouin, A., Napier, B. A., Panicker, N., Kumar, M., Buckwalter, M. S., Rowitch, D. H., Dawson, V. L., Dawson, T. M., … Barres,

B. A. (2017). Neurotoxic reactive astrocytes are induced by activated microglia. *Nature*, *541*(7638), 481–487. https://doi.org/10.1038/nature21029

Lista, Faltraco, F., Prvulovic, D., & Hampel, H. (2013). Blood and plasma-based proteomic biomarker research in Alzheimer's disease. *Progress in Neurobiology*, *101–102*(1), 1–17. https://doi.org/10.1016/j.pneurobio.2012.06.007

Liu, Althaus, J. S., Ellerbrock, B. R., Becker, D. A., & Gurney, M. E. (1998). Enhanced oxygen radical production in a transgenic mouse model of familial amyotrophic lateral sclerosis. *Annals of Neurology*, *44*(5), 763–770. https://doi.org/10.1002/ana.410440510

Livingston, G., Huntley, J., Sommerlad, A., Ames, D., Ballard, C., Banerjee, S., Brayne, C., Burns, A., Cohen-Mansfield, J., Cooper, C., Costafreda, S. G., Dias, A., Fox, N., Gitlin, L. N., Howard, R., Kales, H. C., Kivimäki, M., Larson, E. B., Ogunniyi, A., … Mukadam, N. (2020). Dementia prevention, intervention, and care: 2020 report of the Lancet Commission. In *The Lancet* (Vol. 396, Issue 10248, pp. 413–446). Lancet Publishing Group. https://doi.org/10.1016/S0140-6736(20)30367-6

Lizhnyak, P. N., & Ottens, A. K. (2015). Proteomics: in pursuit of effective traumatic brain injury therapeutics. *Expert Rev Proteomics.*, *12*(1), 75–82. https://doi.org/10.1586/14789450.2015.1000869.Proteomics

Loane, D. J., & Byrnes, K. R. (2010). Role of Microglia in Neurotrauma. *Neurotherapeutics*, *7*, 366–377.

Loane, D. J., & Kumar, A. (2016). Microglia in the TBI Brain: The Good, The Bad and The Dysregulted. *Exp Neurol.*, *275*(0 3), 316–327. https://doi.org/10.1016/j.expneurol.2015.08.018.Microglia

Loane, D. J., Kumar, A., Stoica, B. A., Cabatbat, R., & Faden, A. I. (2014). Progressive Neurodegeneration after experimental brain trauma; Association with chronic microglial activation. *Journal of Neuropathology & Experimental Neurology*, *73*(1), 14–29. https://doi.org/10.1086/498510.Parasitic

LoBue, C., Munro Cullum, C., Didehbani, N., Yeatman, K., Jones, B., Kraut, M. A., & Hart, J. (2018). Neurodegenerative dementias after traumatic brain injury. *Journal of Neuropsychiatry and Clinical Neurosciences*, *30*(1), 7–13. https://doi.org/10.1176/appi.neuropsych.17070145

Loeffler, C., Dietz, K., Schleich, A., Schlaszus, H., Stoll, M., Meyermann, R., & Mittelbronn, M. (2011). Immune surveillance of the normal human CNS takes place in dependence of the locoregional blood-brain barrier configuration and is mainly performed by CD3+/CD8+ lymphocytes. *Neuropathology*, *31*(3), 230–238. https://doi.org/10.1111/j.1440-1789.2010.01167.x

Lõpez-González, I., Carmona, M., Blanco, R., Luna-Muñoz, J., Martínez-Mandonado, A., Mena, R., & Ferrer, I. (2013). Characterization of thorn-shaped astrocytes in white matter of temporal lobe in alzheimers disease brains. *Brain Pathology*, *23*(2), 144–153. https://doi.org/10.1111/j.1750-3639.2012.00627.x

López-Otín, C., Blasco, M. A., Partridge, L., Serrano, M., & Kroemer, G. (2013). The hallmarks of aging. In *Cell* (Vol. 153, Issue 6, p. 1194). Elsevier B.V. https://doi.org/10.1016/j.cell.2013.05.039

Lowe, V. J., Kemp, B. J., Jack, C. R., Senjem, M., Weigand, S., Shiung, M., Smith, G., Knopman, D., Boeve, B., Mullan, B., & Petersen, R. C. (2009). Comparison of 18F-FDG and PiB PET in cognitive impairment. *Journal of*

Nuclear Medicine, *50*(6), 878–886. https://doi.org/10.2967/jnumed.108.058529

Lücking, C. B., & Brice, A. (2000). Review Alpha-synuclein and Parkinson's disease. In *CMLS, Cell. Mol. Life Sci* (Vol. 57).

Lye, T. C., & Shores, E. A. (2000). Traumatic Brain Injury as a Risk Factor for Alzheimer's Disease: A Review. *Neuropsychology Review*, *10*(2), 115–129.

Maas, A. I. R., Menon, D. K., David Adelson, P. D., Andelic, N., Bell, M. J., Belli, A., Bragge, P., Brazinova, A., Büki, A., Chesnut, R. M., Citerio, G., Coburn, M., Jamie Cooper, D., Tamara Crowder, A., Czeiter, E., Czosnyka, M., Diaz-Arrastia, R., Dreier, J. P., Duhaime, A. C., … Zemek, R. (2017). Traumatic brain injury: Integrated approaches to improve prevention, clinical care, and research. In *The Lancet Neurology* (Vol. 16, Issue 12, pp. 987–1048). Lancet Publishing Group. https://doi.org/10.1016/S1474-4422(17)30371-X

Maas, A. I. R., Menon, D. K., Manley, G. T., Abrams, M., Åkerlund, C., Andelic, N., Aries, M., Bashford, T., Bell, M. J., Bodien, Y. G., Brett, B. L., Büki, A., Chesnut, R. M., Citerio, G., Clark, D., Clasby, B., Cooper, D. J., Czeiter, E., Czosnyka, M., … Zemek, R. (2022). Traumatic brain injury: progress and challenges in prevention, clinical care, and research. In *The Lancet Neurology* (Vol. 21, Issue 11, pp. 1004–1060). Elsevier Ltd. https://doi.org/10.1016/S1474-4422(22)00309-X

Maas, A. I. R., Stocchetti, N., & Bullock, R. (2008). Moderate and severe traumatic brain injury in adults. In *www.thelancet.com/neurology* (Vol. 7). http://www.crash2.lshtm.

Mackay, D. F., Russell, E. R., Stewart, K., MacLean, J. A., Pell, J. P., & Stewart, W. (2019). Neurodegenerative Disease Mortality among Former Professional Soccer Players. *New England Journal of Medicine*, *381*(19), 1801–1808. https://doi.org/10.1056/nejmoa1908483

Magistretti, & Allaman, I. (2015). A Cellular Perspective on Brain Energy Metabolism and Functional Imaging. *Neuron*, *86*(4), 883–901. https://doi.org/10.1016/j.neuron.2015.03.035

Malek-Ahmadi, M., Perez, S. E., Chen, K., & Mufson, E. J. (2016). Neuritic and Diffuse Plaque Associations with Memory in Non-Cognitively Impaired Elderly. *Journal of Alzheimer's Disease*, *53*(4), 1641–1652. https://doi.org/10.3233/JAD-160365

Mannix, & Whalen, M. J. (2012). Traumatic brain injury, microglia, and beta amyloid. *International Journal of Alzheimer's Disease*. https://doi.org/10.1155/2012/608732

Marincowitz, C., Lecky, F., Allgar, V., & Sheldon, T. (2019). Evaluation of the impact of the NICE head injury guidelines on inpatient mortality from traumatic brain injury: An interrupted time series analysis. *BMJ Open*, *9*(6). https://doi.org/10.1136/bmjopen-2019-028912

Martland, H. S. (1928). Punch Drunk. *Food Manufacture*, *101*(12), 41. https://doi.org/10.1001/jama.1928.02700150029009

Mathys, Davila-Velderrain, J., Peng, Z., Gao, F., Mohammadi, S., Young, J. Z., Menon, M., He, L., Abdurrob, F., Jiang, X., Martorell, A. J., Ransohoff, R. M., Hafler, B. P., Bennett, D. A., Kellis, M., & Tsai, L. H. (2019). Single-cell transcriptomic analysis of Alzheimer's disease. *Nature*, *570*(7761), 332–337. https://doi.org/10.1038/s41586-019-1195-2

Mawdsley, C., & Ferguson, F. R. (1963). Neurological disease in boxers. *The Lancet*, *282*(7312), 795–801.

Maxwell, Bartlett, E., & Morgan, H. (2015). Wallerian Degeneration in the Optic Nerve Stretch-Injury Model of Traumatic Brain Injury: A Stereological

Analysis. *Journal of Neurotrauma*, *32*(11), 780–790. https://doi.org/10.1089/neu.2014.3369

Maxwell, W. L., Dhillon, K., Harper, L., Espin, J., Macintosh, T. K., Smith, D. H., & Graham, D. I. (2003). There Is Differential Loss of Pyramidal Cells from the Human Hippocampus with Survival after Blunt Head Injury. In *Journal of Neuropathology and Experimental Neurology* (Vol. 62, Issue 3).

Maxwell, W. L., Mackinnon, M. A., Smith, D. H., Mcintosh, T. K., & Graham, D. I. (2006). Thalamic Nuclei After Human Blunt Head Injury. *Journal of Neuropathology*, *65*(5), 478–488.

McKee, A., Cairns, N. J., Dickson, D. W., Folkerth, R. D., Dirk Keene, C., Litvan, I., Perl, D. P., Stein, T. D., Vonsattel, J. P., Stewart, W., Tripodis, Y., Crary, J. F., Bieniek, K. F., Dams-O'Connor, K., Alvarez, V. E., & Gordon, W. A. (2016). The first NINDS/NIBIB consensus meeting to define neuropathological criteria for the diagnosis of chronic traumatic encephalopathy. *Acta Neuropathologica*, *131*(1), 75–86. https://doi.org/10.1007/s00401-015-1515-z

McKee, A., Cantu, R., Nowinski, C. J., Hedley-Whyte, T., Gavett, B. E., Budson, A. E., Santini, V. E., Lee, H. S., Kubilus, C. A., & Stern, R. A. (2009). Chronic Traumatic Encephalopathy in Athletes: Progressive Tauopathy After Repeated Head Injury. *J Neuropathol Exp Neurol*, *68*(7), 709–735.

McKee, A., Gavett, B. E., Stern, R. A., Nowinski, C. J., Cantu, R. C., Kowall, N. W., Perl, D. P., Hedley-Whyte, E. T., Price, B., Sullivan, C., Morin, P., Lee, H., Kubilus, C. A., Daneshvar, D. H., Wulff, M., & Budson, A. E. (2010). TDP-43 proteinopathy and motor neuron disease in chronic traumatic encephalopathy. *Journal of Neuropathology and Experimental Neurology*, *69*(9), 918–929. https://doi.org/10.1097/NEN.0b013e3181ee7d85

McKee, A., Stein, T. D., Kiernan, P. T., & Alvarez, V. (2015). The neuropathology of chronic traumatic encephalopathy. *Brain Pathology*, *25*(3), 350–364. https://doi.org/10.1111/bpa.12248

McKee, A., Stein, T. D., Nowinski, C. J., Stern, R. A., Daneshvar, D. H., Alvarez, V. E., Lee, H., Hall, G., Wojtowicz, S. M., Baugh, C. M., Riley, D. O., Kubilus, C. A., Cormier, K. A., Jacobs, M. A., Martin, B. R., Abraham, C. R., Ikezu, T., Reichard, R. R., Wolozin, B. L., … Cantu, R. C. (2013). The spectrum of disease in chronic traumatic encephalopathy. *Brain*, *136*(1), 43–64. https://doi.org/10.1093/brain/aws307

McKee, C., & Lukens, J. R. (2016). Emerging roles for the immune system in traumatic brain injury. *Frontiers in Immunology*, *7*(DEC), 1–17. https://doi.org/10.3389/fimmu.2016.00556

McKeith, Boeve, B. F., Dickson, D. W., Halliday, G., Taylor, J.-P., Weintraub, D., Aarsland, D., Galvin, J., Attems, J., Ballard, C. G., Bayston, A., Beach, T. G., Blanc, F., Bohnen, N., Bonanni, L., Bras, J., Brundin, P., Burn, D., Chen-Plotkin, A., … Iranzo, A. (2017). Diagnosis and management of dementia with Lewy bodies. *Neurology*, *89*, 88–100.

McManus, R. M., Mills, K. H. G., & Lynch, M. A. (2015). T Cells—Protective or Pathogenic in Alzheimer's Disease? *Journal of Neuroimmune Pharmacology*, *10*(4), 547–560. https://doi.org/10.1007/s11481-015-9612-2

Meaney, Smith, D. H., Shreiber, D. I., Bain, A. C., Miller, R. T., Ross, D. T., & Gennarelli, T. A. (1995). Biomechanical analysis of experimental DAI. *Journal of Neurotrauma*, *12*(4), 689–694.

Mecocci, Boccardi, V., Cecchetti, R., Bastiani, P., Scamosci, M., Ruggiero, C., & Baroni, M. (2018). A Long Journey into Aging, Brain Aging, and Alzheimer's

Disease Following the Oxidative Stress Tracks. *Journal of Alzheimer's Disease*, *62*(3), 1319–1335. https://doi.org/10.3233/JAD-170732

Mecocci, P., MacGarvey, U., Kaufman, A. E., Koontz, D., Shoffner, J. M., Wallace, D. C., & Beal, M. F. (1993). Oxidative damage to mitochondrial DNA shows marked age-dependent increases in human brain. *Annals of Neurology*, *34*(4), 609–616. https://doi.org/10.1002/ana.410340416

Metting, Z., Wilczak, N., Rodiger, L. A., Schaaf, J. M., & Van Der Naalt, J. (2012). GFAP and S100B in the acute phase of mild traumatic brain injury. *Neurology*, *78*(18), 1428–1433. https://doi.org/10.1212/WNL.0b013e318253d5c7

Mez, J., Daneshvar, D. H., Kiernan, P. T., Abdolmohammadi, B., Alvarez, V. E., Huber, B. R., Alosco, M. L., Solomon, T. M., Nowinski, C. J., McHale, L., Cormier, K. A., Kubilus, C. A., Martin, B. M., Murphy, L., Baugh, C. M., Montenigro, P. H., Chaisson, C. E., Tripodis, Y., Kowall, N. W., … McKee, A. C. (2017). Clinicopathological evaluation of chronic traumatic encephalopathy in players of American football. *JAMA - Journal of the American Medical Association*, *318*(4), 360–370. https://doi.org/10.1001/jama.2017.8334

Mezey, Dehejia, A., Harta, G., Papp, M. I., Polymeropoulos, M. H., & Brownstein, M. J. (1998). Alpha synuclein in neurodegenerative disorders: Murderer or accomplice? *Nature Medicine*, *4*(7), 755–757.

Mi, J., Shevchenko, G., Musunuri, S., Hillered, L., Marklund, N., Abu Hamdeh, S., & Bergquist, J. (2014). Brain proteomics analysis of patients with traumatic brain injury reveals biomarkers for post-TBI complications. *J Proteomics Bioinform*, *7*(7), 4172. https://doi.org/10.4172/0974-276X.S1.073

Michinaga, Inoue, A., Sonoda, K., Mizuguchi, H., & Koyama, Y. (2021). Down-regulation of astrocytic sonic hedgehog by activation of endothelin ETB receptors: Involvement in traumatic brain injury-induced disruption of blood brain barrier in a mouse model. *Neurochemistry International*, *146*. https://doi.org/10.1016/j.neuint.2021.105042

Michinaga, S., & Koyama, Y. (2019). Dual roles of astrocyte-derived factors in regulation of blood-brain barrier function after brain damage. *International Journal of Molecular Sciences*, *20*(571). https://doi.org/10.3390/ijms20030571

Mikolaenko, Pletnikova, O., Kawas, C. H., O'Brien, R., Resnick, S. M., Crain, B., & Troncoso, J. C. (2005). Alpha-synuclein lesions in normal aging, Parkinson disease, and Alzheimer disease: Evidence from the Baltimore Longitudinal Study of Aging (BLSA). *Journal of Neuropathology and Experimental Neurology*, *64*(2), 156–162. https://doi.org/10.1093/jnen/64.2.156

Millspaugh, J. A. (1937). Dementia pugilistica. *US Naval Med Bull*, *35*(297), e303.

Minagar, A., & Alexander, J. S. (2003). Blood-brain barrier disruption in multiple sclerosis. In *Multiple Sclerosis* (Vol. 9, Issue 6, pp. 540–549). https://doi.org/10.1191/1352458503ms965oa

Mink, Blumenschine, R. J., & Adams, D. B. (1981). Ratio of central nervous system to body metabolism in vertebrates: its constancy and functional basis. *American Physiological Society*, *241*(3), R203–R212.

Mintun, M. A., Larossa, G. N., Sheline, Y. I., Dence, C. S., Lee, S. Y., MacH, R. H., Klunk, W. E., Mathis, C. A., Dekosky, S. T., & Morris, J. C. (2006). [11C]PIB in a nondemented population: Potential antecedent marker of Alzheimer disease. *Neurology*, *67*(3), 446–452. https://doi.org/10.1212/01.wnl.0000228230.26044.a4

Mirra, S. S., Heyman, A., McKeel, D., Sumi, S. M., Crain, B. J., Brownlee, L. M., Vogel, F. S., Hughes, J. P., Van Belle, G., & Berg, L. (1991). The Consortium to Establish a Registry for Alzheimer's Disease (CERAD): Part II. Standardization of the neuropathologic assessment of Alzheimer's disease. *Neurology*, *41*(4), 479.

Mittal, K., Eremenko, E., Berner, O., Elyahu, Y., Strominger, I., Apelblat, D., Nemirovsky, A., Spiegel, I., & Monsonego, A. (2019). CD4 T Cells Induce A Subset of MHCII-Expressing Microglia that Attenuates Alzheimer Pathology. *IScience*, *16*, 298–311. https://doi.org/10.1016/j.isci.2019.05.039

Molgaard, C. A., Stanford, E. P., Morton, D. J., Ryden, L. A., Schubert, K. R., & Golbeck, A. L. (1990). Epidemiology of head trauma and neurocognitive impairment in a multi-ethnic population. *Neuroepidemiology*, *9*(5), 233–242.

Mondello, Papa, L., Buki, A., Bullock, M. R., Czeiter, E., Tortella, F. C., Wang, K. K., & Hayes, R. L. (2011). Neuronal and glial markers are differently associated with computed tomography findings and outcome in patients with severe traumatic brain injury: A case control study. *Critical Care*, *15*(3). https://doi.org/10.1186/cc10286

Mondello, S., Buki, A., Italiano, D., & Jeromin, A. (2013). a-Synuclein in CSF of patients with severe traumatic brain injury. *American Academy of Neurology*, *80*, 1662–1668. www.neurology.org.

Montagne, A., Barnes, S. R., Sweeney, M. D., Halliday, M. R., Sagare, A. P., Zhao, Z., Toga, A. W., Jacobs, R. E., Liu, C. Y., Amezcua, L., Harrington, M. G., Chui, H. C., Law, M., & Zlokovic, B. V. (2015). Blood-Brain barrier breakdown in the aging human hippocampus. *Neuron*, *85*(2), 296–302. https://doi.org/10.1016/j.neuron.2014.12.032

Morganti-kossmann, M. C., Hans, V. H. J., Lenzlinger, P. M., Dubs, R., Ludwig, E., Trentz, O., & Kossmann, T. (1999). TGF-beta Is Elevated in the CSF of Patients with Severe Traumatic Brain Injuries and Parallels Blood-Brain Barrier Function. *Journal of Neurotrauma*, *16*(7), 617–628.

Morganti-kossmann, M. C., Rancan, M., Stahel, P. F., & Kossmann, T. (2002). Inflammatory response in acute traumatic brain injury : a double-edged sword. *Current Opinion in Critical Care*, *8*, 101–105.

Morganti-Kossmann, M. C., Semple, B. D., Hellewell, S. C., Bye, N., & Ziebell, J. M. (2019). The complexity of neuroinflammation consequent to traumatic brain injury: from research evidence to potential treatments. In *Acta Neuropathologica* (Vol. 137, Issue 5, pp. 731–755). Springer Verlag. https://doi.org/10.1007/s00401-018-1944-6

Morin, A. (2022). *Subacute and chronic proteomic and phosphoproteomic analyses of a mouse model of traumatic brain injury at two timepoints and the comparison with chronic traumatic encephalopathy in human samples*. https://doi.org/10.21203/rs.3.rs-1569233/v1

Morris, J. C., Storandt, ; M, Mckeel, ; D W, Rubin, ; E H, Price, ; J L, Grant, ; E A, & Berg, L. (1996). Cerebral amyloid deposition and diffuse plaques in "normal" aging: Evidence for presymptomatic and very mild Alzheimer's disease. *Neurology*, *46*, 707–719.

Morris, J. C., Storandt, M., McKeel, D. W., Rubin, E. H., Price, J. L., Grant, E. A., & Berg, L. (1996). Cerebral amyloid deposition and diffuse plaques in``normal''aging: Evidence for presymptomatic and very mild Alzheimer's disease. *Neurology*, *46*(3), 707–719.

Mortimer, J. A., Van Duijn, C. M., Chandra, V., Fratiglioni, L., Graves, A. B., Heyman, A., Jorm, A. F., Kokmen, E., Kondo, K., Rocca, W. A., Shalat, S. L., Soininen, H., & Hofman, A. (1991). Head trauma as a risk factor for

Alzheimer's disease: A collaborative re-analysis of case-control studies. *International Journal of Epidemiology*, *20*(SUPPL. 2), S28–S35. https://doi.org/10.1093/ije/20.Supplement_2.S28

Mosenthal, A. C., Lavery, R. F., Addis, M., Kaul, S., Ross, S., Marburger, R., Deitch, E. A., & Livingston, D. H. (2002). Isolated traumatic brain injury; age is an independent predictor of mortality and early outcome. *Journal of Trauma*, *52*(5), 907–911. https://doi.org/10.1097/00005373-200205000-00015

Mosenthal, A. C., Livingston, D. H., Lavery, R. F., Knudson, M. M., Lee, S., Morabito, D., Manley, G. T., Nathens, A., Jurkovich, G., Hoyt, D. B., & Coimbra, R. (2004). The effect of age on functional outcome in mild traumatic brain injury: 6-Month report of a prospective multicenter trial. *Journal of Trauma - Injury, Infection and Critical Care*, *56*(5), 1042–1048. https://doi.org/10.1097/01.TA.0000127767.83267.33

Mouzon, B., Bachmeier, C., Ojo, J., Acker, C., Ferguson, S., Crynen, G., Davies, P., Mullan, M., Stewart, W., & Crawford, F. (2019). Chronic White Matter Degeneration, but No Tau Pathology at One-Year Post-Repetitive Mild Traumatic Brain Injury in a Tau Transgenic Model. *Journal of Neurotrauma*, *36*(4), 576–588. https://doi.org/10.1089/neu.2018.5720

Munro, P. T., Smith, R. D., & Parke, T. R. J. (2002). Effect of patients' age on management of acute intracranial haematoma: Prospective national study. *British Medical Journal*, *325*(7371), 1001–1003. https://doi.org/10.1136/bmj.325.7371.1001

Myer, D. J., Gurkoff, G. G., Lee, S. M., Hovda, D. A., & Sofroniew, M. V. (2006). Essential protective roles of reactive astrocytes in traumatic brain injury. *Brain*, *129*(10), 2761–2772. https://doi.org/10.1093/brain/awl165

Nagelhus, E. A., Mathiisen, T. M., & Ottersen, O. P. (2004). Aquaporin-4 in the central nervous system: Cellular and subcellular distribution and coexpression with KIR4.1. *Neuroscience*, *129*(4), 905–913. https://doi.org/10.1016/j.neuroscience.2004.08.053

Nakagawa, Y., Reed, L., Nakamura, M., McIntosh, T. K., Smith, D. H., Saatman, K. E., Raghupathi, R., Clemens, J., Saido, T. C., Lee, V. M. Y., & Trojanowski, J. Q. (2000). Brain trauma in aged transgenic mice induces regression of established Aß deposits. *Experimental Neurology*, *163*(1), 244–252. https://doi.org/10.1006/exnr.2000.7375

Nakajima, Amano, W., Fujita, A., Fukuhara, A., Azuma, Y. T., Hata, F., Inui, T., & Takeuchi, T. (2007). The active site cysteine of the proapoptotic protein glyceraldehyde-3- phosphate dehydrogenase is essential in oxidative stress-induced aggregation and cell death. *Journal of Biological Chemistry*, *282*(36), 26562–26574. https://doi.org/10.1074/jbc.M704199200

Narayana, P. A. (2017). White matter changes in patients with mild traumatic brain injury: MRI perspective. *Concussion*, *2*(2). https://doi.org/10.2217/cnc-2016-0028

Neri, M., Frati, A., Turillazzi, E., Cantatore, S., Cipolloni, L., Di Paolo, M., Frati, P., La Russa, R., Maiese, A., Scopetti, M., Santurro, A., Sessa, F., Zamparese, R., & Fineschi, V. (2018). Immunohistochemical evaluation of aquaporin-4 and its correlation with CD68, IBA-1, HIF-1α, GFAP, and CD15 expressions in fatal traumatic brain injury. *International Journal of Molecular Sciences*, *19*(11). https://doi.org/10.3390/ijms19113544

Neselius, S., Brisby, H., Theodorsson, A., Blennow, K., Zetterberg, H., & Marcusson, J. (2012). Csf-biomarkers in olympic boxing: Diagnosis and

effects of repetitive head trauma. *PLoS ONE*, *7*(4). https://doi.org/10.1371/journal.pone.0033606

Neubuerger, Sinton, D. W., & Denst, J. (1959). Cerebral Atrophy Associated with Boxing permitted the report of Case The only papers that describe the cerebral lesions in "dementia pugilistica." *AMA Archives of Neurology and Psychiatry*, *81*, 19–24. https://jamanetwork.com/

Neumann, M., Kwong, L. K., Truax, A. C., Vanmassenhove, B., Kretzschmar, H. A., Van Deerlin, V. M., Clark, C. M., Grossman, M., Miller, B. L., Trojanowski, J. Q., & M-Y Lee, V. (2007). TDP-43-Positive White Matter Pathology in Frontotemporal Lobar Degeneration With Ubiquitin-Positive Inclusions. *J Neuropathol Exp Neurol*, *66*(3), 177–183. https://academic.oup.com/jnen/article/66/3/177/2916740

Neumann, M., Sampathu, D. M., Kwong, L. K., Truax, A. C., Micsenyi, M. C., Chou, T. T., Bruce, J., Schuck, T., Grossman, M., Clark, C. M., McCluskey, L. F., Miller, B. L., Masliah, E., Mackenzie, I. R., Feldman, H., Feiden, W., Kretzschmar, H. A., Trojanowski, J. Q., & M-Y Lee, V. (2006). Ubiquitinated TDP-43 in Frontotemporal Lobar Degeneration and Amyotrophic Lateral Sclerosis. *Science*, *314*, 130–133. http://science.sciencemag.org/

Newell, K., Boyer, P., Gomez-Tortosa, E., Hobbs, W., Hedley-Whyte, E. T., Vonsattel, J., & Hyman, B. (1999). Alpha-synuclein immunoreactivity is present in axonal swellings in neuroaxonal dystrophy and acute TBI. *Journal of Neuropathology and Experimental Neurology*, *58*(12), 1263–1268.

Ng, K., Mikulis, D. J., Glazer, J., Kabani, N., Till, C., Greenberg, G., Thompson, A., Lazinski, D., Agid, R., Colella, B., & Green, R. E. (2008). Magnetic Resonance Imaging Evidence of Progression of Subacute Brain Atrophy in Moderate to Severe Traumatic Brain Injury. *Archives of Physical Medicine and Rehabilitation*, *89*(12 SUPPL.). https://doi.org/10.1016/j.apmr.2008.07.006

Nielsen, Nagelhus, E. A., Amiry-Moghaddam, M., Bourque, C., Agre, P., & Ottersen, O. P. (1997). Specialized Membrane Domains for Water Transport in Glial Cells: High-Resolution Immunogold Cytochemistry of Aquaporin-4 in Rat Brain. *Journal of Neuroscience*, *17*(1), 171–180.

Nielsen, S., Nagelhus, E. A., Amiry-Moghaddam, M., Bourque, C., Agre, P., & Ottersen, O. P. (1996). Specialized Membrane Domains for Water Transport in Glial Cells: High-Resolution Immunogold Cytochemistry of Aquaporin-4 in Rat Brain. *The Journal of Neuroscience*, *17*(1), 171–180.

Nizamutdinov, D., & Shapiro, L. A. (2017). Overview of traumatic brain injury: An immunological context. *Brain Sciences*, *7*(1). https://doi.org/10.3390/brainsci7010011

Nordström, A., & Nordström, P. (2018). Traumatic brain injury and the risk of dementia diagnosis: A nationwide cohort study. *PLoS Medicine*, *15*(1). https://doi.org/10.1371/journal.pmed.1002496

Norup, A., Kruse, M., Soendergaard, P. L., Rasmussen, K. W., & Biering-Sørensen, F. (2020). Socioeconomic Consequences of Traumatic Brain Injury: A Danish Nationwide Register-Based Study. *Journal of Neurotrauma*, *37*(24), 2694–2702. https://doi.org/10.1089/neu.2020.7064

Nowak, L. A., Smith, G. G., & Reyes, P. F. (2009). Dementia in a retired world boxing champion: case report and literature review. *Clinical Neuropathology*, *28*(4), 275–280.

Nylander, & Hafler, D. A. (2012). Multiple Sclerosis. *The Journal of Clinical Investigation*, *122*(4), 1180–1188.

Nylén, Öst, M., Csajbok, L. Z., Nilsson, I., Blennow, K., Nellgård, B., & Rosengren, L. (2006). Increased serum-GFAP in patients with severe traumatic brain injury is related to outcome. *Journal of the Neurological Sciences*, *240*(1–2), 85–91. https://doi.org/10.1016/j.jns.2005.09.007

Oberstein, T. J., Spitzer, P., Klafki, H. W., Linning, P., Neff, F., Knölker, H. J., Lewczuk, P., Wiltfang, J., Kornhuber, J., & Maler, J. M. (2015). Astrocytes and microglia but not neurons preferentially generate N-terminally truncated Aß peptides. *Neurobiology of Disease*, *73*, 24–35. https://doi.org/10.1016/j.nbd.2014.08.031

Omalu, Bailes, J., Hamilton, R. L., Kamboh, M. I., Hammers, J., Case, M., & Fitzsimmons, R. (2011). Emerging histomorphologic phenotypes of chronic traumatic encephalopathy in american athletes. *Neurosurgery*, *69*(1), 173–183. https://doi.org/10.1227/NEU.0b013e318212bc7b

Omalu, DeKosky, S. T., Hamilton, R. L., Minster, R. L., Kamboh, M. I., Shakir, A. M., & Wecht, C. H. (2006). Chronic traumatic encephalopathy in a National Football League player: Part II. *Neurosurgery*, *59*(5), 1086–1092. https://doi.org/10.1227/01.NEU.0000245601.69451.27

Omalu, DeKosky, S. T., Minster, R. L., Kamboh, M. I., Hamilton, R. L., & Wecht, C. H. (2005). Chronic traumatic encephalopathy in a National Football League player. *Neurosurgery*, *57*(1), 128–133. https://doi.org/10.1227/01.NEU.0000163407.92769.ED

Omalu, Fitzsimmons, R. P., Hammers, J., & Bailes, J. (2010). Chronic traumatic encephalopathy in a professional American wrestler. *Journal of Forensic Nursing*, *6*(3), 130–136.

Omalu, Hamilton, R. L., Kamboh, M. I., DeKosky, S. T., & Bailes, J. (2010). Chronic traumatic encephalopathy (cte) in a national football league player: Case report and emerging medicolegal practice questions. *Journal of Forensic Nursing*, *6*(1), 40–46. https://doi.org/10.1111/j.1939-3938.2009.01064.x

O'Meara, E. S., Morris, M. C., Evans, D. A., Hebert, L. E., & Bienias, J. L. (1997). Head Injury and Risk of Alzheimer's Disease by Apolipoprotein E Genotype. *American Journal of Epidemiology*, *149*(5), 373–384. https://doi.org/10.1126/science.3.53.32

Onyszchuk, G., He, Y. Y., Berman, N. E. J., & Brooks, W. M. (2008). Detrimental effects of aging on outcome from traumatic brain injury: A behavioral, magnetic resonance imaging, and histological study in mice. *Journal of Neurotrauma*, *25*(2), 153–171. https://doi.org/10.1089/neu.2007.0430

Onyszchuk, G., LeVine, S. M., Brooks, W. M., & Berman, N. E. J. (2009). Post-acute pathological changes in the thalamus and internal capsule in aged mice following controlled cortical impact injury: A magnetic resonance imaging, iron histochemical, and glial immunohistochemical study. *Neuroscience Letters*, *452*(2), 204–208. https://doi.org/10.1016/j.neulet.2009.01.049

Opii, W. O., Nukala, V. N., Sultana, R., Pandya, J. D., Day, K. M., Merchant, M. L., Klein, J. B., Sullivan, P. G., & Butterfield, D. A. (2007). Proteomic identification of oxidized mitochondrial proteins following experimental traumatic brain injury. *Journal of Neurotrauma*, *24*(5), 772–789. https://doi.org/10.1089/neu.2006.0229

Orr, M. E., Sullivan, A. C., & Frost, B. (2017). A Brief Overview of Tauopathy: Causes, Consequences, and Therapeutic Strategies. In *Trends in Pharmacological Sciences* (Vol. 38, Issue 7, pp. 637–648). Elsevier Ltd. https://doi.org/10.1016/j.tips.2017.03.011

Ortiz, G. G., Pacheco-Moisés, F. P., Macías-Islas, M. Á., Flores-Alvarado, L. J., Mireles-Ramírez, M. A., González-Renovato, E. D., Hernández-Navarro, V. E., Sánchez-López, A. L., & Alatorre-Jiménez, M. A. (2014). Role of the Blood-Brain Barrier in Multiple Sclerosis. *Archives of Medical Research*, *45*(8), 687–697. https://doi.org/10.1016/j.arcmed.2014.11.013

Osnato, M., & Giliberti, V. (1926). Postconcussion neurosis-traumatic encephalitis. *American Neurological Association*.

Ostasiewicz, P., & Wiśniewski, J. R. (2017). A Protocol for Large-Scale Proteomic Analysis of Microdissected Formalin Fixed and Paraffin Embedded Tissue. *Methods in Enzymology*, *585*, 159–176. https://doi.org/10.1016/bs.mie.2016.09.017

Ostasiewicz, P., Zielinska, D. F., Mann, M., & Wisniewski, J. R. (2010). Proteome, phosphoproteome, and N-glycoproteome are quantitatively preserved in formalin-fixed paraffin-embedded tissue and analyzable by high-resolution mass spectrometry. *Journal of Proteome Research*, *9*(7), 3688–3700. https://doi.org/10.1021/pr100234w

Ousman, S. S., & Kubes, P. (2012). Immune surveillance in the central nervous system. *Nature Neuroscience*, *15*(8), 1096–1101. https://doi.org/10.1038/nn.3161

Panza, F., Lozupone, M., Logroscino, G., & Imbimbo, B. P. (2019). A critical appraisal of amyloid-ß-targeting therapies for Alzheimer disease. *Nature Reviews Neurology*, *15*(2), 73–88. https://doi.org/10.1038/s41582-018-0116-6

Papa, Lewis, L. M., Falk, J. L., Zhang, Z., Silvestri, S., Giordano, P., Brophy, G. M., Demery, J. A., Dixit, N. K., Ferguson, I., Liu, M. C., Mo, J., Akinyi, L., Schmid, K., Mondello, S., Robertson, C. S., Tortella, F. C., Hayes, R. L., & Wang, K. K. W. (2012). Elevated levels of serum glial fibrillary acidic protein breakdown products in mild and moderate traumatic brain injury are associated with intracranial lesions and neurosurgical intervention. *Annals of Emergency Medicine*, *59*(6), 471–483. https://doi.org/10.1016/j.annemergmed.2011.08.021

Papadopoulos, M. C., Manley, G. T., Krishna, S., & Verkman, A. S. (2004). Aquaporin-4 facilitates reabsorption of excess fluid in vasogenic brain edema. *The FASEB Journal*, *18*(11), 1291–1293. https://doi.org/10.1096/fj.04-1723fje

Papadopoulos, & Verkman, A. S. (2007). Aquaporin-4 and brain edema. *Pediatric Nephrology*, *22*(6), 778–784. https://doi.org/10.1007/s00467-006-0411-0

Papadopoulos, & Verkman, A. S. (2013). Aquaporin water channels in the nervous system. *Nat Rev Neurosci.*, *14*(4), 265–277. https://doi.org/10.1038/jid.2014.371

Parsonage, M. (2016). *REPORT An economic analysis Traumatic brain injury and offending*.

Payne, E. E. (1968). Brains of boxers. *Neurochirurgia*, *11*(05), 173–188.

Pekny, M., Wilhelmsson, U., & Pekna, M. (2014). The dual role of astrocyte activation and reactive gliosis. In *Neuroscience Letters* (Vol. 565, pp. 30–38). Elsevier Ireland Ltd. https://doi.org/10.1016/j.neulet.2013.12.071

Pelinka, Kroepfl, A., Schmidhammer, R., Krenn, M., Buchinger, W., Redl, H., & Raabe, A. (2004). Glial fibrillary acidic protein in serum after traumatic brain injury and multiple trauma. *Journal of Trauma - Injury, Infection and Critical Care*, *57*(5), 1006–1012. https://doi.org/10.1097/01.TA.0000108998.48026.C3

Pellerin, L., Bouzier-Sore, A. K., Aubert, A., Serres, S., Merle, M., Costalat, R., & Magistretti, P. J. (2007). Activity-dependent regulation of energy metabolism by astrocytes: An update. In *GLIA* (Vol. 55, Issue 12, pp. 1251–1262). https://doi.org/10.1002/glia.20528

Perez-Nievas, B. G., & Serrano-Pozo, A. (2018). Deciphering the astrocyte reaction in Alzheimer's disease. In *Frontiers in Aging Neuroscience* (Vol. 10, Issue APR). Frontiers Media S.A. https://doi.org/10.3389/fnagi.2018.00114

Perl, D. P. (2010). Neuropathology of Alzheimer's disease. In *Mount Sinai Journal of Medicine* (Vol. 77, Issue 1, pp. 32–42). https://doi.org/10.1002/msj.20157

Perry, V. H., Nicoll, J. A. R., & Holmes, C. (2010). Microglia in neurodegenerative disease. In *Nature Reviews Neurology* (Vol. 6, Issue 4, pp. 193–201). https://doi.org/10.1038/nrneurol.2010.17

Peters, R. (2006). Ageing and the brain. *Postgraduate Medical Journal*, *82*, 84–88. https://doi.org/10.1136/pgmj.2005.036665

Petzold. (2015). Glial fibrillary acidic protein is a body fluid biomarker for glial pathology in human disease. *Brain Research*, *1600*, 17–31. https://doi.org/10.1016/j.brainres.2014.12.027

Phillips, L. M., & Lampson, L. A. (1999). Site-specific control of T cell traffic in the brain: T cell entry to brainstem vs. hippocampus after local injection of IFN-γ. *Journal of Neuroimmunology*, *96*(2), 218–227.

Pierce, J. E. S., Trojanowski, J. Q., Graham, D. I., Smith, D. H., & Mcintosh', T. K. (1996). lmmunohistochemical Characterization of Alterations in the Distribution of Amyloid Precursor Proteins and P-Amyloid Peptide after Experimental Brain Injury in the Rat. In *The Journal of Neuroscience* (Vol. 76, Issue 3).

Pike, K. E., Savage, G., Villemagne, V. L., Ng, S., Moss, S. A., Maruff, P., Mathis, C. A., Klunk, W. E., Masters, C. L., & Rowe, C. C. (2007). Β-amyloid imaging and memory in non-demented individuals: Evidence for preclinical Alzheimer's disease. *Brain*, *130*(11), 2837–2844. https://doi.org/10.1093/brain/awm238

Plassman, & Grafman, J. (2015). Traumatic brain injury and late-life dementia. In *Handbook of Clinical Neurology* (1st ed., Vol. 128). Elsevier Ltd. https://doi.org/10.1016/B978-0-444-63521-1.00044-3

Plassman, Havlik, RJ., Steffens, DC., Helms, MJ., Newman, TN., Drosdick, D., Phillips, C., Gau, Ba., Welsh–Bohmer, Ka., Burke, JR., Guralnik, JM., & Breitner, JCS. (2000). Documented head injury in early adulthood and risk of Alzheimer's disease and other dementias. *Neurology*, *55*(2), 1158–1166. https://doi.org/10.1212/WNL.55.8.1158

Plummer, S., Van Den Heuvel, C., Thornton, E., Corrigan, F., & Cappai, R. (2016). The neuroprotective properties of the amyloid precursor protein following traumatic brain injury. In *Aging and Disease* (Vol. 7, Issue 2, pp. 163–179). International Society on Aging and Disease. https://doi.org/10.14336/AD.2015.0907

Polymeropoulos, M. H., Lavedan, C., Leroy, E., Ide, S. E., Dehejia, A., Dutra, A., Pike, B., Root, H., Rubenstein, J., Boyer, R., Stenroos, E. S., Chandrasekharappa, S., Athanassiadou, A., Papapetropoulos, T., Johnson, W. G., Lazzarini, A. M., Duvoisin, R. C., Di Iorio, G., Golbe, L. I., & Nussbaum, R. L. (1997). Mutation in the α-synuclein gene identified in families with Parkinson's disease. *Science*, *276*(5321), 2045–2047. https://doi.org/10.1126/science.276.5321.2045

Pontecorvo, M. J., Devous, M. D., Kennedy, I., Navitsky, M., Lu, M., Galante, N., Salloway, S., Murali Doraiswamy, P., Southekal, S., Arora, A. K., McGeehan, A., Lim, N. C., Xiong, H., Truocchio, S. P., Joshi, A. D., Shcherbinin, S., Teske, B., Fleisher, A. S., & Mintun, M. A. (2019). A multicentre longitudinal study of flortaucipir (18F) in normal ageing, mild cognitive impairment and Alzheimer's disease dementia. *Brain*, *142*(6), 1723–1735. https://doi.org/10.1093/brain/awz090

Poon, Hensley, K., Thongboonkerd, V., Merchant, M. L., Lynn, B. C., Pierce, W. M., Klein, J. B., Calabrese, V., & Butterfield, A. D. (2005). Redox proteomics analysis of oxidatively modified proteins in G93A-SOD1 transgenic mice - A model of familial amyotrophic lateral sclerosis. *Free Radical Biology and Medicine*, *39*(4), 453–462. https://doi.org/10.1016/j.freeradbiomed.2005.03.030

Potter, H., & Wisniewski, T. (2012). Apolipoprotein E: Essential catalyst of the Alzheimer amyloid cascade. In *International Journal of Alzheimer's Disease*. https://doi.org/10.1155/2012/489428

Povlishock. (1992). The Role of oxygen radicals in the pathobiology of TBI. *Human Cell*, *5*(4), 345–353.

Povlishock, & Katz, D. I. (2005). Update of Neuropathology and Neurological Recovery After Traumatic Brain Injury. *J Head Trauma Rehabil*, *20*(1), 76–94. www.headtraumarehab.com

Price, J. L., & Morris, J. C. (1999). Tangles and plaques in nondemented aging and "preclinical" alzheimer's disease. *Annals of Neurology*, *45*(3), 358–368. https://doi.org/10.1002/1531-8249(199903)45:3<358::AID-ANA12>3.0.CO;2-X

Pumiglia, Williams, A. M., Kemp, M. T., Wakam, G. K., Alam, H. B., & Biesterveld, B. E. (2021). Brain proteomic changes by histone deacetylase inhibition after traumatic brain injury. *Trauma Surgery and Acute Care Open*, *6*(1). https://doi.org/10.1136/tsaco-2021-000682

Pupillo, E., Bianchi, E., Vanacore, N., Montalto, C., Ricca, G., Robustelli Della Cuna, F. S., Fumagalli, F., Castellani, M., Poli, F., Romeo, F., Tommasi, D., Lazzaro, P., & Beghi, E. (2020). Increased risk and early onset of ALS in professional players from Italian Soccer Teams. *Amyotrophic Lateral Sclerosis and Frontotemporal Degeneration*, *21*(5–6), 403–409. https://doi.org/10.1080/21678421.2020.1752250

Qin, L., Liu, Y., Cooper, C., Liu, B., Wilson, B., & Hong, J. (2002). Microglia enhance b -amyloid peptide-induced toxicity in cortical and mesencephalic neurons by producing reactive oxygen species. *Journal of Neurochemistry*, *83*, 973–983.

Quigley, H., Colloby, S. J., & O'Brien, J. T. (2011). PET imaging of brain amyloid in dementia: A review. *International Journal of Geriatric Psychiatry*, *26*(10), 991–999. https://doi.org/10.1002/gps.2640

Raina, A. K., Templeton, D. J., Deak, J. C., Perry, G., & Smith, M. A. (2013). Quinone reductase (NQO1), a sensitive redox indicator, is increased in Alzheimer's disease. *Redox Report*, *4*(1–2), 23–27. https://doi.org/10.1179/135100099101534701

Raj, R., Kaprio, J., Jousilahti, P., Korja, M., & Siironen, J. (2022). Risk of Dementia After Hospitalization Due to Traumatic Brain Injury. *Neurology*, *98*(23), E2377–E2386. https://doi.org/10.1212/WNL.0000000000200290

Ramanathan, D. M., McWilliams, N., Schatz, P., & Hillary, F. G. (2012). Epidemiological shifts in elderly traumatic brain injury: 18-year trends in

Pennsylvania. *Journal of Neurotrauma*, *29*(7), 1371–1378. https://doi.org/10.1089/neu.2011.2197

Ramlackhansingh, A. F., Brooks, D. J., Greenwood, R. J., Bose, S. K., Turkheimer, F. E., Kinnunen, K. M., Gentleman, S., Heckemann, R. A., Gunanayagam, K., Gelosa, G., & Sharp, D. J. (2011). Inflammation after trauma: Microglial activation and traumatic brain injury. *Annals of Neurology*, *70*(3), 374–383. https://doi.org/10.1002/ana.22455

Rash, J. E., Yasumura, T., Hudson, C. S., Agre, P., & Nielsen, S. (1998). Direct immunogold labeling of aquaporin-4 in square arrays of astrocyte and ependymocyte plasma membranes in rat brain and spinal cord. In *National Institutes of Health* (Vol. 95). www.pnas.org.

Raut, M. K. (2019). Global age-specific denominator estimation for monitoring of health and nutrition SDGs and indicators based on population projections of the UN world population prospects, 2017 revision, for the year 2018. *Int J Community Med Public Health*, *6*(1), 177.

Ray, Huang, B. W., & Tsuji, Y. (2012). Reactive oxygen species (ROS) homeostasis and redox regulation in cellular signaling. *Cellular Signalling*, *24*(5), 981–990. https://doi.org/10.1016/j.cellsig.2012.01.008

Reijn, Abdo, W. F., Schelhaas, H. J., & Verbeek, M. M. (2009). CSF neurofilament protein analysis in the differential diagnosis of ALS. *Journal of Neurology*, *256*, 615–619. https://doi.org/10.1007/s00415-009-0131-z

Ren, Z., Iliff, J., Yang, L., Yang, J., Chen, X., Chen, M. J., Giese, R. N., Wang, B., Shi, X., & Nedergaard, M. (2013). "Hit & Run" model of closed-skull traumatic brain injury (TBI) reveals complex patterns of post-traumatic AQP4 dysregulation. *Journal of Cerebral Blood Flow and Metabolism*, *33*(6), 834–845. https://doi.org/10.1038/jcbfm.2013.30

Ritzel, R. M., Doran, S. J., Barrett, J. P., Henry, R. J., Ma, E. L., Faden, A. I., & Loane, D. J. (2018). Chronic Alterations in Systemic Immune Function after Traumatic Brain Injury. *Journal of Neurotrauma*, *35*(13), 1419–1436. https://doi.org/10.1089/neu.2017.5399

Rivas-Arancibia, S., Guevara-Guzmán, R., López-Vidal, Y., Rodríguez-Martínez, E., Zanardo-Gomes, M., Angoa-Pérez, M., & Raisman-Vozari, R. (2009). Oxidative stress caused by ozone exposure induces loss of brain repair in the hippocampus of adult rats. *Toxicological Sciences*, *113*(1), 187–197. https://doi.org/10.1093/toxsci/kfp252

Robberecht, W., & Philips, T. (2013). The changing scene of amyotrophic lateral sclerosis. In *Nature Reviews Neuroscience* (Vol. 14, Issue 4, pp. 248–264). https://doi.org/10.1038/nrn3430

Roberts, A. H. (1969). *Brain damage in boxers: a study of the prevalence of traumatic encephalopathy among ex-professional boxers*. Pitman Medical & Scientific Publishing Company, Limited.

Roberts, G. W., Allsop, D., & Bruton, C. (1990). The occult aftermath of boxing. *Journal of Neurology Neurosurgery and Psychiatry*, *53*(5), 373–378. https://doi.org/10.1136/jnnp.53.5.373

Roberts, G. W., Gentleman, S. M., Lynch, A., & Graham, D. I. (1991). βA4 amyloid protein deposition in brain after head trauma. *The Lancet*, *338*(8780), 1422–1423. https://doi.org/10.1016/0140-6736(91)92724-G

Roberts, G. W., Gentleman, S. M., Lynch, A., Murray, L., Landon, M., & Graham, D. I. (1994). Beta Amyloid protein deposition in the brain after severe head injury : implications for the pathogenesis of Alzheimer ' s disease. *Journal of Neurology, Neurosurgery, and Psychiatry*, *57*(June 1993), 419–425.

Rodney, T., Osier, N., & Gill, J. (2018). Pro- and anti-inflammatory biomarkers and traumatic brain injury outcomes: A review. In *Cytokine* (Vol. 110, pp. 248–256). Academic Press. https://doi.org/10.1016/j.cyto.2018.01.012

Rodrigue, K., Kennedy, K., Rieck, J., Hebrank, B. A., Diaz-Arrastia, B. R., Mathews, D., & Park, D. (2012). *Amyloid burden in healthy aging Regional distribution and cognitive consequences From the Center for Vital Longevity (K Supplemental data at www.neurology.org*. www.neurology.org

Rodrigue, K. M., Kennedy, K. M., & Park, D. C. (2009). Beta-amyloid deposition in the aging brain. *Neuropsychol Rev*, *19*(4), 436–450. https://doi.org/10.1007/s11065-009-9118-x.Beta-Amyloid

Rosen, Siddiquet, T., Pattersont, D., Figlewicz, D. A., Sapp, P., Hentatit, A., Donaldsont, D., Goto, J., O'Regan, J. P., Dengt, H.-X., Rahmanit, Z., Krizus, A., McKenna-Yasek, D., Cayabyabt, A., Gaston, S. M., Bergert, R., Tanzi, R. E., Halperin, J. J., Herzfeldtt, B., … Brown Jr, R. H. (1993). Mutations in Cu/Zn superoxide dismutase gene are associated with familial amyotrophic lateral sclerosis. *Nature*, *362*, 59–62.

Rosenfeld, V., Rey, J., Maas, A. I., Bragge, P., Morganti-Kossmann, C., Rey, G., Manley, T., & Gruen, R. L. (2012). Early management of severe traumatic brain injury. In *Lancet* (Vol. 380). http://www.

Ross, D. E. (2011). Review of longitudinal studies of MRI brain volumetry in patients with traumatic brain injury. In *Brain Injury* (Vol. 25, Issues 13–14, pp. 1271–1278). Informa Healthcare. https://doi.org/10.3109/02699052.2011.624568

Ross, D. E., Ochs, A. L., Seabaugh, J. M., Demark, M. F., Shrader, C. R., Marwitz, J. H., & Havranek, M. D. (2012). Progressive brain atrophy in patients with chronic neuropsychiatric symptoms after mild traumatic brain injury: A preliminary study. *Brain Injury*, *26*(12), 1500–1509. https://doi.org/10.3109/02699052.2012.694570

Ross, & Siegel, D. (2018). NQO1 in protection against oxidative stress. *Current Opinion in Toxicology*, *7*, 67–72. https://doi.org/10.1016/j.cotox.2017.10.005

Rowe, Ellis, K. A., Rimajova, M., Bourgeat, P., Pike, K. E., Jones, G., Fripp, J., Tochon-Danguy, H., Morandeau, L., O'Keefe, G., Price, R., Raniga, P., Robins, P., Acosta, O., Lenzo, N., Szoeke, C., Salvado, O., Head, R., Martins, R., … Villemagne, V. L. (2010). Amyloid imaging results from the Australian Imaging, Biomarkers and Lifestyle (AIBL) study of aging. *Neurobiology of Aging*, *31*(8), 1275–1283. https://doi.org/10.1016/j.neurobiolaging.2010.04.007

Rowe, Ng, S., Ackermann, U., Gong, S., Pike, K., Savage, G., Cowie, T., Dickinson, K., Maruff, P., Darby, D., Smith, C., Woodward, M., Merory, J., Tochon-Danguy, H., O'Keefe, G., Klunk, W., Mathis, C., Price, J., Masters, C., & Villemagne, V. (2007). Imaging amyloid-beta burden in aging and dementia. *Neurology*, *68*, 1718–1725.

Royal College of Physicians of London. Committee on Boxing. (1969). *Report on the medical aspects of boxing*. Royal College of Physicians of London.

Rugbjerg, K., Ritz, B., Korbo, L., Martinussen, N., & Olsen, J. H. (2009). Risk of Parkinson's disease after hospital contact for head injury: Population based case-control study. *BMJ (Online)*, *338*(7685), 34–36. https://doi.org/10.1136/bmj.a2494

Russell, E. R., Mackay, D. F., Lyall, D., Stewart, K., MacLean, J. A., Robson, J., Pell, JJ. P., & Stewart, W. (2022). Neurodegenerative disease risk among former international rugby union players. *Journal of Neurology,*

Neurosurgery & Psychiatry, jnnp-2022-329675. https://doi.org/10.1136/jnnp-2022-329675

Russell, E. R., MacKay, D. F., Stewart, K., MacLean, J. A., Pell, J. P., & Stewart, W. (2021). Association of Field Position and Career Length with Risk of Neurodegenerative Disease in Male Former Professional Soccer Players. *JAMA Neurology*, *78*(9), 1057–1063. https://doi.org/10.1001/jamaneurol.2021.2403

Russell, E. R., Stewart, K., Mackay, D. F., Maclean, J., Pell, J. P., & Stewart, W. (2019). Football's InfluencE on Lifelong health and Dementia risk (FIELD): Protocol for a retrospective cohort study of former professional footballers. *BMJ Open*, *9*(5). https://doi.org/10.1136/bmjopen-2018-028654

Russo, & McGavern, D. B. (2016). Inflammatory neuroprotection following TBI. *Neuroimmunology*, *353*, 783–785. https://doi.org/10.1126/science.aag2590

Saing, T., Dick, M., Nelson, P. T., Kim, R. C., Cribbs, D. H., & Head, E. (2012). Frontal cortex neuropathology in dementia pugilistica. *Journal of Neurotrauma*, *29*(6), 1054–1070. https://doi.org/10.1089/neu.2011.1957

SantaCruz, K. S., Yazlovitskaya, E., Collins, J., Johnson, J., & DeCarli, C. (2004). Regional NAD(P)H:quinone oxidoreductase activity in Alzheimer's disease. *Neurobiology of Aging*, *25*(1), 63–69. https://doi.org/10.1016/S0197-4580(03)00117-9

Saw, M. M., Chamberlain, J., Barr, M., Morgan, M. P. G., Burnett, J. R., & Ho, K. M. (2014). Differential disruption of blood-brain barrier in severe traumatic brain injury. *Neurocritical Care*, *20*(2), 209–216. https://doi.org/10.1007/s12028-013-9933-z

Schaffert, J., LoBue, C., White, C. L., Chiang, H. S., Didehbani, N., Lacritz, L., Rossetti, H., Dieppa, M., Hart, J., & Cullum, C. M. (2018). Traumatic brain injury history is associated with an earlier age of dementia onset in autopsy-confirmed Alzheimer's disease. *Neuropsychology*, *32*(4), 410–416. https://doi.org/10.1037/neu0000423

Schmidt, S., Kwee, L. C., Allen, K. D., & Oddone, E. Z. (2010). Association of ALS with head injury, cigarette smoking and APOE genotypes. *Journal of the Neurological Sciences*, *291*(1–2), 22–29. https://doi.org/10.1016/j.jns.2010.01.011

Schmidt., Zhukareva, V., Newell, K. L., Lee, V. M. Y., & Trojanowski, J. Q. (2001). Tau isoform profile and phosphorylation state in dementia pugilistica recapitulate Alzheimer's disease. *Acta Neuropathologica*, *101*(5), 518–524. https://doi.org/10.1007/s004010000330

Schofield, P. W., Tang, M., Marder, K., Bell, K., Dooneief, G., Chun, M., Sano, M., Stern, Y., & Mayeux, R. (1997). Alzheimer's disease after remote head injury: an incidence study. *J. Neurol. Neurosurg. Psychiatry*, *62*, 119–124.

Schöll, M., Lockhart, S. N., Schonhaut, D. R., O'Neil, J. P., Janabi, M., Ossenkoppele, R., Baker, S. L., Vogel, J. W., Faria, J., Schwimmer, H. D., Rabinovici, G. D., & Jagust, W. J. (2016). PET Imaging of Tau Deposition in the Aging Human Brain. *Neuron*, *89*(5), 971–982. https://doi.org/10.1016/j.neuron.2016.01.028

Schuchat, A., Director, A., Griffin, P. M., Rasmussen, S. A., Leahy, M. A., Martinroe, J. C., Spriggs, S. R., Yang, T., Doan, Q. M., King, P. H., Starr, T. M., Yang, M., Jones, T. F., Boulton, M. L., Caine, V. A., Daniel, K. L., Fielding, J. E., Fleming, D. W., Halperin, W. E., … Schaffner, W. (2017). Traumatic Brain Injury-Related Emergency Department Visits, Hospitalizations, and Deaths-United States, 2007 and 2013. In *Summ* (Vol. 66).

Scott, G., Hellyer, P. J., Ramlackhansingh, A. F., Brooks, D. J., Matthews, P. M., & Sharp, D. J. (2015). Thalamic inflammation after brain trauma is associated with thalamo-cortical white matter damage. *Journal of Neuroinflammation*, *12*(1), 224. https://doi.org/10.1186/s12974-015-0445-y

Seals, R. M., Hansen, J., Gredal, O., & Weisskopf, M. G. (2016). Physical Trauma and Amyotrophic Lateral Sclerosis: A Population-Based Study Using Danish National Registries. *American Journal of Epidemiology*, *183*(4), 294–301. https://doi.org/10.1093/aje/kwv169

Seidler, A., Hellenbrand, W., Robra, B.-P., Vieregge, P., Nischan, P., Joerg, J., Oertel, W. H., Ulm, G., & Schneider, E. (1996). Possible environmental, occupational, and other etiologic factors for Parkinson's disease. *Neurology*, *46*(5), 1275. https://doi.org/10.1212/WNL.46.5.1275

Selkoe, D. J., & Hardy, J. (2016). The amyloid hypothesis of Alzheimer's disease at 25 years. *EMBO Molecular Medicine*, *8*(6), 595–608. https://doi.org/10.15252/emmm.201606210

Shaw, K., MacKinnon, M. A., Raghupathi, R., Saatman, K. E., McLntosh, T. K., & Graham, D. I. (2001). TUNEL-positive staining in white and grey matter after fatal head injury in man. *Clinical Neuropathology*, *20*(3), 106–112.

Sheean, R. K., McKay, F. C., Cretney, E., Bye, C. R., Perera, N. D., Tomas, D., Weston, R. A., Scheller, K. J., Djouma, E., Menon, P., Schibeci, S. D., Marmash, N., Yerbury, J. J., Nutt, S. L., Booth, D. R., Stewart, G. J., Kiernan, M. C., Vucic, S., & Turner, B. J. (2018). Association of regulatory T-Cell Expansion with progression of amyotrophic lateral sclerosis a study of humans and a transgenic mouse model. *JAMA Neurology*, *75*(6), 681–689. https://doi.org/10.1001/jamaneurol.2018.0035

Sherriff, F. E., Bridges, L. R., & Sivaloganathan, S. (1994). Early detection of axonal injury after human head trauma using immunocytochemistry for ß-amyloid precursor protein. *Acta Neuropathologica*, *87*(1), 55–62. https://doi.org/10.1007/BF00386254

Shi, M., Chu, F., Zhu, F., & Zhu, J. (2022). Impact of Anti-amyloid-ß Monoclonal Antibodies on the Pathology and Clinical Profile of Alzheimer's Disease: A Focus on Aducanumab and Lecanemab. In *Frontiers in Aging Neuroscience* (Vol. 14). Frontiers Media S.A. https://doi.org/10.3389/fnagi.2022.870517

Shibahashi, K., Doi, T., Tanaka, S., Hoda, H., Chikuda, H., Sawada, Y., Takasu, Y., Chiba, K., Nozaki, T., Hamabe, Y., & Ogata, T. (2016). The Serum Phosphorylated Neurofilament Heavy Subunit as a Predictive Marker for Outcome in Adult Patients after Traumatic Brain Injury. *Journal of Neurotrauma*, *33*(20), 1826–1833. https://doi.org/10.1089/neu.2015.4237

Shiozaki, T., Hayakata, T., Tasaki, O., Hosotubo, H., Fuijita, K., Mouri, T., Tajima, G., Kajino, K., Nakae, H., Tanaka, H., Shimazu, T., & Sugimoto, H. (2005). Cerebrospinal fluid concentrations of anti-inflammatory mediators in early-phase severe traumatic brain injury. *Shock*, *23*(5), 406–410. https://doi.org/10.1097/01.shk.0000161385.62758.24

Shishido, H., Ueno, M., Sato, K., Matsumura, M., Toyota, Y., Kirino, Y., Tamiya, T., Kawai, N., & Kishimoto, Y. (2019). Traumatic brain injury by weight-drop method causes transient amyloid-ß deposition and acute cognitive deficits in mice. *Behavioural Neurology*, *2019*. https://doi.org/10.1155/2019/3248519

Shivaji, T., Lee, A., Dougall, N., McMillan, T., & Stark, C. (2014). The epidemiology of hospital treated traumatic brain injury in Scotland. *BMC Neurology*, *14*(1). https://doi.org/10.1186/1471-2377-14-2

Shively, S. B., Edgerton, S. L., Iacono, D., Purohit, D. P., Qu, B. X., Haroutunian, V., Davis, K. L., Diaz-Arrastia, R., & Perl, D. P. (2017). Localized cortical chronic traumatic encephalopathy pathology after single, severe axonal injury in human brain. *Acta Neuropathologica*, *133*(3), 353–366. https://doi.org/10.1007/s00401-016-1649-7

Shively, S. B., Horkayne-Szakaly, I., Jones, R. V., Kelly, J. P., Armstrong, R. C., & Perl, D. P. (2016). Characterisation of interface astroglial scarring in the human brain after blast exposure: a post-mortem case series. *The Lancet Neurology*, *15*(9), 944–953. https://doi.org/10.1016/S1474-4422(16)30057-6

Shlosberg, D., Benifla, M., Kaufer, D., & Friedman, A. (2010). Blood-brain barrier breakdown as a therapeutic target in traumatic brain injury. *Nature Reviews Neurology*, *6*(7), 393–403. https://doi.org/10.1038/nrneurol.2010.74

Simon, C., Soga, T., Okano, H. J., & Parhar, I. (2021). α-Synuclein-mediated neurodegeneration in Dementia with Lewy bodies: the pathobiology of a paradox. In *Cell and Bioscience* (Vol. 11, Issue 1). BioMed Central Ltd. https://doi.org/10.1186/s13578-021-00709-y

Simon, D., McGeachy, M. J., Baylr, H., Clark, R. S. B., Loane, D. J., & Kochanek, P. M. (2017). The far-reaching scope of neuroinflammation after traumatic brain injury. In *Nature Reviews Neurology* (Vol. 13, Issue 3, pp. 171–191). Nature Publishing Group. https://doi.org/10.1038/nrneurol.2017.13

Simpson, J. E., Ince, P. G., Lace, G., Forster, G., Shaw, P. J., Matthews, F., Savva, G., Brayne, C., & Wharton, S. B. (2010). Astrocyte phenotype in relation to Alzheimer-type pathology in the ageing brain. *Neurobiology of Aging*, *31*(4), 578–590. https://doi.org/10.1016/j.neurobiolaging.2008.05.015

Singh, S., Raj, K., & Sharma, V. V. (2019). Exploring the Role of Protein Biomarkers in Traumatic Brain Injury: Preclinical and Clinical Highlights. *Journal of Cellular and Molecular Pharmacology*, *3*(1). https://doi.org/10.4172/jcmp.1000105

Sirko, S., Irmler, M., Gascón, S., Bek, S., Schneider, S., Dimou, L., Obermann, J., De Souza Paiva, D., Poirier, F., Beckers, J., Hauck, S. M., Barde, Y. A., & Götz, M. (2015). Astrocyte reactivity after brain injury-: The role of galectins 1 and 3. *GLIA*, *63*(12), 2340–2361. https://doi.org/10.1002/glia.22898

Sisodia, S. S., & Price, D. L. (1995). Role of the 3-amyloid in Alzheimer ' s Maryland. *Faseb*, *9*(5), 366–370. file:///C:/Users/Public/Documents/KU Leuven/Master 2/Thesis/Papers AD/Role of Abeta in AD.pdf

Sivanandam, T. M., & Thakur, M. K. (2012). Traumatic brain injury: A risk factor for Alzheimer's disease. *Neuroscience and Biobehavioral Reviews*, *36*(5), 1376–1381. https://doi.org/10.1016/j.neubiorev.2012.02.013

Small, B. J., Gagnon, E., & Robinson, B. (2007). Early identification of cognitive deficits. *Geriatrics*, *62*(4).

Smith, A., Duan, T., & Verkman, A. S. (2019). Aquaporin-4 reduces neuropathology in a mouse model of Alzheimer's disease by remodeling peri-plaque astrocyte structure. *Acta Neuropathologica Communications*, *7*(1), 74. https://doi.org/10.1186/s40478-019-0728-0

Smith, C. (2013). Review : The long-term consequences of microglial activation following acute traumatic brain injury. *Neuropathology and Applied Neurobiology*, *39*, 35–44. https://doi.org/10.1111/nan.12006

Smith, C., Graham, D. I., Murray, L. S., & Nicoll, J. A. R. (2003). Tau immunohistochemistry in acute brain injury. *Neuropathology and Applied Neurobiology*, *29*, 496–502.

Smith, D. (1999). *Accumulation of Amyloid -beta and tau and the formation of neurofilament inclusions following diffuse brain injury in the pig*.

Smith, D. (2013). Chronic neuropathologies of single and repetitive TBI: substrates of dementia? *Nat Rev Neurol*, *9*(4), 211–221. https://doi.org/10.1038/nrneurol.2013.29.Chronic

Smith, D. (2016). Neuromechanics and Pathophysiology of Diffuse Axonal Injury in Concussion. In *Smith and Meaney*.

Smith, D., Chen, X.-H., Iwata, A., & Graham, D. I. (2003). Amyloid-beta accumulation in axons after traumatic brain injury in humans. *J Neurosurg*, *98*, 1072–1077.

Smith, D., Dollé, J. P., Ameen-Ali, K. E., Bretzin, A., Cortes, E., Crary, J. F., Dams-O'Connor, K., Diaz-Arrastia, R., Edlow, B. L., Folkerth, R., Hazrati, L. N., Hinds, S. R., Iacono, D., Johnson, V. E., Keene, C. D., Kofler, J., Kovacs, G. G., Lee, E. B., Manley, G., … Stewart, W. (2021). COllaborative Neuropathology NEtwork Characterizing ouTcomes of TBI (CONNECT-TBI). *Acta Neuropathologica Communications*, *9*(1). https://doi.org/10.1186/s40478-021-01122-9

Smith, D., Johnson, V. E., & Stewart, W. (2013a). Chronic neuropathologies of single and repetitive TBI: Substrates of dementia? *Nature Reviews Neurology*, *9*(4), 211–221. https://doi.org/10.1038/nrneurol.2013.29

Smith, D., Johnson, V. E., & Stewart, W. (2013b). Chronic neuropathologies of single and repetitive TBI: substrates of dementia? *Nature Reviews Neurology*, *9*(4), 211–221. https://doi.org/10.1038/nrneurol.2013.29

Smith, D., Johnson, V. E., Trojanowski, J. Q., & Stewart, W. (2019). Chronic traumatic encephalopathy — confusion and controversies. In *Nature Reviews Neurology* (Vol. 15, Issue 3, pp. 179–183). Nature Publishing Group. https://doi.org/10.1038/s41582-018-0114-8

Smith, D., & Meaney, D. F. (2000). Axonal Damage in Traumatic Brain Injury. *Progress in Clinical Neuroscience*, *6*(6), 483–495.

Soares, H. D., Hicks, R. R., Smith, D., & McIntosh, T. K. (1995). Inflammatory leukocytic recruitment and diffuse neuronal degeneration are separate pathological processes resulting from traumatic brain injury. *The Journal of Neuroscience*, *15*(12), 8223–8233. http://www.ncbi.nlm.nih.gov/pubmed/8613756

Sofroniew, M. V. (2009). Molecular dissection of reactive astrogliosis and glial scar formation. *Trends in Neuroscience*, *32*(12), 638–647. https://doi.org/10.1016/j.tins.2009.08.002.Molecular

Sofroniew, M. V. (2013). Multiple Roles for Astrocytes as Effectors of Cytokines and Inflammatory Mediators. *The Neuroscientist*, *20*(2), 160–172. https://doi.org/10.1177/1073858413504466

Sofroniew, M. V. (2015). Astrogliosis. *Cold Spring Harbor Perspectives in Biology*, *7*(2). https://doi.org/10.1101/cshperspect.a020420

Sofroniew, M. V, & Vinters, H. V. (2010). Astrocytes : biology and pathology. *Acta Neuropathologica*, *119*, 7–35. https://doi.org/10.1007/s00401-009-0619-8

Solleiro-Villavicencio, H., & Rivas-Arancibia, S. (2018). Effect of chronic oxidative stress on neuroinflammatory response mediated by CD4+T cells in neurodegenerative diseases. In *Frontiers in Cellular Neuroscience* (Vol. 12). Frontiers Media S.A. https://doi.org/10.3389/fncel.2018.00114

Song, W. M., & Colonna, M. (2018). The identity and function of microglia in neurodegeneration. In *Nature Immunology* (Vol. 19, Issue 10, pp. 1048–1058). Nature Publishing Group. https://doi.org/10.1038/s41590-018-0212-1

Spillane, J. D. (1962). FIVE BOXERS. *British Medical Journal*, 1205–1212.

Spillantini, M. G., Schmidt, M. L., Lee, V. M. Y., Trojanowski, J. Q., Jakes, R., & Goedert, M. (1997). a-Synuclein in Lewy bodies. *Nature*, *388*, 839–840.

Stahel, P. F., Shohami, T., Younis, M., Kariya, K., Otto, V. I., Lenzlinger, P. M., Grosjean, M. B., Eugster, H.-P., Trentz, O., Kossmann, T., & Morganti-Kossmann, M. C. (2000). Experimental Closed Head Injury: Analysis of Neurological Outcome, Blood-Brain Barrier Dysfunction, Intracranial Neutrophil Infiltration, and Neuronal Cell Death in Mice Deficient in Genes for Pro-Inflammatory Cytokines. *Journal of Cerebral Blood Flow and Metabolism*, *20*, 369–380.

Stanwell, P., Iverson, G. L., Van Patten, R., Castellani, R. J., McCrory, P., & Gardner, A. J. (2022). Examining for Cavum Septum Pellucidum and Ventricular Enlargement in Retired Elite-Level Rugby League Players. *Frontiers in Neurology*, *13*. https://doi.org/10.3389/fneur.2022.817709

Stark, S. L., Roe, C. M., Grant, E. A., Hollingsworth, H., Benzinger, T. L., Fagan, A. M., Buckles, V. D., & Morris, J. C. (2013). Preclinical Alzheimer disease and risk of falls. *Neurology*, *81*, 437–443.

Stefanis, L. (2012). α-Synuclein in Parkinson's disease. *Cold Spring Harbor Perspectives in Medicine*, *2*(2). https://doi.org/10.1101/cshperspect.a009399

Stein, T. D., Montenigro, P. H., Alvarez, V. E., Xia, W., Crary, J. F., Tripodis, Y., Daneshvar, D. H., Mez, J., Solomon, T., Meng, G., Kubilus, C. A., Cormier, K. A., Meng, S., Babcock, K., Kiernan, P., Murphy, L., Nowinski, C. J., Martin, B., Dixon, D., … McKee, A. C. (2015). Beta-amyloid deposition in chronic traumatic encephalopathy. *Acta Neuropathologica*, *130*(1), 21–34. https://doi.org/10.1007/s00401-015-1435-y

Steinacker, Feneberg, E., Weishaupt, J., Brettschneider, J., Tumani, H., Andersen, P. M., Arnim, C., Böhm, S., Kassubek, J., Kubisch, C., Lulé, D., Müller, H. P., Muche, R., Pinkhardt, E., Oeckl, P., Rosenbohm, A., Anderl-Straub, S., Volk, A. E., Weydt, P., … Otto, M. (2016). Neurofilaments in the diagnosis of motoneuron diseases: A prospective study on 455 patients. *Journal of Neurology, Neurosurgery and Psychiatry*, *87*(1), 12–20. https://doi.org/10.1136/jnnp-2015-311387

Stewart, W., McNamara, P. H., Lawlor, B., Hutchinson, S., & Farrell, M. (2016). Chronic traumatic encephalopathy: A potential late and under recognized consequence of rugby union? *Qjm*, *109*(1), 11–15. https://doi.org/10.1093/qjmed/hcv070

Sulhan, S., Lyon, K. A., Shapiro, L. A., & Huang, J. H. (2020). Neuroinflammation and blood–brain barrier disruption following traumatic brain injury: Pathophysiology and potential therapeutic targets. In *Journal of Neuroscience Research* (Vol. 98, Issue 1, pp. 19–28). John Wiley and Sons Inc. https://doi.org/10.1002/jnr.24331

Sultana, R., Reed, T., Perluigi, M., Coccia, R., Pierce, W. M., & Butterfield, D. A. (2007). Proteomic identification of nitrated brain proteins in amnestic mild cognitive impairment: A regional study. *Journal of Cellular and Molecular Medicine*, *11*(4), 839–851. https://doi.org/10.1111/j.1582-4934.2007.00065.x

Sun, M.-C., Honey, C., Berk, C., Wong, N., & Tsui, J. (2003). Regulation in AQP4 in TBI model in rats. *Journal of Neurosurgery*, *98*, 565–569.

Susie Zoltewicz, J., Scharf, D., Yang, B., Chawla, A., Newsom, K. J., & Fang, L. (2012). Characterization of antibodies that detect human GFAP after

traumatic brain injury. *Biomarker Insights*, *7*, 71–79. https://doi.org/10.4137/BMI.S9873

Susman, M., DiRusso, S. M., Sullivan, T., Risucci, D., Nealon, P., Cuff, S., & Benzil, D. (2002). Traumatic brain injury in the elderly: Increased mortality and worse functional outcome at discharge despite lower injury severity. *Journal of Trauma*, *53*(2), 219–224. https://doi.org/10.1097/00005373-200208000-00004

Suzuki, R., Okuda, M., Asai, J., Nagashima, G., Itokawa, H., Matsunaga, A., Fukimoto, T., & Suzuki, T. (2006). Astrocytes co-express AQP4 and VEGF in TBI. *Acta. Neurochir*, *96*, 368–401.

Tagliaferri, F., Compagnone, C., Korsic, M., Servadei, F., & Kraus, J. (2006). A systematic review of brain injury epidemiology in Europe. *Acta Neurochirurgica*, *148*(3), 255–267. https://doi.org/10.1007/s00701-005-0651-y

Takata, F., Nakagawa, S., Matsumoto, J., & Dohgu, S. (2021). Blood-Brain Barrier Dysfunction Amplifies the Development of Neuroinflammation: Understanding of Cellular Events in Brain Microvascular Endothelial Cells for Prevention and Treatment of BBB Dysfunction. In *Frontiers in Cellular Neuroscience* (Vol. 15). Frontiers Media S.A. https://doi.org/10.3389/fncel.2021.661838

Tanca, A., Pagnozzi, D., & Addis, M. F. (2012). Setting proteins free: Progresses and achievements in proteomics of formalin-fixed, paraffin-embedded tissues. *Proteomics - Clinical Applications*, *6*(1–2), 7–21. https://doi.org/10.1002/prca.201100044

Tate, D. F., & Bigler, E. D. (2000). Fornix and hippocampal atrophy in traumatic brain injury. *Learning and Memory*, *7*(6), 442–446. https://doi.org/10.1101/lm.33000

Taylor, C. A., Bell, J. M., Breiding, M. J., & Xu, L. (2017). Traumatic Brain Injury–Related Emergency Department Visits, Hospitalizations, and Deaths — United States, 2007 and 2013. *Centers for Disease Control and Prevention: Morbitity and Mortality Weekly Report*, *66*(9), 1–16. https://doi.org/10.15585/mmwr.ss6609a1

Teismann, P., Vila, M., Choi, D. K., Tieu, K., Wu, D. C., Jackson-Lewis, V., & Przedborski, S. (2003). COX-2 and neurodegeneration in Parkinson's disease. *Annals of the New York Academy of Sciences*, *991*, 272–277. https://doi.org/10.1111/j.1749-6632.2003.tb07482.x

Teissier, T., Boulanger, E., & Deramecourt, V. (2020a). Normal ageing of the brain: Histological and biological aspects. In *Revue Neurologique* (Vol. 176, Issue 9, pp. 649–660). Elsevier Masson s.r.l. https://doi.org/10.1016/j.neurol.2020.03.017

Teissier, T., Boulanger, E., & Deramecourt, V. (2020b). Normal ageing of the brain: Histological and biological aspects. In *Revue Neurologique* (Vol. 176, Issue 9, pp. 649–660). Elsevier Masson s.r.l. https://doi.org/10.1016/j.neurol.2020.03.017

Thal, D. R., Attems, J., & Ewers, M. (2014). Spreading of amyloid, tau, and microvascular pathology in alzheimer's disease: Findings from neuropathological and neuroimaging studies. In *Journal of Alzheimer's Disease* (Vol. 42, pp. S421–S429). IOS Press. https://doi.org/10.3233/JAD-141461

Thal, D. R., Del Tredici, K., & Braak, H. (2004). Neurodegeneration in Normal Brain Aging and Disease. *Science of Aging Knowledge Environment*, *2004*(23), pe26–pe26. https://doi.org/10.1126/sageke.2004.23.pe26

Thal, D., Rüb, U., Orantes, M., & Braak, H. (2002). Phases of Aß-deposition in the human brain and its relevance for the development of AD. *Neurology*, *58*(12), 1791–1800. www.neurology.org

Thelin, E. P., Tajsic, T., Zeiler, F. A., Menon, D. K., Hutchinson, P. J. A., Carpenter, K. L. H., Morganti-Kossmann, M. C., & Helmy, A. (2017). Monitoring the neuroinflammatory response following acute brain injury. In *Frontiers in Neurology* (Vol. 8, Issue JUL). Frontiers Media S.A. https://doi.org/10.3389/fneur.2017.00351

Thompson, H. J., McCormick, W. C., & Kagan, S. H. (2006). Traumatic Brain Injuriy in Older Adults: Epidemiology, Outcomes and Furture Implications. *J Am Geriatr Soc.*, *54*(10), 1590–1595. https://doi.org/10.1039/b800799c.O

Thomsen, Ma, A. M., Ko, A., Harada, M. Y., Wyss, L., Haro, P. S., Vit, J. P., Shelest, O., Rhee, P., Svendsen, C. N., & Ley, E. J. (2016). A model of recurrent concussion that leads to long-term motor deficits, CTE-like tauopathy and exacerbation of an ALS phenotype. *Journal of Trauma and Acute Care Surgery*, *81*, 1070–1078. https://doi.org/10.1097/TA.0000000000001248

Thornton, E., Vink, R., Blumbergs, P. C., & Van Den Heuvel, C. (2006). Soluble amyloid precursor protein α reduces neuronal injury and improves functional outcome following diffuse traumatic brain injury in rats. *Brain Research*, *1094*(1), 38–46. https://doi.org/10.1016/j.brainres.2006.03.107

Tisdale. (2002). Glyceraldehyde-3-phosphate dehydrogenase is phosphorylated by protein kinase Cιλ and plays a role in microtubule dynamics in the early secretory pathway. *Journal of Biological Chemistry*, *277*(5), 3334–3341. https://doi.org/10.1074/jbc.M109744200

Tobin, R. P., Mukherjee, S., Kain, J. M., Rogers, S. K., Henderson, S. K., Motal, H. L., Rogers, M. K. N., & Shapiro, L. A. (2014). Traumatic brain injury causes selective, CD74-dependent peripheral lymphocyte activation that exacerbates neurodegeneration. *Acta Neuropathologica Communications*, *2*(1), 1–10. https://doi.org/10.1186/s40478-014-0143-5

Tokuda, T., Ikeda, S., Yanagisawa, N., Ihara, Y., & Glenner, G. G. (1991). Re-examination of ex-boxers' brains using immunohistochemistry with antibodies to amyloid ß-protein and tau protein. *Acta Neuropathologica*, *82*(4), 280–285. https://doi.org/10.1007/BF00308813

Tolppanen, A. M., Taipale, H., & Hartikainen, S. (2017). Head or brain injuries and Alzheimer's disease: A nested case-control register study. *Alzheimer's and Dementia*, *13*(12), 1371–1379. https://doi.org/10.1016/j.jalz.2017.04.010

Tomaiuolo, F., Carlesimo, G. A., Di Paola, M., Petrides, M., Fera, F., Bonanni, R., Formisano, R., Pasqualetti, P., & Caltagirone, C. (2004). Gross morphology and morphometric sequelae in the hippocampus, fornix, and corpus callosum of patients with severe non-missile traumatic brain injury without macroscopically detectable lesions: A T1 weighted MRI study. *Journal of Neurology, Neurosurgery and Psychiatry*, *75*(9), 1314–1322. https://doi.org/10.1136/jnnp.2003.017046

Tomkins, O., Feintuch, A., Benifla, M., Cohen, A., Friedman, A., & Shelef, I. (2011). Blood-brain barrier breakdown following traumatic brain injury: A possible role in posttraumatic epilepsy. *Cardiovascular Psychiatry and Neurology*. https://doi.org/10.1155/2011/765923

Tran, D., Daniels, M., Colson, B., Aivazian, D., Boccia, A., Joseph, I., Ho, S., French, S., Buko, A., & Wei, J. (2011). Sample Preparation of Formalin-Fixed Paraffin-Embedded (FFPE) Tissue for Proteomic Analyses. In *Sample*

Preparation in Biological Mass Spectrometry (pp. 159–170). Springer Netherlands. https://doi.org/10.1007/978-94-007-0828-0_10

Tran, Daniels, M., Colson, B., Aivazian, D., Boccia, A., Joseph, I., Ho, S., French, S., Buko, A., & Wei, J. (2011). Sample Preparation of Formalin-Fixed Paraffin-Embedded (FFPE) Tissue for Proteomic Analyses. In *Sample Preparation in Biological Mass Spectrometry* (pp. 159–170). Springer Netherlands. https://doi.org/10.1007/978-94-007-0828-0_10

Tran, H. T., LaFerla, F. M., Holtzman, D. M., & Brody, D. L. (2011). Controlled cortical impact traumatic brain injury in 3xTg-AD mice causes acute intra-axonal amyloid-ß accumulation and independently accelerates the development of tau abnormalities. *Journal of Neuroscience*, *31*(26), 9513–9525. https://doi.org/10.1523/JNEUROSCI.0858-11.2011

Trist, B. G., Davies, K. M., Cottam, V., Genoud, S., Ortega, R., Roudeau, S., Carmona, A., De Silva, K., Wasinger, V., Lewis, S. J. G., Sachdev, P., Smith, B., Troakes, C., Vance, C., Shaw, C., Al-Sarraj, S., Ball, H. J., Halliday, G. M., Hare, D. J., & Double, K. L. (2017). Amyotrophic lateral sclerosis-like superoxide dismutase 1 proteinopathy is associated with neuronal loss in Parkinson's disease brain. *Acta Neuropathologica*, *134*(1), 113–127. https://doi.org/10.1007/s00401-017-1726-6

Trojanowski, & Virginia M-Y.L. (1998). Aggregation of Neurofilament and-Synuclein Proteins in Lewy Bodies Implications for the Pathogenesis of Parkinson Disease and Lewy Body Dementia. *Arch Neurol*, *55*, 151–152. https://jamanetwork.com/

Troost, D., van den Oord, J. J., de Jong, J. M. B. V., & Swaab, D. F. (1989). Lymphocytic infiltration in the spinal chord of patients with ALS. *Clinical Neuropathology*, *8*(6), 289–294.

Ulusoy, A., & Di Monte, D. A. (2013). α-Synuclein elevation in human neurodegenerative diseases: experimental, pathogenetic, and therapeutic implications. In *Molecular neurobiology* (Vol. 47, Issue 2, pp. 484–494). https://doi.org/10.1007/s12035-012-8329-y

Urano, Sato, Y., Otonari, T., Makabe, S., Suzuki, S., Ogata, M., & Endo, T. (1998). Aging and oxidative stress in neurodegeneration. *BioFactors*, *7*(1–2), 103–112. https://doi.org/10.1002/biof.5520070114

Uryu, K., Chen, X. H., Martinez, D., Browne, K. D., Johnson, V. E., Graham, D. I., Lee, V. M. Y., Trojanowski, J. Q., & Smith, D. H. (2007). Multiple proteins implicated in neurodegenerative diseases accumulate in axons after brain trauma in humans. *Experimental Neurology*, *208*(2), 185–192. https://doi.org/10.1016/j.expneurol.2007.06.018

Uryu, K., Laurer, H., McIntosh, T., Praticò, D., Martinez, D., Leight, S., M-Y Lee, V., & Trojanowski, J. (2002). Repetitive Mild Brain Trauma Accelerates A Deposition, Lipid Peroxidation, and Cognitive Impairment in a Transgenic Mouse Model of Alzheimer Amyloidosis. *The Journal of Neuroscience*, *22*(2), 446–454.

Van Den Heuvel, C., Thornton, E., & Vink, R. (2007). Traumatic brain injury and Alzheimer's disease: a review. In *Progress in Brain Research* (Vol. 161, pp. 303–316). https://doi.org/10.1016/S0079-6123(06)61021-2

van Dyck, C. H., Swanson, C. J., Aisen, P., Bateman, R. J., Chen, C., Gee, M., Kanekiyo, M., Li, D., Reyderman, L., Cohen, S., Froelich, L., Katayama, S., Sabbagh, M., Vellas, B., Watson, D., Dhadda, S., Irizarry, M., Kramer, L. D., & Iwatsubo, T. (2022). Lecanemab in Early Alzheimer's Disease. *The New England Journal of Medicine*. https://doi.org/10.1056/NEJMoa2212948

Van Muiswinkel, F. L., De Vos, R. A. I., Bol, J. G. J. M., Andringa, G., Jansen Steur, E. N. H., Ross, D., Siegel, D., & Drukarch, B. (2004). Expression of NAD(P)H:quinone oxidoreductase in the normal and Parkinsonian substantia nigra. *Neurobiology of Aging*, *25*(9), 1253–1262. https://doi.org/10.1016/j.neurobiolaging.2003.12.010

Van Steenoven, Koel-Simmelink, M. J. A., Vergouw, L. J. M., Tijms, B. M., Piersma, S. R., Pham, T. V., Bridel, C., Ferri, G. L., Cocco, C., Noli, B., Worley, P. F., Xiao, M. F., Xu, D., Oeckl, P., Otto, M., Van Der Flier, W. M., De Jong, F. J., Jimenez, C. R., Lemstra, A. W., & Teunissen, C. E. (2020). Identification of novel cerebrospinal fluid biomarker candidates for dementia with Lewy bodies: a proteomic approach. *Molecular Neurodegeneration*, *15*(36). https://doi.org/10.1186/s13024-020-00388-2

Vargas, M. R., & Johnson, J. A. (2017). The Nrf2-ARE cytoprotective pathway in astrocytes. *Expert Reviews in Molecular Medicine*, *11*, 1–25. https://doi.org/10.1017/S1462399409001094

Vasile, F., Dossi, E., & Rouach, N. (2017). Human astrocytes: structure and functions in the healthy brain. In *Brain Structure and Function* (Vol. 222, Issue 5, pp. 2017–2029). Springer Verlag. https://doi.org/10.1007/s00429-017-1383-5

Venero, J. L., Vizuete, M. L., Machado, A., & Cano, J. (2001). Aquaporins in the central nervous system. In *Progress in Neurobiology* (Vol. 63). www.elsevier.com/locate/pneurobio

Villemagne, V. L., Doré, V., Burnham, S., & Rowe, C. C. (2021). Aß Imaging in Aging, Alzheimer's Disease, and Other Neurodegenerative Conditions. In *PET and SPECT in Neurology* (pp. 283–343). Springer International Publishing. https://doi.org/10.1007/978-3-030-53168-3_10

Vlassenko, A. G., Benzinger, T. L. S., & Morris, J. C. (2012). PET amyloid-beta imaging in preclinical Alzheimer's disease. In *Biochimica et Biophysica Acta - Molecular Basis of Disease* (Vol. 1822, Issue 3, pp. 370–379). https://doi.org/10.1016/j.bbadis.2011.11.005

Vos, Jacobs, B., Andriessen, T. M. J. C., Lamers, K. J. B., Borm, G. F., Beems, T., Edwards, M., Rosmalen, C. F., & Vissers, J. L. M. (2010). GFAP and S100B are biomarkers of traumatic brain injury An observational cohort study. *Neurology*, *75*, 1786–1793.

Wada, Ren, C. H., Koyama, S., Arawaka, S., Kawakatsu, S., Kimura, H., Nagasawa, H., Kawanami, T., Kurita, K., Daimon, M., Hirano, A., & Kato, T. (2004). A human granin-like neuroendocrine peptide precursor (proSAAS) immunoreactivity in tau inclusions of Alzheimer's disease and parkinsonism-dementia complex on Guam. *Neuroscience Letters*, *356*(1), 49–52. https://doi.org/10.1016/j.neulet.2003.11.028

Walker, F. R., Beynon, S. B., Jones, K. A., Zhao, Z., Kongsui, R., Cairns, M., & Nilsson, M. (2014). Dynamic structural remodelling of microglia in health and disease: A review of the models, the signals and the mechanisms. In *Brain, Behavior, and Immunity* (Vol. 37, pp. 1–14). https://doi.org/10.1016/j.bbi.2013.12.010

Wang, Cunningham, R., Zetterberg, Asthana, S., Carlsson, C., Okonkwo, O., & Li, L. (2016). Label-free quantitative comparison of cerebrospinal fluid glycoproteins and endogenous peptides in subjects with Alzheimer's disease, mild cognitive impairment, and healthy individuals. *Proteomics - Clinical Applications*, *10*(12), 1225–1241. https://doi.org/10.1002/prca.201600009

Wang, H. K., Lin, S. H., Sung, P. S., Wu, M. H., Hung, K. W., Wang, L. C., Huang, C. Y., Lu, K., Chen, H. J., & Tsai, K. J. (2012). Population based study on

patients with traumatic brain injury suggests increased risk of dementia. *Journal of Neurology, Neurosurgery and Psychiatry*, *83*(11), 1080–1085. https://doi.org/10.1136/jnnp-2012-302633

Wang, H., Song, G., Chuang, H., Chiu, C., Abdelmaksoud, A., Ye, Y., & Zhao, L. (2018). Portrait of glial scar in neurological diseases. In *International Journal of Immunopathology and Pharmacology* (Vol. 31, pp. 1–6). SAGE Publications Inc. https://doi.org/10.1177/2058738418801406

Wang, K., Ottens, A., Haskins, W., Liu, M. C., Kobeissy, F., Denslow, N., Chen, S. S., & Hayes, R. L. (2004). Proteomics studies of traumatic brain injury. *International Review of Neurobiology*, *61*, 215–240. https://doi.org/10.1016/S0074-7742(04)61009-9

Wang, K., Yang, Z., Yue, J. K., Zhang, Z., Winkler, E. A., Puccio, A. M., Diaz-Arrastia, R., Lingsma, H. F., Yuh, E. L., Mukherjee, P., Valadka, A. B., Gordon, W. A., Okonkwo, D. O., Manley, G. T., Cooper, S. R., Dams-O'Connor, K., Hricik, A. J., Inoue, T., Maas, A. I. R., … Vassar, M. J. (2016). Plasma Anti-Glial Fibrillary Acidic Protein Autoantibody Levels during the Acute and Chronic Phases of Traumatic Brain Injury: A Transforming Research and Clinical Knowledge in Traumatic Brain Injury Pilot Study. *Journal of Neurotrauma*, *33*(13), 1270–1277. https://doi.org/10.1089/neu.2015.3881

Wang, Q., Woltjer, R. L., Cimino, P. J., Pan, C., Montine, K. S., Zhang, J., & Montine, T. J. (2005). Proteomic analysis of neurofibrillary tangles in Alzheimer disease identifies GAPDH as a detergent-insoluble paired helical filament tau binding protein. *The FASEB Journal*, *19*(7), 1–12. https://doi.org/10.1096/fj.04-3210fje

Wang, Y., Santa-Cruz, K., Decarli, C., & Johnson, J. A. (2000). NAD(P)H:quinone oxidoreductase activity is increased in hippocampal pyramidal neurons of patients with Alzheimer's disease. *Neurobiology of Aging*, *21*(4), 525–531. https://doi.org/10.1016/S0197-4580(00)00114-7

Warner, M. A., Youn, T. S., Davis, T., Chandra, A., Marquez De La Plata, C., Moore, C., Harper, C., Madden, C. J., Spence, J., McColl, R., Devous, M., King, R. D., & Diaz-Arrastia, R. (2010). Regionally selective atrophy after traumatic axonal injury. *Archives of Neurology*, *67*(11), 1336–1344. https://doi.org/10.1001/archneurol.2010.149

Washington, P. M., Morffy, N., Parsadanian, M., Zapple, D. N., & Burns, M. P. (2014). Experimental traumatic brain injury induces rapid aggregation and oligomerization of amyloid-beta in an Alzheimer's disease mouse model. *Journal of Neurotrauma*, *31*(1), 125–134. https://doi.org/10.1089/neu.2013.3017

Washington, P. M., Villapol, S., & Burns, M. P. (2016). Polypathology and dementia after brain trauma: Does brain injury trigger distinct neurodegenerative diseases, or should they be classified together as traumatic encephalopathy? *Experimental Neurology*, *275*, 381–388. https://doi.org/10.1016/j.expneurol.2015.06.015

Weckbach, S., Neher, M., Losacco, J. T., Bolden, A. L., Kulik, L., Flierl, M. A., Bell, S. E., Holers, V. M., & Stahel, P. F. (2012). Challenging the Role of Adaptive Immunity in Neurotrauma: *Rag1* $^{-/-}$ Mice Lacking Mature B and T Cells Do Not Show Neuroprotection after Closed Head Injury. *Journal of Neurotrauma*, *29*(6), 1233–1242. https://doi.org/10.1089/neu.2011.2169

Weissberg, I., Veksler, R., Kamintsky, L., Saar-ashkenazy, R., Milikovsky, D., Shelef, I., & Friedman, A. (2014). Imaging Blood-Brain Barrier Dysfunction in

Football Players. *JAMA Neurology*, *71*(11), 1453–1455. https://jamanetwork.com/

Werner, C., & Engelhard, K. (2007). Pathophysiology of traumatic brain injury. *British Journal of Anaesthesia*, *99*(1), 4–9. https://doi.org/10.1093/bja/aem131

Werner, C. J., Heyny-von Haussen, R., Mall, G., & Wolf, S. (2008). Proteome analysis of human substantia nigra in Parkinson's disease. *Proteome Science*, *6*. https://doi.org/10.1186/1477-5956-6-8

Williams. (1995). Oxidative stress, age-related neurodegeneration, and the potential for neurotrophic treatment. *Cerebrovascular and Brain Metabolism Reviews*, *7*(1), 55—73. http://europepmc.org/abstract/MED/7742172

Williams, D., & Tannenberg, A. E. G. (1996). Dementia pugilistica in an alcoholic achondroplastic dwarf. *Pathology*, *28*(1), 102–104.

Williams, S., Raghupathi, R., MacKinnon, M. A., McIntosh, T. K., Saatman, K. E., & Graham, D. I. (2001). In situ DNA fragmentation occurs in white matter up to 12 months after head injury in man. *Acta Neuropathologica*, *102*(6), 581–590. https://doi.org/10.1007/s004010100410

Williams-Gray, C. H., Mason, S. L., Evans, J. R., Foltynie, T., Brayne, C., Robbins, T. W., & Barker, R. A. (2013). The CamPaIGN study of Parkinson's disease: 10-year outlook in an incident population-based cohort. *Journal of Neurology, Neurosurgery and Psychiatry*, *84*(11), 1258–1264. https://doi.org/10.1136/jnnp-2013-305277

Wilson, L., Stewart, W., Dams-O'Connor, K., Diaz-Arrastia, R., Horton, L., Menon, D. K., & Polinder, S. (2017). The chronic and evolving neurological consequences of traumatic brain injury. *The Lancet Neurology*, *16*(10), 813–825. https://doi.org/10.1016/S1474-4422(17)30279-X

Wiśniewski, J. R., Ostasiewicz, P., Duś, K., Zielińska, D. F., Gnad, F., & Mann, M. (2012). Extensive quantitative remodeling of the proteome between normal colon tissue and adenocarcinoma. *Molecular Systems Biology*, *8*. https://doi.org/10.1038/msb.2012.44

Witcher, Bray, C. E., Chunchai, T., Zhao, F., O'Neil, S. M., Gordillo, A. J., Campbell, W. A., McKim, D. B., Liu, X., Dziabis, J. E., Quan, N., Eiferman, D. S., Fischer, A. J., Kokiko-Cochran, Olga. N., Askwith, C., & Godbout, J. P. (2021). Traumatic brain injury causes chronic cortical inflammation and neuronal dysfunction mediated by Microglia. *Journal of Neuroscience*, *41*(7), 1597–1616. https://doi.org/10.1523/JNEUROSCI.2469-20.2020

Wright, D., Liu, S., Van Der Poel, C., McDonald, S. J., Brady, R. D., Taylor, L., Yang, L., Gardner, A. J., Ordidge, R., O'Brien, T., Johnston, L. A., & Shultz, S. R. (2017). Traumatic brain injury results in cellular, structural and functional changes resembling motor neuron disease. *Cerebral Cortex*, *27*(9), 4503–4515. https://doi.org/10.1093/cercor/bhw254

Yan, W., Wang, H. D., Hu, Z. G., Wang, Q. F., & Yin, H. X. (2008). Activation of Nrf2-ARE pathway in brain after traumatic brain injury. *Neuroscience Letters*, *431*(2), 150–154. https://doi.org/10.1016/j.neulet.2007.11.060

Yeager, M. P., DeLeo, J. A., Hoopes, P. J., Hartov, A., Hildebrandt, L., & Hickey, W. F. (2000). Trauma and inflammation modulate lymphocyte localization in vivo: Quantitation of tissue entry and retention using indium-111-labeled lymphocytes. *Critical Care Medicine*, *28*(5), 1477–1482. https://doi.org/10.1097/00003246-200005000-00037

Yuan, & Nixon, R. A. (2021). Neurofilament Proteins as Biomarkers to Monitor Neurological Diseases and the Efficacy of Therapies. *Frontiers in Neuroscience*, *15*. https://doi.org/10.3389/fnins.2021.689938

Yuan, Rao, M. V., Veeranna, & Nixon, R. A. (2017). Neurofilaments and neurofilament proteins in health and disease. *Cold Spring Harbor Perspectives in Biology*, *9*(4). https://doi.org/10.1101/cshperspect.a018309

Zanier, E. R., Bertani, I., Sammali, E., Pischiutta, F., Chiaravalloti, M. A., Vegliante, G., Masone, A., Corbelli, A., Smith, D. H., Menon, D. K., Stocchetti, N., Fiordaliso, F., De Simoni, M. G., Stewart, W., & Chiesa, R. (2018). Induction of a transmissible tau pathology by traumatic brain injury. *Brain*, *141*(9), 2685–2699. https://doi.org/10.1093/brain/awy193

Zanier, E. R., Fumagalli, S., Perego, C., Pischiutta, F., & De Simoni, M. G. (2015). Shape descriptors of the "never resting" microglia in three different acute brain injury models in mice. *Intensive Care Medicine Experimental* , *3*(1), 1–18. https://doi.org/10.1186/s40635-015-0039-0

Zetterberg, H., Smith, D. H., & Blennow, K. (2013). Biomarkers of mild traumatic brain injury in cerebrospinal fluid and blood. *Nature Reviews Neurology*, *9*(4), 201–210. https://doi.org/10.1038/nrneurol.2013.9

Zgorzynska, E., Dziedzic, B., & Walczewska, A. (2021). An overview of the nrf2/are pathway and its role in neurodegenerative diseases. In *International Journal of Molecular Sciences* (Vol. 22, Issue 17). MDPI. https://doi.org/10.3390/ijms22179592

Zhang, Z. W., Liang, J., Yan, J. X., Ye, Y. C., Wang, J. J., Chen, C., Sun, H. T., Chen, F., Tu, Y., & Li, X. H. (2020). TBHQ improved neurological recovery after traumatic brain injury by inhibiting the overactivation of astrocytes. *Brain Research*, *1739*. https://doi.org/10.1016/j.brainres.2020.146818

Zhang, Z., Zoltewicz, J. S., Mondello, S., Newsom, K. J., Yang, Z., Yang, B., Kobeissy, F., Guingab, J., Glushakova, O., Robicsek, S., Heaton, S., Buki, A., Hannay, J., Gold, M. S., Rubenstein, R., Lu, X. C. M., Dave, J. R., Schmid, K., Tortella, F., … Wang, K. K. W. (2014). Human traumatic brain injury induces autoantibody response against glial fibrillary acidic protein and its breakdown products. *PLoS ONE*, *9*(3), 1–16. https://doi.org/10.1371/journal.pone.0092698

Zhao, Y., & Zhao, B. (2013). Oxidative stress and the pathogenesis of alzheimer's disease. In *Oxidative Medicine and Cellular Longevity*. https://doi.org/10.1155/2013/316523

Zhao, Z. A., Li, P., Ye, S. Y., Ning, Y. L., Wang, H., Peng, Y., Yang, N., Zhao, Y., Zhang, Z. H., Chen, J. F., & Zhou, Y. G. (2017). Perivascular AQP4 dysregulation in the hippocampal CA1 area after traumatic brain injury is alleviated by adenosine A2Areceptor inactivation. *Scientific Reports*, *7*(1), 1–10. https://doi.org/10.1038/s41598-017-02505-6

Zhou, B., Zuo, Y. X., & Jiang, R. T. (2019). Astrocyte morphology: Diversity, plasticity, and role in neurological diseases. In *CNS Neuroscience and Therapeutics* (Vol. 25, Issue 6, pp. 665–673). Blackwell Publishing Ltd. https://doi.org/10.1111/cns.13123

Zhu, Weiss, T., Zhang, Q., Sun, R., Wang, B., Yi, X., Wu, Z., Gao, H., Cai, X., Ruan, G., Zhu, T., Xu, C., Lou, S., Yu, X., Gillet, L., Blattmann, P., Saba, K., Fankhauser, C. D., Schmid, M. B., … Guo, T. (2019). High-throughput proteomic analysis of FFPE tissue samples facilitates tumor stratification. *Molecular Oncology*, *13*(11), 2305–2328. https://doi.org/10.1002/1878-0261.12570

Ziebell, J. M., & Morganti-Kossmann, M. C. (2010). Involvement of Pro-and Anti-Inflammatory Cytokines and Chemokines in the Pathophysiology of Traumatic Brain Injury. *Neurotherapeutics*, *7*, 22–30.

Zlokovic, B. V. (2008). The Blood-Brain Barrier in Health and Chronic Neurodegenerative Disorders. *Neuron*, *57*(2), 178–201. https://doi.org/10.1016/j.neuron.2008.01.003

Zlokovic, B. V. (2011). Neurovascular pathways to neurodegeneration in Alzheimer's disease and other disorders. In *Nature Reviews Neuroscience* (Vol. 12, Issue 12). https://doi.org/10.1038/nrn3114

Zlokovic, B. V., Deane, R., Sagare, A. P., Bell, R. D., & Winkler, E. A. (2010). Low-density lipoprotein receptor-related protein-1: A serial clearance homeostatic mechanism controlling Alzheimer's amyloid ß-peptide elimination from the brain. *Journal of Neurochemistry*, *115*(5), 1077–1089. https://doi.org/10.1111/j.1471-4159.2010.07002.x

Zucchi, Bonetto, V., Sorarù, G., Martinelli, I., Parchi, P., Liguori, R., & Mandrioli, J. (2020). Neurofilaments in motor neuron disorders: towards promising diagnostic and prognostic biomarkers. *Molecular Neurodegeneration*, *15*(58). https://doi.org/10.1186/s13024-020-00406-3